PSL UNIVERSITÉ PARIS

Université Paris Cité

SAPIENZA UNIVERSITÀ DI ROMA

THÈSE DE DOCTORAT

DE L'UNIVERSITÉ PSL

Préparée à l'École normale supérieure

Affiner la limite cinétique du gaz de Rayleigh non-idéal

Refining the kinetic limit of the nonideal Rayleigh gas

Soutenue par

Florent FOUGÈRES

Le 3 juillet 2026

École doctorale n°386

École doctorale de Sciences Mathématiques de Paris Centre

Spécialité

Mathématiques

Composition du jury :

Isabelle Gallagher Professeure, Université Paris Cité	*Directrice de thèse*
Sergio Simonella Full professor, Sapienza Università di Roma	*Directeur de thèse*
François Golse Professeur, École polytechnique	*Rapporteur*
Karsten Matthies Senior Lecturer, University of Bath	*Rapporteur*
Nathalie Ayi Maîtresse de conférence, Sorbonne université	*Examinatrice*
Giada Basile Associate professor, Sapienza Università di Roma	*Examinatrice*
Cécile Huneau Directrice de recherche CNRS, École normale supérieure	*Examinatrice*

ENS | PSL

Cette thèse est dédiée à la description du comportement des fluides,
la définition d'un fluide étant prise dans un sens relativement général.

Je suis conscient que la plupart des résultats de telles études servent à la construction et au fonctionnement de pesantes machines, aux usages plus ou moins excessifs.

Aussi, je vous invite avant de parcourir ces pages à prendre un instant la mesure de la vie qui nous habite.

L'air qui gonfle nos poumons.

Le sang qui bat dans nos veines et abreuve nos membres,

la salive,

l'urine,

la moelle,

les larmes.

Je me plais à croire que cette vie est belle, et qu'il est bon de la chérir sous les formes variées qu'elle revêt.

J'aimerais que cette thèse soit aussi l'occasion de retrouver la conscience des fluides biologiques qui rendent possible la vaste expérience de cette existence, pour nous personnes humaines, et pour la foule d'êtres qui partagent avec nous l'air, l'eau, et la vie.

Thèse préparée au Département de mathématiques et applications de l'École normale supérieure de Paris, puis en partie au Département de mathématiques Guido Castelnuovo de l'Université de Rome Sapienza, et à l'Institut de mathématiques de Jussieu – Paris Rive Gauche, de l'Université Paris Cité.

Sous la direction d'Isabelle Gallagher et Sergio Simonella.

Cette thèse débute avec un rapide résumé en français et en anglais,
suivi d'une double-page de remerciements.

La partie principale qui compose la thèse est rédigée en anglais et débute à la page 15,
par la table des matières, suivie d'une introduction qui contextualise notre étude
et en détaille les enjeux principaux.

Pour le lectorat francophone, cette partie substancielle est précédée d'un résumé détaillé
de quelques pages en français.

Résumé

Dans cette thèse, nous nous intéressons à préciser la limite cinétique du gaz de Rayleigh non-idéal, qui consiste à observer l'évolution d'une petite fraction de particules marquées dans un gaz à l'équilibre. Plus précisément, dans la continuité des travaux mathématiques initiés par Oscar Lanford en 1975, autour de la dérivation de l'équation de Boltzmann à partir des équations microscopiques des gaz, nous cherchons à analyser le comportement limite d'une panoplie d'objets statistiques servant à décrire le comportement moyen de leur dynamique.

Ce modèle possède la spécificité de faire apparaître dans sa limite des équations linéaires, pour lesquelles l'analyse en temps long est drastiquement simplifiée par rapport au cas général, dans lequel de nombreux résultats sont restreints à des temps très courts. Grâce à la proximité du gaz à son équilibre, de nouvelles méthodes de dérivation apparaissent, qui utilisent des bornes a priori sur les marginales de la densité du gaz.

Afin de décrire statistiquement la dynamique des particules marquées, nous commençons par généraliser le modèle existant du gaz de Rayleigh à un nombre asymptotiquement infini de ces particules, grâce à un système de particules étiquetées. Pour ce modèle, nous montrons sur des temps longs la convergence des fonctions de corrélation vers des limites données par l'équation de Rayleigh–Boltzmann linéaire. Nous généralisons ainsi les résultats pré-existants, en améliorant également leurs taux de convergence quantitatifs grâce à une nouvelle méthode de découpe temporelle adaptative. Ces résultats fournissent un premier corollaire sur le comportement asymptotique de la mesure empirique du gaz.

Pour affiner ce résultat, nous décrivons ensuite le comportement limite du champ de fluctuation et des grandes déviations de cette mesure empirique. Cette étude s'appuie sur l'analyse des cumulants de la dynamique, objets statistiques visant à décrire ses évènements rares. Nous étudions leur généralisation à notre système, en montrant des estimées et des résultats de convergence vers des équations de type Boltzmann linéaires, dont nous interrogeons finalement le cadre fonctionnel.

Grâce à une étude géométrique approfondie des trajectoires de la dynamique des particules, et à de nouvelles techniques de gestion de leurs singularités, nous améliorons par ailleurs le taux de convergence des cumulants. Ces méthodes géométriques optimisées s'appliquent d'ailleurs également dans le cadre général non-linéaire.

Grâce à cette étude, nous montrons la convergence des fluctuations vers un processus stochastique trivial, en exhibant au passage l'absence de transition de phase de ce comportement dans la limite sur-diluée. À l'ordre suivant, nous décrivons en temps long le système de Boltzmann–Hamilton–Jacobi linéaire qui gouvernent les grandes déviations de la mesure empirique, bien que de son côté le résultat de grandes déviations que nous démontrons reste restreint à des temps courts.

En effet, la question de la dérivation en temps long de résultats décrivant la dynamique des particules est centrale dans cette étude cinétique, et nous consacrons un chapitre à la présentation des diverses difficultés qui y sont liées, ainsi que des possibles solutions qui apparaissent dans certains cadres particuliers. Dans cette optique, nous présentons également une heuristique visant à déplacer certaines de ces obstructions, de façon à mieux en appréhender la nature. Cette étude se base sur un argument de grandes déviations et nous amène jusqu'à montrer certains résultats préliminaires, qui améliorent encore les estimées que l'on peut avoir sur les convergences en temps longs des fonctions de corrélation.

Enfin, cette thèse se conclut sur des perspectives de poursuite de notre étude, notamment autour de l'analyse des cumulants en temps long.

Abstract

In this thesis, we are interested in precising the kinetic limit of the nonideal Rayleigh gas, which consists in observing the evolution of a small fraction of tagged particles in a gas at thermodynamic equilibrium. More precisely, following the mathematical works initiated by Oscar Lanford in 1975, around the derivation of the Boltzmann equation from the microscopic Newton equations for gases, we try to analyse the limit behaviour of a panoply of statistical objects that describe the average behaviour of their dynamics.

This model makes appear linear equations in its limit, for which the long time analysis is far simpler than in the general case, for which numerous results are restricted to short times. Thanks to the proximity to equilibrium, new methods appear, that rely on a priori bounds on the marginals of the gas density.

So as to describe statistically the dynamics of tagged particles, we start by generalizing the existing Rayleigh gas model to an asymptotically infinite number of those particles, using a labelled mixture model. In this framework, we show the long time convergence of the correlation functions to limits governed by the linear Rayleigh–Boltzmann equation. We thus generalize the preexisting results, also improving their quantitative convergence rates thanks to a new method of adaptive time cutting. These results yield a first corollary on the asymptotic behaviour of the empirical measure of the gas.

To refine this result, we then describe the limit behaviour of the fluctuation field and large deviations of this empirical measure. This further study is based on the analysis of the dynamics' cumulants, which are statistical objects describing its rare events. We study their generalization to our system, showing estimates and convergence results to linear Boltzmann-like equations, of which we eventually interrogate the functional framework.

Thanks to a deepened geometrical study of the trajectories involved in the particles' dynamics, and using new techniques to handle their singularities, we also improve the existing convergence rate for the cumulants. These optimized geometrical methods also apply in the general nonlinear case.

With this analysis, we show the convergence of the fluctuations to a trivial stochastic process, exhibiting on the way the absence of phase transition for this behaviour in the overdilute regime. At the next order, we describe on large times the linear Boltzmann–Hamilton–Jacobi system driving the large deviations of the empirical measure, although this large deviation result is still shown only for short times.

Actually, the question of the long-time derivation of results describing the particles' dynamics is foremost in our kinetic study, and we dedicate a chapter to the presentation of various associated difficulties, along with possible solutions that emerge in some specific frameworks. In this idea, we also expose a heuristics to displace some of these hindrances, so as to better understand them. This study relies on a large deviation argument, and eventually leads us to prove preliminary results that improve once again the estimates that we can obtain on the long-time convergence of the correlation functions.

Eventually, this thesis ends with some perspectives on the continuation of our study, especially around the long-time analysis of cumulants.

Remerciements

Quelques mots pour remercier chaleureusement ma direction de thèse, Isabelle et Sergio, pour leur bienveillance et leur confiance dès les premiers contacts et tout au long de la thèse, pour leur enthousiasme quand ils parlent de ces sujets qui les passionnent, pour leur patience dans une énième explication et leurs relectures assidues. Un grand merci à vous deux également pour le soutien humain et moral que vous avez su m'apporter dans les moments difficiles comme dans les périodes de joie, et pour tout votre accompagnement et vos idées sans lesquels cette thèse n'aurait pu voir le jour !

I would also like to thank warmly my thesis *rapporteurs*, François Golse and Karsten Matthies, for having accepted to read and review my work. Merci grandement également aux examinatrices de mon jury Nathalie Ayi, Giada Basile et Cécile Huneau, pour leur relecture et leur présence lors des discussions de ma soutenance.

Je voudrais aussi remercier l'équipe du DMA pour leur accueil et leur soutien pendant ces trois années, merci à toute l'équipe d'analyse, merci à mes co-bureaux qui ont patiemment enduré ma propension à la croissance entropique, et égayé mes journées de longues discussions qu'elles soient mathématiques ou non ; merci à Alexis pour beaucoup trop de choses, à Arthur surtout pour son énergie inépuisable, à Alejandro pour son enthousiasme contagieux, à Shuoxing pour son mode de vie inspirant, à Matija pour sa générosité et à Quentin pour sa simplicité ; merci à Ons qui à la fin faisait presqu'autant partie du bureau pour notre plus grand plaisir !

Par ordre alphabétique, et de façon non-exhaustive, merci à Alexandre pour les belles chemises, Alexis pour les pauses au soleil, Bertrand pour sa poésie, Cécile pour sa bonté, Claire pour son franc-parler, Corentin pour les échanges matinaux, Cyril pour toutes nos discussions musicales, Djalil pour les diverses discussions et le soutien indéfectible sur l'enseignement, Émeric pour les moment partagés autour du Spike, Frédéric pour son humour, Gaspard pour son rire, Igor pour sa passion, Jimmy pour le repas à l'air libre, Julie pour son engagement remotivant, Julien pour sa complicité, Laure pour sa combativité et sa bonne humeur, Lino et Louis-Pierre pour le refuge de leur bureau et de leurs conversations, Maël pour le séminaire des doctorants, Milan pour me faire régulièrement travailler l'anglais, Nicolas pour l'image de son violoncelle, Romain pour les sourires, Sam bien sûr, Soham pour son imaginaire, Thomas pour sa calme sagesse, Vanessa pour son accompagnement dans les affres de l'éducation nationale, Yannick pour son short de vélo, et enfin évidemment Yue pour sa gaieté et son aide précieuses au quotidien !

Merci également à tous ceux que j'ai dû oublier, en espérant qu'il ne m'en tienne pas trop rigueur. Je voudrais également remercier les équipes de Paris-Cité et de la Sapienza, pour leur accueil chaleureux malgré la brièveté de mes passages.

Merci tout particulièrement à Fabienne, Cyril et Emmanuel pour leur accueil dans le laboratoire depuis mon stage et jusqu'à la fin de cette thèse, plein d'une bienveillance précieuse et rare.

Je voudrais aussi fortement remercier Théophile, Pierre et Corentin pour m'avoir précédé et accompagné dans cette aventure en bons demis-frères qu'ils sont, ainsi qu'Ambre qui m'y a suivie de près, et enfin Aksel pour sa cuisine et sa belle amitié !

Un merci particulier à Mathieu Lewin, qui m'a initié et formé au plaisir de la recherche et de la rédaction de belles mathématiques.

Si cette thèse est arrivée à son terme, lentement mais sûrement, c'est aussi grâce à tous mes complices de musique, qui m'ont permis de me changer les idées durant ces trois années. Un grand merci à *Meandres*, Arnaud, David, Gaspard et Théo pour leur patience, pour nos retraites et pour ces belles chansons dans lesquelles je m'évade dans les moments difficiles. Merci beaucoup aux *Bavards*, et encore bravo à Thierry, Thibaud et Béatrice pour ce beau bébé, merci à tous les membres présents et passés de cette tendre troupe aux allures de famille recomposée ! Merci également à l'orchestre et au chœur d'Oya Kephale, à l'atelier Demodocos et à mes compagnons improvisés de la salle Mu !

Un grand merci aussi à toute l'équipe d'Hackens, d'Enselle, et de la cycloffycine d'Ivry pour les dépannages et les moments de bricolage partagés, merci à tous les sportifs d'A2CMieux pour leur mentalité d'acier, merci aux petites et grandes amitiés, aux moments éphémères d'humanité glanés, qui me donnent au quotidien l'énergie dont j'ai besoin pour avancer.

Enfin, j'ai pour habitude de dire que mes plus grandes qualités sont mes amis et ma famille ; ces derniers savent à quel point je leur dois et à quel point je suis reconnaissant pour la personne qu'ils m'ont aidé à devenir, et la tendresse qu'ils m'aident à conserver. Merci Romane de m'avoir toujours soutenu de façon inconditionnelle, avec ton grand courage. Et puis force à Thomas dans cette page qui s'ouvre pour lui aussi ; et bon courage à toi aussi maa sœur ; et prends soin de toi mon frangin de la montagne !

Résumé détaillé en français

Le corps principal de la présente thèse, rédigé en anglais, débute par une introduction historique qui raconte l'émergence de la théorie atomique dans l'effervescence scientifique de l'Europe du XVIIIe siècle. John Dalton fut le premier à proposer un modèle complet de la matière comme composée de particules élémentaires, classifiées en catégories de propriétés identiques, qui dans un gaz évoluent librement dans le vide en interagissant les unes avec les autres. Cette description amena de proche en proche Ludwig Boltzmann à proposer un modèle statistique pour ces gaz, et à écrire l'équation qui porte désormais son nom, afin de décrire leur évolution mésoscopique à partir des équations microscopiques des particules. Cette étude marqua le commencement de la théorie cinétique, dont nous décrivons en partie l'avancée jusqu'à nos jours.

Cette introduction historique nous permet de contextualiser notre étude, en exposant les résultats mathématiques existants, et ceux que l'on est encore en droit d'espérer, ainsi que la façon dont nos problématiques s'y insèrent. Le reste de l'introduction propose un survol relativement détaillé des techniques, écueils et solutions rencontrées et utilisées dans l'ensemble de la thèse.

Les détails techniques apparaissent dans le deuxième chapitre, destiné à présenter le modèle que nous utilisons, qui est un cas particulier de gaz de Rayleigh non-idéal. Ce modèle consiste en l'observation de particules marquées dans un gaz globalement à l'équilibre, dans une proportion suffisamment faible pour que l'équation limite qui décrive leur évolution soit linéaire. Il s'agit en l'occurence de l'équation de Rayleigh–Boltzmann, que nous présentons rapidement dans ce même chapitre. Nous commençons donc par une présentation générale du modèle des sphères dures qui sert de base à notre étude, puis par une exposition d'outils techniques permettant de paramétriser les collisions entre les particules, en fonction des divers angles caractérisant la dispersion. Nous donnons ensuite les détails de la représentation statistique que nous faisons du gaz : pour les besoins de notre étude, nous élargissons ainsi le modèle du gaz de Rayleigh à un modèle de gaz mélangé, basé sur des particules étiquetées. Cette représentation permet de symétriser notre système, et d'introduire divers objets statistiques qui seront au cœur de notre analyse: la mesure empirique, son champ de fluctuation, ainsi que les fonctions de corrélation et leurs cumulants.

Pour conclure ce chapitre, nous calculons en détails la hiérarchie BBGKY satisfaite par les fonctions de corrélation de notre système, en écrivant ainsi certaines spécificités et détails techniques qui sont généralement omis dans la littérature.

Le troisième chapitre présente ensuite les équations de Boltzmann linéaires, et la façon dont elles apparaissent à partir de l'équation de Boltzmann quadratique. Après une rapide description des termes qui composent cette équation, nous pouvons alors détailler les raisons intuitives pour lesquelles certains termes linéaires apparaissent, quand d'autres sont absents, lorsque l'on observe les équations limites de divers systèmes proches de l'équilibre. On s'intéresse alors plus précisément au caractère bien posé de ces équations, en particulier de celles qui vont émerger comme comportement limite de notre gaz, à savoir l'équation de Rayleigh–Boltzmann linéaire, et un système linéaire de Hamilton–Jacobi dont la structure est très proche de celle de l'équation de Boltzmann. À partir d'une étude détaillée des opérateurs de collision qui apparaissent dans ces équations, et à travers divers changements d'inconnues, on se ramène à définir un cadre fonctionnel dans lequel nos équations linéaires possèdent des solutions uniques et globales.

Alors, le quatrième chapitre montre la convergence en temps long des fonctions de corrélation vers un équilibre perturbé par la solution de l'équation de Rayleigh–Boltzmann linéaire. Cette preuve est une adaptation de la littérature existante à notre nouveau modèle, et nous généralisons également les bornes quantitatives précédentes à l'ensemble des fonctions de corrélation en temps long, quand

elles avaient seules été montrées pour la première de ces fonctions. Nous exhibons au passage dans ce cas de figure l'apparition de constantes pathologiques qui dégradent les estimées quantitatives pour les hauts ordres de fonctions de corrélation, dues à la méthode standard que nous employons. Par ailleurs, nous donnons comme corollaire de ce théorème un résultat de convergence sur la mesure empirique, de type Loi des grands nombres. Ce corollaire est une première description statistique du comportement asymptotique de la dynamique.

La preuve du théorème passe par la représentation des séries de Duhamel itérées comme des intégrales sur des pseudo-trajectoires. Nous définissons donc ces pseudo-trajectoires dans un formalisme adapté à notre modèle, avant de suivre la méthode de preuve classique à partir de cette représentation: graĉe à des estimées de continuité et à l'étude géométrique des trajectoires des particules, nous ramenons la différence au temps t, entre la dynamique microscopique et la solution de l'équation limite, à cette même différence au temps initial, où l'erreur est explicite compte tenu du choix des données initiales. Afin de prolonger ce résultat à des temps longs, on utilise un procédé de découpage de l'intervalle de temps en petits intervalles : on impose une condition sur le nombre de collisions ayant lieu sur chacun de ces intervalles, de sorte qu'il nous faut ensuite justifier que cette approximation n'entraîne pas une erreur trop importante qui empêcherait de montrer la convergence. En pratique, l'erreur due à cette approximation est l'ordre dominant dans les taux de convergence que nous montrons.

Par rapport aux preuves existantes, les bornes a priori pour ce cadre de mélange grand-canonique demandent un effort combinatoire supplémentaire, et une étude détaillée de la fonction de partition de notre système. Ces résultats reposent sur une analyse fine des cumulants de l'exclusion, effectuée dans le chapitre dédié aux cumulants. Un autre point apparaissant spécifiquement dans le cadre de notre étude est la justification du fait que les particules marquées interagissent suffisamment peu entre elles pour qu'à la limite, les collisions entre elles n'aient aucune influence sur la dynamique.

De plus, nous améliorons grandement les résultats pré-existants, qui se basaient sur un découpage temporelle uniforme, en adaptant la taille de chaque petit intervalle à la condition sur le nombre de collisions qu'il doit contenir. De cette façon, l'erreur est répartie de façon régulière sur chacun de ces intervalles, qui sont similaires d'un point de vue de l'échelle physique : nous nous débarassons ainsi de près de deux logarithmes qui ralentissaient grandement les taux de convergence. La condition sur les collisions étant exponentielle, ce découpage temporel adaptatif peut être vu comme paramétrisé par une échelle logarithmique en temps.

La suite de notre étude consiste en un raffinement du corollaire statistique de type Loi des grands nombres montré dans le quatrième chapitre, en décrivant les ordres supérieurs de cette convergence. Cette analyse se base sur l'étude d'objets qui encodent les défauts de factorisation des fonctions de corrélation : les *cumulants*. Notre cinquième chapitre est donc dédié à une étude générale de ces objets et de leurs premières propriétés. Après les avoir définis à partir des fonctions de corrélation, et commentés, nous détaillons les ressorts combinatoires qui permettent de prouver leur injectivité grâce à une formule d'inversion. Dans la littérature existante, l'identité au cœur de cette preuve est usuellement prouvée grâce à des séries de Taylor analytique ; nous en donnons ici une preuve complètement combinatoire, qui s'appuie sur la structure propre aux partitions qui définissent les cumulants.

Dans un second temps, nous nous intéressons plus précisément aux cumulants de fonctions possédant la même structure caractéristique que la condition d'exclusion des sphères dures. Pour ces *cumulants de l'exclusion*, nous exhibons l'apparition d'une formule basée sur des graphes connexes d'exclusion, qui nous permet de prouver une estimée puissante sur ces cumulants particuliers. Nous détaillons le schéma de partition, dû à Roger Penrose, qui permet de prouver cette estimée. Nous utilisons ensuite ces résultats pour prouver les bornes sur la fonction de partition que nous avons utilisées au chapitre précédent, encore une fois basées sur une étude combinatoire. Nous en profitons

pour énoncer également des résulats sur les fonctions de partitions canoniques, qui précisent l'estimée sur la proximité des données initiales à l'équilibre.

Notre sixième chapitre est le plus conséquent, et le plus dense techniquement. Nous y étudions précisément les cumulants du gaz de Rayleigh, de façon à obtenir sur ces objets des bornes et des résultats de convergence. Il débute avec l'introduction de la fonction génératrice de ces cumulants, que l'on montre être directement liée aux moments de la mesure empirique. Cette propriété justifie l'utilisation de ces objets afin d'étudier les ordres fins de son comportement statistique asymptotique. Avant d'entrer directement dans notre étude de ces cumulants, nous commençons en décrivant naïvement les équations aux dérivées partielles satisfaites par ces objets, de façon à montrer qu'elles présentent une complexité autrement supérieure aux équations sur les fonctions de corrélation. Nous en profitons pour présenter une façon de simplifier les cumulants qui est parfois utilisée dans la littérature, en révélant toute la chaîne simplificatrice qui y amène depuis les cumulants que nous utilisons.

Alors, ces calculs justifient la nécessité d'observer une expansion des cumulants en fonction des pseudo-trajectoires introduites précédemment, et plus précisément en fonction des évènements rares qui apparaissent dans ces trajectoires. En effet, on montre dans la suite que ces évènements rares décrivent précisément l'évolution des cumulants, et même qu'à la limite le n-ème cumulant est gouverné par les trajectoires présentant $(n-1)$ de ces évènements rares, qui peuvent être de deux sortes, appelées recollision et superposition. Cette expansion fait apparaître au temps initial des cumulants plus grossiers, appelés cumulants initiaux en grappes, pour lesquels nous donnons une formule explicite en fonction des cumulants de l'exclusion.

Pour faire apparaître la dépendance de ces cumulants en les évènements rares évoqués plus haut, et plus spécifiquement pour faire apparaître la petite taille des cumulants due à la faible probabilité d'apparition de trajectoires contenant des évènements rares, nous reparamétrisons toutes les trajectoires à partir des conditions imposées par ces évènements. Ces conditions sont alors enregistrées dans un *arbre de dynamique*, qui permet de reconstruire la trajectoire à partir de cette nouvelle paramétrisation. Nous obtenons finalement une formule pour les cumulants, en conditionnant sur l'arbre de dynamique associé à chaque pseudo-trajectoire, qui met en évidence les recollisions et les superpositions, avec leurs paramétrisations correspondantes, au même niveau que les collisions déjà contenues dans les pseudo-trajectoires.

Alors, on peut démontrer des bornes sur les cumulants directement à partir de cette formule. D'une part, on utilise les cumulants de l'exclusion pour dominer les cumulants initiaux en grappes, en détaillant la combinatoire des arbres sous-jacents. D'autre part, on utilise l'argument de Cauchy–Schwarz classique pour contrôler les sections efficaces associées aux collisions, recollisions et superpositions. Enfin, on conclut en décomposant les partitions qui apparaissent dans la formule trouvée plus haut. Ce travail est grandement simplifié par la nouvelle formule explicite en question dans laquelle apparaissent clairement tous les éléments à contrôler.

Enfin, on peut donc s'intéresser à la limite des cumulants, en justifiant qu'ils convergent effectivement vers la limite formelle de leur formule explicite, avec de bons taux de convergence. Pour ce faire, on commence par contrôler la partie correspondant aux trajectoires dans lesquelles on rencontre fortuitement des particules marquées. Comme leur proportion dans le gaz tend vers 0, cette partie des cumulants est négligeable à la limite. On justifie alors le fait que les trajectoires contenant trop de rencontres rares, qui présentent donc des cycles, sont également négligeables à la limite. Les arguments géométriques qui soutiennent ce résultat sont repoussés au chapitre 8. Grâce à un travail détaillé sur les arguments géométriques en question, on optimise le contrôle pré-existant dans la littérature sur ces trajectoires contenant des cycles, de façon à améliorer les taux de convergence des cumulants. Cette amélioration reste par ailleurs valide dans le cas général quadratique de l'équation de Boltzmann.

On parvient alors à montrer que les cumulants tendent effectivement vers leur limite formelle dans la formule explicite exhibant les évènements rares qui gouvernent leur évolution. On peut alors s'intéresser à cette limite, dans laquelle l'utilisation de symétries propres à l'état d'équilibre initial permet de simplifier un nombre important de termes. On retrouve notamment l'équation de Rayleigh–Boltzmann linéaire pour le premier cumulant.

Grâce à ces résultats, on prouve finalement que pour les particules marquées, la limite de la fonction génératrice des cumulants dépend uniquement du premier cumulant, qui est aussi la première fonction de corrélation. En effet, la taille des cumulants dépend de la probabilité des évènements rares dans les pseudo-trajectoires, qui dépend de la limite de Boltzmann–Grad pour le potentiel chimique μ de l'ensemble du gaz, tandis que pour obtenir les moments de la mesure empirique, ces cumulants sont renormalisés selon le potentiel chimique λ des particules marquées. Comme le rapport des deux potentiels chimiques tend vers zéro à la limite, à partir du second cumulant, tous les ordres ont un impact négligeable sur la fonction génératrice des cumulants.

Ainsi, l'équation hamiltonienne satisfaite par cette fonction génératrice limite se révèle linéaire. Nous montrons donc comment apparaît cette équation puis, en définissant le cadre fonctionnel dans lequel se place la fonction limite, nous l'identifions avec une solution issue de méthodes constructrices à partir du système de Hamilton–Jacobi associé. C'est cette équation qui décrit le principe de grandes déviations dont il est question dans la suite.

On entre alors dans le septième chapitre, dans laquelle on peut finalement énoncer les résultats de raffinement statistique de l'étude de la mesure empirique : on y décrit le comportement limite de ses fluctuations et de ses grandes déviations. Dans cette partie, on détaille surtout la preuve de ces résultats dans un sens faible, qui repose essentiellement sur la convergence des cumulants prouvée dans le chapitre précédent. On justifie alors que ce sens faible correspond effectivement aux asymptotiques annoncées pour les fluctuations et grandes déviations, en invoquant l'étude menée sur ces résultats dans le cas général non-linéaire, et qui s'applique à l'identique à notre modèle une fois prouvés les résultats sur la fonction génératrice des cumulants. On donne simplement une preuve sur l'espérance du nombre de particules qui n'était pas détaillée dans l'étude précédemment évoquée, d'autant que cette preuve nécessite une légère adaptation par rapport au cas général à cause de la structure du mélange gazeux que nous modélisons.

On montre alors que dans notre choix d'échelle de Rayleigh–Boltzmann, le champ de fluctuations de la mesure empirique converge vers un processus stochastique trivial qui ne dépend que du comportement limite du premier cumulant, contrairement au cas général dans lequel l'ordre 2 garde asymptotiquement une influence déterminante sur les fluctuations. À la limite, il est donc impossible de garder la trace, dans les fluctuations de la mesure empirique, de l'interaction entre paires de particules marquées. Ce résultat est d'autant plus intéressant qu'il est vrai quelque soit l'échelle choisie pour le potentiel chimique λ des particules marquées, à partir du moment où il reste en-dessous de la limite diluée (qui est l'échelle de l'ensemble des particules). Ainsi, on peut observer l'absence de transition de phase dans tout le régime sur-dilué ; aucun seuil n'apparaît dans l'étude des corrélations au deuxième ordre. La limite de Boltzmann–Grad, dans laquelle se manifeste l'équation de Boltzmann, est donc exactement la bonne échelle pour commencer à voir apparaître des interactions non-triviales entre particules à l'ordre 2 ; et plus généralement à tous les ordres supérieurs, comme le montre le résultat suivant.

En effet, de la même façon, le résultat de grandes déviations, lequel comprend l'information sur tous les ordres de corrélation dans les cumulants sur lesquels il s'appuie, se comporte également sans transition de phase dans la limite sur-diluée. Ces grandes déviations suivent un taux déterminé, comme c'est généralement le cas, par la transformée de Legendre d'une certaine fonctionelle. Cette fonctionelle de grandes déviations est donnée par la limite de la fonction génératrice des cumulants, qui selon notre étude des cumulants dépend uniquement du comportement asymptotique du premier

cumulant, assujeti à l'équation de Rayleigh–Boltzmann linéaire. On montre ainsi que cette fonctionelle satisfait l'équation hamiltonienne discutée dans le sixième chapitre, et peut ainsi être identifiée avec la solution constructive du système de Hamilton–Jacobi associé, qui dans un changement d'inconnues adapté présente une structure très proche de celle de l'équation de Rayleigh–Boltzmann linéaire.

Dans le huitième chapitre, on détaille les arguments géométriques qui justifient que les trajectoires présentant des cycles (c'est-à-dire trop de rencontres rares) sont négligeables asymptotiquement. C'est le résultat qui a été utilisé dans le chapitre 6 pour en déduire la limite des cumulants. Nous adaptons les résultats existant à notre système, en utilisant fortement les estimées déjà prouvées sur les rencontres de particules dans les cumulants. De plus, nous en profitons pour préciser les arguments se trouvant dans la littérature, de façon à en optimiser le résultat quantitatif, se débarassant d'un logarithme pour parvenir enfin à la puissance complète de ε (le diamètre des sphères dures) qu'il est naturel d'attendre d'un tel résultat.

Pour cela, on modifie la disjonction de cas opérée dans la littérature pré-existante, qui repose sur l'histoire passée, dans la pseudo-trajectoire, des particules impliquées dans un cycle. Selon si l'une de ces particules a précédemment été déviée ou non, la paramétrisation du cycle selon les conditions de collisions de la trajectoire varie. Notre nouvelle méthode permet une formule générale de cette paramétrisation qui regroupe tous les cas dans lesquels une particule a subi une déflexion : l'intégration sur les paramètres de la collision associée fait apparaître un petit facteur qui rend cette trajectoire négligeable. Grâce à la généralisation de tous ces cas, le cas non-dévié ne contient pas beaucoup de différentes situations possibles, et alors l'absence de déflexion dans ces dynamiques permet un contrôle bien plus simple des trajectoires correspondantes, et en particulier des singularités qui apparaissent à cause des faibles vitesses relatives entre les collisions. Pour traiter ces singularités analytiquement, nous utilisons des arguments simples et efficaces qui s'appuient sur un choix de coordonnées hypersphériques.

L'avant-dernier chapitre est dédié à la question du temps long et interroge plus précisément les méthodes que nous utilisons, en particulier dans les troisième et quatrième chapitres, dans l'étude des fonctions de corrélation, et qui ne s'appliquent pas directement dans l'étude des cumulants. La première partie de ce chapitre est une discussion sur le rôle de la mémoire de l'histoire passée des trajectoires dans ces méthodes, et sur la façon dont cela se répercute sur la technique d'élagage des dynamique que nous utilisons pour parvenir à des résultats en temps longs, ainsi que sur les bornes a priori qu'elle nécessite.

La seconde partie de cet avant-dernier chapitre est la présentation d'une méthode heuristique permettant de mieux appréhender les obstacles au temps long, en les déplaçant d'une obstruction sur le nombre excessif de collisions, à un blocage dû à la perte de contrôle sur la température du système. Cette heuristique fonctionne dans des espaces $\mathbb{L}^1$, car elle repose sur des arguments de grandes déviations. Au passage, elle permet également de montrer comment de tels résultats de grandes déviations peuvent être exploités, dans un cas largement plus simple que le résultat de grandes déviations que nous montrons dans le septième chapitre.

Au-delà de ces éléments heuristiques, la méthode exposée permet aussi de démontrer des résultats préliminaires qui améliorent encore le taux de convergence des fonctions de corrélation dans un contexte $\mathbb{L}^1$, dans l'optique de se débarasser des constantes pathologiques qui apparaissent dans le quatrième chapitre à cause de la méthode de découpage temporel, pour les ordres élevés de fonctions de corrélation.

Enfin, l'ultime chapitre de cette thèse ouvre sur les perspectives de poursuite de cette étude, et sur les méthodes envisageables pour généraliser certains des résultats qui y sont présentés.

Contents

Chapter 1

Introduction

Figure 1.1: Isaac Newton, James Maxwell, Ludwig Boltzmann, Oscar Lanford

1.1 Historical and mathematical context

One can hardly find the origin of the first sparkle in a human eye, of the first glimpse of curiosity leading in cascade to people getting interested in kinetic theory; so let us start arbitrarily our introduction with the genesis of modern atomic theory. In the scientific effervescence of the European 18th century, the antique idea of Democritus that matter was microscopically composed of elementary particles eventually found a favourable echo. Stemming from the study of various gases, such as nitric oxyde or dioxygen, which were already synthesized at the time, and comparing their pressure, volume and temperature, chemists and physicists among which William Higgins, Louis Gay-Lussac or Robert Boyle emphasized the fact that, when a composite gas is decomposed, its components keep their mass systematically in fixed proportions of the original mixture mass. Based on these observations, John Dalton published in 1808 [22] the theory formalizing the modern molecular perspective, representing gases as molecules composed of atoms, classified in categories of identical properties, and restlessly moving in the void. He was then followed by Amedeo Avogadro, who let his name to the famous constant, and Johann Josef Loschmidt, who paved the way to modern organic chemistry. The latter's work greatly inspired our main character, Ludwig Eduard Boltzmann, who got interested in using the classical equations of celestial movement, known from the 1687 works of Isaac Newton, to describe the microscopic movement of these atoms. From another of his mentors, James Clerk Maxwell, he took the idea of a statistical description of gases, to apprehend the behaviour of an enormous amount of interacting bodies. Eventually, he published in 1872 the famous equation that now bears his name [15], to describe the evolution of the density (in positions and velocities)

of a general class of gases, based on the microscopic collisions of their particles. This work opened the gates of kinetic theory, and to the uninterrupted adventure to which the present thesis humbly belongs.

This Boltzmann equation (presented in (3.1)) is valid for dilute gases, in which the average number of collisions per particle is finite, and in a specific scaling it can be seen as the description of an intermediate mesoscopic step, between microscopic and macroscopic scales: it allowed indeed Sydney Chapman and Thomas George Cowling [21], then Harold Grad [40], to formally derive the equations of fluid mechanics from the classical Newton equations. This issue is part of the sixth of the problems introduced by David Hilbert for the last century, and continues to fascinate the scientific community. The full rigorous derivation, from microscopic particles to hydrodynamics, is still incomplete at the time, yet in the 90s Claude Bardos, François Golse, Dave Levermore and Laure Saint-Raymond mathematically proved [6, 7] the part of the derivation going from the Boltzmann equation to the Navier–Stokes [39] and Euler equations [56]. Because of the time scaling involved in this limit, the full derivation lacks a long time derivation of the Boltzmann equation, despite the recent breakthroughs on this subject. This model is nevertheless very used nowadays, whether in quantitative hydrodynamic simulations [63, 36], in neutronics [62], or even (in a more general setting) to model crowds [5, 43], flocks [23] and opinions [16, 17].

Moreover, back in the 19th century, the Boltzmann equation yielded a deep qualitative understanding of the intrinsic statistical behaviour of fluid matter. Indeed, springing from his equation, Boltzmann introduced the concept of *statistical entropy* as a Lyapunov functional of the particle system, showing that the density of particles irreversibly converges towards an equilibrium on large time scales. This equilibrium is now known as the Maxwellian state, and is very natural to consider: the gas occupies uniformly the available space, and the velocities of the particles are distributed according to the Maxwell Gaussian distribution (see (2.11)), which only depends on the temperature of the system. However, since the microscopic evolution of the gas, from which is derived the Boltzmann equation, follows classical Newton equations in a completely time reversible way, most of Boltzmann's contemporaries got confused from this seeming paradox. In fact, this even appeared as a counterargument to doubt the validity of the atomistic model. The key point to resolve this paradox is to understand that the irreversible quantity encoded in the statistical density and in the entropy, is a measure of our knowledge of the system, which is deeply partial and simply describes the most likely evolution of the gas from a mesoscopic point of view. The understanding of statistics and information theory has been profoundly fueled by Boltzmann's work, and still owes him a lot.

From a mathematical point of view, the rigorous derivation of the Boltzmann equation from the microscopic Newton equations has however waited until 1975 to be proved rigorously by Oscar Erasmus Lanford III [45, 46], in the case of hard sphere interactions, in parallel of the work of Seiji Ukai on the Boltzmann equation [59]. The method that Lanford used is very rigid in the tracking of particles' trajectories, hindering to prove his result for time scales larger than very small times, when only about a fifth of particles have collided. The major obstruction to large time scales is the emergence of correlations between colliding particles. Indeed, Boltzmann's model relies on precollisional independence between meeting particles, but with Lanford's method, the quantitative estimates on the system's chaoticity deteriorate over time, making it impossible to deal with recollisions of particles. Since this short time proof of the derivation, various mathematicians tried to resolve this limitation, first in the 90s with Carlo Cercignani, Reinhard Illner and Mario Pulvirenti [19]. Then a few decades later, in 2013, when Isabelle Gallagher, Laure Saint-Raymond and Benjamin Texier completed the work of Lanford and his former student Francis Gordon King [44], generalizing their proof to the case of compactly supported potentials, and providing in parallel precise quantitative estimates on the convergence rate of the derivation, yet still on short times. And eventually, very recently, Yu Deng, Zaher Hani and Xiao Ma [24] showed that assuming uniform bounds on the regular solutions to the Boltzmann equation, the derivation is valid for long times. Their work relies on a very fine combi-

natorial analysis of the dynamics' geometry and interacting structure. This thesis does not harness their latest methods—yet one could want to use them to extend some of the results presented here to large times—but it exposes the major difficulties and obstructions that they had to overcome to reach large time results.

Fortunately for future researchers, the sixth Hilbert problem still remains to achieve, since the solutions to the Boltzmann equations are not yet understood enough to prove Deng, Hani and Ma's assumptions; and the generalization of this result to different potentials—such as the ones describing the perfect gases—is still an open problem, along with the understanding of the generation of chaos in such systems.

But as a matter of fact, when looking at the behaviour of the gases close to their thermodynamic equilibrium (described by the Maxwellian state discussed above), the statistical stability of the dynamics guarantees a certain amount of chaos over large times, allowing a very strong control of the correlations. In the *Rayleigh gas framework*, describing the behaviour of a small fraction of tagged particles near equilibrium [57], a proof relying on the same ideas as Lanford's yielded the derivation *on large time scales* of a linear version of the Boltzmann equation, called the linear Rayleigh–Boltzmann equation. This was the work of Henk van Beijeren, Lanford, Joel Louis Lebowitz and Herbert Spohn in 1980 [60], later completed with applications to color-changing boundary conditions [47].

Eventually, these estimates led in 2016 to an article by Thierry Bodineau, Gallagher and Saint-Raymond on the convergence rate in the linear case, and its dependence on the long time scaling, so as to infer Brownian hydrodynamic limits [9]. We improved these quantitative estimates on the convergence rates in 2024, introducing an adaptive time cutting [31], that we present with more details in Section 4.6.

Stemming from their work [9], the authors, joined by Sergio Simonella, also studied the symmetric linearization of the Boltzmann equation on long time scales [11, 13], using similar methods along with a well-chosen time cutting, and even precising their study so as to capture rarer dynamics events that are involved in fine correlations between particles. Eventually, they completed this analysis of the fine scales of the dynamics in 2023, describing the finest correlations of the system through its *cumulants* (defined in (5.1)), exhibiting the equations governing the fluctuations of the empirical measure around its expected limit, along with its large deviations [12]. Indeed, they showed that the fluctuation field of the dynamics is described at the limit by a stochastic differential equation, driven on the one hand by a Gaussian process due to the correlations growing in the system, and on the other hand by a linear part corresponding to a linearized Boltzmann equation. For the large deviations, they identified a limit functional describing asymptotically the probability that the empirical measure of the system diverges significantly from its expected limit. This functional is the Legendre transform (as it is usual for large deviations) of the solution to a Hamilton–Jacobi system, where once again the associated Hamiltonian has a Boltzmann-like collisional form. They showed this result for a certain class of functions, which are solution to a certain biased Boltzmann equation, hence not completely different from the Boltzmann solution expected as limit of the empirical measure.

In the present thesis, we perform such a study in the Rayleigh gas setting, where the expected limit of the empirical measure is solution to the linear Rayleigh–Boltzmann equation. We thus refine the first-order statistical limit of the nonideal Rayleigh gas, presented in [9, 31]. The pre-existing model for the Rayleigh gas, containing a single tagged, perturbed particle, did not allow to consider statistical quantities such as the empirical measure, or its fluctuation field, to describe the behaviour of tagged particles. We thus had to introduce a relevant model for this purpose, in which the number of tagged particles goes to infinity with the average number of particles, yet in a vanishing fraction. Most of the particles are initially distributed according to the equilibrium state, and in the low-density regime: for general initial data this scaling leads to the quadratic Boltzmann equation, but perfect equilibrium initial data would make it trivial. Meanwhile, some other tagged particles are initially perturbed from this equilibrium; they need to remain in a more dilute regime, so that their

asymptotic behaviour remains described by the linear Rayleigh setting. The first part of this thesis is dedicated to define this new model, and to describe its first-order statistical behaviour.

We then focus on the fluctuations and large deviations of this system. The corresponding study is based on the analysis of the cumulants, which deeply relies on symmetries of the system, that are guaranteed by the grand canonical ensemble, in which most of the correlations, that could appear because of the number of particles being fixed, vanish. As this model allows to study the statistical behaviour of the perturbed particles, it permits in particular to explore the phase transition around the low-density scaling. Indeed, when looking at the fluctuations of the empirical measure of tagged particles, we show that there is no threshold ahead of this scaling, which is thus the exact regime to consider, to observe the appearance of correlations at the limit. This way, in the limit stochastic differential equation describing the fluctuations of the Rayleigh gas, the only source term is a Gaussian noise due to the correlations with particles at equilibrium, without retroaction of the fluctuation field on itself. For the large deviation principle that we exhibit, the limit Hamilton–Jacobi system that describes the large deviation functional is a linear version of the low-density quadratic case, whose wellposedness can thus be proved in large times.

But, although in the first order study of the Rayleigh gas and of its empirical measure, one can harness the structure of equilibrium to prove long time results, the evolution of cumulants behaves very differently with respect to the proximity with equilibrium, so that the fluctuation and large deviation results that we present in this thesis are still restricted to short times, despite the uniform bounds that we prove on the limit Hamilton–Jacobi system describing these limit cumulants.

Nevertheless, one could consider to apply Deng, Hani and Ma combinatorial method to the statistical results presented in this thesis, to extend their time validity, especially since the hypothesis they make in their method precisely require the uniform bounds of the limit equations, which are satisfied thanks to the linear framework.

Some other contextual elements can be found in each particular section, so that we end here this general introduction. In the following, we announce a detailed plan of this thesis, and also introduce specifically some of its main topics.

1.2 Plan of the thesis

Let us present the different chapters that will henceforth structure this thesis. After the previous historical contextualization, and the present section, our first introducing chapter will give an insight on the linear Boltzmann equations, and on the Rayleigh gas model in which they appear, presenting the novelties due to our mixture setting. The next topic discussed in this introduction will be dedicated to the cumulants, which are complex objects, specifically useful to describe the small statistical scales of our dynamics implied in fluctuations and large deviations. A small section will then introduce the geometrical methods on which rely the whole kinetic derivation. And finally, we will make introducing comments on the large time methods, which will be later completed by the specific Chapter 9.

After this first introducing chapter, we enter the technical details in Chapter 2 and define our new mixture model for the Rayleigh gas, well adapted for statistical descriptions, based on particle tags and a mixture grand canonical description. We also detail the microscopic description of the gas, and the statistical objects used to describe it mesoscopically. The last part of this chapter gives the technical computations to recover the corresponding BBGKY hierarchy for this new model.

Once exposed the microscopic model, we focus in Chapter 3 on the equations describing its limit behaviour. We give some insights on the way the linear Rayleigh–Boltzmann equation (and the Hamilton–Jacobi system that stems from it) appear from the Boltzmann equations and its linearizations, up to the appropriate approximations and change of variable. A precise study of these linear equations is then given, with the study of the collisional operators that drive them, and of their

wellposedness in their specific functional settings.

Thanks to these preliminary results, the first main theorem of this thesis appears in Chapter 4, dedicated to the long time convergence of the correlation functions of the mixture Rayleigh gas, deriving the linear Rayleigh–Boltzmann equation. The proof of this theorem is based on the pseudo-trajectory method due to Lanford, that we adapt to our formalism. Compared to the pre-existing litterature, this new model makes appear new combinatorial difficulties, especially in the proofs of the a priori bounds, essential for the long time derivation. Moreover, we choose to extend the existing long time study to the convergence of all the correlation functions of the system, while only the first one was proved in [9], hence adapting the existing methods to this new result, and to this new model. Eventually, we present in the said chapter the adaptive tree pruning process that allowed us to improve the convergence rates in [31], presenting in detail the method, and even improving the time scaling of our previous paper.

Chapter 5 enters the statistical refinements, defining the cumulants and proving their general basic properties. We introduce a new way of proving the inversion formula on which is based their injectivity, harnessing the combinatorial structure of the decomposition in partitions that allows to define them. We also focus on the general properties of a specific kind of cumulants, appearing in our study as cumulants of the exclusion conditions that define the hard sphere potential. These cumulants benefit from a decomposition in connected graphs, which yields a strong control on them through the *tree inequality*, which we detail along with its proof and the Penrose partition scheme on which it is based. Eventually, we exploit these results on the cumulants to refine our description of the grand canonical quantities, through the analysis of its partition functions. This anaylsis provides in particular a proof for the combinatorial results used in the previous chapter to compute the a priori bounds on the correlation functions.

After this general presentation of the cumulants, the dynamical evolution of the cumulants of the mixture Rayleigh gas is the subject of Chapter 6. This chapter is the most technical, and hence the most detailed. We propose in it a new manner of formalizing the decomposition in dynamics trees of these cumulants, as we adapt their study to the Rayleigh framework. Indeed, we provide an explicit full decomposition which allows to better understand how each component of the pseudo-dynamics is bounded when estimating the cumulants, and what becomes of the limit interactions between these components. This explicit formula also simplifies the way we perform the geometrical control of the dynamics' cycles (see Section 1.5 and Chapter 8). It eventually allows us to compute the limit of the cumulant generating function, which is precisely the functional tuning the large deviation principle for the empirical measure. We show that the evolution of this functional follows a Hamilton–Jacobi equation, which is a linear version of the low-density quadratic Hamilton–Jacobi equation studied in [12]. Through the associated linear Boltzmann–Hamilton–Jacobi system studied in Chapter 3, we prove the wellposedness of this equation, globally on large times. Nevertheless, we can only prove on short times the fact that the cumulants of the Rayleigh gas are indeed asymptotically described by this functional, thanks to which we prove the large deviation principle. As it will be detailed in the following, we lack *a priori* bounds on the cumulants, since their evolution with respect to equilibrium is very different from the evolution of the correlation functions.

In the end, the results from the previous chapter yield the two theorems refining the statistical study of the Rayleigh gas, in Chapter 7: the description of the limit fluctuation field, and the large deviation principle for the empirical measure of the tagged particles. For the proof of these theorems, the intrinsic computations, linked to the dynamics of our mixture Rayleigh gas, are all encoded in the cumulants, whose bounds and convergence are the subject of Chapter 6. Chapter 7 is thus essentially an adaptation of the algebraic calculus presented in [12], to establish the probabilistic results from the convergence of the cumulants. Harnessing the stronger decay of the cumulants of the Rayleigh gas compared to the standard low density gas, we hence highlight the triviality of the limit fluctuation field, on short times, for any regime of tagged particles more dilute than the Boltzmann–Grad scaling.

This result brings out a answer to the foremost question of the intermediate regimes preceding the low density limit, exhibiting the absence of phase transition as the mean free path scales above the order $O(1)$. The only relevant threshold for dilute gases is hence the Boltzmann–Grad scaling, on any statistical scale. On the side of large deviations indeed, the decay of cumulants is such that at the limit, the cumulant generating function only depends on the limit of the first cumulant, which is exactly the limit of the first correlation function, satisfying the linear Rayleigh–Boltzmann equation. The large deviation principle is then governed by a linear Boltzmann–Hamilton–Jacobi system, yielding a broader functional framework than in the quadratic case, and global results of existence for the limit solution.

Chapter 8 is dedicated to the geometric control of the dynamics' cycles. Indeed, the proof of the convergence of the cumulants is based on the microscopic analysis of the billiards dynamics, through the geometry of particles' trajectories and collisions. The key point is to prove that the dynamics can be well approximated by a dynamics without cycle. In fact, this approximating error is often the biggest error, at least in short times, and is thus often the limiting one for the quantitative bounds. We introduce here an optimized method, through a precise case disjunction and an optimal control of the singularities, eventually reaching the full natural approximating error of size ε. This new analysis, which is a completed adaptation of the method from [11], is hence detailed in the said chapter, supported by a few figures illustrating its geometric stakes.

Eventually, since the long time problem is a key question, both for conceptual reasons and for the derivation of hydrodynamic limits, we discuss the various obstacles to the derivation on large times, in Chapter 9. In a kind of meta-analysis of our methods, we start by discarding a wide class of methods doomed to fail, before explaining how the tree pruning method works, from a conceptual and technical point of view, to overcome this difficulty. We naturally then discuss the method used to obtain a priori bounds on the correlation functions, as they are crucial for the tree pruning estimates, and we interrogate the reasons why they do not apply to other objects such as the cumulants. The last part of this epistemological chapter illustrates the techniques at stake in the long time derivation, proposing a heuristic method based on a large deviation argument. More precisely, we present an alternative way of controlling the collision operators, displacing the obstacles to large time derivations from a control of collisions to a control of temperature, to better apprehend this technical difficulty. Moreover, this heuristic method proposes a way to get rid of the big combinatorial factors that appear in the convergence rates of high correlation functions, because we adapted the tree pruning methods to all the correlation functions. For a closer introduction to this method, see Section 1.6.

To conclude this thesis, Chapter 10 opens on some perspectives to deepen the present study, mostly on the long-time analysis of cumulants, proposing different methods to extend Theorems 2 and 3. Additionally, we evoke some further work to better describe the limit cumulant behaviour, or possibly to study the evolution of the cumulants in neighbouring simpler models.

In the end, a notation index gathers the various choices of writings at page 155.

1.3 Linear framework for a Boltzmann collisional study

We introduce here the framework in which linear versions of the Boltzmann equation appear, first presenting briefly the microscopic model, then describing the specificities of the said linear equations.

1.3.1 The Rayleigh gas

The basic microscopic model for gases consists, in the classical description, in a certain number of particles evolving in a given domain, each one of them characterized by its position and its velocity (quantum models also occupy an important part of kinetic theory, see for example [48]). These particles might belong to different categories, among which they are assumed to be identical and

indistinguishable. Their evolution, i.e. the evolution of their positions and velocities, are given by the classical Newton laws, on the basis of a potential of interaction between them. Boltzmann's collisional model is based on localized interactions: localized in space, with a short range of the potential, and thus localized in time, assuming that two particles get quickly away of their range of interaction. These interactions are nonetheless very strong, and each encounter between two particles changes completely their trajectories. This model is the exact opposite of the mean field model, in which each particle interacts with all the others, yet very weakly.

The simplest, and most explicit, of collisional models consists in considering an infinite repulsion of particles when they get closer than a certain distance $\varepsilon > 0$, which thus corresponds to their diameter. This way, when two particles meet, they collide instantaneously, like in an ideal billiards, in any dimension greater than 2. This microscopic model for the particles' interactions, pictured in Figure 1.2, is called the *hard sphere model*. Our thesis only considers this hard-sphere model,

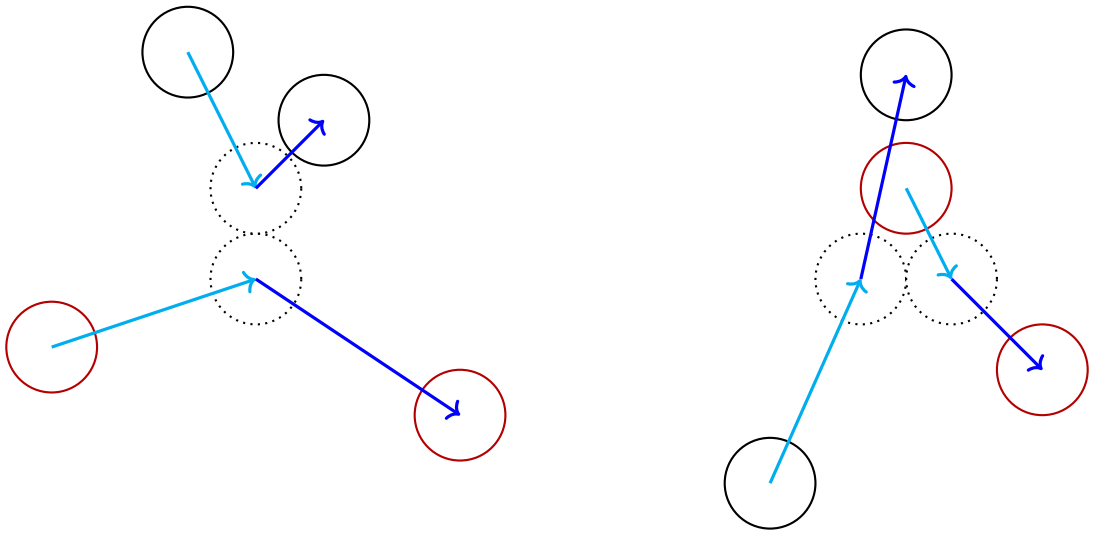

Figure 1.2: Billiards-like collisions of hard sphere particles (colored for clarity)

archetype of Boltzmann's collisional model. Note that the paper by Gallagher, Saint-Raymond and Texier also considers the case of short-range potentials, which does not change deeply the spirit of the proofs, but adds a lot of technical difficulties. In any case, the collisions are always tuned by a diameter parameter, whether the range of the short-range potential or the actual diameter of the hard spheres. The emergence of the Boltzmann equation when the number of particles goes to infinity, and their diameter to zero, depends directly on the scaling between these two quantities. As we will detail in Section 2.3, the relevant parameter to obtain Boltzmann's limit is the *mean free path*, corresponding to the average distance gone through by a particle on a typical time interval. Should the mean free path converge to zero, the particles would eventually get constantly in contact at the limit, which corresponds to the hydrodynamic limit, leading to the equations of fluid mechanics. Should this mean free path converge to infinity, the particles would eventually be so dilute that they would not interact anymore at the limit.

Actually, this thesis can be seen partially as an exploration of this overdilute regime, showing that at any statistical scale it is indeed trivial. The relevant scaling for the Boltzmann equation is hence the one called *low-density* limit, or Boltzmann—Grad limit, in which the mean free path remains of order $O(1)$. Now, the Rayleigh gas historically consists in a gas at equilibrium, taken in this low-density regime, in which a single tagged particle is perturbed away from equilibrium. There is hence a symmetry defect in this model, one particle being considered distinguishable so as to track its trajectory. Actually, this model corresponds deeply with the first modelization of a Brownian

motion: historically, the biologist Robert Brown introduced this rough trajectory to describe the movement of a pollen particle being collided by water molecules at equilibrium. And indeed, it was shown by Bodineau, Gallagher and Saint-Raymond that in the hydrodynamic limit, the Rayleigh gas leads to an actual stochastic Brownian motion for the tagged particle [9].

As we said in the introducing section, the Boltzmann equation takes place on an intermediate mesoscopic scale between microscopic and macroscopic limits. In the case of the Rayleigh gas, in between the tagged particle model and the Brownian motion (which corresponds from a PDE point of view to the heat equation), there is the linear Rayleigh–Boltzmann equation (2.13), which is a linear version of the Boltzmann equation. It is thanks to the structure of the equilibrium and to the linearity of the limit that one was able to prove hydrodynamic limits for this system, since these limits systematically imply a time rescaling that imposes to have long time results in the mesoscopic scale.

In this thesis, we consider a *nonideal* Rayleigh gas, which merely means that all the particles are interacting together, in the most microscopically relevant way. However, as most of the particles are initially at equilibrium, it can be an interesting approximation to suppose that they do not interact one with another; indeed, the reservoir of nontagged particles is such that morally they should all remain at equilibrium, which is globally what happens when they do not interact one with another [47]. This model of *ideal* Rayleigh gas allows to ignore the component of particles that are perturbed in cascade by the tagged particle, component that grows exponentially fast, by assuming that the global equilibrium regulates that perturbation. In this case, as the perturbation does not propagate, the component of perturbed particles grows linearly, as some equilibrium particles meet the tagged one. Thanks to this powerful approximation, Karsten Matthies and Theodora Syntaka were able to get an excellent convergence rate to the solution of the linear Rayleigh–Boltzmann equation, on a very long time scale, using semigroup methods on probability measures weighting the collision trees [50]. Eventually, this model is to compare with the Lorentz gas, in which the particles at equilibrium are completely frozen in a random Poisson distribution, defining a fixed background in which the tagged particle evolves, eventually leading to a kinetic Lorentz equation [38].

Now, the particularity of our nonideal Rayleigh gas model is the fact that the species of tagged particles is not restrained to a single individual. To get a statistical description of the tagged particle, we need to consider a large number of them, so as to deal with their average behaviour and their eventual correlations. This all boils down to consider a mixture gas, composed of two different species, like the composite gases studied by the chemists of our historical introduction. This model has already been studied in short times in the Lanford framework [3], with a canonical description: for each fixed value of diameter ε, the number of particles of each kind is fixed, and both species are scaled in the low-density regime, eventually deriving a mixed Boltzmann equation depending on the ratio between both species. In our case, the tagged particles necessarily have to remain in a subdense regime, if we want to keep a hope of reaching a linear Rayleigh–Boltzmann equation. The fraction of initially perturbed particles, among the ones initially distributed according to equilibrium, hence converges to zero, yet the number of tagged particles still goes to infinity. Moreover, our statistical description, based on the cumulants of the dynamics, is made way more natural in a grand canonical setting: the number of particles of each species follows a Poisson-like law, tuned by two different chemical potentials. This eliminates the correlations appearing between marginals of different orders in the canonical framework, due to the fact that the number of particles is fixed, and that the high marginals thus lose degrees of freedom.

It is thanks to this representation, that we are able to explore the overdilute regime, tuning the chemical potential of the tagged particles close to the low density regime, describing the fine statistical scales of the dynamics, and looking for a possible phase transition. We show on short times that there is no other relevant threshold than the Boltzmann–Grad one (Chapter 7). Nevertheless, in our long time results (in Chapter 4), the non-optimality of the tree pruning method, and of our a priori

bounds, leads to a technical threshold on this chemical potential, which is not to be thought of as physically pertinent.

Eventually, we partially validate the hypothesis made in the study on the ideal Rayleigh gas, showing that at least at the limit, the correlations between particles at equilibrium do not depend on the perturbation. Yet the a priori sub-optimality of our quantitative bounds does not yet allow to quantify precisely the approximation error that is made, due to this simplification.

1.3.2 Studying linear versions of the Boltzmann equation

The general version of the Boltzmann equation (3.1) is composed of a free transport part, and of a source term corresponding to the collisions between the particles. The density of the gas is impacted by the collisions between pairs of particles, each particle being distributed according to the said density, whence the quadratic structure of the collision kernel of this equation. This kernel is usually written in a symmetric form, since both particles are distributed according to the same distribution, but when looking at the linearizations of this equation, it is useful to decompose it into two asymmetric kernels.

More precisely, linearizing this equation consists in writing the equation satisfied by a small perturbation of a reference solution, hence written as a sum, making appear two cross products and a small quadratic remainder (see Section 3.2 for technical details). The two cross products correspond respectively to the collisional influence of the perturbation on the reference solution, and symmetrically to the impact of the reference solution on the perturbation. The quadratic remainder corresponds to the action of the perturbation on itself, but is of a lower order.

This understanding of the linearized operators justifies the fact that the linear Rayleigh–Boltzmann equation (2.13) is only composed of one of these two cross products: indeed, since the fraction of tagged particles is asymptotically negligible compared to the particles at equilibrium, at the limit they have no influence on the particles at equilibrium; the only remaining term is the one corresponding to the impact, on the density of tagged particles, from a collision with a particle distributed according to equilibrium.

Whereas the general functional setting chosen to study the linearized Boltzmann equation is often a weighted $\mathbb{L}^2$-space to harness its symmetry and the self-adjointness of the linearized collision operator (see [19, 11]), in the Rayleigh case this symmetry is broken and we prefer to exploit the a priori bounds yielded in $\mathbb{L}^\infty$. The structure of the initial data, explicitly very close to equilibrium, allows to easily transport over time a domination by this stationary solution (see Section 4.4). This functional setting is similar to the one used for general initial data in the low density regime, leading to the quadratic Boltzmann equation in short times. The mere fact of having a priori bounds allows to obtain long time results through the tree pruning method detailed later.

These considerations concern the derivation from the microscopic dynamics. On the other hand, when studying only the limit equations, having a linear structure also helps obtaining stronger results. Chapter 3 is dedicated to the functional study of the solutions to these linear equations, looking at their wellposedness and bounds. We hence prove that there exists a unique global solution, on large time intervals, to the linear Rayleigh–Boltzmann equation, and to the linear Boltzmann–Hamilton–Jacobi system that appears to describe the large deviations of the empirical measure, both of them sharing a lot of similarities.

Using classical results of kinetic theory, the study of these equations is brought back to the analysis of the linear collision operators that appear in them. These operators can be decomposed into two signed terms, one participating in making the solution grow, and the other helping to make it shrink. The wellposedness of the equation depends on the fact that the first one is controlled enough, and the bounds on the solution (exponential growth or decay) depend on the comparison between both gain and loss terms.

Actually, in our specific case, the bounds on the gain collision operator are highly dependent on the way how the Gaussian Maxwellian weight is distributed, which can be changed by performing a change of unknown in the linear equation. Multiplying the solution by a power of the Maxwellian state lets all the equation invariant, except for the collision operator in which the decay according to the kinetic energy is displaced. Taking directly the operator appearing in the Rayleigh–Boltzmann equation, we show using a quick argument in hyperspherical coordinates that it is not bounded, impeding the usual method to apply. We then secondly remedy to this obstruction through the adequate change of variable that makes appear a collision operator closer to Boltzmann's, for which we succeed to prove a satisfying bound, eventually shifting the functional framework. Figure 1.3 illustrates this shift of the exponential weight in the radial coordinate: the initial integral kernel is concentrated around the velocity norm $|v|$, but multiplying the unknown by the root of a Maxwellian, the kernel is split into the product of two integral kernels, one concentrated around 0 and the other around $2|v|$, so that its integral is eventually bounded as $|v|$ gets large.

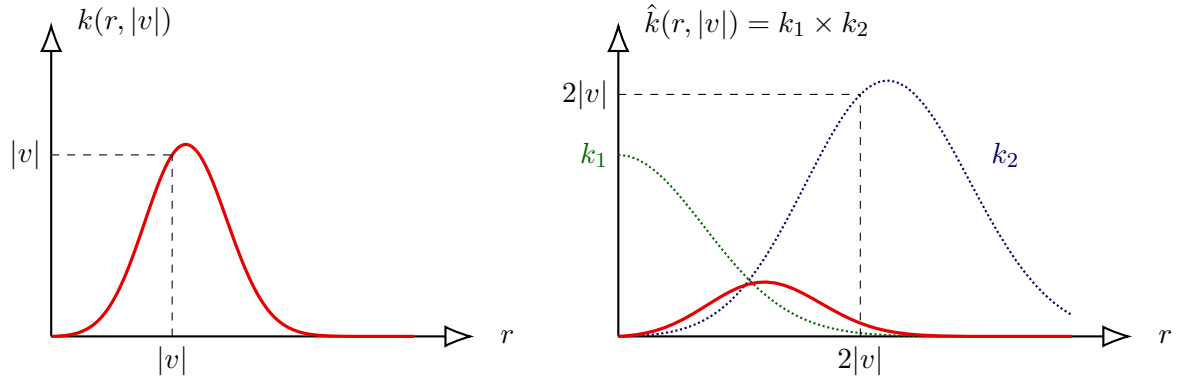

Figure 1.3: Displacing the exponential weights in the collision integral kernel

Note that the main new result that we present is the wellposedness of the linear Boltzmann–Hamilton–Jacobi system (6.38). The solutions to this system do not decay exponentially, because of the observable θ appearing as a gain term. Hence, one can only guarantee a controlled exponential growth on them (unless we assume artificial conditions of smallness on the observable θ). In the precise case where this observable θ is equal to 0, we retrieve the Rayleigh–Boltzmann equation, for which one can harness some elaborate bootstrap method, that we do not detail here, to prove the exponential decay of the solution (see [35, 55]).

Finally, since these global bounds are precisely the hypothesis made by Deng, Hani and Ma for their long time derivation of the Boltzmann equation, one could consider to use their method in the linear case, adapting it to achieve a long time study of the cumulants and eventually proving on large time scales the fluctuation and large deviation results presented in this thesis.

1.4 Statistical study of the empirical measure and cumulants

Let us now introduce the statistical description of gases that we perform, mainly in Chapters 4, 6 and 7. Defining, in Chapter 2, random variables that model the number, tags, positions, and velocities of the particles that compose the gas, we follow the usual probabilistic idea to use observables to characterize their law. Given such an observable, that depends for any particle on its tag, position and velocity, we consider the empirical measure of this observable: this is a random variable that corresponds to the average value of this observed quantity on the whole set of particles.

The first statistical result that we perform is the convergence of this empirical measure, in the sense of square integrable random variables, to a deterministic quantity depending on the chosen

observable and on the solution to the Rayleigh–Boltzmann equation (Corollary 4.1.1). This result, which can be seen as a law of large numbers for the Rayleigh dynamics, is a direct consequence of the convergence of the two first correlation functions. The latter objects are the counterparts of the marginals in the grand canonical ensemble: they project the density of the dynamics on the average behaviour of a certain number of considered particles. There exists an explicit relation (2.19) between these correlation functions and the moments of the empirical measure: the first correlation function describes its expectancy, so that its limit allows to characterize the limit expected value of the empirical measure. To achieve this law of large numbers, it remains to control the limit second correlation function, which describes the asymptotic behaviour of its variance. The long time derivation of the correlation functions is the point of Theorem 1.

To go further than this first statistical result, we naturally want to observe the small fluctuations of the empirical measure around its expected value, in the low density limit. The relevant scaling to observe these fluctuations is the same as for the usual central limit theorem, and we get indeed the convergence in law of this random process to a limit stochastic process in Theorem 2. The foremost observation is the fact that contrary to the usual low density case, this limit process is a trivial Gaussian process that does not depend on any higher scale than the first order Rayleigh–Boltzmann equation, *regardless of the subdense regime* chosen for the tagged particles. Under the mere condition that it is negligible in front of the total number of particles, the correlations between pairs of tagged particles do not influence at all the limit fluctuations.

Finally, to try to capture the finest statistical scales of the dynamics, we get interested in the large deviations of the dynamics, i.e. in the asymptotic decay of the probability for the empirical measure to be far from its expected value. The distance that we choose to formalize this closeness between random processes is the Skorokhod distance, for a specific class of observables that filters the transport part of the dynamics. Indeed, in Theorem 3 we characterize the asymptotic large deviation rate, which corresponds to the rate of the exponential decay of the probability evoked above, thanks to a functional that is identified using Boltzmann-like PDEs. Considering the way we study this large deviation principle, the structure of the associated equation imposes the structure condition chosen for the observable. Like in [12], we show the upper bound for general deviations, which is the most relevant part for applications, but we only show its optimality (proving a lower bound) for a restricted class of deviations, that keep a collisional structure, being solutions to a biased linear Boltzmann equation. The large deviation functional, solution to a linear transport Hamilton–Jacobi equation, is shown to be globally well-posed, contrary to the low density case, where the non-linearity of this equation led to short time results for its wellposedness. However, we only show the large deviation principle on short time, despite the bound on the limit, because of the technical difficulty to control on large times the statistical objects that we harness to describe the fine scales of the dynamics' statistics.

These objects are the *cumulants* of the dynamics. These, like the correlation functions through the moments of the empirical measure, also contain all the statistical information of the system, yet in an alternative way. In fact, what changes is the way the moments are combinatorially adjusted, to encode the fine statistical scales of a nearly independent system. For example, the second cumulant is the difference between the second correlation function and the tensor square of the first correlation function. For independent particles, this quantity would vanish, which is asymptotically the case in our system.

Indeed, a crucial part of Boltzmann's collisional study is the chaoticity of the system, assuming that at the moment when two particles collide, they are independent. This property is taken as initial assumption, and the heart of the proof of the derivation is to propagate this initial chaos estimate. Eventually, the correlation functions evoked above are all shown in Theorem 1 to converge towards tensor products, which correspond to independent random variables.

The cumulants hence allow to identify the defects in the chaoticity of the system, and in the end

to rescale this vanishing defect to characterize its behaviour in a finer way. All of the cumulants are constructed with this idea, the n-th cumulant capturing exactly the defects of independence specific to the n-th and lower correlation functions. And all of the cumulants vanish in a completely chaotic system, apart from the first one that simply is the first correlation function. These objects are hence deeply connected to the measure of correlations in the system.

The beautiful thing when studying the cumulants, and their evolution, is that one can explicitly identify the rare events happening in the dynamics, that contribute to the correlations between particles. In this thesis, it appears through the crucial pseudo-trajectory representation. This formula, on which are based all the derivations of Chapters 4 and 6, allows to express the evolution of correlation functions, and a fortiori of cumulants, according to weighted imaginary trajectories of the particles (see Section 4.2). Summing over all the possible fictional histories that could have led to a given state of the system, one can retrieve the density of the system at any time. Note that it is precisely this summing process that only works on short times.

Let us see now, for instance, how the rare correlations happen in the second cumulant. We look at the state of pairs of particles: the second cumulant is the difference between the sum over pseudo-trajectories, stemming from these two particles and defining the second correlation function, and the ones defining two independent copies of the first correlation function. In the end, most pseudo-trajectories cancel in both sums, and the only remaining ones are those where the trajectories of both particles are connected by a common collision in their history (stemming from the first sum, with a '+' sign), and the ones in which the independent trajectories overlap one another (stemming from the second sum, with a '−' sign). In practice, this decomposition is not exact until the limit, but one can identify the error terms and bound them to show that they vanish asymptotically. Eventually, we show that the n-th limit cumulant is carried by exactly $(n-1)$ of these rare events, called recollisions and overlaps, as pictured in Figure 1.4 for the third cumulant; in this figure, we follow backwards the imaginary history of three given particles, which collide with new ones (numbered 4 and 5). The trajectories on which the third cumulant is supported are the ones implying two of the rare events introduced above (here, a recollision between particles 3 and 5, and an overlap between particles 2 and 3).

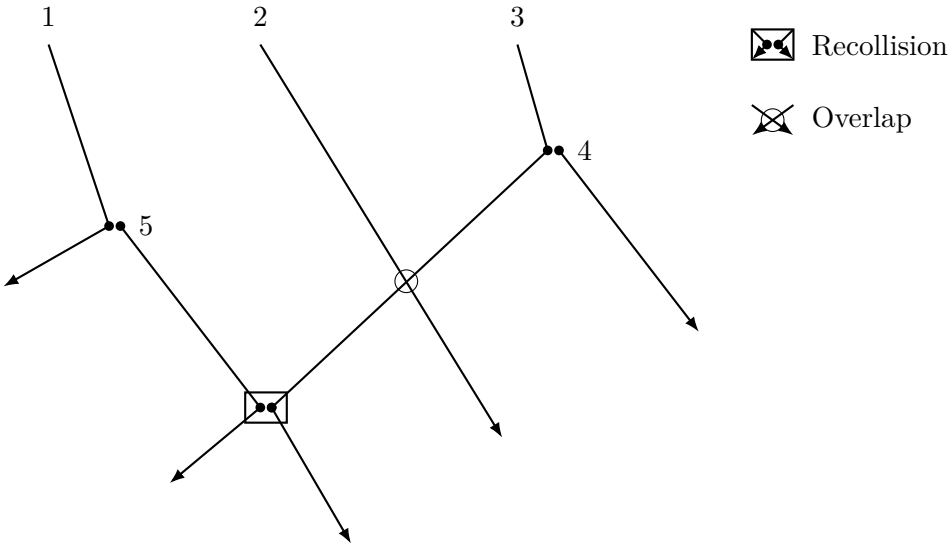

Figure 1.4: Typical pseudo-trajectory supporting the 3rd cumulant

This study is performed through *dynamics trees*, which record all the interactions between particles, and in particular the rare events participating to correlations (see Section 6.4). Decomposing the pseudo-trajectory representation by partitioning according to the associated dynamics tree pro-

vides both a way to bound the cumulants so as to quantify their smallness, based on the rarity of recollisions and overlaps, and a way to characterize their limit. Apart from this construction and the bounds that we prove on this formula, the main difficulty is to eliminate the dynamics graphs containing too many of these rare events: they necessarily contain cycles in their pseudo-trajectories, and cannot be minimally connected as the one in Figure 1.4 is. The elimination of these cycling trajectories is made through geometric methods discussed in the next Section 1.5.

Finally, let us just remark that the two first cumulants are precisely the ones describing the fluctuations of the empirical measure, which hence arise from the correlations between pairs of particles. In our subdense regime, the second cumulant vanishes in the associated scaling, and no 2nd order correlation impacts the fluctuation field. On the other hand, the functional that rates the large deviations is precisely the Legendre transform of the limit cumulant generating function, supported on the rare events that can make deviate the empirical measure from its expected value. As for the fluctuations, only the first cumulant remains at the limit in the case of the Rayleigh gas, yielding a linear equation to characterize the large deviation functional.

1.5 Geometrical methods

The hard sphere model implies dynamics that rely on billiards theory. Even in the case of compactly supported potentials [34], an important part of the computation is based on approximating the dynamics by a collision-like one. This localized model of collisions (instantaneous and local in space) is very rigid and chaotic: shifting a particle's position by a small distance ε can easily avoid a collision, leading to completely different trajectories for the implied particles. Basically, this model is at the opposite of the mean-field methods, in which the interactions are weak and numerous [20].

Nevertheless, one can harness this rigidity through exact geometrical computations close to billiards theory. On the one hand, the exact formula for the collisional cross section (see Section 2.2) can be seen very geometrically: in this thesis, we compute lots of estimates, whose proofs are sometimes difficult to find completely written in the litterature, using hyperspherical coordinates. Introduced in Section 2.2, those coordinates are perfectly adapted to the changes of parametrization of the collisions, through very geometric arguments, and to the calculus of the associated Jacobian (Lemma 2.2.1). They also reveal themselves very useful to find bounds on the linear collision operators appearing in the various versions of the Rayleigh–Boltzmann equation, when studying their integral kernels. Eventually, in Chapter 8, which is the most geometrical part of this thesis, they provide elegant arguments to control the singularities that happen in the analysis of dynamics's cycles, about which we are going to talk right now.

Indeed, as we just wrote, the dynamics is very rigid, and so is Lanford's method to derive the Boltzmann equation: it relies on a very tight control of trajectories of particles (or more precisely pseudo-trajectories, see Section 4.2), and in particular on the fact that these pseudo-trajectories, which contain prescribed collisions, avoid any other collision. These unwanted collisions, which would appear between particles having already collided before, are called *recollisions*, and are directly associated to cycles in the trajectory. When we study the cumulants of the dynamics in Chapters 5 and 6, this notion of recollision is generalized to different kinds of dynamics cycles that we will try to avoid in the pseudo-trajectories we consider (see the discussion on recollisions and overlaps in the previous Section 1.4). To understand this idea of cycle, one can have a look at Figure 1.5, which pictures the most trivial case of recollision: in the dynamics, two particles collide, and one of them is brought back to the other one by a collision with a third particle. This way, two particles, that were already connected through encounters in the dynamics, meet again and thus create a cycle in the dynamics' encounters.

In the rigid method of Lanford, each prescribed collision is parametrized by assigned time and angle of collision. The essential idea in the derivation is to show that the collision parameters leading

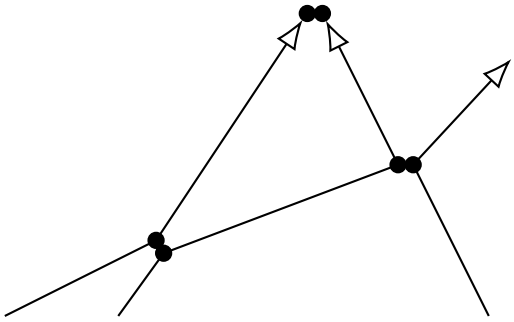

Figure 1.5: A cycle happening in the dynamics

to cycles asymptotically have a negligible impact on the statistics of the dynamics. In fact, through a geometrical study, one can express the algebraic conditions that these parameters should satisfy to generate such a pathological situation, and deduce strong geometrical constraints that will provide smallness on some measure of the set in which they must belong, eventually showing that it vanishes in the limit.

The first full quantitative method to state such a result must be the method used in [34], which is similar in [9]. We use it in Chapter 4, since in the said chapter we adapt the general method of the papers evoked above. The result is stated in Lemma 4.8.3, and can thus be compared to the alternative method that we will discuss below. This method relies first on a bound on the total kinetic energy (allowed by the sub-Gaussian velocity distribution hypothesis), which ensures that the velocities are bounded: this is indispensable to control the particles' dynamics. The second tool is the elimination of the collisions that happen too close in time one from another: indeed, should such a configuration occur, the cone, in which the outgoing velocity must belong to recollide with the particle it just met, would be very wide because of the proximity of the particles. This wideness goes in the opposite direction from the smallness that we want to prove. Eventually, for the same reasons, a lower bound is computed on the velocities so that particles could go sufficiently apart one from another after a collision, for the latter cone to be narrow enough. All of this leads to three approximating parameters $(\mathbf{V}, \delta, \eta)$, which have to be tuned in the conclusion of the derivation. The lack of flexibility of this method provides quantitative estimates which are small powers of ε, when we have the right to expect a convergence in a full power of ε.

Actually, a more subtle method has been introduced in [11], in which the authors made two main observations, to relax the approximating parameters: first of all, should the time between collisions be small, it imposes a strong condition on the encounter times, that provides smallness. This was already the idea used before to justify the fact that the approximation was asymptotically good, yet here they decided to relax these collision times and to integrate over them along with the rest of the parameters: this flexibility optimizes the quantitative result. On the other hand, they observed that the singularities due to small velocities could be resolved by integration over other collision parameters in the dynamics. Indeed, these situations are rare when looking globally at the weighted trajectories. In short, they freed the approximating parameters (δ, η) of time separation and minimum velocity, to integrate over them along with the rest of the computation, eventually leading to a quantitative bound in $\varepsilon|\log\varepsilon|$, very close to the optimal one.

In the first part of this thesis, we use the first non-optimal method to avoid unnecessary technicity, considering moreover that the associated quantitative bound is still smaller than the bigger error due to the tree pruning (despite its adaptive optimization presented in [31] and Section 4.6).

Nevertheless, when studying cumulants in short times (in Chapter 6), we adapt the second better method, improving it to finally reach the optimal bound in a *full power of* ε. This computation relies on a precise geometrical analysis and is presented separately in Chapter 8. Our optimized

computation is based on a finer disjunction of the possible cases that can possibly lead to a cycle in the dynamics. This disjunction is not easy to establish, especially since we need to choose which cases to treat together, adapting the geometric methods to each situation, and obviously considering that we need to treat them exhaustively. The said disjunction is pictured in Figure 8.1 in the corresponding chapter, and allows to generalize as much as possible the arising cases, also to synthesize the proof.

The main idea of the case disjunction is to know over which collision parameters we should integrate to gain smallness. Essentially, if one of the particles involved in the cycle has been deflected sooner in the dynamics, playing with the parameters of this deflection, we reveal a strong retroactive control on these parameters using the cycle condition. Of course, the way how the cycle condition retroactively impacts the integrated parameters depends on the previous history of the dynamics, leading to another case disjunction, yet this latter can be expressed in a quite elegant generalized way, which leads to a common computation. The strength of this first argument is that otherwise, none of the particles has ever been deflected; in this second case, one can directly harness the initial density to describe the velocities!

This simplifies greatly the study of the singularities evoked above, due to small velocities, especially the one implying a sinus, since this one only occurs in the non-deflected case. Nevertheless, we also control the singularities in the deflection case, once again harnessing the hyperspherical coordinates to gain clarity in the arguments, and to utilize as much as possible the geometric structure of the trajectories.

Note eventually that compared to [11], we also free the approximating parameter $\mathbf{V}$ bounding the total kinetic energy, including it in the global integration process, hence finalizing the method that they started to impulse.

1.6 Long time derivations

The question of the long time derivation of the Boltzmann equation has been partially resolved quite recently by Deng, Hani and Ma [24]. Their method combines the usual geometric study of the billiards dynamics with combinatorial results such as the Burago lemma [18], yielding quantitative estimates on the large clusters of recollisions. Then they compute in a very subtle way a combinatorial algorithm of integration on the variables driving the dynamics, to discard the pathological trajectories that imply correlations between several time layers. That eventually allows them to compare the solution of the Boltzmann equation with a well-chosen ansatz close to the original dynamics, propagating good estimates on the defects of independence. For an overview of their computation, see for example the presentation of their paper by Bodineau, Gallagher, Saint-Raymond and Simonella [14].

Before this result, the Lanford theorem for the derivation of the Boltzmann equation was restricted to small times. In some linearized frameworks presented in Chapter 3, the proximity to equilibrium allowed to preserve enough structure and bounds to perform a derivation in large times, as it is the case in our Rayleigh setting. Our study did not need to use their industrious computations, thanks to the a priori bounds discussed in Section 9.3, yet it gets confronted to the same obstacles they had to overcome.

The first one is the necessity of devising a method that takes into consideration the history on the whole considered time interval, when one could want to simply try to restart the Lanford method on independent time layers, provided good enough bounds. Nevertheless, we show by a small argument based on the irreversibility of the limit solution, that such a method is doomed to fail (see Section 9.1).

The other big difficulty is then to guarantee enough chaoticity in our system. In our situation, this is explicitly the question of proximity to the chaotic equilibrium that is at stake, in the form of the *a priori* bounds. Indeed, these bounds are precisely obtained using the fact that the general dynamics preserves the structure of the closeness to equilibrium that we chose, which is simply a multiplication by a small perturbation. This way, one can assert that *at any time*, the correlation

functions are dominated by a good stationary state, with explicit bounds. Now, the reason why this reasoning works is precisely why we cannot obtain such bounds on the cumulants. Uniform a priori bounds on the cumulants would mean a very strong control on the chaoticity of the system over time, yet the sense in which we choose to be *close to equilibrium*, which eventually leads to the Rayleigh-Boltzmann equation, does not behave as well with the equations governing the cumulants. Indeed, the hierarchy on the cumulants (6.5), in addition to being non-linear, rely on fine cancellations that are completely lost when bounding crudely using the triangle inequality (see Section 9.3). In the case of specific cumulants, such as the cumulants of the exclusion (see Section 5.3), using the structure of the connected graphs that support them provides strong bounds without losing too much from the absolute values, but the general cumulants of the Rayleigh dynamics do not have such a structure. This is the reason why the first part of this thesis on the convergence of the correlation functions, is performed for long times, and not the second part on the convergence of the cumulants, which remains restricted to short times.

Let us now have a word about the *pruning method*, presented in Section 4.6 and further discussed in Section 9.2, which is precisely the method allowing to reach large time results from a priori bounds. The central idea is to control the number of collisions on each small time interval, so as to keep long lasting bounds on the pseudo-trajectory expansion of the correlation functions, on which is based the derivation. It relies on the argument that the probability of having a lot of collisions on a small time interval is small, so that we want at once to compute this method with short intervals; but not too short, so as to cover long times.

Technically, this probability appears through the weights associated to each pseudo-trajectory. When one computes an iterated Dyson expansion, the bounds on the implied operators depend on the number of collisions that are present in their associated trajectory's history. These bounds are downgraded as time goes, since the number of collisions grows. A naive solution would be to reduce the size of the time intervals accordingly, but this would force their series to converge very quickly, when we want it to diverge so as to cover large times. In the calculations, the tree pruning consists in putting aside of the expansion the bad factors depending on the number of collisions, to keep the time interval lengths independent from them. Doing so, one needs to keep this big factor controlled, hoping to compensate it with a source of smallness. We thus impose a subexponential growth of the number of collisions on each time interval, and discard the other trajectories in a pruned-out term. In the main term, the bad factor will be compensated by the initial proximity of the distribution; in the remainder, it will be compensated by the small probability of having a lot of collisions on small intervals. This pruning process is illustrated in Figure 4.3.

The first pruning process used to show the long time derivation of the Rayleigh–Boltzmann equation was performed in [9], using a uniform time cutting. The idea that we present in this thesis, to improve greatly the convergence rate of this derivation, is to consider an adaptive time cutting, where the length of the time intervals depends on the number of collisions imposed within. This way, constructing scale-similar intervals containing a number of collisions adapted to their length, in a scaling that is common to all, allows to distribute uniformly the error due to the pruning term, eventually getting rid of almost two logarithms that slowed the convergence rates (see the discussion around Theorem 1).

Finally, we would like to introduce an original perspective that appeared in our attempt to improve the time scaling, and quantitative convergence rates, of the long time derivation of the correlation functions. This method, exposed in Section 9.4, displaces the obstruction to long time from the control on the number of collisions, to a loss of control on the temperature, which are the two main moral limitations that prevent from having bounds on large times. This way, the latter method explains how these limitations can be thought of as competing one with the other. Eventually, the displacement of obstruction allows to gain on the dependency of the quantitative estimates along the rank of the correlation functions, getting rid of the factor n^{cn} that appears in the bound for the n-th

correlation function in Theorem 1.

However, this method only works in an $\mathbb{L}^1$ setting, instead of the $\mathbb{L}^\infty$ results that we present in Chapter 4, since it relies on a large deviation argument. In an adequate twist of fate, it also illustrates to what end might be employed the large deviation results, as the one we prove in Section 7.4. For all these reasons, we present this heuristic proof, even if it is not exhaustive. It relies on the idea that if the velocities are not concentrated around 0, the Gaussian weight in the Maxwellian state, which initially dominates our density, provides a strong bound thanks to the kinetic energy being high enough. Doing so, we emancipate ourselves from the Cauchy–Schwarz method that provided a bad dependency on the number of collisions, but this new method depends more steeply on the temperature of the system (which rates the decay according to the kinetic energy): the obstruction is thus displaced.

Moreover, we have to justify that the velocities do not concentrate around 0, which looking at the collision operators in $\mathbb{L}^1$ corresponds to a probability of large deviations: for velocities expected to behave according to a Gaussian distribution, a realization in which an abnormal fraction of them concentrates on small values constitutes a deviation from the expected density (such a situation is pictured in Figure 1.6).

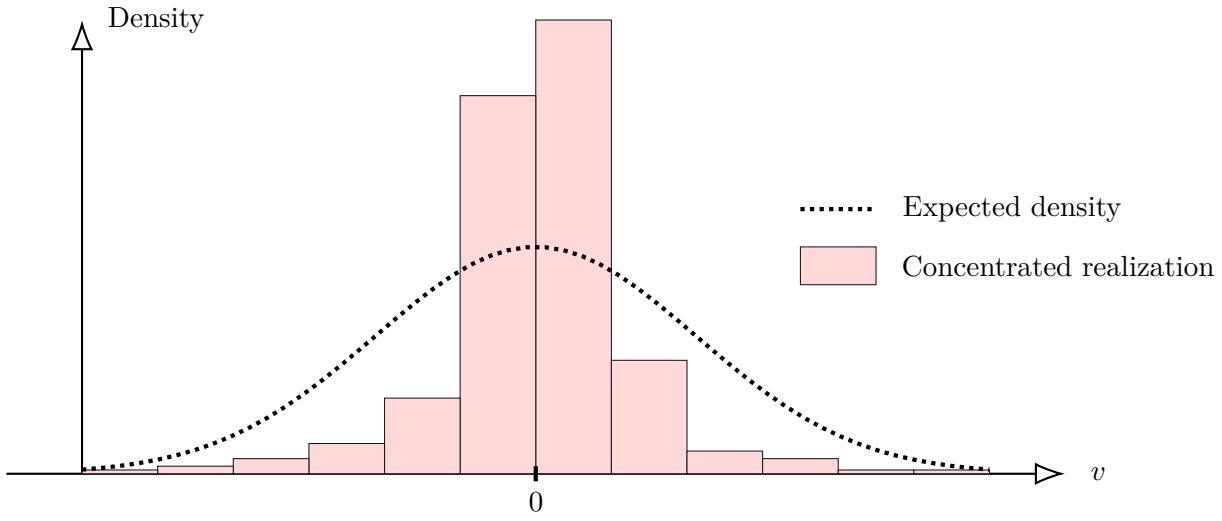

Figure 1.6: An example of large deviation for the velocity Gaussian distribution

For realizations containing a large number of particles, the probability of such an event to occur is precisely described by an explicit large deviation principle (corresponding here to the one of a binomial law). This probability hence decays exponentially fast with respect to the number of particles, with an explicit rate. Note that this method works in $\mathbb{L}^1$, and only for large values of implied particles. Two solutions might be considered to solve the latter problem: the first one is to get rid of the bad bounds due to the big number of particles only when this number of particles is indeed too big, using in particular a refinement of the usual Stirling estimate, keeping the large deviation argument only for these cases. The other, simpler solution is to bring down the information from the high marginals to the lower ones, yet it also requires some adjustements, as the reader will notice if he browses the technical details.

Chapter 2

The nonideal Rayleigh gas as a symmetric mixture model

We enter now the technical details. This section is dedicated to presenting the framework we work with: the classical hard sphere model at microscopic scale, and its statistical description close to equilibrium in a Rayleigh setting. More precisely, we expose how we chose to model an unbalanced mixture in the grand canonical ensemble, introducing our tagged model, which in this chapter is the most specific part to this thesis. Eventually, we define all the statistical objects whose study constitutes the core of our results.

Sections 2.2 and 2.6 are more technical and prove respectively the changes of scattering parametrization, and the foremost BBGKY hierarchy for the setting we concentrate on.

2.1 Microscopic hard sphere model

Microscopically, we consider the hard sphere model, which resembles a perfectly elastic d-dimensional billiards. The state of a gas of N particles is completely determined by the positions (in the d-dimensional torus $\mathbb{T}^d$) and the velocities of every particle, represented by the vector

$$\underline{z}_N = (z_1, \dots, z_N) \doteq (\underline{x}_N, \underline{v}_N) \in \mathcal{D}^N \doteq (\mathbb{T}^d \times \mathbb{R}^d)^N.$$

The *hard sphere* model consists in an exclusion condition, which states that two particles cannot get closer than a certain diameter $\varepsilon > 0$: the positions have to belong to the *hard sphere exclusion set*

$$\mathcal{X}_N^\varepsilon \doteq \{\underline{x}_N \in \mathbb{T}^{dN};\ \forall\, i \neq j,\ d(x_i, x_j) > \varepsilon\}, \tag{2.1}$$

where $d(\cdot,\cdot)$ denotes the distance on the torus; and hence the state of the gas $\underline{z}_N$ must belong to the open domain $\mathcal{D}_N^\varepsilon \doteq \mathcal{X}_N^\varepsilon \times \mathbb{R}^{dN}$.

Within this set, the particles evolve in straight line and their dynamics is hence given by the Newton equations for uniform line movement: for any $i \in [\![1, N]\!]$,

$$\frac{\mathrm{d}x_i}{\mathrm{d}t} = v_i, \qquad \frac{\mathrm{d}v_i}{\mathrm{d}t} = 0.$$

Conversely, on the boundary of $\mathcal{D}_N^\varepsilon$, we have for at least two particles (let us say i and j) the condition $d(x_i, x_j) = \varepsilon$: they collide. In the case where the scalar product $(x_i - x_j) \cdot (v_i - v_j)$ is positive, it means that the particles are exiting the collision in uniform line movement. Otherwise, they are entering the collision and must scatter (see Fig.1.2 and the following Section 2.2) according to the

following system giving the post-collisional velocities (v_i', v_j'):

$$\begin{cases} v_i' = v_i - \left\langle v_i - v_j, \dfrac{x_i - x_j}{\varepsilon} \right\rangle \dfrac{x_i - x_j}{\varepsilon} \\ \\ v_j' = v_j + \left\langle v_i - v_j, \dfrac{x_i - x_j}{\varepsilon} \right\rangle \dfrac{x_i - x_j}{\varepsilon}. \end{cases} \tag{2.2}$$

In the hard sphere case, the interaction is taken instantaneous and elastic: the system above (2.2) stems from the preservation of momentum and kinetic energy, knowing that the exchange of momentum between the particles is carried by the normal to the hard spheres. Indeed, the velocities simply switch their component along this normal.

This dynamics is well-defined up to a zero measure set of initial configurations, in which infinite amounts of collisions might happen in finite times, along with collisions between more than two particles at a time. This result was proved by Roger Keith Alexander [1], and might also be found in [34]. Some other models use non-instantaneous scattering governed by potentials of interaction that can be short-range [34] or long-range [25, 4]. The review by Cédric Villani [61] gives a global overview of collisional kinetic theory.

2.2 Scattering parametrization

The scattering system (2.2) can be parametrized by either one of the following angles,

$$\omega \doteq \frac{x_i - x_j}{\varepsilon} \quad \text{or} \quad \sigma \doteq \frac{v_i' - v_j'}{|v_i' - v_j'|}. \tag{2.3}$$

The angle ω, conditioned for the scattering by the relation $\omega \cdot (v_i - v_j) < 0$, is especially relevant to picture geometrically the exchange of momentum between the particles, in their physical dynamics (see Fig. 2.1).

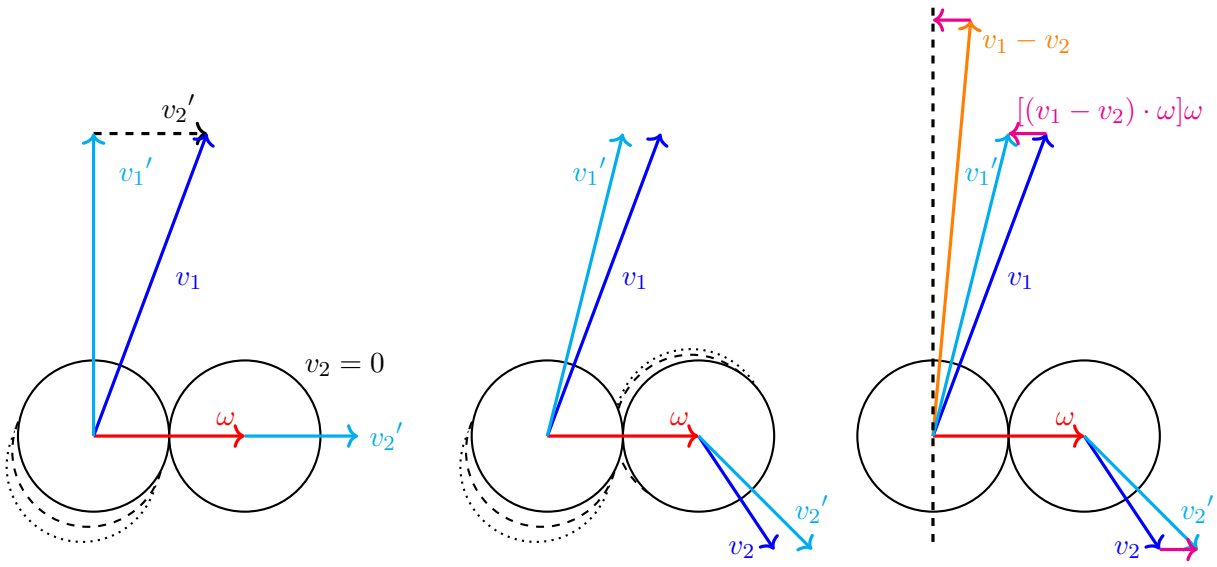

Figure 2.1: Geometric representation of pre- and post-velocities,
from left to right: case $v_2 = 0$, general case, detailed geometric construction

On the other hand, in terms of the scattering angle σ defined above (2.3), denoting $(v, w) \doteq$

(v_i, v_j), the scattering system (2.2) is equivalent to

$$\begin{cases} v' = \dfrac{v+w}{2} + \sigma \dfrac{|v-w|}{2} \\ w' = \dfrac{v+w}{2} - \sigma \dfrac{|v-w|}{2}, \end{cases} \tag{2.4}$$

where σ hence stands for the direction of the deviation with respect to the mean velocity. Since (v, w, v', w') are in the same plane, σ and ω also belong to this same plane (see Fig. 2.2). Thus, we might reduce their dependency to the 1-dimensional circle, where the following holds

$$\sigma = \pi - 2\omega,$$

σ going through the full circle, and ω through the half-circle: at fixed velocities u, v, we denote $\mathbb{S}^{d-1}_-$ the half-sphere that ω ranges, under the condition $(v_i - v_j) \cdot \omega < 0$.

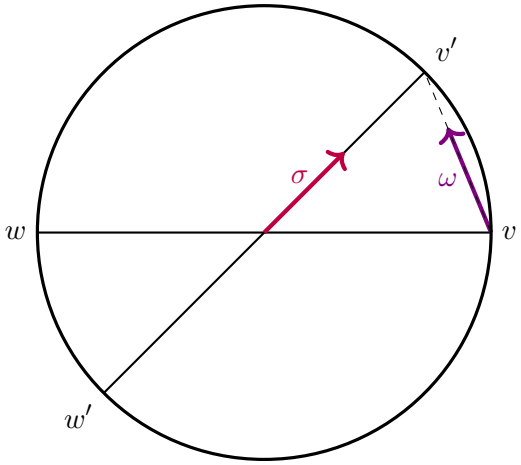

Figure 2.2: Deflection parameters in the velocity space

Throughout this thesis, integrals on the scattering angles will appear, and it will be quite useful to be able to switch from one variable to another, which we will do considering the following formula.

Lemma 2.2.1 (Change of scattering angle)**.** *For any measurable function f, one has*

$$\int_{\mathbb{S}^{d-1}_-} f(\omega)\langle \omega, u\rangle \mathrm{d}\omega = \frac{|u|}{4} \int_{\mathbb{S}^{d-1}} f(\omega)\mathrm{d}\sigma. \tag{2.5}$$

The proof that we give of this lemma, along with other technical results, relies on the *hyperspherical coordinates*, based on the following parametrization of the sphere $\mathbb{S}^{d-1}$:

$$\begin{pmatrix} \cos\theta_1 \\ \sin\theta_1 \cos\theta_2 \\ \vdots \\ \sin\theta_1 \dots \sin\theta_{d-2} \cos\theta_{d-1} \\ \sin\theta_1 \dots \sin\theta_{d-2} \sin\theta_{d-1} \end{pmatrix}, \begin{cases} (\theta_i)_{1\le i\le d-2} \in [0,\pi]^{d-2} \\ \theta_{d-1} \in [0, 2\pi], \end{cases} \tag{2.6}$$

with Jacobian $\sin^{d-2}\theta_1 \sin^{d-3}\theta_2 \dots \sin\theta_{d-2}$.

Proof. Let us denote $u = w - v$ the precollisional relative velocity. We want to change the variable $\omega \in \mathbb{S}^{d-1}_-$ into $\sigma \in \mathbb{S}^{d-1}$ in the following integral, written in hyperspherical coordinates

$$\int_{\mathbb{S}^{d-1}_-} f(\omega)\langle \omega, u\rangle \mathrm{d}\omega = \int f(\omega)|u| \cos(\theta_{d-2}) \sin^{d-2}\theta_1 \sin^{d-3}\theta_2 \dots \sin^2\theta_{d-3} \sin\theta_{d-2}\ \mathrm{d}\underline{\theta}_{d-1},$$

where the $d-2$ first angles $(\theta_i)_{i\leqslant d-2}$ range $[0,\pi]$, and θ_{d-1} ranges $[0,2\pi]$. Thus, choosing the angle $\theta \doteq \widehat{(u,\omega)}$ as θ_{d-2}, the half-sphere that ω ranges corresponds to $\theta \in [0,\pi/2]$. In Fig. 2.2, one can see that $\widehat{(u,\sigma)} = \pi - 2\widehat{(u,\omega)}$, so that we will compute the natural change of variable $\theta = (\pi-\phi)/2$. Denoting $\check{\theta} = (\theta_1, \dots, \theta_{d-3}, \theta_{d-1})$, we get by trigonometry formulas that

$$\begin{aligned}
\int_{\mathbb{S}^{d-1}_-} f(\omega)\langle \omega, u\rangle \mathrm{d}\omega &= \int_0^\pi \int f(\omega)\frac{|u|}{2} \sin\left(\frac{\phi}{2}\right)\cos\left(\frac{\phi}{2}\right) \sin^{d-2}\theta_1 \sin^{d-3}\theta_2 \dots \sin^2\theta_{d-3}\ \mathrm{d}\check{\theta}\mathrm{d}\phi \\
&= \int_0^\pi \int f(\omega)\frac{|u|}{4} \sin(\phi) \sin^{d-2}\theta_1 \sin^{d-3}\theta_2 \dots \sin^2\theta_{d-3}\ \mathrm{d}\check{\theta}\mathrm{d}\phi \\
&= \frac{|u|}{4}\int_{\mathbb{S}^{d-1}} f(\omega)\mathrm{d}\sigma,
\end{aligned}$$

which concludes the proof. □

2.3 Statistical description of the gas

When the number of particles N enlarges, this hard sphere dynamics becomes very difficult to compute, especially because it is very chaotic. Indeed, a small shift of a particle might prevent a collision, which would strongly change its trajectory and cause a macroscopic change in the dynamics. For this reason, we choose to describe the gas statistically. In this thesis, we study a gas of identical particles, yet divided in two distinguishable parts, represented by tags $\underline{\ell}_N = (\ell_1, \dots, \ell_N) \in \{0,1\}^N$: the tag $\ell = 0$ will be attributed to particles initially distributed at thermodynamic equilibrium, and the tag $\ell = 1$ to 'tagged' particles initially perturbed from that equilibrium.

At fixed $N \in \mathbb{N}$ and $\varepsilon > 0$, we consider $W_N^\varepsilon(t, \underline{z}_N, \underline{\ell}_N)$ the *canonical* probability density of presence of particles with tags $\underline{\ell}_N$ on the phase space $\mathcal{D}_N^\varepsilon$ at time $t \geq 0$: by exchangeability, it is invariant by permutation among particles with identical tags. The microscopic dynamics, defined by the Newton equations, provides the Liouville transport equation for W_N^ε within $\mathcal{D}_N^\varepsilon$

$$\partial_t W_N^\varepsilon + \underline{v}_N \cdot \nabla_{\underline{x}_N} W_N^\varepsilon = 0. \tag{2.7}$$

The solutions to this equation are provided by the method of characteristics and expressed in terms of the initial distribution $W_N^\varepsilon(0)$ and of the transport going *back in time*: as long as the positions of the particles remain in the hard sphere exclusion open domain $\mathcal{X}_N^\varepsilon$, using the method of characteristics one can indeed write for any time interval $\delta t > 0$, that

$$W_N(t, \underline{z}_N) = W_N(t - \delta t, \underline{x}_N - \delta t \cdot \underline{v}_N, \underline{v}_N).$$

On the boundary of the domain $\mathcal{D}_N^\varepsilon$, to pursue the backwards characteristics and transport back the density until time 0, we need the following boundary condition when two particles emerge from a collision:

$$d(x_i, x_j) = \varepsilon \text{ and } \langle x_i - x_j, v_i - v_j\rangle > 0 \quad \Rightarrow \quad W_N^\varepsilon(\underline{z}_N) \doteq W_N^\varepsilon(\underline{z}_N^\star), \tag{2.8}$$

where $\underline{z}_N^\star = (z_1, \dots, x_i, {v_i}^\star, \dots, x_j, {v_j}^\star, \dots, z_N)$ denotes the *pre*-collisional state associated to $\underline{z}_N$. Note that by reversibility, the formulas for $(v_i^\star, v_j^\star)$ are the same as for (v_i', v_j').

Note that in reality, in our model the trajectories are deterministic, so that the randomness of this statistical description only stems from the initial condition $W_N^\varepsilon(0)$, and the density $W_N^\varepsilon(t)$ depends

on it in a deterministic way. In Section 2.4, we present the initial distribution associated to the nonideal Rayleigh gas, in a mixture framework, that we introduced in [32]. Eventually, notice that the particles are exchangeable at the condition to also exchange their tags, which appears in the symmetry of the canonical densities:

$$W_N^\varepsilon(z_1,\ell_1,\dots,z_i,\ell_i,\dots,z_j,\ell_j,\dots,z_N,\ell_N) = W_N^\varepsilon(z_1,\ell_1,\dots,z_j,\ell_j,\dots,z_i,\ell_i,\dots,z_N,\ell_N). \tag{2.9}$$

In the previous litterature, the Rayleigh gas essentially contained a single tagged particle. The grand canonical ensemble consists in randomizing the number N of particles to a random variable $\mathcal{N}$, the expectancy of which is tuned by a parameter μ called the *chemical potential* (see Section 2.4). The kinetic limit that we consider is called the *low density limit*, or Boltzmann–Grad limit, and consists in letting this chemical potential μ go to infinity while keeping a constant mean free path

$$\mathrm{MFP} \doteq \mu^{-1}\varepsilon^{1-d} = 1, \tag{2.10}$$

so that the particles' diameter ε goes to 0. The *mean free path* corresponds to the average distance gone through by a particle between two collisions. It is computed such that the cylinders corresponding to the route of the particles between collisions (Fig. 2.3) cover the whole available space (of volume 1). Since the volume of these $\mathcal{N}$ cylinders is proportional to $\varepsilon^{d-1}\times\mathrm{MFP}$, up to multiplicative constants we retrieve the mean free path formula (2.10).

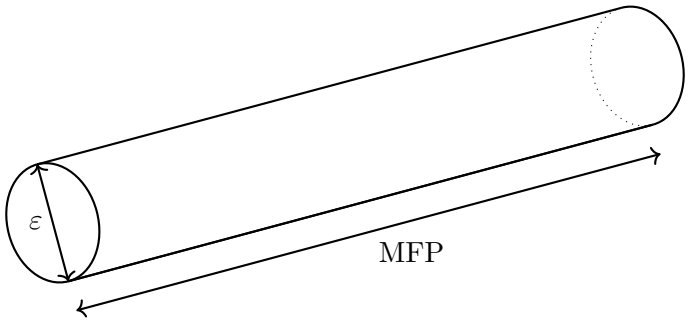

Figure 2.3: The mean free path as height of a particle's route cylinder between collisions

In the low density limit, assuming initial chaos, the first marginal of the density usually converges to the solution of the Boltzmann equation [34, 24]. We discussed in the introduction that this solution to the Boltzmann equation, studied by Boltzmann and Maxwell, when well defined, relaxes in large times to an equilibrium called the *Maxwell state* and defined [15] as

$$M_\beta(x,v) \doteq \left(\frac{\beta}{2\pi}\right)^{d/2} \exp\left(-\frac{\beta}{2}|v|^2\right). \tag{2.11}$$

The parameter β stands for the inverse temperature of the system, tuning its intensive (kinetic) energy. It appears that the density $M_\beta^{\otimes N}\mathbb{1}_{\mathcal{D}_N^\varepsilon}$ is an equilibrium of the microscopic hard sphere dynamics: the *nonideal Rayleigh gas* model [57] consists precisely in considering specific initial conditions that are close to this thermodynamic equilibrium, to retrieve a *linear version* of the Boltzmann equation, whose theory is much simpler and hence might be derived for long time scales. More precisely, we will consider a gas at equilibrium, in which a subset of tagged particles are perturbed from equilibrium, breaking the particles' exchangeability. In the case of a single tagged particle, the derivation of a linear equation has been shown [9, 31] when choosing the following perturbation of equilibrium as initial state

$$W_N^\varepsilon(0,\underline{z}_N) = \frac{\mathbb{1}_{\mathcal{X}_N^\varepsilon}(\underline{x}_N)}{\mathcal{Z}_N^{\varepsilon,\mathrm{c}}}\rho(x_1)M_\beta^{\otimes N}(\underline{z}_N), \tag{2.12}$$

for $\rho \in \mathcal{C}(\mathbb{T}^d)$ a continuous space perturbation on the torus, and $\mathcal{Z}_N^{\varepsilon,\mathrm{c}}$ a normalization constant. Indeed, in the Boltzmann–Grad limit, the first marginal of W_N^ε behaves like the solution $g \doteq M_\beta \varphi$ to the linear *Rayleigh–Boltzmann equation* [9] with initial condition ρ:

$$\left\{ \begin{array}{rcl} \partial_t \varphi + v \cdot \nabla_x \varphi & = & \displaystyle\int_{\mathbb{S}^{d-1}} \int_{\mathbb{R}^d} [\varphi(v^\star) - \varphi(v)] M_\beta(v_c) \langle \omega, v_c - v \rangle_+ \mathrm{d}v_c \mathrm{d}\omega, \\ \varphi(0,x,v) & = & \rho(x). \end{array} \right. \tag{2.13}$$

This linear equation (2.13) is globally well-posed in the velocity-weighted space $\mathbb{L}^\infty_x \mathbb{L}^\infty_v(M_{\beta/2})$ (see Chapter 3, Section 3.3.3), and allows to derive the linear heat equation in the hydrodynamic limit [9].

Some partial results exist for this same model with long-range interactions instead of hard sphere collisions [25, 4], yet the complete derivation of the Rayleigh–Boltzmann equation for general potentials is still an open problem. Other ways to derive the linear Rayleigh–Boltzmann equation for long time scales are the *ideal* Rayleigh gas model, in which the particles at equilibrium do not interact among themselves [30, 49, 51], and the Lorentz gas model, which consists in letting a tagged particle evolve in a frozen random background [58, 19, 38].

2.4 Grand canonical framework for the tagged mixture

As introduced in the previous section, we want to study the behaviour of an arbitrary large subset of tagged particles perturbed away from equilibrium, whose density will follow a linear version of the Boltzmann equation, that we call the Rayleigh–Boltzmann equation (2.13). This derivation has been studied in the case of a finite set [9, 31], but to provide extended statistical results on this gas we hereafter take its size diverging to infinity, yet remaining a tiny fraction of the gas. Our statistical study is based on an analysis in cumulants (see Section 5.1), that highly relies on the symmetry of the system. Hence, to preserve the symmetric structure of the objets that we consider, we work in the grand canonical ensemble and introduce an additional tagging variable, indicating to which set each particle belongs. Each particle is randomly assigned a tag, so that all of them are statistically identical. This approach to describe a gas mixture is different from the canonical one, used by Ioakeim Ampatzoglou, Joseph K. Miller and Nataša Pavlović in their article deriving a mixed Boltzmann equation [3]; indeed their description is made in the canonical ensemble, at fixed numbers of particles of each kind.

The particles at equilibrium are taken in the usual low density (Boltzamnn–Grad) limit, whereas the tagged perturbed particles only occupy a tiny fraction of the gas, smaller than the Boltzmann–Grad density: otherwise indeed they would behave like a classical Boltzmann dilute gas, satisfying the non-linear Boltzmann equation (3.1). This all boils down to the following scaling,

$$\mu \varepsilon^{d-1} = 1 \quad \text{and} \quad 1 \ll \lambda \ll \mu, \tag{$S_{\varepsilon,\mu,\lambda}$}$$

where $\mu > 0$ corresponds to the chemical potential of the particles at equilibrium, and $\lambda > 0$ to that of tagged particles. The notation $\lambda \ll \mu$ simply means that $\lambda \mu^{-1}$ goes to 0, as λ and μ go to infinity. Formally, **the particles at initial equilibrium will be tagged with a 0, and the initially perturbed 'tagged' particles will be tagged with a 1**. The tags of all particles hence form a vector $\underline{\ell}_n \in \Lambda_n \doteq \{0,1\}^n$, identified to the corresponding subset $\underline{\ell}_n \subset [\![1,n]\!]$, with the following notation

$$|\underline{\ell}_n| = \|\underline{\ell}_n\|_1 = |\{i \leq n \ , \ \ell_i = 1\}| \quad \text{and} \quad \varphi_0^{\otimes \underline{\ell}_n}(\underline{z}_{\underline{\ell}_n}) = \prod_{\substack{i \leqslant n \\ \ell_i = 1}} \varphi_0(z_i).$$

Moreover, instead of ρ a perturbation happening in space only, as in [9], we will hereafter consider an initial perturbation $\varphi_0 \in \mathbb{L}^\infty_x \mathbb{L}^\infty_v(M_{\beta/2})$ also happening in velocities. Now, we introduce the

mixed grand canonical ensemble, which consists in relaxing the number of particles, weighting it with a mixed Poisson law depending on the number of tagged particles. More precisely, at fixed λ, and $\mu = \varepsilon^{1-d}$, we take the following weighted canonical initial densities

$$W_n^\varepsilon(0, \underline{z}_n, \underline{\ell}_n) \doteq \frac{\lambda^{|\underline{\ell}_n|}\mu^{n-|\underline{\ell}_n|}}{\mathcal{Z}_\mu} M_\beta^{\otimes n}(\underline{v}_n)\varphi_0^{\otimes \underline{\ell}_n}(\underline{z}_{\underline{\ell}_n})\mathbb{1}_{\mathcal{X}_n^\varepsilon}(\underline{x}_n) \tag{2.14}$$

driven by the Liouville equation (2.7), for a normalizing constant $\mathcal{Z}_\mu$ that we will adjust soon in (2.17). In the grand canonical ensemble, we randomize the total number of particles, and we will study *correlation functions*, that project the dynamics on a finite number of studied particles. Their definition is based on the *marginals* of the canonical densities: looking at configurations $(\tilde{\underline{z}}_N, \tilde{\underline{\ell}}_N) \doteq (\underline{z}_k, \underline{z}^*_{N-k}, \underline{\ell}_k, \underline{\ell}^*_{N-k})$, the marginals average the density over the values of $\underline{z}^*_{N-k}, \underline{\ell}^*_{N-k}$, as

$$W_N^{\varepsilon,(k)}(t, \underline{z}_k, \underline{\ell}_k) = \sum_{\underline{\ell}^*_{N-k} \in \Lambda_{N-k}} \int_{\mathcal{D}^{N-k}} W_N^\varepsilon(t, \tilde{\underline{z}}_N, \tilde{\underline{\ell}}_N)\mathrm{d}\underline{z}^*_{N-k}, \tag{2.15}$$

where the density is prolongated by 0 outside of the hard sphere domain $\mathcal{D}_N^\varepsilon$. The chemical potential λ weights the tagged particles, and μ weights the others. Note that we also take the marginal according to the tags, corresponding to the sum over $\underline{\ell}^*_p \in \Lambda_p$. Since the number N of particles will go to infinity, we need to project their statistics to remain in a fixed functional framework: this is why we study marginals of the density. Then, the correlation functions are defined as

$$\begin{aligned} F_n^\varepsilon(t, \underline{z}_n, \underline{\ell}_n) &\doteq \frac{1}{\mu^{n-|\underline{\ell}_n|}\lambda^{|\underline{\ell}_n|}} \sum_{p\geqslant 0} \frac{1}{p!} W_{n+p}^{\varepsilon,(n)}(t, \underline{z}_n, \underline{\ell}_n) \\ &= \frac{1}{\mathcal{Z}_\mu} \sum_{p\geqslant 0} \sum_{\underline{\ell}^*_p \in \Lambda_p} \frac{\lambda^{|\underline{\ell}^*_p|}\mu^{p-|\underline{\ell}^*_p|}}{p!} \int M_\beta^{\otimes n+p}(\underline{\tilde{v}}_{n+p})\varphi_0^{\otimes \tilde{\underline{\ell}}_{n+p}}(\tilde{\underline{z}}_{\tilde{\underline{\ell}}_{n+p}})\mathbb{1}_{\mathcal{X}_{n+p}^\varepsilon}(\tilde{\underline{x}}_{n+p})\mathrm{d}\underline{z}^*_p, \end{aligned} \tag{2.16}$$

where the normalizing (grand canonical) partition function is hence defined as follows

$$\mathcal{Z}_\mu \doteq \sum_{p\geqslant 0} \sum_{\underline{\ell}_p \in \Lambda_p} \frac{\lambda^{|\underline{\ell}_p|}\mu^{p-|\underline{\ell}_p|}}{p!} \int M_\beta^{\otimes p}(\underline{v}_p)\varphi_0^{\otimes \underline{\ell}_p}(\underline{z}_{\underline{\ell}_p})\mathbb{1}_{\mathcal{X}_p^\varepsilon}(\underline{x}_p)\mathrm{d}\underline{z}_p. \tag{2.17}$$

By construction, the correlation functions satisfy the same symmetry property (2.9) as the canonical densities. One can remark that in the case of a single tagged particle [9, 31], thanks to the invariance by translation of the spatial domain, the partition function does not depend on the perturbation φ_0. Indeed, in the said papers, one can perform the spatial change of variable $y_i = x_i - x_1, i \geq 2$, yielding

$$\begin{aligned} \int_{\mathbb{T}^{dN}} \rho(x_1)\mathbb{1}_{\mathcal{X}_N^\varepsilon}(x_1, \dots, x_N)\mathrm{d}\underline{x}_N &= \int_{\mathbb{T}^{dN}} \rho(x_1)\mathbb{1}_{\mathcal{X}_N^\varepsilon}(x_1, y_2 + x_1, \dots, y_N + x_1)\mathrm{d}x_1\mathrm{d}y_2 \dots \mathrm{d}y_N \\ &= \int_{\mathbb{T}^{dN}} \rho(x_1)\mathbb{1}_{\mathcal{X}_N^\varepsilon}(0, y_2, \dots, y_N)\mathrm{d}x_1\mathrm{d}y_2 \dots \mathrm{d}y_N, \end{aligned}$$

by invariance by translation, which allows to integrate ρ over x_1.

Here, the perturbed particles are correlated one with another, preventing us from using the same argument, which is why the initial perturbation appears in the formula (2.17) above. Note that the velocities of the non-perturbed particles (in the complementary of $\underline{\ell}_p$) may be integrated writing

$$\mathcal{Z}_\mu = \sum_{p\geqslant 0} \sum_{\underline{\ell}_p \in \Lambda_p} \frac{\lambda^{|\underline{\ell}_p|}\mu^{p-|\underline{\ell}_p|}}{p!} \int M_\beta^{\otimes \underline{\ell}_p}(\underline{v}_{\underline{\ell}_p})\varphi_0^{\otimes \underline{\ell}_p}(\underline{z}_{\underline{\ell}_p})\mathbb{1}_{\mathcal{X}_p^\varepsilon}(\underline{x}_p)\mathrm{d}\underline{x}_p\mathrm{d}\underline{v}_{\underline{\ell}_p},$$

using the fact that the equilibrium M_β is of integral 1. We still keep the first formulation for symmetry reasons; a more precise study of this object is made in Section 5.4.

Our probabilistic study is based on the *random variables*

$$(Z_{\varepsilon,i}^{[t]})_{1\leqslant i\leqslant \mathcal{N}}, \text{ and } (L_i)_{1\leqslant i\leqslant \mathcal{N}}, \tag{2.18}$$

respectively giving the states of the particles at time t, and their tags (invariant in time). The probability density of the initial state $(Z_{\varepsilon,i}^{[0]}, L_i)$ has been determined above, and the evolution to time t is a deterministic piecewise affine function of the initial state, following the microscopic hard sphere dynamics. The correlation functions are in fact defined such that for any observable $H_n \in \mathcal{C}_{\mathrm{c}}^\infty(\mathcal{D}^n \times \Lambda_n)$, we have the following link between correlation functions and expectancy of this observable

$$\begin{aligned}\mathbb{E}\left[\sum_{1\leq i_k\neq i_j\leq \mathcal{N}} H_n(Z_{\varepsilon,i_1}^{[t]}, L_{i_1}, \dots, Z_{\varepsilon,i_n}^{[t]}, L_{i_n})\right] &= \mathbb{E}\left[\delta_{\mathcal{N}\geq n}\frac{\mathcal{N}!}{(\mathcal{N}-n)!}H_n(Z_{\varepsilon,1}^{[t]}, L_1, \dots, Z_{\varepsilon,n}^{[t]}, L_n)\right]\\ &= \sum_{p=n}^{\infty}\frac{1}{p!}\frac{p!}{(p-n)!}\sum_{\underline{\ell}_p\in\Lambda_p}\int_{\mathcal{D}_p^\varepsilon} W_p^\varepsilon(t,\underline{z}_p,\underline{\ell}_p)H_n(\underline{z}_n,\underline{\ell}_n)\mathrm{d}\underline{z}_p\\ &= \sum_{\underline{\ell}_n\in\Lambda_n}\mu^{n-|\underline{\ell}_n|}\lambda^{|\underline{\ell}_n|}\int_{\mathcal{D}_n^\varepsilon} F_n^\varepsilon(t,\underline{z}_n,\underline{\ell}_n)H_n(\underline{z}_n,\underline{\ell}_n)\mathrm{d}\underline{z}_n.\end{aligned} \tag{2.19}$$

This formula between the correlation functions and observables will be used in the combinatorial computations of Section 6.1, when expanding the cumulant generating function.

2.5 Panoply of statistical objects

In this short section, we present the objects studied to describe the statistical behaviour of the system defined above. The first ones are the *canonical densities* W_N^ε and their marginals (2.15), which have been historically studied by Lanford in [45], and later in [34]. Further studies [12] took place in the grand canonical ensemble formalism, studying the *correlation functions* F_n^ε defined in the section above (2.16). This is also the case in this thesis, at Chapter 4.

For any observable $H \in \mathcal{C}_{\mathrm{c}}^\infty(\mathcal{D}\times\Lambda_1)$ of the value of the positions and tags of particles, we now define the following random variables: the *empirical measure of all particles*

$$\pi_t^\varepsilon[H] \doteq \frac{1}{\mu}\sum_{i=1}^{\mathcal{N}} H(Z_{\varepsilon,i}^{[t]}, L_i), \tag{2.20}$$

and the *empirical measure of tagged particles*

$$\tilde{\pi}_t^\varepsilon[H] \doteq \frac{1}{\lambda}\sum_{i=1}^{\mathcal{N}} H(Z_{\varepsilon,i}^{[t]}, L_i)\mathbb{1}_{L_i=1}. \tag{2.21}$$

These random variables are defined based on the random positions and tags of the particles, defined in (2.18), to capture the average value of the observable H for the particles of the system, and to describe the gas statistically at the level of a law of large numbers (see Corollary 4.1.1).

Actually, the empirical measures can be seen as the observations of a random measure in a wider space. For example, the empirical measure of the tagged particles can be associated with the random measure $\tilde{\pi}_t^\varepsilon \in \mathcal{M}(\mathcal{D})$ on the domain $\mathcal{D}$, writing

$$\tilde{\pi}_t^\varepsilon[H] = \int H(z)\mathrm{d}\tilde{\pi}_t^\varepsilon(z). \tag{2.22}$$

The family $(\tilde{\pi}^\varepsilon_s)_{0\leqslant s\leqslant t}$ defines a measure on the trajectories of $\mathcal{D}^{[0,t]}$. The set $\mathrm{Traj}([0,t],\mathcal{M}(\mathcal{D}))$ of such measures is endowed with the Skorokhod topology. The large deviations of this trajectory measure is studied in Theorem 3.

Eventually, one may also define the *fluctuation field* of this measure as

$$\zeta^\varepsilon_t = \sqrt{\lambda}(\tilde{\pi}^\varepsilon_t - \mathbb{E}\,[\tilde{\pi}^\varepsilon_t]), \tag{2.23}$$

to capture the next small order after the law of large numbers, in the idea of a central limit theorem. The asymptotical fluctuations of the empirical measure are exposed in Theorem 2.

The paramount statistical objects to describe the evolution of such quantities are the *cumulants* (f^ε_n) of the dynamics, defined in (5.1). They decompose the fine scales of the dynamics contained in the correlation functions, to capture the small-scale correlations of the system. Chapter 5 is dedicated to their combinatorial construction, and their convergence is the subject of Chapter 6.

2.6 BBGKY hierarchy on the density marginals

The marginals (2.15) correspond to the projection of the density of the particles, as their number will greatly enlarge. Each equation satisfied by a marginal implies the closest marginal of higher order, which forms a global hierarchy of equations, which is closed by the Liouville equation (2.7) in the canonical case, and closed at infinity in the grand canonical case. This hierarchy is called BBGKY hierarchy after Nikolaï Bogolioubov, Max Born, Herbert Green, John Kirkwood and Jacques Yvon; and can be formulated as follows in our case. For a tag $\ell \in \{0,1\}$, we first introduce the n-th *collision operator*

$$\mathcal{C}^{\langle\ell\rangle}_n F^\varepsilon_{n+1} \doteq \sum_{i=1}^n \int \langle \omega, v_{\mathrm{c}} - v_i\rangle F^\varepsilon_{n+1}(\underline{z}_s, \underline{\ell}_s, x_i + \varepsilon\omega, v_{\mathrm{c}}, \ell)\mathrm{d}\omega\mathrm{d}v_{\mathrm{c}}, \tag{2.24}$$

which represents the influence of a $(n+1)$-th particle (with tag ℓ) on the average dynamics of n considered particles.

Proposition 2.6.1 (BBGKY hierarchy for the Rayleigh mixture)**.** *For the Rayleigh gas mixture introduced in the beginning of this chapter, the canonical densities' marginals satisfy the following hierarchy*

$$\begin{aligned}\partial_t W^{\varepsilon,(n)}_N + \underline{v}_n \cdot \nabla_{\underline{x}_n} W^{\varepsilon,(n)}_N &= (N-n)\varepsilon^{d-1}\left(\mathcal{C}^{\langle 0\rangle}_n W^{\varepsilon,(n+1)}_N + \mathcal{C}^{\langle 1\rangle}_n W^{\varepsilon,(n+1)}_N\right)\\ &= (N-n)\varepsilon^{d-1}\sum_{\ell=0}^1\sum_{i=1}^n \int \langle \omega, v_{\mathrm{c}} - v_i\rangle W^{\varepsilon,(n+1)}_N(\underline{z}_n, \underline{\ell}_n, x_i+\varepsilon\omega, v_{\mathrm{c}}, \ell)\mathrm{d}\omega\mathrm{d}v_{\mathrm{c}}\end{aligned}$$

for any $n \geq 1$. In our mixed Boltzmann–Grad scaling ($S_{\varepsilon,\mu,\lambda}$), it direcly implies the following BBGKY hierarchy for the correlation functions

$$\partial_t F^\varepsilon_n + \underline{v}_n \cdot \nabla_{\underline{x}_n} F^\varepsilon_n = \mathcal{C}^{\langle 0\rangle}_n F^\varepsilon_{n+1} + \frac{\lambda}{\mu}\mathcal{C}^{\langle 1\rangle}_n F^\varepsilon_{n+1}. \tag{2.25}$$

The proof of this Proposition is detailed in the following Sections 2.6.1 and 2.6.2. To make appear the gain and loss terms of the Boltzmann equations (such as (2.13)), we rewrite the collision operators using the boundary condition (2.8) when $\langle\omega, v_{n+1} - v_i\rangle > 0$, and the change of variable $\omega \mapsto -\omega$ otherwise:

$$\begin{aligned}\mathcal{C}^{\langle\ell\rangle}_n F^\varepsilon_{n+1} = \sum_{i=1}^n \int \mathrm{d}\omega\mathrm{d}v_{n+1}\langle\omega, v_{n+1} - v_i\rangle_+ \times\\ \Big[F^\varepsilon_{n+1}(\underline{z}^\star_n, \underline{\ell}_n, x_i + \varepsilon\omega, v^\star_{n+1}, \ell) - F^\varepsilon_{n+1}(\underline{z}_n, \underline{\ell}_n, x_i - \varepsilon\omega, v_{n+1}, \ell)\Big].\end{aligned} \tag{2.26}$$

Morally, we look at the influence of a $(n+1)$-th particle—with tag ℓ—on the dynamics, colliding with one of the n existing ones with angle ω and velocity v_{n+1}, whence the name *collision operators*. The *cross section* $\langle \omega, v_{n+1} - v_i \rangle_+$ weights the likelihood of such a collision.

Note that [3] derives a mixed Boltzmann equation for a different setting, in a canonical case where the number of particles of each kind is fixed. It could also work in our case, studying canonical densities' marginals of the form

$$W_{N,M}^{(n,m)}(\underline{z}_n, \underline{\zeta}_m) = \int W_{N,M}\left(\underline{z}_n, \underline{z}^*_{N-n}, \underline{\zeta}_m, \underline{\zeta}^*_{M-m}\right) \mathrm{d}\underline{z}^*_{N-n} \mathrm{d}\underline{\zeta}^*_{M-m},$$

where the vectors $\underline{z}_n = (\underline{x}_n, \underline{u}_n)$ and $\underline{\zeta}_m = (\underline{y}_m, \underline{v}_m)$ representing the positions of tagged and non-tagged particles are separated. This would lead to a BBGKY hierarchy of the form

$$\partial_t W_{N,M}^{(n,m)} + \underline{u} \cdot \nabla_{\underline{x}} W_{N,M}^{(n,m)} + \underline{v} \cdot \nabla_{\underline{y}} W_{N,M}^{(n,m)} = \sum_{\ell=0}^{1} \alpha_\varepsilon \mathcal{C}_{n,m}^{\langle \ell \rangle} W_{N,M}^{(n+1,m)} + \beta_\varepsilon \tilde{\mathcal{C}}_{n,m}^{\langle \ell \rangle} W_{N,M}^{(n,m+1)},$$

where the four collision operators represent the influence of the tagged particles on themselves, of the tagged particles on the non-tagged ones, of the non-tagged ones on the tagged ones, etc. with weights $\alpha_\varepsilon, \beta_\varepsilon$ depending on the number of particles of each kind.

Nevertheless, even if our tag model implies specific technical difficulties, it alleviates the notation and most of all it preserves a symmetrical structure that greatly helps to study the cumulants of the system, and makes all the computations formally closer to the non-mixture case.

2.6.1 Proof of the mixed hierarchy

We start with the proof of Proposition 2.6.1, before proving some technical changes of variables that appear in it, in Section 2.6.2.

Proof. We are going to test the Liouville equation (2.7) against observables $\psi \in \mathcal{C}_c^\infty(\mathbb{R}^+ \times \mathcal{D}_s^\varepsilon \times \Lambda_s)$ that satisfy the same symmetry (2.9) and boundary (2.8) conditions as W_N^ε. The time derivative of the Liouville equation will commute with the marginal, by integration by parts with ψ regular enough: recalling the definition of the s-th marginal (2.15) we write

$$\begin{aligned}
&\sum_{\underline{\ell}^*_{N-s}} \int_{\mathbb{R}^+ \times \mathcal{D}^N} \partial_t W_N^\varepsilon \left(t, \underline{z}_N, \underline{\ell}_N\right) \psi(t, \underline{z}_s, \underline{\ell}_s) \mathrm{d}\underline{z}_N \mathrm{d}t \\
&\quad = -\int_{\mathcal{D}^s} W_N^{\varepsilon,(s)}\left(0, \underline{z}_s, \underline{\ell}_s\right) \psi(0, \underline{z}_s, \underline{\ell}_s) \mathrm{d}\underline{z}_s - \int_{\mathbb{R}^+ \times \mathcal{D}^s} W_N^{\varepsilon,(s)}(t, \underline{z}_s, \underline{\ell}_s) \partial_t \psi(t, \underline{z}_s, \underline{\ell}_s) \mathrm{d}\underline{z}_s \mathrm{d}t \\
&\quad = \int_{\mathbb{R}^+ \times \mathcal{D}^s} \partial_t W_N^{\varepsilon,(s)}(t, \underline{z}_s, \underline{\ell}_s) \psi(t, \underline{z}_s, \underline{\ell}_s) \mathrm{d}\underline{z}_s \mathrm{d}t.
\end{aligned}$$

On the other hand, for the transport term of the Liouville equation, we apply the Green formula in space, decomposing the boundary of the hard sphere exclusion set $\mathcal{X}_N^\varepsilon$ into the surfaces of contact between two particles $i, j \leq N$,

$$\Sigma(i,j) \doteq \{\underline{x}_N \in \mathbb{R}^{dN};\ |x_i - x_j| = \varepsilon\},$$

recalling that the collisions implying more than 2 particles are of measure zero [1]. Hence, we get

$$\begin{aligned}
&\sum_{\underline{\ell}_N} \int_{\mathcal{D}_N^\varepsilon} \underline{v}_N \cdot \nabla_{\underline{x}_N} W_N^\varepsilon(\underline{z}_N, \underline{\ell}_N) \psi(\underline{z}_s, \underline{\ell}_s) \mathrm{d}\underline{z}_N \\
&\quad = \sum_{\underline{\ell}_N} \int_{\mathcal{D}_N^\varepsilon} \mathrm{div}_{\underline{x}_N}(\underline{v}_N W_N^\varepsilon(\underline{z}_N, \underline{\ell}_N)) \psi(\underline{z}_s, \underline{\ell}_s) \mathrm{d}\underline{z}_N \\
&\quad = -\sum_{\underline{\ell}_N} \sum_{i=1}^N \int_{\mathcal{D}_N^\varepsilon} W_N^\varepsilon(\underline{z}_N, \underline{\ell}_N) v_i \cdot \nabla_{x_i} \psi(\underline{z}_s, \underline{\ell}_s) \mathrm{d}\underline{z}_N \\
&\qquad + \sum_{1 \le i < j \le N} \sum_{\underline{\ell}_N} \int_{\mathbb{R}^{dN}} \int_{\Sigma(i,j)} n_{i,j} \cdot \underline{v}_N W_N^\varepsilon(\underline{z}_N, \underline{\ell}_N) \psi(\underline{z}_s, \underline{\ell}_s) \mathrm{d}\sigma^{i,j}(\underline{x}_N) \mathrm{d}\underline{v}_N .
\end{aligned}$$

The first term corresponds by integration par parts to the gradient of the s-th marginal $W_N^{\varepsilon,(s)}$.

The second term corresponds to the influence of collisions: since the normal vector is

$$n_{i,j} = \frac{1}{\sqrt{2}\varepsilon} (0, \dots, x_j - x_i, \dots, x_i - x_j, \dots, 0) ,$$

its double sum can be rewritten

$$\sum_{1 \le i < j \le N} \sum_{\underline{\ell}_N} \int_{\mathbb{R}^{dN}} \int_{\Sigma(i,j)} \frac{(x_j - x_i) \cdot (v_i - v_j)}{\sqrt{2}\varepsilon} W_N^\varepsilon(\underline{z}_N, \underline{\ell}_N) \psi(\underline{z}_s, \underline{\ell}_s) \mathrm{d}\sigma^{i,j}(\underline{x}_N) \mathrm{d}\underline{v}_N . \tag{2.27}$$

We henceforth split this sum according to the following Figure 2.4.

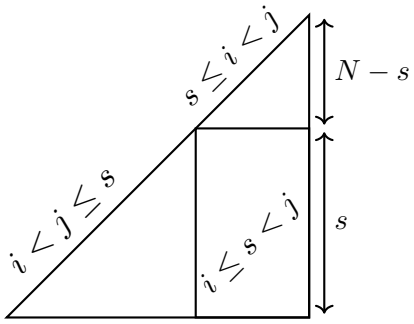

Figure 2.4: Decomposition of the BBGKY interactions

For $1 \le i \le s < j \le N$, we compute a change of variable on x_j from the hypersurface $\Sigma(i,j)$ to the sphere $\mathbb{S}_\varepsilon^{d-1}(x_i)$ of center x_i and radius ε. The technical details of this change of variable, that makes appear a factor $\sqrt{2}$, are postponed to the following Section 2.6.2. We get

$$\begin{aligned}
&\int_{\mathbb{R}^{dN}} \int_{\Sigma(i,j)} \frac{(x_j - x_i) \cdot (v_i - v_j)}{\sqrt{2}\varepsilon} W_N^\varepsilon(\underline{z}_N, \underline{\ell}_N) \psi(\underline{z}_s, \underline{\ell}_s) \mathrm{d}\sigma^{i,j}(\underline{x}_N) \mathrm{d}\underline{v}_N \qquad (2.28) \\
&= \int_{\mathbb{R}^{dN}} \int_{\mathbb{T}^{d(N-1)}} \int_{\mathbb{S}_\varepsilon^{d-1}(x_i)} \frac{(x_j - x_i)}{\varepsilon} \cdot (v_i - v_j) W_N^\varepsilon(\underline{z}_N, \underline{\ell}_N) \psi(\underline{z}_s, \underline{\ell}_s) \mathrm{d}x_1 \dots \mathrm{d}\omega^i(x_j) \dots \mathrm{d}x_N \mathrm{d}\underline{v}_N .
\end{aligned}$$

Now, we parametrize $x_j = x_i + \varepsilon\omega \Leftrightarrow \omega = (x_j - x_i)/\varepsilon$, and use the exchangeability of particles to swap x_j and x_{s+1}: by the definition of the $(s+1)$-th marginal, if $\hat{\underline{\ell}} \doteq (\ell_{s+2}, \dots, \ell_N) \in \Lambda_{N-(s+1)}$, we have

$$\begin{aligned}
&\sum_{\hat{\underline{\ell}}} \int_{\mathbb{R}^{dN}} \int_{\Sigma(i,j)} \frac{(x_j - x_i) \cdot (v_i - v_j)}{\sqrt{2}\varepsilon} W_N^\varepsilon(\underline{z}_N, \underline{\ell}_N) \psi(\underline{z}_s, \underline{\ell}_s) \mathrm{d}\sigma^{i,j}(\underline{x}_N) \mathrm{d}\underline{v}_N \\
&= \varepsilon^{d-1} \int_{\mathbb{R}^{d(s+1)}} \int_{\mathbb{T}^{ds}} \int_{\mathbb{S}^{d-1}} \omega \cdot (v_i - v_{s+1}) W_N^{\varepsilon,(s+1)}(\underline{z}_s, x_i + \varepsilon\omega, v_{s+1}, \underline{\ell}_{s+1}) \psi(\underline{z}_s, \underline{\ell}_s) \mathrm{d}\underline{x}_s \mathrm{d}\omega \mathrm{d}\underline{v}_{s+1} .
\end{aligned}$$

Otherwise, if $i,j \in [\![1,s]\!]$ or $i,j \in [\![s+1,N]\!]$, the associated term will vanish by symmetry of the pre- and post-collisional configurations: let us fix $\underline{x}_N$ such that $\underline{z}_N \in \Sigma(i,j)$. Denoting

$$\underline{v}_N^\star = (v_1, \dots, {v_i}^\star, \dots, {v_j}^\star, \dots, v_N)$$

the precollisional velocities, we will use the fact that the change of variable $(v_i, v_j) \mapsto ({v_i}^\star, {v_j}^\star)$ is of Jacobian 1 (see once again Section 2.6.2). Since by the scattering rules one has

$$\omega \cdot (v_i - v_j) = -\omega(v_i^\star - v_j^\star),$$

and using the boundary condition (2.8) on W_N^ε and ψ, we get

$$\begin{aligned}
&\int_{\mathbb{R}^{dN}} \omega \cdot (v_i - v_j) W_N^\varepsilon(\underline{z}_N)\psi(\underline{z}_s)\mathrm{d}\underline{v}_N \\
&\quad = \int [\omega \cdot (v_i - v_j)]_+ W_N^\varepsilon(\underline{z}_N^\star)\psi(\underline{z}_s^\star)\mathrm{d}\underline{v}_N - \int [\omega \cdot (v_i - v_j)]_- W_N^\varepsilon(\underline{z}_N)\psi(\underline{z}_s)\mathrm{d}\underline{v}_N \\
&\quad = \int [-\omega \cdot ({v_i}^\star - {v_j}^\star)]_+ W_N^\varepsilon(\underline{z}_N^\star)\psi(\underline{z}_s^\star)\mathrm{d}\underline{v}_N^\star - \int [\omega \cdot (v_i - v_j)]_- W_N^\varepsilon(\underline{z}_N)\psi(\underline{z}_s)\mathrm{d}\underline{v}_N = 0.
\end{aligned}$$

Hence, the only contributing terms of the double sum (2.27) are the crossed terms, which at a fixed i appear each one identically $(N-s)$ times by symmetry, so that the double sum is equal to

$$-(N-s)\varepsilon^{d-1} \sum_{i=1}^{s} \sum_{\underline{\ell}_{s+1}} \int_{\mathcal{D}^s} \int_{\mathbb{R}^d} \int_{\mathbb{S}^{d-1}} \omega \cdot (v_{s+1} - v_i) W_N^{\varepsilon,(s+1)}(\underline{z}_s, \underline{\ell}_s, x_i + \varepsilon\omega, v_{s+1}, \ell_{s+1})\mathrm{d}\omega \mathrm{d}v_{s+1}\mathrm{d}\underline{z}_s.$$

One recognizes the collision operator (2.24), so that we retrieve the BBGKY hierarchy of the canonical densities, proving the first part of the proposition. For the correlation functions, we use their definition and the mixed scaling ($S_{\varepsilon,\mu,\lambda}$) to write

$$\begin{aligned}
\partial_t F_n^\varepsilon + \underline{v}_n \cdot \nabla_{\underline{x}_n} F_n^\varepsilon &= \frac{1}{\mu^{n-|\underline{\ell}_n|}\lambda^{|\underline{\ell}_n|}} \sum_{k \geqslant 0} \frac{k\varepsilon^{d-1}}{k!} \left(\mathcal{C}_n^{\langle 0 \rangle} W_{n+k}^{\varepsilon,(n+1)} + \mathcal{C}_n^{\langle 1 \rangle} W_{n+k}^{\varepsilon,(n+1)} \right) \\
&= \frac{\mu\varepsilon^{d-1}}{\mu^{n+1-|\underline{\ell}_n|}\lambda^{|\underline{\ell}_n|}} \sum_{k \geqslant 0} \frac{1}{k!} \mathcal{C}_n^{\langle 0 \rangle} W_{n+k+1}^{\varepsilon,(n+1)} + \frac{\lambda\varepsilon^{d-1}}{\mu^{n-|\underline{\ell}_n|}\lambda^{|\underline{\ell}_n|+1}} \sum_{k \geqslant 0} \frac{\varepsilon^{d-1}}{k!} \mathcal{C}_n^{\langle 1 \rangle} W_{n+k+1}^{\varepsilon,(n+1)} \\
&= \mathcal{C}_n^{\langle 0 \rangle} F_{n+1}^\varepsilon + \frac{\lambda}{\mu} \mathcal{C}_n^{\langle 1 \rangle} F_{n+1}^\varepsilon,
\end{aligned}$$

completing the proof of Proposition 2.6.1 by linearity of the collision operators. □

2.6.2 Technical changes of variable

Change of variable on the hypersurface $\Sigma(i,j)$.

As announced sooner, we hereafter prove the change of variable used in Section 2.6.1, at line (2.28), to prove the BBGKY hierarchy. We use the notation presented in the concerned section, to change the parametrization of the hypersurface $\Sigma(i,j)$ to the sphere $\mathbb{S}_\varepsilon^{d-1}(x_i)$, making appear a factor $\sqrt{2}$.

Let us consider the case of two particles $x = x_i$ and $y = x_j$, since the other ones are free of conditions in $\Sigma(i,j)$. Let us denote $\phi(\theta_1, \dots, \theta_{d-1})$ a parametrization of $\varepsilon \cdot \mathbb{S}^{d-1}$. We thus have the following parametrization of $\Sigma(i,j) \ni (x,y)$ as a union of balls with centers $x = (t_1, \dots, t_d)$ and radiuses ε,

$$\Phi(t_1, \dots, t_d, \theta_1, \dots, \theta_{d-1}) = \Big(t_1; \dots; t_d; t_1 + \phi(\theta_1, \dots, \theta_{d-1}); \dots; t_d + \phi(\theta_1, \dots, t_{d-1}) \Big), \tag{2.29}$$

whose Jacobian is given by

$$J_\Phi = \left(\begin{array}{c|c} I_d & 0 \\ \hline I_d & J_\phi \end{array}\right). \tag{2.30}$$

Then, by integration over a hypersurface, the element of surface of $\Sigma(i,j)$ is given by

$$\mathrm{d}\sigma(x,y) = A_\Phi(T_d, \Theta_{d-1})\mathrm{d}T_d\mathrm{d}\Theta_{d-1}, \tag{2.31}$$

where the area $\mathcal{A}_\Phi(T_d, \Theta_{d-1})$ is yielded by the norm of the cross product of the columns of J_Φ, or differently formulated

$$\mathcal{A}_\Phi^2 = \sum_{i=1}^{2d} \Delta_\Phi(k)^2, \tag{2.32}$$

where $\Delta_\Phi(k)$ is the determinant of J_Φ deprived of its k-th line. A simple computation of matrix calculus using the relation (2.30) between both Jacobians—developping for $k \leq d$ along the k-th column which has only a single 1 in $(d+k)$-th position—yields

$$\Delta_\Phi(k)^2 = \left\{ \begin{array}{l} \Delta_\phi(k)^2 \text{ if } k \leq d \\ \Delta_\phi(k-d)^2 \text{ otherwise,} \end{array}\right. \tag{2.33}$$

so that

$$\mathcal{A}_\Phi^2 = 2\mathcal{A}_\phi^2, \tag{2.34}$$

i.e. eventually

$$\mathrm{d}\sigma(x,y) = \sqrt{2}\cdot \mathrm{d}x\mathrm{d}\omega(y), \tag{2.35}$$

whence the $\sqrt{2}$ factor, concluding the proof. □

Change of variable from pre- to post-collisional velocities.

At fixed ω, the map $(v, v_c) \mapsto (v^\star, {v_c}^\star)$ has Jacobian 1. Indeed, denoting $\Omega_2 = \omega \times {}^t\omega$, we have

$$J = \left(\begin{array}{c|c} I - \Omega_2 & \Omega_2 \\ \hline \Omega_2 & I - \Omega_2 \end{array}\right). \tag{2.36}$$

Inspired by the scalar case, we conjugate by $\left(\begin{array}{c|c} I & I \\ \hline I & -I \end{array}\right)$, and then diagonalize Ω_2 of rank 1 with the eigenpair $(|\omega|^2, \omega)$, to eventually get

$$\det J = \det(I)\cdot\det(I - 2\Omega_2) = 1 - 2|\omega|^2 = -1, \tag{2.37}$$

completing the computation. □

Chapter 3

Linear Boltzmann equations

This chapter is dedicated to the introduction of the Boltzmann equation, and of various of its linear versions, appearing in different statistical descriptions of the particles's system.

We insist on the Rayleigh–Boltzmann equation (2.13), along with the linear Boltzmann–Hamilton–Jacobi system that appears in the study of the large deviation principle exposed in Theorem 3 (see Section 6.6.5) . We study the properties and wellposedness of these equations respectively in Sections 3.3 and 3.4.

3.1 The Boltzmann equation

The Boltzmann equation was introduced by Ludwig Eduard Boltzmann in 1872, based on a statistical description of a microscopically atomistic gas. For a density of particles $F(t,x,v)$ on the position-velocity phase space $\mathcal{D}\times\mathbb{R}^d$, it reads

$$\partial_t F + v\cdot\nabla_x F = \int_{\mathbb{S}^{d-1}}\int_{\mathbb{R}^d}\left[F(v^\star)F(v_c^\star) - F(v)F(v_c)\right]\langle\omega, v_c - v\rangle_+ \mathrm{d}v_c\mathrm{d}\omega \tag{3.1}$$

in the case of the hard sphere potential, with the notation of previous chapter. This equation usually goes along with an initial condition $F(0,x,v)$. Note that this equation is transport-like from its left side, the right side corresponding to the influence of collisions on the dynamics. It is valid in the case of dilute gases, in which the collisions might be considered binary, implying only two particles at a time, hence quite localized in time and space. The choice of another microscopical potential would merely change the cross section $\langle\omega, v_c - v\rangle_+$. This equation directly stems from the BBGKY hierarchy (see Proposition 2.6.1): indeed, it is the formal limit of the equation on the first marginal, under the *assumption of chaoticity*

$$F_2 = F_1^{\otimes 2},$$

introduced by Maxwell, and historically called *Stoßzahlansatz* by Paul and Tatiana Ehrenfest [29]. Eventually, it highly relies on the microscopical reversibility, in part due to the elasticity of the collisions. Recently, Théophile Dolmaire and Juan José López Velázquez studied an inelastic version of the atomistic gas [27], and Dolmaire and Alessia Nota derived an inelastic version of the Boltzmann equation [26].

The derivation of this equation in the hard sphere case has been performed in 1975 by Lanford [45], and extended to compactly supported potentials in 2013 [34], yet its derivation for general potentials is still an open problem. For a review of the existing results on the Boltzmann equation and its Cauchy problem, see the review by Villani [61].

3.2 Linearizations

Let us denote

$$Q(F,G) \doteq \int_{\mathbb{S}^{d-1}} \int_{\mathbb{R}^d} \left[F(v^\star)G(v_c^\star) - F(v)G(v_c)\right] \langle \omega, v_c - v\rangle_+ \mathrm{d}v_c \mathrm{d}\omega$$

the non-symmetrical bilinear Boltzmann collision operator. Linear versions of the Boltzmann equation appear in situations close to some known solution

$$\partial_t \overline{F} + v \cdot \nabla_x \overline{F} = Q(\overline{F}, \overline{F}), \tag{3.2}$$

yet the notion of closeness can take different shapes. First, one may look at small perturbations of the form

$$F = \overline{F} + \varepsilon f^\varepsilon.$$

Using the fact that $\overline{F}$ satisfies (3.2), the rescaled perturbation f^ε satisfies

$$\partial_t f^\varepsilon + v \cdot \nabla_x f^\varepsilon = Q(\overline{F}, f^\varepsilon) + Q(f^\varepsilon, \overline{F}) + \varepsilon Q(f^\varepsilon, f^\varepsilon).$$

Hence, at first order as ε gets small, it is driven by the *linearized Boltzmann operator*

$$L_{\overline{F}} f^\varepsilon = Q(\overline{F}, f^\varepsilon) + Q(f^\varepsilon, \overline{F}). \tag{3.3}$$

In particular, one can study small perturbations around the thermodynamic equilibrium $\overline{F} = M_\beta$ (defined in (2.11)), to get uniform bounds on the linear operator (see [19] for details).

On the other hand, the linearization can appear in a mixture case, when the fraction of a kind of particles goes to 0 at the limit (which is in particular the case for a single tagged particle). Indeed, looking the mixture BBGKY hierarchy given in Proposition 2.6.1, one can see that the influence of tagged particles is weighted by a factor λ/μ, vanishing in the scaling ($S_{\varepsilon,\mu,\lambda}$). Hence, in the limit equation for the density of tagged particles, the quadratic term vanishes and we retrieve the linear Rayleigh–Boltzmann equation (2.13) exposed in the previous chapter: it corresponds to half the linear operator L_{M_β} defined above (3.3), with only its part $Q(f, M_\beta)$, up to a change of variable. Indeed, if φ satisfies the Rayleigh–Boltzmann equation, one can check that $F = M_\beta \varphi$ is a solution of the equation

$$\partial_t F + v \cdot \nabla_x F = Q(F, M_\beta).$$

For further details, see the following sections, in which we juggle with various changes of unknowns. Though the first linearized Boltzmann operator is generally studied in a weighted $\mathbb{L}^2$ space to harness the fact that it is self-adjoint, the linear Rayleigh–Boltzmann equation can here be treated in a weighted $\mathbb{L}^\infty$ space. Next section is dedicated to its study.

3.3 The linear Rayleigh–Boltzmann equation

3.3.1 Rayleigh–Boltzmann integral kernel

To get existence and uniqueness results on the linear Rayleigh–Boltzmann equation, we proceed to a similar decomposition as in [37], and compute the integrals in the hyperspherical coordinates given in (2.6). The linear Rayleigh–Boltzmann equation (2.13) might be written

$$\partial_t \varphi + v \cdot \nabla_x \varphi = \mathcal{K}\varphi(v) - \nu_\beta(v)\varphi(v)$$

where the gain operator is

$$\mathcal{K}\varphi(v) \doteq \int \langle v_c - v, \omega\rangle_+ M_\beta(v_c)\varphi(v^\star)\mathrm{d}\omega\mathrm{d}v_c \tag{3.4}$$

and the loss factor is

$$\nu_\beta(v) \doteq \int \langle v_c - v, \omega\rangle_+ M_\beta(v_c) \mathrm{d}\omega \mathrm{d}v_c. \tag{3.5}$$

The loss factor being bounded below in v, it will provide some decay of the solution, while the gain operator will rather make it grow. We will prove that it can be made nonetheless bounded, starting with the following lemma.

Lemma 3.3.1 (Integral kernel of the gain part)**.** *The gain operator $\mathcal{K}$ defined above (3.4) has the following kernel integral formula*

$$\mathcal{K}\varphi(v) = \sqrt{\frac{\beta}{2\pi}} \int \frac{\varphi(\eta)}{|\eta - v|^{d-2}} \exp\left(-\beta\left[\frac{|\eta - v|^2}{8} + \frac{|\eta|^2 - |v|^2}{4} + \frac{\left(|\eta|^2 - |v|^2\right)^2}{8|\eta - v|^2}\right]\right) \mathrm{d}\eta.$$

Proof. We start by the translated change of variable $V \doteq v_c - v$. Additionally, changing the angle ω into $-\omega$ merely changes the collision kernel to $|\langle v_c - v, \omega\rangle_-|$, so that up to dividing the integral over ω by two, it can be made on the whole sphere $\mathbb{S}^{d-1}$. Eventually, at fixed angle ω, we isolate the part of $V = v_c - v$ supported on ω, whose norm appears in the collision kernel: we write

$$V \doteq V_\omega\, \omega + U_\perp\ , \qquad \text{with } U_\perp \cdot \omega = 0.$$

Then, recalling the scattering formula (2.2) in which the projection of V on ω also appears, we have

$$\mathcal{K}\varphi(v) = \frac{1}{2}\int |V_\omega| M_\beta(v + V)\varphi(v + V_\omega\omega)\mathrm{d}\omega\mathrm{d}V.$$

The key computation is now to relax the angle ω, and to introduce the variable

$$\xi \doteq V_\omega\omega,$$

going twice across $\mathbb{R}^d$, and satisfying $U_\perp \cdot \xi = 0$. We perform the change of variable

$$\begin{aligned}\mathrm{d}\omega\mathrm{d}V &= \mathrm{d}\omega\ \mathrm{d}V_\omega\ \mathrm{d}U_\perp \\ &= 2\frac{\mathrm{d}\xi}{|\xi|^{d-1}}\ \mathrm{d}U_\perp.\end{aligned}$$

Eventually, we perform the translated change of variable $\xi \mapsto v + \xi \doteq \eta$, so that

$$\begin{aligned}\mathcal{K}\varphi(v) &= \int |\xi| M_\beta(v + \xi + U_\perp)\varphi(v + \xi)\frac{\mathrm{d}\xi}{|\xi|^{d-1}}\mathrm{d}U_\perp \\ &= \int \frac{1}{|\eta - v|^{d-2}} M_\beta(\eta + U_\perp)\varphi(\eta)\ \mathrm{d}\eta\ \mathrm{d}U_\perp.\end{aligned} \tag{3.6}$$

To compute the integral over $U^\perp$, it is useful to harness a vector whose scalar product with $\xi = \eta - v$ is easy to calculate: we set

$$\alpha \doteq \frac{v + \eta}{2}.$$

At lign (3.6), the Maxwellian M_β depends on the square of the velocities (2.11), and so makes appear

$$\begin{aligned}|\eta + U_\perp + \alpha - \alpha|^2 &= |U_\perp + \alpha|^2 + |\eta - \alpha|^2 + 2\langle U_\perp + \alpha, \eta - \alpha\rangle \\ &= |U_\perp + \alpha|^2 + \frac{|\eta - v|^2}{4} + \frac{1}{2}\langle 2U_\perp + \eta + v, \eta - v\rangle,\end{aligned}$$

so that using the fact that $\langle U_\perp, \eta - v\rangle = 0$, we have

$$|\eta + U_\perp|^2 = |U_\perp + \alpha|^2 + \frac{|\eta - v|^2}{4} + \frac{|\eta|^2 - |v|^2}{2}.$$

Decomposing α according to ξ as

$$\alpha = \alpha_1 + \alpha_\perp \in \mathrm{Span}(\xi) \oplus \xi^\perp,$$

it all boils down to writing

$$\begin{aligned}\int M_\beta(\eta + U_\perp)\mathrm{d}U_\perp &= \left(\frac{\beta}{2\pi}\right)^{\frac{d}{2}} e^{-\frac{\beta}{2}\left[|\alpha_1|^2 + \frac{|\eta-v|^2}{4} + \frac{|\eta|^2-|v|^2}{2}\right]} \int e^{-\frac{\beta}{2}|\alpha_\perp + U_\perp|^2}\mathrm{d}U_\perp \\ &= \sqrt{\frac{\beta}{2\pi}} e^{-\frac{\beta}{2}\left[|\alpha_1|^2 + \frac{|\eta-v|^2}{4} + \frac{|\eta|^2-|v|^2}{2}\right]}.\end{aligned}$$

The result follows from the computation above and formula (3.6), observing that

$$|\alpha_1|^2 = \left|\frac{v+\eta}{2} \cdot \frac{\xi}{|\xi|}\right|^2 = \frac{\left(|\eta|^2 - |v|^2\right)^2}{4|\eta - v|^2}.$$

□

To get existence results on large times, we would like this kernel to be bounded, yet in this form it is not, as shown in the following lemma.

Lemma 3.3.2 (Estimate on the kernel)**.** *There exist constants c_β and C_β depending only on the dimension and the temperature, such that the integral kernel from Lemma 3.3.1 satisfies for all $v \in R^d$*

$$c_\beta(1 + |v|) \leq \int \frac{\mathrm{d}\eta}{|\eta - v|^{d-2}} e^{-\beta\left[\frac{|\eta-v|^2}{8} + \frac{|\eta|^2-|v|^2}{4} + \frac{\left(|\eta|^2-|v|^2\right)^2}{8|\eta-v|^2}\right]} \leq C_\beta(1 + |v|).$$

Proof. We start denoting $u \doteq v - \eta$, so that

$$|\eta|^2 - |v|^2 = |v - u|^2 - |v|^2 = |u|^2 - 2u \cdot v.$$

Thus, in hyperspherical coordinates (see (2.6) in Section 2.2) with respect to v, denoting $\mathrm{d}J(\underline{\theta})$ the Jacobian corresponding to the measure on the unit sphere, and $\theta = \theta_{d-2} \doteq \widehat{(u, v)}$, one has

$$\begin{aligned}\int \frac{\mathrm{d}\eta}{|\eta - v|^{d-2}} e^{-\beta\left[\frac{|\eta-v|^2}{8} + \frac{|\eta|^2-|v|^2}{4} + \frac{\left(|\eta|^2-|v|^2\right)^2}{8|\eta-v|^2}\right]} &= \int \mathrm{d}r\mathrm{d}J(\underline{\theta}_{d-1}) r e^{-\beta\left[\frac{r^2}{8} + \frac{r^2 - 2r|v|\cos\theta}{4} + \frac{\left(r-2|v|\cos\theta\right)^2}{8}\right]} \\ &= \int \mathrm{d}r\mathrm{d}J(\underline{\theta}_{d-1}) r e^{-\frac{\beta}{2}(r - |v|\cos\theta)^2}.\end{aligned}$$

The last equality above merely results from developing and refactorizing the term in brackets. The final estimate follows from recognizing the expectancy of a non-normalized Gaussian centered around $|v|\cos\theta$, then integrating over θ, which provides the constants depending on the dimension and temperature, concluding the proof. □

3.3.2 Modified Rayleigh–Boltzmann equation

Hence, this kernel is not bounded in v and it is necessary to compute a change of unknown in the linear Rayleigh-Boltzmann equation (2.13), to better distribute the exponential decay and get a bounded operator. Setting

$$R = M_\beta^{\frac{1}{2}}\varphi,$$

the Rayleigh–Boltzmann equation becomes

$$\partial_t R + v\cdot\nabla_x R = \hat{\mathcal{K}}R(v) - \nu_\beta(v)R(v), \tag{3.7}$$

for the new operator

$$\hat{\mathcal{K}}R(v) \doteq \int \langle v_c - v, \omega\rangle_+ M_\beta(v_c) M_\beta^{\frac{1}{2}}(v) M_\beta^{-\frac{1}{2}}(v') R(v') \mathrm{d}\omega \mathrm{d}v_c. \tag{3.8}$$

Lemma 3.3.3 (Integral kernel of the modified gain part)**.** *The new gain operator $\hat{\mathcal{K}}$ defined above (3.8) has the following kernel integral formula*

$$\hat{\mathcal{K}}R(v) = \sqrt{\frac{\beta}{2\pi}}\int \frac{R(\eta)}{|\eta - v|^{d-2}} \exp\left(-\beta\left[\frac{|\eta - v|^2}{8} + \frac{\left(|\eta|^2 - |v|^2\right)^2}{8|\eta - v|^2}\right]\right)\mathrm{d}\eta,$$

and is bounded on $\mathbb{L}^\infty(\mathcal{D})$ as a consequence of the following estimate on its integral kernel

$$\sqrt{\frac{\beta}{2\pi}}\int \frac{R(\eta)}{|\eta - v|^{d-2}} \exp\left(-\beta\left[\frac{|\eta - v|^2}{8} + \frac{\left(|\eta|^2 - |v|^2\right)^2}{8|\eta - v|^2}\right]\right)\mathrm{d}\eta \leq \frac{17|\mathbb{S}^{d-1}|}{\beta|v|}.$$

Proof. The only difference between both operators is the factor $M_\beta^{\frac{1}{2}}(v)M_\beta^{-\frac{1}{2}}(v') = \exp(\beta(|v|^2 - |\eta|^2)/4)$ in the change of variable of the proof of Lemma 3.3.1, proving the new kernel formula.

Using once again the hyperspherical coordinates (see (2.6) and above), we have

$$\int \frac{\mathrm{d}\eta}{|\eta - v|^{d-2}} e^{-\beta\left[\frac{|\eta-v|^2}{8} + \frac{\left(|\eta|^2-|v|^2\right)^2}{8|\eta-v|^2}\right]} = \int \mathrm{d}r\mathrm{d}J(\underline{\theta}_{d-1}) r e^{-\frac{\beta}{8}\left[r^2 + (r - 2|v|\cos\theta)^2\right]}.$$

Now, one can integrate

$$\int_0^\infty r e^{-\frac{\beta}{8}\left[r^2+(r-2|v|\cos\theta)^2\right]}\mathrm{d}r = \left[\frac{-2}{\beta}e^{-\frac{\beta}{8}\left[r^2+(r-2|v|\cos\theta)^2\right]}\right]_0^\infty + |v|\cos\theta\int_0^\infty r e^{-\frac{\beta}{8}\left[r^2+(r-2|v|\cos\theta)^2\right]}\mathrm{d}r.$$

In the second integral, part of the weight concentrates around 0, and the rest around $2|v|\cos\theta$, so it can be split into

$$\begin{aligned}\int_0^{|v|\cos\theta} e^{-\frac{\beta}{8}\left[r^2+(r-2|v|\cos\theta)^2\right]}\mathrm{d}r &\leq \int_{|v|\cos\theta}^\infty e^{-\frac{\beta}{8}u^2}\mathrm{d}u \\ &\leq \frac{8}{\beta|v|\cos\theta}e^{-\frac{\beta}{8}|v|^2\cos^2\theta}\end{aligned}$$

(bounding by standard estimates on the Gaussian cumulative distribution function), and similarly

$$\int_{|v|\cos\theta}^\infty e^{-\frac{\beta}{8}\left[r^2+(r-2|v|\cos\theta)^2\right]}\mathrm{d}r \leq \frac{8}{\beta|v|\cos\theta}e^{-\frac{\beta}{8}|v|^2\cos^2\theta}.$$

In the end, we get

$$\int_0^\infty r e^{-\frac{\beta}{8}\left[r^2+(r-2|v|\cos\theta)^2\right]}\mathrm{d}r \leq \frac{2}{\beta}e^{-\frac{\beta}{8}[2|v|\cos\theta]^2} + \frac{16}{\beta}e^{-\frac{\beta}{8}|v|^2\cos^2\theta}.$$

It remains to integrate over θ as

$$\int_0^\pi \sin\theta e^{-\frac{\beta}{8}|v|^2\cos^2\theta}\mathrm{d}\theta = \int_{-1}^1 e^{-\frac{\beta}{8}|v|^2x^2}\mathrm{d}x \leq \frac{1}{|v|}\sqrt{\frac{8\pi}{\beta}}.$$

The contribution of the integral over θ to the volume of the sphere is 2, so that the integral over the other angles yields $|\mathbb{S}^{d-1}|/2$. In the end,

$$\int_0^\infty r e^{-\frac{\beta}{8}\left[r^2+(r-2|v|\cos\theta)^2\right]}\mathrm{d}r \leq \frac{|\mathbb{S}^{d-1}|}{2}\left(\frac{2}{\beta}\cdot\frac{1}{|v|}\sqrt{\frac{2\pi}{\beta}} + \frac{16}{\beta}\cdot\frac{1}{|v|}\sqrt{\frac{8\pi}{\beta}}\right),$$

which concludes the proof when multiplying by the factor $\sqrt{\beta(2\pi)^{-1}}$. The kernel is also bounded for small values of $|v|$ in dimensions $d \geqslant 2$, so that the operator is bounded from $\mathbb{L}^\infty(\mathcal{D})$ to itself.

We refer to the introducing Section 1.3.2, and Figure 1.3, for a graphical visualization of the way we displaced the exponential weight by computing the change of unknown. □

3.3.3 Wellposedness of the linear Rayleigh–Boltzmann equation

Thanks to the bound on the modified operator $\hat{\mathcal{K}}$ in Lemma 3.3.3 above, we get the global existence and uniqueness of the original Rayleigh–Boltzmann equation (2.13) in the velocity-weighted space $\mathcal{F}_{1,-\beta/4} \doteq \mathbb{L}^\infty_x\mathbb{L}^\infty_v(M_{\beta/2})$ (see (4.14) for a generalization of this space), endowed with the norm

$$\operatorname*{supess}_{z\in\mathcal{D}}\left|f(z)\exp\left(-\frac{\beta}{4}\|v\|^2\right)\right| < \infty,$$

as for the existence and uniqueness of the following Boltzmann–Hamilton–Jacobi system (3.9). Note that we assume indeed that our initial condition φ_0 is in that space. We refer to the course [2] on Transport and diffusion for details: we want to construct a solution R in the integral formulation

$$\begin{aligned} R(t,z) &= e^{-\int_0^t \nu_\beta(s,v)\mathrm{d}s}R(0,x-tv,v) + \int_0^t \hat{\mathcal{K}}R(s,x+(s-t)v,v)e^{-\int_s^t \nu_\beta(\tau,v)\mathrm{d}\tau}\mathrm{d}s \\ &\doteq e^{-\int_0^t \nu_\beta(s,v)\mathrm{d}s}R(0,x-tv,v) + \Xi R(t,z). \end{aligned}$$

Using the fixed point method, we construct it as

$$R(t,z) \doteq \sum_{n\geqslant 0}\Xi^n\left[e^{-\int_0^t \nu_\beta(s,v)\mathrm{d}s}R(0,x-tv,v)\right],$$

converging thanks to the bound on $\hat{\mathcal{K}}$. We give a bit more details in the following proof of Proposition 3.4.1.

3.4 The Boltzmann–Hamilton–Jacobi system

We expose here a last linear Boltzmann-like system, appearing in the description of the large deviations of the tagged empirical measure of the system, that we call Boltzmann–Hamilton–Jacobi system (see Section 6.6.5, Proposition 6.6.5) . It consists in two linear Rayleigh–Boltzmann equations, one of them constructed forward on an interval $[0,t]$ with an initial condition, the second

one constructed backward with a final condition, both with an additional linear term driven by an observable $\theta_t \in \mathbb{L}^\infty(\mathcal{D})$:

$$\begin{cases} (\partial_s - v\cdot\nabla_x)\chi = -\theta\chi + \displaystyle\int \mathrm{d}v_2\mathrm{d}\omega\langle v - v_2,\omega\rangle_+\Big(M_\beta(v_2')\chi(z') - M_\beta(v_2)\chi(z)\Big) \\ (\partial_s - v\cdot\nabla_x)\eta = +\theta\eta - \displaystyle\int \mathrm{d}v_2\mathrm{d}\omega\langle v - v_2,\omega\rangle_+ M_\beta(v_2)\Big(\eta(z') - \eta(z)\Big), \end{cases} \tag{3.9}$$

of unknowns (χ,η), with the boundary conditions

$$\begin{cases} \chi(0) = M_\beta\varphi_0 \\ \eta(t) = \gamma(t) \in \mathcal{F}_{1,-\beta/4}. \end{cases}$$

It is a linear version of the quadratic case [12, Section 7.2], which has been studied by Chenjiayue Qi in long times in the case of small initial data [55]. Note that their collision operators are identical up to a change of unknown, as discussed at the end of Section 3.2.

To obtain the boundedness of the gain operator appearing in the Rayleigh–Boltzmann equation, we computed a change of unknown that distributed differently the exponential weights. However, doing so, we caused the new gain operator to be greater than the loss factor for small velocities, so that the latter do not compensate totally the gain operator. Because of this, they will not immediately provide a maximum principle.

In the specific case of the system (3.9) that we study here, we have no hope of a maximum principle, because of the gain terms $-\theta_t\chi_t$ and $\theta_t\eta_t$ that depend on the observable θ_t.

We use once again the notation $\mathcal{F}_{1,\beta/4}$ for the set of functions decaying faster than the $\dfrac{\beta}{2}-$Gaussian in velocities.

Proposition 3.4.1 (Wellposedness of the Boltzmann–Hamilton–Jacobi system)**.** *For any time $t > 0$, for a bounded gain weight $\theta \in \mathbb{L}^\infty(\mathcal{D})$, and boundary conditions*

$$\begin{cases} \chi(0) = M_\beta\varphi_0 \in \mathcal{F}_{1,\beta/4} \\ \eta(t) = \gamma(t) \in \mathcal{F}_{1,-\beta/4}, \end{cases}$$

the system (3.9) has a unique global positive solution $(\chi,\eta) \in \mathbb{L}^\infty\Big([0,t],\ \mathcal{F}_{1,\beta/4}\times\mathcal{F}_{1,-\beta/4}\Big)$.

Proof. We will compute a different change of unknown to go from the operators of the Boltzmann–Hamilton–Jacobi system (3.9) to the bounded operator $\hat{\mathcal{K}}$ defined in (3.8). Considering $\chi(0) \in \mathcal{F}_{1,\beta/4}$, we will look at $R(0) \doteq M_\beta^{-\frac{1}{2}}\chi(0) \in \mathbb{L}^\infty(\mathcal{D})$. The existence of a global solution for the first equation of the system (3.9) above, on χ in $\mathcal{F}_{1,\beta/4}$, is thus equivalent to the global existence in $\mathbb{L}^\infty(\mathcal{D})$ of the modified Rayleigh–Boltzmann equation

$$\partial_t R + v\cdot\nabla_x R = \hat{\mathcal{K}}R(v) - \theta R - \nu_\beta(v)R(v),$$

with the modified gain operator $\hat{\mathcal{K}}$, which is shown to be bounded in $\mathbb{L}^\infty(\mathcal{D})$ (Lemma 3.3.3). Hence, the operator $R \mapsto \hat{\mathcal{K}}R - \theta R$ is also bounded for $\theta \in \mathbb{L}^\infty(\mathcal{D})$. Classical results in kinetic theory [2] states that there exists a global unique positive solution to this equation, with the bound, for any time $t \geqslant 0$,

$$\|R(t)\|_{\mathbb{L}^\infty} \leq \|R(0)\|_{\mathbb{L}^\infty}e^{Ct},$$

where the constant C depends on the operators' kernels as

$$C = \sup_{z\in\mathcal{D}}\left[\int_{\mathbb{R}^d}\frac{\sqrt{\beta(2\pi)^{-1}}}{|u-v|^{d-2}}\cdot e^{-\beta\left[\frac{|u-v|^2}{8} + \frac{\left(|u|^2-|v|^2\right)^2}{8|u-v|^2}\right]}\mathrm{d}u \ - \theta(z) - \nu_\beta(v)\right].$$

This concludes the proof, returning to the variable $\chi \in \mathcal{F}_{1,\beta/4}$. The same computation holds backwards in time for η, observing that $M_\beta \eta$ satisfies a linear Boltzmann-like equation with the same collision operator as χ. Note that even in the case $\theta = 0$, one can check that the constant C is positive because of small velocities. In this case nevertheless, one can still prove a maximum principle using more elaborate methods implying a bootstrap argument to fall back in spaces in which a complete spectral study is possible (see for example [35, Section 3.1], or more recently [55]). □

Chapter 4

Long-time convergence of the correlation functions

In this chapter, we show the convergence of the correlation functions (F_n^ε) defined in (2.16) to the family $(M_\beta^{\otimes n}\varphi^{\otimes \ell_n})_{n\geqslant 1}$, where φ is the solution of the linear Rayleigh–Boltzmann equation (2.13). Indeed, this family satisfies the formal limit of the BBGKY hierarchy (2.25) with initial conditions (2.14). This work has been originally written in [32].

Section 4.1 exposes the result, along with the law of large numbers that is its consequence. The following Section 4.2 introduces the crucial concept of pseudo-trajectories, and explains how the strategy of the proof is structured around this object, which is done in the last sections of this paper. Note the presence of Section 4.6, dedicated to the adaptive pruning method used to improve greatly the convergence rate in Theorem 1.

4.1 Convergence result, a law of large numbers

The following theorem provides a convergence rate of the mixed correlation functions to the solutions of the Rayleigh–Boltzmann equation, which is a generalization of [31, 9] with a time scale of validity improved by a power 1/4 thanks to a more precise computation (see the proof of Proposition 4.6.1). Moreover, here for completeness the result is extended to all the correlation functions (not only the first one), yet at the cost of a bad constant n^{cn} stemming from the time cutting method we use. This constant, which did not appear in the convergence of the first marginal, is due to an accumulation of errors at each time step of our cutting. Note finally that we use the pruning method discussed in the introducing Section 1.6, with the adaptive time cutting introduced in [31], improving greatly the convergence rate compared to [9]. Note that Section 9.4 introduces an alternative method, based on a large deviation argument, to get rid of the bad constant n^{cn} in an $\mathbb{L}^1$ framework.

Theorem 1 (Convergence of the correlation functions)**.** *For some sets $\Delta_n^\varepsilon \subset \mathcal{D}^n$ whose measure goes to 0 with ε, there exists a constant c_β depending only on the temperature and the dimension such that, for any $\alpha \in (0, 3/4)$, as long as*

$$t \lesssim (\log|c_\beta \log\varepsilon|)^{\frac{3}{4}-\alpha} \quad \text{and} \quad \lambda \lesssim |\log\varepsilon|^{1-\alpha}, \tag{4.1}$$

and for ε small enough, one has the following convergence rate of the correlation functions to the linear Rayleigh–Boltzmann solutions in our mixed low density scaling ($S_{\varepsilon,\mu,\lambda}$), for a constant $c > 0$;

$$\|F_n^\varepsilon - M_\beta^{\otimes n}\varphi^{\otimes \ell_n}\|_{\mathbb{L}^\infty([0,t]\times\mathcal{D}^n\setminus\Delta_n^\varepsilon)} \leq n^{cn}\exp\left(-c_\beta|\log\varepsilon|^{1-\alpha}\right).$$

The notation $t \lesssim (\log|c_\beta \log\varepsilon|)^{\frac{3}{4}-\alpha}$ means that, for a good constant $c>0$ depending only on the dimension d and the inverse temperature β, one has

$$t \leq c\,(\log|c_\beta \log\varepsilon|)^{\frac{3}{4}-\alpha}.$$

The proof of this theorem is the subject of Sections 4.2 to 4.8. It is close to the proof presented in [31], but in the mixed grand canonical framework and for all the correlation functions instead of the first marginal only.

This theorem provides a first corollary on the statistical behaviour of the gas. Recall the definitions (2.21) of the empirical measures

$$\pi_t^\varepsilon[H] \doteq \frac{1}{\mu}\sum_{i=1}^{\mathcal{N}} H(Z_{\varepsilon,i}^{[t]}, L_i),$$

along with its tagged version

$$\tilde{\pi}_t^\varepsilon[H] \doteq \frac{1}{\lambda}\sum_{i=1}^{\mathcal{N}} H(Z_{\varepsilon,i}^{[t]}, L_i)\mathbb{1}_{L_i=1}.$$

Thanks to Theorem 1, one can deduce the convergence of these empirical measures, hence providing a law of large numbers for the hard sphere dynamics. This result is given in the space $\mathbf{L}^2$ of *square-integrable random variables*, embedded with the norm $\mathbb{E}\left[|\cdot|^2\right]$.

Corollary 4.1.1 (Law of large numbers for the dynamics)**.** *The empirical measures converge as random variables in* $\mathbf{L}^2$*, the non-tagged particles towards an equilibrium state, and the tagged ones to a state described by the linear Rayleigh–Boltzmann equation* (2.13)*, in the following way*

$$\pi_t^\varepsilon[H] \xrightarrow[\varepsilon\to 0]{\mathbf{L}^2} \int M_\beta(v)H(z,0)\mathrm{d}z, \tag{4.2}$$

and

$$\tilde{\pi}_t^\varepsilon[H] \xrightarrow[\varepsilon\to 0]{\mathbf{L}^2} \int M_\beta(v)\varphi(t,z)H(z,1)\mathrm{d}z. \tag{4.3}$$

Proof. To show that the random variable $\pi_t^\varepsilon[H]$ converges in $\mathbf{L}^2$ to a deterministic limit $a\in\mathbb{R}$, writing

$$\pi_t^\varepsilon[H] - a = \pi_t^\varepsilon[H] - \mathbb{E}\big[\pi_t^\varepsilon[H]\big] + \mathbb{E}\big[\pi_t^\varepsilon[H]\big] - a,$$

it is enough to show that $\mathbb{E}\big[\pi_t^\varepsilon[H]\big] \xrightarrow[\varepsilon\to 0]{} a$ and $\mathbb{E}\left[\left|\pi_t^\varepsilon[H] - \mathbb{E}\big[\pi_t^\varepsilon[H]\big]\right|^2\right] \xrightarrow[\varepsilon\to 0]{} 0$. Using formula (2.19), one can write

$$\mathbb{E}\left[\frac{1}{\mu}\sum_{i=1}^{\mathcal{N}} H(Z_{\varepsilon,i}^{[t]}, L_i)\right] = \int F_1^\varepsilon(t,z_1,0)H(z_1,0)\mathrm{d}z_1 + \frac{\lambda}{\mu}\int F_1^\varepsilon(t,z_1,1)H(z_1,1)\mathrm{d}z_1,$$

so that the expectancies converge by Theorem 1 above. For concision, we show the fact that the variance vanishes in the tagged case, denoting $h \doteq H(\cdot,1)$. The equilibrium case is treated in a similar though simpler way. Let us compute, once again by formula (2.19),

$$\begin{aligned}
\mathbb{E}\left[\left|\tilde{\pi}_t^\varepsilon - \mathbb{E}\big[\tilde{\pi}_t^\varepsilon[H]\big]\right|^2\right] &= \frac{1}{\lambda^2}\mathbb{E}\left[\sum_{i,j=1}^{n} h(Z_{\varepsilon,i}^{[t]})h(Z_{\varepsilon,j}^{[t]})\right] - \frac{2}{\lambda}\mathbb{E}\left[\sum_{i=1}^{n} h(Z_{\varepsilon,i}^{[t]})\int F_1^\varepsilon(1)h\right] + \left(\int F_1^\varepsilon(1)h\right)^2 \\
&= \int F_2^\varepsilon(1,1)h^{\otimes 2} + \frac{1}{\lambda}\int F_1^\varepsilon(1)h^2 - 2\left(\int F_1^\varepsilon(1)h\right)^2 + \left(\int F_1^\varepsilon(1)h\right)^2 \\
&\xrightarrow[\varepsilon\to 0]{} \int M_\beta^{\otimes 2}\varphi^{\otimes 2} + 0 - \left(\int M_\beta\varphi\right)^2 = 0,
\end{aligned}$$

thanks to the convergence of the correlation functions (Theorem 1). The other convergence (4.2) follows similarly in our scaling ($S_{\varepsilon,\mu,\lambda}$), using the fact that $\dfrac{\lambda}{\mu}$ goes to 0. □

4.2 Pseudo-trajectories and strategy of proof

We denote $p_\mu \doteq \dfrac{\lambda}{\mu}$ the fraction of initially perturbed particles, so that iterating Duhamel formula as in [34] or [9], we can write the Dyson expansion

$$F_n^\varepsilon(t) = \sum_{k\geqslant 0} \sum_{\underline{\ell}_k^* \in \Lambda_k} p_\mu^{|\underline{\ell}_k^*|} Q_{n,\underline{\ell}_k^*}(t) F_{n+k}^\varepsilon(0), \tag{4.4}$$

developing the choice of the encountered tags $\underline{\ell}_k^* \doteq (\tilde{\ell}_{n+1}, \dots, \tilde{\ell}_{n+k})$, with the successive-collision operators defined as

$$Q_{n,\underline{\ell}_k^*}(t) \doteq \int_{T_k(t)} \Theta_n(t-t_1)\mathcal{C}_n^{\tilde{\ell}_{n+1}}\Theta_{n+1}(t_1-t_2)\dots\mathcal{C}_{n+k-1}^{\tilde{\ell}_{n+k}}\Theta_{n+k}(t_k)\mathrm{d}\underline{t}_k, \tag{4.5}$$

where $\Theta_n(\tau)$ denotes the transport semi-group operator in $\mathcal{D}_n^\varepsilon$ with specular reflections, for a time τ. The collision times are integrated over

$$T_k(t) \doteq \Big\{ \underline{t}_k \;\Big|\; 0 \doteq t_{k+1} \leq t_k \leq \dots \leq t_1 \leq t_0 \doteq t \Big\}. \tag{4.6}$$

The main idea of the proof, coming from Lanford's original paper [45], is to use a coupling between this expansion and its limit version, implying imaginary histories of the particles, among those that eventually lead to the state $\underline{z}_n$ at time t. These histories, called *pseudo-trajectories*, are non-physical trajectories that—in a way—allow to extend the method of characteristics for the successive-collision operators.

Indeed, the transport operators appearing in (4.5) correspond to following the characteristics of free transport, with specular reflections: taking the first operator $\Theta_n(t-t_1)$ of a functional is equivalent to considering this functional at time t_1, in a state $\underline{z}_n^{[t_1]}$ given by the backwards hard sphere dynamics.

Then, the first collision operator (2.26) writes

$$\mathcal{C}_n^\ell F_{n+1}^\varepsilon = \sum_{i=1}^n \sum_{s_1=\pm 1} s_1 \int \mathrm{d}\omega_1 \mathrm{d}v_{n+1} \langle \omega_1, v_{n+1}-v_i\rangle_+ F_{n+1}^\varepsilon(\underline{z}_n^{\langle s_1\rangle}, \underline{\ell}_n, x_i + s_1\varepsilon\omega_1, v_{n+1}^{\langle s_1\rangle}, \ell),$$

where $\underline{z}_n^{\langle +1\rangle} = \underline{z}_n^\star$ and $\underline{z}_n^{\langle -1\rangle} = \underline{z}_n$, scattered for the gain term, and let unchanged for the loss term, so that the collision is always incoming, allowing to pursue the backwards method of characteristics with the next transport operator. Hence, for given collision parameters $(i, s_1, \omega_1, v_{n+1})$, this operator can be seen as a weighted adjunction of a particle to the characteristics—or pseudo-trajectory—which scatters (or not, according to s_1) with particle i, creating a new state $\underline{z}_{n+1}^{[t_1]} \doteq (\underline{z}_n^{[t_1]}, x_i + s_1\varepsilon\omega_1, v_{n+1}^{\langle s_1\rangle})$. The integration and sum over these collision parameters will yield an integral over pseudo-trajectories. Iterating this extended method of characteristics and tracking the pseudo-trajectories $(\underline{z}_{n+j}^{[t_j]})$ thus constructed, we bring the analysis back to the value of the functional at time $\tau = 0$, in the state $\underline{z}_{n+k}^{[0]}$.

We will have to record the numbering labels of the existing particles meeting the new ones, the velocities of the particles that spring up, the angles at which the encounters happen, and whether they scatter or not. The pseudo-trajectories will also keep track of the tags of the encountered particles.

Here is precisely how we construct the pseudo-trajectories. The choice of the successive encountered tags is registered in $\underline{\ell}_k^* = (\tilde{\ell}_{n+1}, \dots, \tilde{\ell}_{n+k})$, and expanding all the sums in all the collision operators (4.5), we can sum them up to the history $(m_1, \dots, m_k)$ of which particle encountered the $(n+i)$-th new one. These particles naturally belong to the following set

$$\mathcal{M}_{n,k} \doteq \Big\{ (m_1, \dots, m_k) \;\Big|\; \forall i \leq k, m_i \leq n+i-1 \Big\}.$$

We consider the scattering labels $(s_1, \dots, s_k) \in \{\pm 1\}^k$. The fact that some encounters do not scatter, along with the fact that some particles are artificially added, is why the pseudo-trajectories are not physical trajectories. Once the total history

$$\chi_k \doteq (\underline{m}_k, \underline{\ell}_k^*, \underline{s}_k) \in \mathcal{H}_{n,k} \doteq \mathcal{M}_{n,k} \times \Lambda_k \times \{\pm 1\}^k \tag{4.7}$$

is fixed, for given collision parameters $(\underline{\omega}_k, v_{n+1}, \dots, v_{n+k})$, we can construct the pseudo-trajectories for every endstate $\underline{z}_n = \underline{z}_n^{[t]}$, backwards in time to an initial configuration $\underline{z}_{n+m}^{[0]}$, following the inductive procedure below:

$$\begin{cases} \underline{z}_n^{[t]} \doteq \underline{z}_n \\ \forall\ i \in [\![0, k]\!],\ \forall \tau \in (t_{i+1}, t_i),\ \underline{z}_{n+i}^{[\tau]} \text{ follows (backwards) the physical hard sphere dynamics} \\ \forall\ i \in [\![1, k]\!],\ \underline{z}_{n+i}^{[t_i]} = \left(\underline{z}_{n+i-1}^{[t_i^+], \langle s_i \rangle}, x_{m_i} + s_i \varepsilon \omega_i, v_{n+1}^{\langle s_i \rangle} \right). \end{cases} \tag{4.8}$$

One may observe that the change of velocities in the last step is automatic by the hard sphere dynamics' boundary condition, but it will not be for the limit version of pseudo-trajectories, since the limit particles are formally pointwise. In the end, one can write the *pseudo-trajectory formulation* of the Dyson expansion

$$F_n^\varepsilon(t) = \sum_{k \geqslant 0} \sum_{\chi_k} p_\mu^{|\underline{\ell}_k^*|} \int_{T_k(t)} \mathrm{d}\underline{t}_k \int \mathrm{d}\underline{\omega}_k \mathrm{d}v_{n+1} \dots \mathrm{d}v_{n+k} \prod_{i=1}^k s_i \langle \omega_i, v_{n+i} - v_{m_i}^{[t_i^+]} \rangle_+ F_{n+k}^\varepsilon(0, \underline{z}_{n+k}^{[0]}, \underline{\tilde{\ell}}_{n+k}). \tag{4.9}$$

A small technical detail lies in the fact that the added particles must satisfy the exclusion condition. A way to deal with it may be to impose a condition on the domain of integration of the collision angles [12], yet here to simplify we merely change the definition of the pseudo-trajectories: if at any moment the exclusion condition is violated by the adjunction of a particle, then the trajectories are frozen in this state until time $\tau = 0$, so that the integral formally vanishes thanks to the initial distribution $F_{n+k}^\varepsilon(0)$ being 0 outside of $\mathcal{D}_{n+k}^\varepsilon$.

Figure 4.1 pictures the backwards contruction of a pseudo-trajectory, in one dimension, for a given history $\underline{m}_3 = (1, 1, 2)$ with scattering labels $\underline{s}_3 = (+1, +1, -1)$. One can observe a recollision between times $\tau = 0$ and t_3, due to the hard sphere flow. A paramount stake in the following study will be to avoid these recollisions, since as one will see, they are absent from the limit pseudo-trajectories defined below.

Our goal is now to prove the convergence of the correlation functions to the **limit densities**

$$G_n(t, \underline{z}_n, \underline{\ell}_n) \doteq M_\beta^{\otimes n}(\underline{v}_n) \varphi^{\otimes \underline{\ell}_n}(t, \underline{z}_{\underline{\ell}_n}),$$

where φ is the solution of the linear Rayleigh–Boltzmann equation (2.13). Because of the structure of this equation, this family satisfies the following hierarchy

$$(\partial_t + \underline{v} \cdot \nabla_{\underline{x}}) G_n = \sum_{i=1}^n \sum_{s_c = \pm 1} s_c \int \mathrm{d}\omega \mathrm{d}v_{n+1} \langle \omega, v_{n+1} - v_i \rangle_+ G_{n+1}(\underline{z}_n^{\langle s_c \rangle}, \underline{\ell}_n, x_i, v_{n+1}^{\langle s_c \rangle}, 0), \tag{4.10}$$

noticing that the terms vanish when the scattering occur between two particles distributed according to the equilibrium $M_\beta^{\otimes n}$. This equation is the formal limit of the BBGKY hierarchy (2.25) in the mixed low density regime ($S_{\varepsilon,\mu,\lambda}$): it makes only appear the collision operator linked to equilibrum particles, tagged 0, since the other one has a factor λ/μ that vanishes at the limit. It leads to the following limit version of the Dyson expansion (4.4)

$$G_n(t) = \sum_{k \geqslant 0} Q_{n, \underline{0}_k}^{\lim}(t) G_{n+k}(0), \tag{4.11}$$

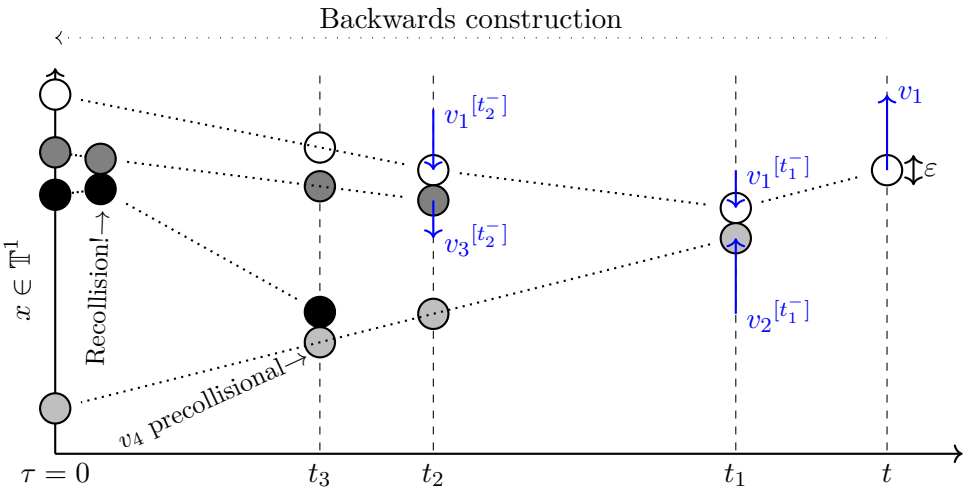

Figure 4.1: Backwards construction of a 1D-pseudo-trajectory

where the following successive-collision operators contain only collisions with particles at equilibrium, and limit free transport of pointwise particles, without scattering:

$$Q^{\lim}_{n,\underline{0}_k}(t) \doteq \int_{T_k(t)} \Theta^{\lim}_n(t-t_1)\mathcal{C}^{\langle 0\rangle,\lim}_n \Theta^{\lim}_{n+1}(t_1-t_2)\dots\mathcal{C}^{\langle 0\rangle,\lim}_{n+k-1}\Theta^{\lim}_{n+k}(t_k)\mathrm{d}\underline{t}_k. \tag{4.12}$$

The limit collision operators $\mathcal{C}^{\langle 0\rangle,\lim}_n$ are the formal limit of the collision operators (2.26), for $\varepsilon = 0$. The same computation as below for this limit hierarchy leads to a similar writing in terms of pseudo-trajectories

$$G_n(t) = \sum_{k\geqslant 0}\sum_{\underline{\chi}_k} \mathbb{1}_{\underline{\ell}^*_k=\underline{0}_k}\int_{T_k(t)}\mathrm{d}\underline{t}_k\int \mathrm{d}\underline{\omega}_k\mathrm{d}v_{n+1}\dots\mathrm{d}v_{n+k}\prod_{i=1}^{k} s_i\langle\omega_i, v_{n+i}-v^{[t_i^+]}_{m_i}\rangle_+ G_{n+k}(0,\underline{\zeta}^{[0]}_{n+k},\underline{\tilde{\ell}}_{n+k}), \tag{4.13}$$

where the limit pseudo-trajectories $(\underline{\zeta}^{[t_i]}_{n+i})_{i\leqslant k}$ are defined as their hard sphere versions (4.8) for $\varepsilon = 0$, with the noticeable difference that in the dynamics followed on each time interval (t_{i+1}, t_i), the particles are pointwise and hence follow the free flow without any scattering.

Strategy of proof We will couple both pseudo-trajectory formulations (4.9) and (4.13), bringing down the difference at a certain time $(F^\varepsilon_n - G_n)(t,\underline{z}_n)$ to the difference at time 0 of higher correlation functions $\left[F^\varepsilon_{n+k}(0,\underline{z}^{[0]}_{n+k}) - G_{n+k}(0,\underline{\zeta}^{[0]}_{n+k})\right]$. For these hierarchies to be well coupled, the two pseudo-trajectories must be close; the classical argument is to show that the transport operators Θ_k, appearing between the collision operators, do not imply additional recollisions, since the trajectories would diverge from the limit transport operator $\Theta^{\lim}_k$, defined on the whole space $\mathcal{D}^k$ without recollisions.

Indeed with this method, it will be enough to use **continuity estimates** on the operators to bring the convergence back to time $\tau = 0$ where we can use explicit **initial proximity**. Nevertheless, these continuity estimates demand to work with trajectories that do not contain too many particles, so that we will first compute a **tree pruning**, and control the pruned-out term using some **a priori estimates** on the densities. The last step before proving the **convergence** will be to **discard the pseudo-trajectories** in which some perturbed particles are encountered, as this situation does not happen in the limit pseudo-trajectories. This strategy will be followed in the following sections.

4.3 Initial proximity

The total kinetic energy, preserved at fixed number of particles by the transport and by elastic collisions, will be denoted

$$\|\underline{v}_k\|^2 \doteq \sum_{i=1}^{k} |v_i|^2,$$

where $|v_i|$ is the Euclidean norm of the velocity $v_i \in \mathbb{R}^d$ of particle i. For an inverse temperature $\beta > 0$ and $k \in \mathbb{N}^*$, we consider the space $\mathcal{F}_{k,\beta}$ of measurable functions defined almost everywhere on the domain $\mathcal{D}^k$ such that

$$\|f_k\|_{k,\beta} \doteq \operatorname*{supess}_{\underline{z}_k \in \mathcal{D}^k} |f_k(\underline{z}_k) \exp(\beta \|\underline{v}_k\|^2)| < \infty, \tag{4.14}$$

hence decreasing at least as the Gaussian equilibrium $M_{2\beta}^{\otimes k}$ in velocities. We denote

$$C_0 \doteq \max \left[\|M_\beta\|_{1,\beta/2} \; ; \; \|M_\beta \varphi_0\|_{1,\beta/4} \; ; \; \left\| M_\beta M_{\beta/2}^{-\frac{1}{2}} \varphi_0 \right\|_{\mathbb{L}^\infty(\mathcal{D})} \right]. \tag{4.15}$$

The initial error between the microscopic densities and the limit ones is mainly due to the exclusion condition, of which we can compute an explicit control.

Proposition 4.3.1 (Initial proximity)**.** *For all $n \in \mathbb{N}$ and tags $\underline{\ell}_n \in \Lambda_n$, for any $\lambda, \mu > 0$ in the scaling ($S_{\varepsilon,\mu,\lambda}$), one has*

$$\left\| \mathbb{1}_{\mathcal{X}_n^\varepsilon} M_\beta^{\otimes n} \varphi_0^{\otimes \underline{\ell}_n} - F_n^\varepsilon(0, \underline{\ell}_n) \right\|_{n,\beta/4} \leq C_0^n \varepsilon. \tag{4.16}$$

Proof of the proposition. We denote $\mathbb{1}_{i \not\sim j} \doteq \mathbb{1}_{d(x_i,x_j)>\varepsilon}$ and $\mathbb{1}_{i \sim j} \doteq \mathbb{1}_{d(x_i,x_j)\leq\varepsilon}$ the indicator of exclusion between i and j and its complementary. Recalling that $\mathbb{1}_{\mathcal{X}_N^\varepsilon}$ denotes the exclusion condition (2.1) and by definition (2.17) of the partition function $\mathcal{Z}_\mu$, we can write, once again denoting $\tilde{\underline{\ell}}_{n+p} \doteq (\underline{\ell}_n, \underline{\ell}_p^*)$:

$$\begin{aligned}
&\mathbb{1}_{\mathcal{X}_n^\varepsilon} M_\beta^{\otimes n} \varphi_0^{\otimes \underline{\ell}_n} - F_n^\varepsilon(0) \\
&\quad = \frac{1}{\mathcal{Z}_\mu} \sum_{p \geqslant 0} \frac{1}{p!} \left[\sum_{\underline{\ell}_p^* \in \Lambda_p} \lambda^{|\underline{\ell}_p^*|} \mu^{p - |\underline{\ell}_p^*|} \mathbb{1}_{\mathcal{X}_n^\varepsilon} M_\beta^{\otimes n} \varphi_0^{\otimes \underline{\ell}_n} \int \varphi_0^{\otimes \underline{\ell}_p^*} M_\beta^{\otimes p} \mathbb{1}_{\mathcal{X}_p^\varepsilon} - \left(\varphi_0^{\otimes \tilde{\underline{\ell}}_{n+p}} M_\beta^{\otimes n+p} \mathbb{1}_{\mathcal{X}_{n+p}^\varepsilon} \right)^{(n)} \right].
\end{aligned}$$

Expanding the marginals' formula (2.15), the following term appears, in which we decompose the exclusion indicator $\mathbb{1}_{\mathcal{X}_{n+p}^\varepsilon}$ as

$$\begin{aligned}
&\mathbb{1}_{\mathcal{X}_n^\varepsilon} M_\beta^{\otimes n} \varphi_0^{\otimes \underline{\ell}_n} \int \varphi_0^{\otimes \underline{\ell}_p^*} M_\beta^{\otimes p} \mathbb{1}_{\mathcal{X}_p^\varepsilon} - \int \varphi_0^{\otimes \tilde{\underline{\ell}}_{n+p}} M_\beta^{\otimes n+p} \mathbb{1}_{\mathcal{X}_{n+p}^\varepsilon} \mathrm{d}\underline{z}_p^* \\
&\qquad = \mathbb{1}_{\mathcal{X}_n^\varepsilon} M_\beta^{\otimes n} \varphi_0^{\otimes \underline{\ell}_n} \int (M_\beta \varphi_0)^{\otimes \underline{\ell}_p^*} (\underline{z}_{\underline{\ell}_p^*}^*) \mathbb{1}_{\mathcal{X}_p^\varepsilon}(\underline{x}_p^*) \left(1 - \prod_{\substack{1 \leqslant i \leqslant n \\ 1 \leqslant j \leqslant p}} \mathbb{1}_{x_i \not\sim x_j^*} \right) \mathrm{d}\underline{x}_p^* \underline{v}_{\underline{\ell}_p^*}^*,
\end{aligned}$$

using that M_β is of integral 1. Then, we will harness the following basic set property,

$$1 - \prod_{\substack{1 \leqslant i \leqslant n \\ 1 \leqslant j \leqslant p}} \mathbb{1}_{x_i \not\sim x_j^*} \leq \sum_{\substack{1 \leqslant i \leqslant n \\ 1 \leqslant j \leqslant p}} \mathbb{1}_{x_i \sim x_j^*},$$

yielding

$$\left| \mathbb{1}_{\mathcal{X}_n^\varepsilon} M_\beta^{\otimes n} \varphi_0^{\otimes \underline{\ell}_n} - F_n^\varepsilon(0) \right| \leq \frac{\mathbb{1}_{\mathcal{X}_n^\varepsilon} M_\beta^{\otimes n} \varphi_0^{\otimes \underline{\ell}_n}}{\mathcal{Z}_\mu} \sum_{p \geqslant 0} \sum_{\underline{\ell}_p^* \in \Lambda_p} \frac{\lambda^{|\underline{\ell}_p^*|} \mu^{p - |\underline{\ell}_p^*|}}{p!} \sum_{\substack{1 \leqslant i \leqslant n \\ 1 \leqslant j \leqslant p}} \int (M_\beta \varphi_0)^{\otimes \underline{\ell}_p^*} \mathbb{1}_{\mathcal{X}_p^\varepsilon} \mathbb{1}_{x_i \sim x_j^*} \mathrm{d}\underline{x}_p^* \mathrm{d}\underline{v}_{\underline{\ell}_p^*}^*.$$

To be able to integrate over x_j^*, we denote $\underline{\check{\ell}}_p^{(j)} \doteq (\ell_1^*, \dots, \ell_{j-1}^*, \ell_{j+1}^*, \dots, \ell_p^*)$ the vector of all tags apart from j. Using the definition (4.15) of C_0 and summing over ℓ_j^*, we get

$$\begin{aligned}
&\left\| \mathbb{1}_{\mathcal{X}_n^\varepsilon} M_\beta^{\otimes n} \varphi_0^{\otimes \underline{\ell}_n} - F_n^\varepsilon(0) \right\|_{n,\beta} \\
&\qquad \leq \frac{C_0^n}{\mathcal{Z}_\mu} \sum_{p \geqslant 0} \sum_{\substack{1 \leqslant i \leqslant n \\ 1 \leqslant j \leqslant p}} \sum_{\underline{\check{\ell}}_p^{(j)} \in \Lambda_{p-1}} \frac{\lambda^{|\underline{\check{\ell}}_p^{(j)}|} \mu^{p-1-|\underline{\check{\ell}}_p^{(j)}|}}{p!} (\lambda C_0 + \mu) \int (M_\beta \varphi_0)^{\otimes \underline{\check{\ell}}_p^{(j)}} \mathbb{1}_{\mathcal{X}_p^\varepsilon} \mathbb{1}_{x_i \sim x_j^*} \\
&\qquad \leq \frac{C_0^n}{\mathcal{Z}_\mu} \sum_{p \geqslant 0} np \sum_{\underline{\ell}_{p-1}^* \in \Lambda_{p-1}} \frac{\lambda^{|\underline{\ell}_{p-1}^*|} \mu^{p-1-|\underline{\ell}_{p-1}^*|}}{p!} 2\mu |\mathbb{S}^{d-1}| \varepsilon^d \int (M_\beta \varphi_0)^{\otimes \underline{\ell}_{p-1}^*} \mathbb{1}_{\mathcal{X}_{p-1}^\varepsilon}
\end{aligned}$$

using the exchangeability of identical particles, integrating over x_j^* and using the fact that $C_0 \lambda < \mu$. We get in the mixed low density scaling ($S_{\varepsilon,\mu,\lambda}$)

$$\left\| \mathbb{1}_{\mathcal{X}_n^\varepsilon} M_\beta^{\otimes n} \varphi_0^{\otimes \underline{\ell}_n} - F_n^\varepsilon(0) \right\|_{n,\beta} \leq 2|\mathbb{S}^{d-1}| \varepsilon \frac{C_0^n}{\mathcal{Z}_\mu} n \sum_{p \geqslant 1} \sum_{\underline{\ell}_{p-1}^* \in \Lambda_{p-1}} \frac{\lambda^{|\underline{\ell}_{p-1}^*|} \mu^{p-1-|\underline{\ell}_{p-1}^*|}}{(p-1)!} \int (M_\beta \varphi_0)^{\otimes \underline{\ell}_{p-1}^*} \mathbb{1}_{\mathcal{X}_{p-1}^\varepsilon},$$

which concludes the proof recognizing the partition function $\mathcal{Z}_\mu$ (2.17) after an index shift. □

4.4 A priori estimates

As in the previous works [9, 31] about the Rayleigh gas, the long-time derivation is allowed thanks to a priori estimates yielded by the rigid structure of the equilibrium. Here, some additional technical difficulties, dealt with in Section 5.4, appear in the proof of these estimates because of the structure of the grand canonical mixture and its partition function. First, let us observe that the initial canonical densities defined in (2.14) satisfy for all $(\underline{z}_n, \underline{\ell}_n) \in \mathcal{D}^n \times \Lambda_n$ that

$$W_n^\varepsilon(0, \underline{z}_n, \underline{\ell}_n) \leq \frac{\lambda^{|\underline{\ell}_n|} \mu^{n-|\underline{\ell}_n|}}{\mathcal{Z}_\mu} \left\| M_\beta M_{\beta/2}^{-\frac{1}{2}} \varphi_0 \right\|_{\mathbb{L}^\infty}^{|\underline{\ell}_n|} M_{\beta/2}^{\otimes n}(\underline{v}_n) \mathbb{1}_{\mathcal{X}_n^\varepsilon}(\underline{x}_n). \tag{4.17}$$

Since their evolution is simply given by the global transport of n particles, by which the equilibrium $M_{\beta/2}^{\otimes n} \mathbb{1}_{\mathcal{X}_n^\varepsilon}$ is invariant, for all times $t \geq 0$ the bound (4.17) is propagated by the transport and remains true. Hence, taking the marginals we get

$$\begin{aligned}
W_n^{\varepsilon,(k)}(t, \underline{z}_k, \underline{\ell}_k) &\leq \sum_{\underline{\ell}_{n-k}^* \in \Lambda_{n-k}} \frac{(\lambda C_0)^{|\underline{\ell}_k| + |\underline{\ell}_{n-k}^*|} \mu^{n-|\underline{\ell}_k|-|\underline{\ell}_{n-k}^*|}}{\mathcal{Z}_\mu} M_{\beta/2}^{\otimes k}(\underline{v}_k) \left(\mathbb{1}_{\mathcal{X}_n^\varepsilon} \right)^{(k)} (\underline{x}_k) \\
&\leq (\lambda C_0 + \mu)^{n-k} \frac{(\lambda C_0)^{|\underline{\ell}_k|} \mu^{k-|\underline{\ell}_k|}}{\mathcal{Z}_\mu} M_{\beta/2}^{\otimes k}(\underline{v}_k) \mathbb{1}_{\mathcal{X}_n^\varepsilon}^{(k)}(\underline{x}_k),
\end{aligned}$$

where the factor $(\lambda C_0 + \mu)^{n-k}$ stems from the sum over $\underline{\ell}_{n-k}^*$, using the binomial theorem. The main difference in the linear case, compared to the general non-linear one, is that the bound (4.17) on the canonical densities uses the invariant density $M_{\beta/2}^{\otimes n}$, that passes to the k-th marginals to become $M_{\beta/2}^{\otimes k}$, contrary to the constant C_0^n in the general case.

Eventually, these bounds over the marginals of the canonical densities leaves the following a priori

estimate for the correlation functions

$$\begin{aligned} F_n^\varepsilon(t,\underline{z}_n,\underline{\ell}_n) &\leq \frac{M_{\beta/2}^{\otimes n}}{\mu^{n-|\underline{\ell}_n|}\lambda^{|\underline{\ell}_n|}} \sum_{p\geqslant 0} \frac{1}{p!} \frac{(\lambda C_0+\mu)^p (\lambda C_0)^{|\underline{\ell}_n|}\mu^{n-|\underline{\ell}_n|}}{\mathcal{Z}_\mu} \mathbb{1}_{\mathcal{X}_{n+p}^\varepsilon}^{(n)} \\ &\leq \frac{C_0^{|\underline{\ell}_n|} M_{\beta/2}^{\otimes n}}{\mathcal{Z}_\mu} \sum_{p\geqslant 0} \frac{(\lambda C_0+\mu)^p}{p!} \int \mathbb{1}_{\mathcal{X}_p^\varepsilon} \\ &\leq \frac{C_0^{|\underline{\ell}_n|} M_{\beta/2}^{\otimes n}}{\mathcal{Z}_\mu} \sum_{q,r\geqslant 0} \frac{(\lambda C_0)^q \mu^r}{q!r!} \int \mathbb{1}_{\mathcal{X}_{q+r}^\varepsilon} \end{aligned} \tag{4.18}$$

where at line (4.18) we computed a direct binomial theorem. The key point to end our a priori estimate is now to control the remaining quotient implying the partition function $\mathcal{Z}_\mu$ and the slightly modified version of it, which is the following proposition.

Proposition 4.4.1. *There exists a constant C_d depending only on the dimension such that for μ large enough, in our mixed Boltzmann-Grad scaling ($S_{\varepsilon,\mu,\lambda}$), we have*

$$\frac{1}{\mathcal{Z}_\mu} \sum_{q,r\geqslant 0} \frac{(\lambda C_0)^q \mu^r}{q!r!} \int \mathbb{1}_{\mathcal{X}_{q+r}^\varepsilon} \leq C_d^{C_0\lambda}.$$

The proof of this technical result is given in Section 5.4, using an explicit expansion of the partition function according to the cumulants of the exclusion. Eventually, this leads to the following proposition, which is the main argument of our long time analysis.

Proposition 4.4.2 (A priori estimates for the correlation functions)**.** *For any $n \in \mathbb{N}$ and $\varepsilon > 0$ in the mixed scaling ($S_{\varepsilon,\mu,\lambda}$), one has*

$$F_n^\varepsilon(t,\underline{z}_n,\underline{\ell}_n) \leq C_0^{|\underline{\ell}_n|} M_{\beta/2}^{\otimes n} \times C^{C_0\lambda}. \tag{4.19}$$

4.5 Continuity estimates

Thanks to the a priori estimates (4.19) given in the previous Section 4.4, all the correlation functions (F_n^ε) extended by 0 out of $\mathcal{D}_n^\varepsilon$ belong to the space $\mathcal{F}_{n,\beta/4}$ defined in (4.14).

In the following, up to change the initial temperature β to 4β, to simplify the notation in the computation below we will assume that they belong to the space $\mathcal{F}_{n,\beta}$, with

$$\sup_{t\geqslant 0} \|F_n^\varepsilon(t)\|_{n,\beta} \leq C_0^n C^{C_0\lambda}, \tag{4.20}$$

thanks to the estimates above, and similarly for the initial proximity, from Proposition 4.3.1,

$$\left\| \mathbb{1}_{\mathcal{X}_n^\varepsilon} M_\beta^{\otimes n} \varphi_0^{\otimes \underline{\ell}_n} - F_n^\varepsilon(0,\underline{\ell}_n) \right\|_{n,\beta} \leq C_0^n \varepsilon. \tag{4.21}$$

Our whole long time derivation is allowed thanks to the fact that the a priori bounds (4.20) are valid for every time with the same inverse temperature β. Indeed, in the non-linear case, this parameter is downgraded over time until vanishing in finite time [34, Section 5].

Technically, the downgrading of this norm parameter stems from the fact that to control the collision operators, the sum over the velocities is resorbed thanks to a fraction of the sub-Gaussian decreasing, eventually providing the following continuity estimates.

Proposition 4.5.1 (Continuity of the successive-collision operators)**.**
There exists a constant C_d depending only on the dimension such that for all $n, s \in \mathbb{N}^*$, and all times $t > 0$, fixing tags $\underline{\ell}_s \in \Lambda_k$ and choosing two inverse temperature $\beta' < \beta$, we have

$$f_{n+s} \in \mathcal{F}_{n+s,\beta} \Rightarrow Q_{n,\underline{\ell}_s}(t) f_{n+s} \in \mathcal{F}_{n,\beta'}, \text{ with}$$

$$\left\| Q_{n,\underline{\ell}_s}(t) f_{n+s} \right\|_{n,\beta'} \leq e^n \left(\frac{C_d\, t}{\sqrt{\beta^d(\beta - \beta')}} \right)^s \|f_{n+s}\|_{n+s,\beta}. \tag{4.22}$$

The proof of this proposition is written in [31], adapted from the article by Bodineau, Gallagher and Saint-Raymond [9].

Proof. First of all, let us observe that the transport operators preserve all of the weighted norms $(\| \cdot \|_{n,\beta})_{n,\beta}$, since the weight depends only on the kinetic energy of the system. In the following, we fix the tags $\underline{\ell}_s$ and omit to write them, as they do not change the bounds on the collision operators.

Recall the definition (4.5) of the successive-collision operators. Then, for $j \leq N$, let us compute for $f_{j+1} \in \mathcal{F}_{j+1,\beta}$, making appear its $\| \cdot \|_{j+1,\beta}$ norm,

$$\begin{aligned}
\left| \Theta_j(-\tau) \mathcal{C}_j \Theta_{j+1}(\tau) f_{j+1} \right| &\leq \left| \Theta_j(-\tau) \sum_{i=1}^{j} \int \omega \cdot (v_{j+1} - v_i) \Theta_{j+1}(\tau) f_{j+1}(\underline{z}_j, x_i + \varepsilon\omega, v_{j+1}) \mathrm{d}\omega \mathrm{d}v_{j+1} \right| \\
&\leq \sum_{i=1}^{j} \int_{\mathbb{S}^{d-1} \times \mathbb{R}^d} (|v_{j+1}| + |v_i|) \|f_{j+1}\|_{j+1,\beta} \exp\left[-\beta \|\underline{v}_{j+1}\|^2 \right] \mathrm{d}\omega \mathrm{d}v_{j+1} \\
&= |\mathbb{S}^{d-1}| \cdot \|f_{j+1}\|_{j+1,\beta} \sum_{i=1}^{j} \int_{\mathbb{R}^d} (|v_{j+1}| + |v_i|) \exp\left[-\beta \sum_{k=1}^{j+1} |v_k|^2 \right] \mathrm{d}v_{j+1}.
\end{aligned}$$

The latter integrals may be written explicitly, up to constants depending only on the dimension d, after a radial change of variable and a dilation by $\beta^{-\frac{1}{2}}$,

$$\begin{aligned}
\int (|v_{j+1}| + |v_i|) \exp\left[-\beta \sum_{k=1}^{j+1} |v_k|^2 \right] \mathrm{d}v_{j+1} &= C_d \int (r + |v_i|) \exp\left[-\beta \sum_{k=1}^{j} |v_k|^2 \right] r^{d-1} e^{-\beta r^2} \mathrm{d}r \\
&= C_d \exp\left[-\beta \|\underline{v}_j\|^2 \right] \left(c_d \sqrt{\beta^{-(d+1)}} + |v_i| \tilde{c}_d \sqrt{\beta^{-d}} \right).
\end{aligned} \tag{4.23}$$

This way, applying this to f_{n+s}, summing (4.23) over i and accepting to downgrade by $(\beta - \beta')/s$ the considered norm so as to later resorb the factors $|v_i|$, we get that

$$\begin{aligned}
&\left\| \Theta_{n+s-1}(-t_s) \mathcal{C}_{n+s-1} \Theta_{n+s}(t_s) f_{n+s} \right\|_{n+s-1,\beta-(\beta-\beta')/s} \\
&\quad \leq \widetilde{C}_d \left((n+s-1) \sqrt{\beta^{-(d+1)}} + \sqrt{\beta^{-d}} \sum_{i=1}^{n+s-1} |v_i| \right) \exp\left[-\frac{\beta - \beta'}{s} \|\underline{v}_{n+s-1}\|^2 \right] \|f_{n+s}\|_{n+s,\beta}.
\end{aligned} \tag{4.24}$$

But using the Cauchy–Schwarz inequality and the fact that $xe^{-x} \leq e^{-1}$ for any $x \geq 0$, we have

$$\begin{aligned}
\left(\sum_{i=1}^{n+s-1} |v_i| \right) \exp\left[-\frac{\beta - \beta'}{s} \sum_{k=1}^{n+s-1} |v_k|^2 \right] &\leq \left(\frac{s(n+s-1)}{2(\beta - \beta')} \right)^{\frac{1}{2}} \left(2 \frac{\beta - \beta'}{s} \|\underline{v}_{n+s-1}\|^2 \right)^{\frac{1}{2}} e^{-\frac{\beta - \beta'}{s} \|\underline{v}_{n+s-1}\|^2} \\
&\leq \frac{(n+s)}{\sqrt{2e}\sqrt{\beta - \beta'}},
\end{aligned} \tag{4.25}$$

so that (4.24) yields

$$\left\|\Theta_{n+s-1}(-t_s)\mathcal{C}_{n+s-1}\Theta_{n+s}(t_s)f_{n+s}\right\|_{n+s-1,\beta-(\beta-\beta')/s} \leq \frac{\widehat{C}_d(n+s)}{\beta^{\frac{d}{2}}\sqrt{\beta-\beta'}}\|f_{n+s}\|_{n+s,\beta}.$$

To retrieve $Q_{n,\underline{\ell}_s}(t)$, we have to iterate this calculus s times, downgrading the norm parameter by $(\beta-\beta')/s$ at each step. In the end, we get

$$\begin{aligned}\left\|Q_{n,\underline{\ell}_s}(t)f_{n+s}\right\|_{n,\beta'} &\leq \left(\overline{C}_d(n+s)\sqrt{\beta^{-d}(\beta-\beta')^{-1}}\right)^s \int_{0\leq t_s\leq\cdots\leq t_1\leq t} \mathrm{d}t_1\cdots\mathrm{d}t_s\|f_{n+s}\|_{n+s,\beta}\\ &\leq \left(\overline{C}_d\sqrt{\beta^{-d}(\beta-\beta')^{-1}}\right)^s (n+s)^s\ \frac{t^s}{s!}\ \|f_{n+s}\|_{n+s,\beta}\\ &\leq \left(\overline{C}_d\sqrt{\beta^{-d}(\beta-\beta')^{-1}}\right)^s e^{n+s}\ t^s\ \|f_{n+s}\|_{n+s,\beta}\ ,\end{aligned}$$

where the factor $s!$ comes from the imposed order of collision times $t_s \leq \cdots \leq t_1$, and allows to control the term $(n+s)^s$, concluding the proof. □

4.6 Adaptive tree pruning of the Dyson expansion for long times

The continuity estimates presented in the previous section justify the wellposedness of the Dyson series (4.4) for short times. To perform a derivation for long times, we will iterate the Dyson series, but each iteration will make appear a factor e^n stemming from the estimate of Proposition 4.5.1. These factors stack, so that, without further adjustment, at each iteration the successive times would decrease extremely fast and their sum would eventually be summable, leaving the derivation on a finite short time (see Section 9.2 for details). The method we use here, introduced in [9], consists in putting aside these stacking factors e^n and to control them by bounding the number of collisions appearing in the Dyson series.

More precisely, for a fixed time $t > 1$ we will split the time interval $[0,t]$ into K pieces and impose a piece-dependent amount of collisions on each small interval of this cutting. The number K will be tuned in the end of the proof, and henceforth we write

$$t = \sum_{i=1}^{K} h_i, \text{ with time steps } t_k^{\mathrm{p}} \doteq t - \sum_{j=1}^{k} h_i, \tag{4.26}$$

so that $t_K^{\mathrm{p}} = 0$. Like in [31], and contrary to [9], we will not choose a uniform cutting, but an adaptive one. At the k-th time quantum of length h_k, we want at most 2^k collisions to have happened; we prune the collision tree every time it becomes more than exponentially big. Explicitly, between t and $t_1^{\mathrm{p}} = t - h_1$, we first truncate the Dyson series (4.4) to 2 collisions, then expand it again between $t-h_1$ and $t-h_2$ truncated to 2^2 collisions, and iterate this process K times.

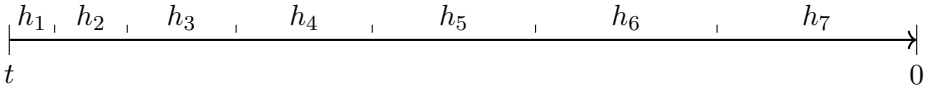

Figure 4.2: Backwards division of the time interval under study

We denote the step number of added tagged particles and the step total number of particles

$$L_k \doteq \sum_{i=1}^{k} |\underline{\ell}_{j_i}^*| \quad \text{and} \quad N_k \doteq n + j_1 + \cdots + j_k. \tag{4.27}$$

This yields, similarly as in [9, 31], the following pruned expansion

$$F_n^\varepsilon(t) = \sum_{\substack{(j_i \leqslant 2^i \\ \underline{\ell}^*_{j_i} \in \Lambda_{j_i})_{1\leqslant i\leqslant K}}} p_\mu^{L_K} Q_{n,\underline{\ell}^*_{j_1}}(h_1)\dots Q_{N_{K-1},\underline{\ell}^*_{j_K}}(h_K) F^\varepsilon_{N_K}(0) + R_n^{[K]}(t) \tag{4.28}$$

where the remainder is defined as

$$R_n^{[K]}(t) \doteq \sum_{k=1}^{K} \sum_{\substack{(j_i \leqslant 2^i \\ \underline{\ell}^*_{j_i} \in \Lambda_{j_i})_{i\leqslant k-1}}} Q_{n,\underline{\ell}^*_{j_1}}(h_1)\dots Q_{N_{k-2},\underline{\ell}^*_{j_{k-1}}}(h_{k-1}) \sum_{j_k > 2^k} \sum_{\underline{\ell}^*_{j_k} \in \Lambda_{j_k}} p_\mu^{L_k} Q_{N_{k-1},\underline{\ell}^*_{j_k}}(h_k) F^\varepsilon_{N_k}(t_k^{\mathrm{p}}). \tag{4.29}$$

Based on the limit expansion (4.11), one can write the same decomposition for the limit family $(G_n)_{n\geqslant 0}$:

$$G_n(t) = \sum_{(j_i \leqslant 2^i)_{1\leqslant i\leqslant K}} Q^{\lim}_{n,\underline{0}_{j_1}}(h_1)\dots Q^{\lim}_{N_{K-1},\underline{0}_{j_K}}(h_K) G_{N_K}(0) + R_n^{[K],\lim}(t). \tag{4.30}$$

Let us denote $\widehat{G}_n(t) \doteq G_n(t) - R_n^{[K],\lim}(t)$ the limit pruned expansion. Since the chosen condition of a sub-exponential number of collisions is very restrictive at first, and then gradually relaxed, the adaptive cutting times are chosen small at first and then progressively bigger (see Fig. 4.2). Figure 4.3 pictures why one talks about pruning trees: one could think of the procedure as removing exceeding collisions in the trees drawn by the pseudo-trajectories, yet formally we rather discard entirely the pseudo-trajectories containing too many collisions. The bound on the pruned-out remainder is given in the following proposition.

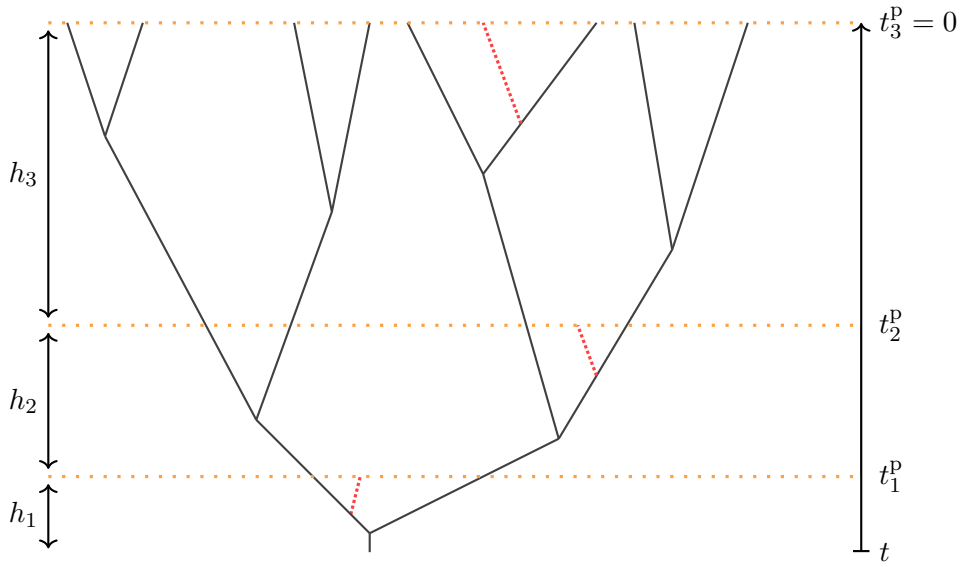

Figure 4.3: Pruning out the collisions exceeding the maximal amount (dotted in red) on each interval

Proposition 4.6.1 (Estimate of the pruned-out term)**.** *With the previous notation, for any choice of power $\alpha \in (0, 3/4)$, and K large enough satisfying $t \lesssim K^{\frac{3}{4}-\alpha}$, a good choice of time cutting*

$$\underline{h} = (h_1, \dots, h_K)$$

provides the following estimate

$$\left\| R_n^{[K]}(t) \right\|_{\mathbb{L}^\infty(\mathcal{D}^d)} + \left\| R_n^{[K],\lim}(t) \right\|_{\mathbb{L}^\infty(\mathcal{D}^d)} \leq C^{C_0\lambda} n^{cn} e^{-2^{K-K^\alpha}}. \tag{4.31}$$

Note that this estimate imposes a technical condition on the mixed scaling of λ and K for the error to be small; we will tune this scaling in Section 4.8. The factor n^{cn} stems from the fact that we generalize the result to all the correlation functions, and not only the first one. Indeed, one will see that this factor is due to the usual bound C^n stacking at each iteration of the cutting.

Proof. The proof is very similar to the one found in [31]. We give it for the hard sphere version, since the limit version is identical. Using the a priori estimates (4.19) on the densities and the continuity estimate on successive-collision operators given in Proposition 4.5.1, at given $(\underline{\ell}^*_{j_i})_{i\leq k-1}$ one has for every $k \in [\![1, K]\!]$

$$\begin{aligned}\left\| \sum_{j_k>2^k} \sum_{\underline{\ell}^*_{j_k}\in\Lambda_{j_k}} p_\mu^{L_k} Q_{N_{k-1},\underline{\ell}^*_{j_k}}(h_k) F^\varepsilon_{N_k}(t^{\mathrm{p}}_k) \right\|_{N_{k-1},\beta/2} &\leq e^{N_{k-1}} \sum_{j_k>2^k} \sum_{\underline{\ell}^*_{j_k}\in\Lambda_{j_k}} p_\mu^{L_k} \left(\frac{\sqrt{2}C_d h_k}{\beta^{(d+1)/2}}\right)^{j_k} \left\|F^\varepsilon_{N_k}(t^{\mathrm{p}}_k)\right\|_{N_k,\beta} \\ &\leq e^{N_{k-1}} \sum_{j_k>2^k} \sum_{\underline{\ell}^*_{j_k}\in\Lambda_{j_k}} p_\mu^{L_k} \left(\frac{\sqrt{2}C_d h_k}{\beta^{(d+1)/2}}\right)^{j_k} C^{N_k} C^{C_0\lambda}.\end{aligned}$$

For μ large enough in the scaling $(S_{\varepsilon,\mu,\lambda})$, we have $p_\mu \leq 1$, so that the sum over $\underline{\ell}^*_{j_k} \in \Lambda_{j_k}$ only gives a factor 2^{N_k} that can be resorbed in the term C^{N_k}. We then iterate Proposition 4.5.1, downgrading the parameter $\beta/2$ by $\beta/(4k)$ at each step, so that it remains greater than $\beta/4$. Hence we can write, grouping $C^{N_{k-1}}$ and all the appearing terms of the form e^{N_i} together as a power of a constant $\hat{C}$, that

$$\begin{aligned}&\left\| Q_{n,\underline{\ell}^*_{j_1}}(h_1)\dots Q_{N_{k-2},\underline{\ell}^*_{j_{k-1}}}(h_{k-1}) \sum_{j_k>2^k} \sum_{\underline{\ell}^*_{j_k}\in\Lambda_{j_k}} p_\mu^{L_k} Q_{N_{k-1},\underline{\ell}^*_{j_k}}(h_k) F_{N_k}(t^{\mathrm{p}}_k) \right\|_{n,\beta/4} \\ &\leq C^{C_0\lambda} \hat{C}^{\sum_{i=0}^{k-1} N_i} \left(\left(\frac{4}{\beta}\right)^{\frac{d+1}{2}} \sqrt{4k} C_d h_1\right)^{j_1} \dots \left(\left(\frac{4}{\beta}\right)^{\frac{d+1}{2}} \sqrt{4k} C_d h_{k-1}\right)^{j_{k-1}} \sum_{j_k>2^k} \left(\frac{\sqrt{2}C_d h_k}{\sqrt{\beta}}\right)^{j_k}.\end{aligned} \tag{4.32}$$

We now observe, on the one hand, that recalling notation (4.27) for N_i and since for $i \leq k-1$, $j_i \leq 2^i$, we have $\sum_{i=0}^{k-1} N_i \leq nk + 2^{k+1}$. On the other hand, we can also put aside from the sum the following factors

$$\left(\left(\frac{4}{\beta}\right)^{\frac{d+1}{2}} 2k^{\frac{1}{4}-\alpha} C_d\right)^{\sum_{i=0}^{k-1} j_i} \leq (\hat{C}_\beta k^{\frac{1}{4}-\alpha})^{2^k}.$$

This computation is what allows us to gain a power $\frac{1}{4}$ on the time scaling that we imposed in Theorem 1, compared to [31]. Indeed, in the following, the computation above harnesses the full power decay of the last time interval h_k, whereas some of it was lost in [31]. In the end, for a possibly larger constant C depending on d and β, we get

$$\left\|R^{[K]}_n(t)\right\|_{\mathbb{L}^\infty} \leq C^{C_0\lambda} \sum_{k=1}^{K} C^{nk} (Ck^{\frac{1}{4}-\alpha})^{2^k} \sum_{j_1=0}^{2} \dots \sum_{j_{k-1}=0}^{2^{k-1}} (k^{\frac{1}{4}+\alpha} h_1)^{j_1} \dots (k^{\frac{1}{4}+\alpha} h_{k-1})^{j_{k-1}} \sum_{j_k>2^k} (Ch_k)^{j_k}.$$

Eventually, we consider similarly as in [31], for all $1 \leq i \leq K$,

$$\tilde{h}_i \doteq \frac{e^{-2^{(K-K^{1-\alpha}-i)}}}{2K^{\frac{1}{4}+\alpha}} \leq \frac{1}{2K^{\frac{1}{4}+\alpha}}, \tag{4.33}$$

and renormalize them such that

$$h_i \doteq \frac{t}{\sum_{j=1}^{K} \tilde{h}_j} \tilde{h}_i \leq \tilde{h}_i.$$

Indeed, as soon as $t \lesssim K^{\frac{3}{4}-2\alpha}$, we can write

$$\begin{aligned}\frac{1}{t}\sum_{i=1}^{K}\tilde{h}_i &\geq \frac{1}{t}\sum_{j=0}^{\lfloor K^{1-\alpha}\rfloor}\tilde{h}_{K-j}\\ &\geq \frac{1}{t}\sum_{j=0}^{\lfloor K^{1-\alpha}\rfloor}\frac{e^{-1}}{2K^{\frac{1}{4}+\alpha}} \geq 1.\end{aligned}$$

Now, the time interval lengths $(h_i)_{1\leqslant i\leqslant K}$ cover t as imposed by (4.26), and their choice provides, summing the geometric series over $(j_i)_{1\leqslant i\leqslant K}$,

$$\begin{aligned}\left\|R_n^{[K]}(t)\right\|_{\mathbb{L}^\infty} &\leq C^{C_0\lambda}\sum_{k=1}^{K}C^{nk}(Ck^{\frac{1}{4}-\alpha})^{2^k}\times 2^k\sum_{j_k>2^k}\left(\frac{e^{-2^{K-K^{1-\alpha}-k}}}{2K^{\frac{1}{4}+\alpha}}\right)^{j_k}\\ &\leq C^{C_0\lambda}\sum_{k=1}^{K}C^{nk}\left(\frac{CK^{\frac{1}{4}-\alpha}}{K^{\frac{1}{4}+\alpha}}\right)^{2^k}\left(\frac{e^{-2^{K-K^{1-\alpha}-k}}}{2}\right)^{2^k}.\end{aligned}$$

Observe now that there exists a constant c such that $(k \geq c\log n) \Rightarrow (nk \leq 2^k)$, so that in this case the factor C^{nk} is absorbed by C^{2^k}, and for $k \leq c\log n$, then $C^{nk} \leq C^{cn\log n} = n^{(c\log C)n}$. Now, the denominator $K^{\frac{1}{4}+\alpha}$ crushes the term $CK^{\frac{1}{4}-\alpha}$ for K large enough and we end up with

$$\left\|R_n^{[K]}(t)\right\|_{\mathbb{L}^\infty} \leq C^{C_0\lambda}\tilde{C}^{n\log n}e^{-2^{K-K^{1-\alpha}}}.$$

This completes the proof of Proposition 4.6.1. □

4.7 Discarding trajectories implying several labelled particles

Since the limit pseudo-trajectories defined from the limit hierarchy (4.13) only imply collisions with particles at equilibrium (which are in wide majority), we must get rid of the ones including collisions with perturbed tagged particles. We hence write our pruned expansion as

$$\begin{aligned}&\sum_{\substack{(j_i\leqslant 2^i\\ \underline{\ell}^*_{j_i}\in\Lambda_{j_i})_{1\leqslant i\leqslant K}}} p_\mu^{L_K}Q_{n,\underline{\ell}^*_{j_1}}(h_1)\dots Q_{N_{K-1},\underline{\ell}^*_{j_K}}(h_K)F^\varepsilon_{N_K}(0)\\ &\quad= \sum_{(j_i\leqslant 2^i)_{1\leqslant i\leqslant K}} Q_{n,\underline{0}_{j_1}}(h_1)\dots Q_{N_{K-1},\underline{0}_{j_K}}(h_K)F^\varepsilon_{N_K}(0) \qquad (4.34)\\ &\quad\quad+\sum_{(j_i\leqslant 2^i)}\sum_{k=1}^{K}\sum_{\substack{(\underline{\ell}^*_{j_i})_{i\leqslant K}\\ \underline{\ell}^*_{j_k}\neq\underline{0}_{j_k}}} p_\mu^{L_K}Q_{n,\underline{\ell}^*_{j_1}}(h_1)\dots Q_{N_{K-1},\underline{\ell}^*_{j_K}}(h_K)F^\varepsilon_{N_K}(0), \qquad (4.35)\\ &\quad\doteq \widehat{F}^\varepsilon_n(t)+F^{\varepsilon,\text{u.e.}}_n(t),\end{aligned}$$

where we denote $\widehat{F}^\varepsilon_n(t)$ the main term (4.34) containing only collisions with equilibrium, and $F^{\varepsilon,\text{u.e.}}_n(t)$ the one implying unwanted encounters (4.35). We bound the latter in the following proposition.

Proposition 4.7.1 (Encountering tagged particles is rare)**.** *As long as*

$$p_\mu \leq \frac{1}{2^K},$$

in the same time setting as in Proposition 4.6.1, the unwanted pseudotrajectories implying tagged particles are bounded by

$$\|F^{\varepsilon,\text{u.e.}}_n(t)\|_{\mathbb{L}^\infty(\mathcal{D}^d)} \leq C^{nK+A^K}\ p_\mu. \qquad (4.36)$$

The reader may think of the factor C^{A^K} as a small negative power of ε in the final scaling, which we will compute in the following Section 4.8: the scaling proportion p_μ will have to compensate it.

Proof of the proposition. A computation directly adapted from the initial proximity bound (4.21) leads to the estimate

$$\left\| F^\varepsilon_{N_K}(0, \tilde{\underline{\ell}}_{N_K}) \right\|_{N_K,\beta} \leq (C_0)^{N_K},$$

so that, using the binomial identity

$$\sum_{\underline{\ell}^*_{j_i} \in \Lambda_{j_i}} p_\mu^{|\underline{\ell}^*_{j_i}|} = (1+p_\mu)^{j_i}$$

and the same continuity estimates on the successive-collision operators as in the proof of Proposition 4.6.1, one has

$$\|F_n^{\varepsilon,\mathrm{u.e.}}(t)\|_{\mathbb{L}^\infty(\mathcal{D}^d)} \leq C^{nK}(CK^{\frac{1}{4}-\alpha})^{2^K} \sum_{(j_i \leqslant 2^i)_{i\leqslant K}} \sum_{k=1}^K \left((1+p_\mu)^{j_k}-1\right) \prod_{i=1}^K \left(\frac{1}{2}\right)^{j_i}.$$

Notice on the one hand that

$$\begin{aligned}(CK^{\frac{1}{4}-\alpha})^{2^K} &= \exp\left[2^K \log(CK^{\frac{1}{4}-\alpha})\right] \\ &\leq \exp\left(A^K\right)\end{aligned}$$

for any $A > 2$ as long as K is large enough (depending on A). On the other hand, using $j_k \leq 2^k$ and taking $p_\mu \leq 2^{-K} \leq 2^{-k}$, we have by convexity on $[0, 2^{-k}]$ that

$$\begin{aligned}(1+p_\mu)^{j_k} - 1 &\leq (1+p_\mu)^{2^k} - 1 \\ &\leq (e-1)2^k p_\mu,\end{aligned}$$

so that eventually

$$\begin{aligned}\|F_n^{\varepsilon,\mathrm{u.e.}}(t)\|_{\mathbb{L}^\infty(\mathcal{D}^d)} &\leq (e-1)p_\mu \times C^{nK+A^K} \sum_{k=1}^K 2^k \sum_{(j_i\leqslant 2^i)_{i\leqslant K}} \prod_{i=1}^K \left(\frac{1}{2}\right)^{j_i} \\ &\leq p_\mu\ \widehat{C}^{nK+A^K}\end{aligned}$$

for another constant $\widehat{C}$ absorbing the factor $(e-1)2^{K+1} \times 2^K$, concluding the proof. □

4.8 Proof of the convergence

Now that the pruned-out terms have been controlled, we want to compare the pruned terms $\widehat{F}^\varepsilon_n(t)$ and $\widehat{G}_n(t)$, which is the last step before our choice of scaling for K and the conclusion of Theorem 1. As explained in Section 4.2, our strategy relies on considering pseudo-trajectories without recollisions. This method is an adaptation of [9, Section 5] which is now classical; it follows from several approximations: an energy truncation and a time separation of the collisions are operated, so as to be able to construct a small set of bad collision parameters, outside of which there will be no recollision.

This time separation method does not yield the best quantitative estimates, but in our study in long time the worst error is made with the pruned-out terms, so that here we use this method anyway. This allows concision on the one hand, and on the other hand one can thus compare it with the optimized method presented in Chapter 8.

Like in [31], we still refine the quantitative bounds using the same control on

$$Q_{n,\underline{\ell}^*_{j_1}}(h_1)\dots Q_{N_{K-1},\underline{\ell}^*_{j_K}}(h_K)$$

as in Propositions 4.6.1 and 4.7.1, which induces our factor ${C_\beta}^{nK+A^K}$, instead of the original crude bound with $|Q|_{1,J_k}(t)$, which gave a factor $(Ct)^{2^K}$ (see [9]). From a physical perspective, we decompose the time interval into small pieces whose lengths are adapted to the maximum number of particles that may appear in them, so that the dynamics behaves similarly during each one of them. Hence, as long as time does not get too big with respect to the number of pieces, none of the estimates depends on the total time length.

Pseudo-trajectory formulation First of all, let us notice that the pruned expansion (4.28) has a pseudo-trajectory formulation similar to the original one (4.9), summing over the successive numbers of collisions $(j_i \leq 2^i)_{i\leq K}$, with the following additional condition on the collision times, located between the time steps (4.26):

$$\underline{t}_{J_K} \in T_{\underline{j}_K}(t) \doteq \Big\{(t_1,\dots,t_{J_K}) \in T_{J_K}(t)\ ,\ \{t_{J_k+1},\dots,t_{J_{k+1}}\} \subset [t^{\mathrm{p}}_{k+1}, t^{\mathrm{p}}_k]\Big\},$$

where $J_K \doteq N_K - n = j_1 + \dots + j_K$ denotes the step number of collisions. As announced above, we start by computing a few approximations, initiated by an energy truncation, so as to work with bounded velocities.

Energy truncation We hence consider the following functionals with truncated energy

$$\widehat{F}^{\varepsilon,[\mathbf{V}]}_n(t) \doteq \sum_{\underline{j}_K} \sum_{L_K=0}^{\chi_{J_K}} \int_{T_{\underline{j}_K}(t)} \mathrm{d}\underline{t}_{J_K} \int \mathrm{d}\underline{\omega}_{J_K} \mathrm{d}v_{n+1}\dots\mathrm{d}v_{N_K} \prod_{i=1}^{J_K} s_i\langle \omega_i, v_{n+i} - v^{[t_i^+]}_{m_i}\rangle_+ \times F^{\varepsilon}_{N_K}(0,\underline{z}^{[0]}_{N_K})\mathbb{1}_{\left\|\underline{v}^{[0]}_{N_K}\right\|^2 \leqslant \mathbf{V}^2}, \tag{4.37}$$

and similarly the truncated limit functions $\widehat{G}^{[\mathbf{V}]}_n$. The error made by truncating the velocities is

$$\widehat{F}^{\varepsilon}_n(t) - \widehat{F}^{\varepsilon,[\mathbf{V}]}_n(t) = \sum_{(j_i\leqslant 2^i)} Q_{n,\underline{0}_{j_1}}(h_1)\dots Q_{N_{K-1},\underline{0}_{j_K}}(h_K)\left[F^{\varepsilon}_{N_K}(0)\mathbb{1}_{\left\|\underline{v}^{[0]}_{N_K}\right\|^2 \geqslant \mathbf{V}^2}\right],$$

with the following estimate on the initial functional on the right:

$$\begin{aligned}\left\|F^{\varepsilon}_{N_K}(0,\underline{z}^{[0]}_{N_K},\underline{\tilde{\ell}}_{N_K})\mathbb{1}_{\left\|\underline{v}^{[0]}_{N_K}\right\|^2 \geqslant \mathbf{V}^2}\right\|_{N_K,\beta/2} &\leq \sup_{\underline{u}_{N_K}\in\mathbb{R}^{dN_K}} \left|F^{\varepsilon}_{N_K}(0) e^{\beta\left\|\underline{u}_{N_K}\right\|^2} e^{-\frac{\beta}{2}\left\|\underline{u}_{N_K}\right\|^2} \mathbb{1}_{\left\|\underline{u}_{N_K}\right\|^2 \geqslant \mathbf{V}^2}\right| \\ &\leq \left\|F^{\varepsilon}_{N_K}(0)\right\|_{N_K,\beta} e^{-\frac{\beta}{2}\mathbf{V}^2}.\end{aligned}$$

Hence, applying the same bounds as in Propositions 4.6.1 and 4.7.1 in the same setting, we end up with the following lemma.

Lemma 4.8.1 (Energy truncation error)**.** *The error due to the energy truncation is bounded by*

$$\|\widehat{F}^{\varepsilon}_n(t) - \widehat{F}^{\varepsilon,[\mathbf{V}]}_n(t)\|_{\mathbb{L}^\infty} \leq C^{nK+A^K} \exp\left(-\frac{\beta}{2}\mathbf{V}^2\right). \tag{4.38}$$

The same holds for its limit version $\widehat{G}_n(t) - \widehat{G}^{[\mathbf{V}]}_n(t)$.

Time separation We now need the successive collisions to be separated enough in time, to avoid pathological geometric recollisions. Like in the previous section, let us define

$$\widehat{F}_n^{\varepsilon,[\mathbf{V},\delta]}(t) \doteq \sum_{\underline{j}_K} \sum_{\substack{\chi_{J_K} \\ L_K=0}} \int_{T^{[\delta]}_{\underline{j}_K}(t)} \mathrm{d}\underline{t}_{J_K} \int \mathrm{d}\underline{\omega}_{J_K} \mathrm{d}v_{n+1} \dots \mathrm{d}v_{N_K} \prod_{i=1}^{J_K} s_i \langle \omega_i, v_{n+i} - v_{m_i}^{[t_i^+]} \rangle_+ \times F^{\varepsilon}_{N_K}(0, \underline{z}^{[0]}_{N_K}) \mathbb{1}_{\left\| \underline{v}^{[0]}_{N_K} \right\|^2 \leqslant \mathbf{V}^2}, \tag{4.39}$$

with the separation condition encoded in the following time set, over which we integrate,

$$T^{[\delta]}_{\underline{j}_K}(t) = \left\{ \underline{t} \in T_{\underline{j}_K}(t) \ , \ t_{i-1} - t_i > \delta \right\}. \tag{4.40}$$

The limit version $\widehat{G}_n^{[\mathbf{V},\delta]}$ is defined by the same time restriction. The error of time separation is

$$\widehat{F}_n^{\varepsilon,[\mathbf{V}]} - \widehat{F}_n^{\varepsilon,[\mathbf{V},\delta]} \doteq \sum_{\underline{j}_K} \sum_{\substack{\chi_{J_K} \\ L_K=0}} \int_{\left(T^{[\delta]}_{\underline{j}_K}(t)\right)^c} \mathrm{d}\underline{t}_{J_K} \int \mathrm{d}\underline{\omega}_{J_K} \mathrm{d}v_{n+1} \dots \mathrm{d}v_{N_K} \times \prod_{i=1}^{J_K} s_i \langle \omega_i, v_{m_i}^{[t_i^+]} - v_{n+i} \rangle_+ \times F^{\varepsilon}_{N_K}(0, \underline{z}^{[0]}_{N_K}) \mathbb{1}_{\left\| \underline{v}^{[0]}_{N_K} \right\|^2 \leqslant \mathbf{V}^2},$$

where one can write

$$\left(T^{[\delta]}_{\underline{j}_K}(t)\right)^c = \bigcup_{i=1}^{J_K - 1} \left\{ \underline{t} \in T_{\underline{j}_K}(t) \ , \ t_i - t_{i+1} \leqslant \delta \right\}. \tag{4.41}$$

Now, the integral in time over one of these sets, using the same method as before, changes the estimate of the corresponding successive-collision operator from $\frac{h_k^{j_k}}{j_k!}$ to $\frac{\delta h_k^{j_k - 1}}{(j_k - 1)!}$. Since the loss of $\frac{h_k}{j_k}$ and the factor $(J_K - 1)$ coming from the union (4.41) easily resorb into the bigger factor C^{A^K}, we get in the end the following lemma.

Lemma 4.8.2 (Time separation error)**.** *For this error, we have the following estimate*

$$\| \widehat{F}_n^{\varepsilon,[\mathbf{V}]} - \widehat{F}_n^{\varepsilon,[\mathbf{V},\delta]} \|_{\mathbb{L}^\infty} \leq C^{mK + A^K} \delta. \tag{4.42}$$

Once again, the same holds for its limit version $\widehat{G}_n^{[\mathbf{V}]} - \widehat{G}_n^{[\mathbf{V},\delta]}$ for similar reasons.

Restriction to non-pathological collision parameters Finally, at fixed ε, we have to restrict the collision parameters to non-pathological configurations, leading to no recollision during the transport flow. Figure 4.4 illustrates, in a cartoonish way, how choosing wisely the collision angle and velocity of the collision on the right of the figure can allow to avoid the cone of outgoing velocities that would lead to a recollision of both particles. First, to compute the convergence of the n-th marginal, we have to consider final configurations $\underline{z}_n = \underline{z}_n^{[t]}$ that do not directly lead to recollisions, i.e. that belong to the following set of past-excluding configurations, with some extra room $\varepsilon_d \doteq \varepsilon^{\frac{d}{d+1}}$:

$$\mathcal{E}_n^t(\varepsilon_d) \doteq \left\{ \underline{z}_n \in \mathcal{D}_n^{\varepsilon} \ \middle| \ \forall \tau \in [0,t], \ (\underline{x}_n - \tau \underline{v}_n) \in \mathcal{D}_n^{\varepsilon_d} \right\}. \tag{4.43}$$

This set is the whole domain for $n = 1$, like in [9, 31]. Then, the restriction on the collision parameters is done based on the following geometric result, proved in [34, 9] and formalizing the arguments of Lanford [45], based on billiards theory.

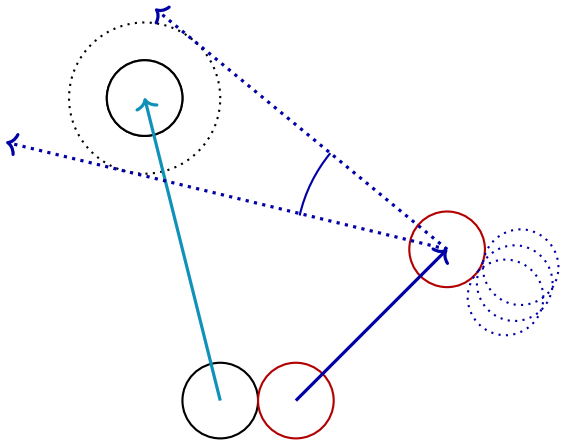

Figure 4.4: Identifying collision parameters leading to recollisions

Similarly to the notation $\underline{z}_n^{[\tau]} = (\underline{x}_n^{[\tau]}, \underline{v}_n^{[\tau]})$ for the hard sphere pseudo-trajectories, let us denote $\underline{\zeta}_n^{[\tau]} = (\underline{y}_n^{[\tau]}, \underline{u}_n^{[\tau]})$ the limit pseudo-trajectories, and $N[\tau]$ the number of particles in the trajectory at time $\tau \in [0,t]$, from $N[t] = n$ to $N[0] = N_K$. Hence, the following lemma asserts that once the previous truncations computed, choosing collision parameters away from a set of small measure, the hard sphere and limit pseudo-trajectories are easy to compare. The proof of this lemma relies on similar geometric estimates as one can find in Chapter 8, in which we perform a similar study for different objects.

Lemma 4.8.3. *Considering a history $(\underline{j}_K, \underline{\chi}_{J_K})$ with collision times $\underline{t}_{J_K} \in T^{[\delta]}_{\underline{j}_K}(t)$ (δ-separated) and a final configuration $\underline{z}_n^{[t]}$, given a maximum energy $\mathbf{V}^2 > 0$, there exists a set of pathological collision parameters*

$$\Pi(\underline{z}_n^{[t]}, \underline{j}_K, \underline{\chi}_{J_K}) \subset (\mathbb{S}^{d-1} \times \mathbb{R}^d)^{J_K}$$

with small volume

$$|\Pi(\underline{z}_n^{[t]}, \underline{j}_K, \underline{\chi}_{J_K})| \leq C J_K N_K \left(\varepsilon^{\frac{d}{d+2}} + \mathbf{V}^d \times \varepsilon^{\frac{d-1}{3(d+1)}} + \mathbf{V}^{\frac{d+1}{2}} \left(\frac{\varepsilon^{\frac{d}{d+1}}}{\delta} \right)^{\frac{d-1}{2}} \right), \tag{4.44}$$

and such that, assuming

i. the collision parameters are non-pathological: $(\underline{\omega}_{J_K}, v_{n+1}, \dots, v_{N_K}) \notin \Pi(\underline{z}_n^{[t]}, \underline{j}_K, \underline{\chi}_{J_K})$

ii. the energy of the corresponding pseudo-trajectory remains bounded: $\|\underline{v}_{N_K}^{[0]}\|^2 \leq \mathbf{V}^2$

iii. the final configuration is past-excluding for the free-flow: $\underline{z}_n^{[t]} \in \mathcal{E}_n^t(\varepsilon_d)$,

then

1. *the hard sphere pseudo-positions remain sufficiently far away: $\forall \tau \in [0,t],\ \underline{x}_{N[\tau]}^{[\tau]} \in \mathcal{D}_{N[\tau]}^{\varepsilon_d/2}$*

2. *the* velocities *of the hard sphere and limit trajectories coincide: $\forall \tau \in [0,t],\ \underline{v}_{N[\tau]}^{[\tau]} = \underline{u}_{N[\tau]}^{[\tau]}$*

3. *the* positions *of both trajectories remain close: $\forall \tau \in [0,t], \forall i \leq N[\tau], d(x_i^{[\tau]}, y_i^{[\tau]}) \leq J_K \varepsilon$.*

Let us observe that *3.* is a consequence of *2.* since, when the velocities coincide, the only difference between the positions is the shift of $\varepsilon\omega_i$ that happens at each particle adjunction. Furthermore, *2.* is a consequence of *1.* since when the collision parameters are the same, and if the particles do not collide between the particle adjunctions, the velocities of both pseudo-trajectories are identically determined. This result has been proved [34, 9] for a one-species gas, but the dynamics is strictly identical for our mixture gas.

Hence, we consider the following functional restricted to non-pathological collision parameters

$$\widetilde{F}_n^{\varepsilon,[\mathbf{V},\delta]}(t) \doteq \sum_{\underline{j}_K} \sum_{\substack{\underline{\chi}_{J_K} \\ L_K=0}} \int_{T_{\underline{j}_K}^{[\delta]}(t)} \mathrm{d}\underline{t}_{J_K} \int_{\Pi(\underline{z}_n^{[t]},\underline{j}_K,\underline{\chi}_{J_K})^c} \mathrm{d}\underline{\omega}_{J_K} \mathrm{d}v_{n+1} \dots \mathrm{d}v_{N_K} \tag{4.45}$$
$$\times \prod_{i=1}^{J_K} s_i \langle \omega_i, v_{n+i} - v_{m_i}^{[t_i^+]} \rangle_+ \times F_{N_K}^{\varepsilon}(0, \underline{z}_{N_K}^{[0]}) \mathbb{1}_{\left\| \underline{v}_{N_K}^{[0]} \right\|^2 \leqslant \mathbf{V}^2},$$

and its limit version $\widetilde{G}_n^{[\mathbf{V},\delta]}$. Now, the error $\widetilde{F}_n^{\varepsilon,[\mathbf{V},\delta]} - \widehat{F}_n^{\varepsilon,[\mathbf{V},\delta]}$ is supported on $\Pi(\underline{z}_n^{[t]}, \underline{j}_K, \underline{\chi}_{J_K})$, so that we will use the control on its volume (4.44) to control the successive-collision operators, concluding the bounds with the usual computation. More precisely, in the proof [31] of Proposition 4.5.1, we bound the collision operators (2.26) in the following way:

$$e^{\beta\|\underline{v}_j\|^2} \left| \mathcal{C}_j^{\ell} f_{j+1} \right| \leq \sum_{i=1}^{j} \int \mathrm{d}\omega_j \mathrm{d}v_{j+1} \, |v_{j+1} - v_i| \cdot \|f_{j+1}\|_{j+1,\beta'} \times e^{-(\beta'-\beta)\|\underline{v}_j\|^2 - \beta'|v_{j+1}|^2}$$
$$\leq \|f_{j+1}\|_{j+1,\beta'} \int \mathrm{d}\omega_j \mathrm{d}v_{j+1} \left(j \, |v_{j+1}| + \sum_{i=1}^{j} |v_i| \right) e^{-(\beta'-\beta)\|\underline{v}_j\|^2 - \beta'|v_{j+1}|^2}.$$

By the Cauchy-Schwarz inequality, we used to bound, like at lign (4.25),

$$e^{\beta\|\underline{v}_j\|^2} \left| \mathcal{C}_j^{\ell} f_{j+1} \right| \leq \|f_{j+1}\|_{j+1,\beta'} \int \mathrm{d}\omega_j \mathrm{d}v_{j+1} \left(j \, |v_{j+1}| + \sqrt{\frac{j}{2e(\beta'-\beta)}} \right) e^{-\beta'|v_{j+1}|^2}$$
$$\leq \|f_{j+1}\|_{j+1,\beta'} \left(j \frac{c_d}{\sqrt{\beta'^{d+1}}} + \sqrt{\frac{j}{2e(\beta'-\beta)}} \frac{\tilde{c}_d}{\sqrt{\beta'^{d}}} \right),$$

for some constants $c_d, \tilde{c}_d$ depending only on the dimension. For the present bound, one can write instead

$$\int \mathrm{d}\omega_j \mathrm{d}v_{j+1} \left(j|v_{j+1}| + \sqrt{\frac{j}{2e(\beta'-\beta)}} \right) e^{-\beta'|v_{j+1}|^2} \leq \int \mathrm{d}\omega_j \mathrm{d}v_j \left(\frac{1}{\sqrt{2e\beta}} + \sqrt{\frac{e^{-1}}{\beta-\beta'}} \right),$$

making appear the volume of collision parameters bounded in (4.44), leading to the following estimate (the factors J_K and N_K resorb in the bigger factor C^{nK+A^K}, for a slightly different constant C depending on β).

Lemma 4.8.4 (Error of restriction to non-pathological collision parameters)**.** *The restriction of considering only collision parameters chosen so as to avoid recollisions, leads to an error of order*

$$\|\widetilde{F}_n^{\varepsilon,[\mathbf{V},\delta]} - \widehat{F}_n^{[\mathbf{V},\delta]}\|_{\mathbb{L}^\infty} \leq C^{nK+A^K} \left(\varepsilon^{\frac{d}{d+2}} + \mathbf{V}^d \times \varepsilon^{\frac{d-1}{3(d+1)}} + \mathbf{V}^{\frac{d+1}{2}} \left(\frac{\varepsilon^{\frac{d}{d+1}}}{\delta} \right)^{\frac{d-1}{2}} \right), \tag{4.46}$$

and similarly for the limit $\widehat{G}_n^{[\mathbf{V}]} - \widehat{G}_n^{[\mathbf{V},\delta]}$ from the same computation.

Harnessing initial proximity Now that we have constructed approximations of our distributions that avoid recollisions, we can at last compare both the BBGKY and limiting distributions thanks to the coupled pseudo-trajectories. Indeed, we can write the coupling

$$\widetilde{F}_n^{\varepsilon,[\mathbf{V},\delta]} - \widetilde{G}_n^{[\mathbf{V},\delta]} = \sum_{\underline{j}_K} \sum_{\underline{\chi}_{J_K}} p_\mu^{|\underline{\ell}^*_{J_K}|} \int_{T^{[\delta]}_{\underline{j}_K}(t)} \mathrm{d}\underline{t}_{J_K} \int_{\Pi(\underline{z}_n^{[t]}, \underline{j}_K, \underline{\chi}_{J_K})^c} \mathrm{d}\underline{\omega}_{J_K} \mathrm{d}v_{n+1} \dots \mathrm{d}v_{N_K}$$
$$\times \prod_{i=1}^{J_K} s_i \langle \omega_i, v_{n+i} - v_{m_i}^{[t_i^+]} \rangle_+ \left[F^\varepsilon_{N_K}(0, \underline{z}^{[0]}_{N_K}) - G_{N_K}(0, \underline{\zeta}^{[0]}_{N_K}) \right] \mathbb{1}_{\left\| \underline{v}^{[0]}_{N_K} \right\|^2 \leqslant \mathbf{V}^2},$$

with the same collision parameters for both pseudo-trajectories, the hard-sphere one and the limit one. Since by construction $\underline{x}_n^{[t]} = \underline{y}_n^{[t]}$, and by Lemma 4.8.3 for $\underline{z}_n^{[t]} \in \mathcal{E}_n^t(\varepsilon_d)$, the n first particles also have identical velocities on $[0,t]$, then for all times $\tau \in [0,t]$, we have $\underline{z}_n^{[\tau]} = \underline{\zeta}_n^{[\tau]}$ also in positions. Henceforth, since by the work done in Section 4.7 all the added particles are particles at equilibrium tagged 0, one has (as $\underline{\ell}_n \subset [\![1,n]\!]$),

$$\begin{aligned} G_{N_K}(0, \underline{\zeta}^{[0]}_{N_K}) &= M_\beta^{\otimes N_K}(\underline{u}^{[0]}_{N_K}) \varphi_0^{\otimes \underline{\ell}_n}(\underline{\zeta}^{[0]}_{\underline{\ell}_n}) \\ &= M_\beta^{\otimes N_K}(\underline{v}^{[0]}_{N_K}) \varphi_0^{\otimes \underline{\ell}_n}(\underline{z}^{[0]}_{\underline{\ell}_n}), \end{aligned} \tag{4.47}$$

and so

$$\begin{aligned} \left| F^\varepsilon_{N_K}(0, \underline{z}^{[0]}_{N_K}) - G_{N_K}(0, \underline{\zeta}^{[0]}_{N_K}) \right| &= \left| F^\varepsilon_{N_K}(0, \underline{z}^{[0]}_{N_K}) - G_{N_K}(0, \underline{z}^{[0]}_{N_K}) \right| \\ &\leq (C_0)^{N_K} e^{-\beta \|\underline{v}^{[0]}_{N_K}\|^2} \cdot \varepsilon \end{aligned}$$

by the initial proximity result (4.21). Hence, the previous estimates on the successive-collision operators eventually yield the following result.

Lemma 4.8.5 (Initial value error)**.** *Conditionally to $\underline{z}_n \in \mathcal{E}_n^t(\varepsilon_d)$, the initial error is bounded by*

$$\left\| \widetilde{F}_n^{\varepsilon,[\mathbf{V},\delta]} - \widetilde{G}_n^{[\mathbf{V},\delta]} \right\|_{\mathbb{L}^\infty(\mathcal{E}_n^t(\varepsilon_d))} \leq C^{nK + A^K} \varepsilon. \tag{4.48}$$

Coherent choice of truncation parameters $(K, \mathbf{V}, \delta)$ Eventually, the last step is to tune the truncation parameters according to ε, so as to obtain the convergence we want. Actually, there is room to choose the scaling, since one can set all the errors as powers of ε, except for the pruning error (4.31) which is significantly bigger. Explicitly, stacking all the errors (pruning (4.31), removing additional tagged particle (4.36), energy truncation (4.38), time separation (4.42) and removing pathological trajectories (4.46)) then using the coupling result (4.48), one has

$$\begin{aligned} \|F_n^\varepsilon(t) - G_n(t)\|_{\mathbb{L}^\infty(\mathcal{E}_n^t(\varepsilon_d))} &\leq C^{C_0 \lambda} n^{cn} e^{-2^{K - K^\alpha}} \\ &+ C^{nK + A^K} \left(p_\mu + e^{-\frac{\beta}{2}\mathbf{V}^2} + \delta + \left[\varepsilon^{\frac{d}{d+2}} + \mathbf{V}^d \times \varepsilon^{\frac{d-1}{3(d+1)}} + \frac{\mathbf{V}^{\frac{d+1}{2}} \varepsilon^{\frac{d(d-1)}{2(d+1)}}}{\delta^{\frac{d-1}{2}}} \right] + \varepsilon \right). \end{aligned}$$

Hence, choosing the scaling

$$\delta = \varepsilon^{\frac{d-1}{d+1}}, \quad \text{and } \mathbf{V}^2 = \frac{2}{\beta} |\log \varepsilon|,$$

one gets

$$\begin{aligned} e^{-\frac{\beta}{2}\mathbf{V}^2} + \delta + \mathbf{V}^d \times \varepsilon^{\frac{d-1}{4(d+1)}} + \frac{\mathbf{V}^{\frac{d+1}{2}} \varepsilon^{\frac{d(d-1)}{2(d+1)}}}{\delta^{\frac{d-1}{2}}} &\leq \varepsilon + \varepsilon^{\frac{d-1}{d+1}} + \left| \frac{2}{\beta} \log \varepsilon \right|^{\frac{d}{2}} \varepsilon^{\frac{d-1}{3(d+1)}} + \left| \frac{2}{\beta} \log \varepsilon \right|^{\frac{d+1}{4}} \varepsilon^{\frac{d-1}{2(d+1)}} \\ &\leq \varepsilon^{\frac{d-1}{4(d+1)}} \end{aligned} \tag{4.49}$$

for ε small enough. This way, if we pick

$$K = \left\lfloor \frac{1}{\log A} \log\left(\frac{(d-1)|\log\varepsilon|}{8(d+1)\log C} \right) \right\rfloor,$$

then $C^{A^K} \leq \varepsilon^{-\frac{d-1}{8(d+1)}}$, and we can deal with the term C^{nK} like in the proof of Proposition 4.6.1, yielding the same factor n^{cn}. Hence, for K large enough, denoting $c_\beta \doteq (d-1)/8(d+1)\log C$, we have

$$e^{-2^{K-K^\alpha}} \leq e^{-2^{(1-\alpha)K}} \leq \exp\left(-c_\beta |\log\varepsilon|^{(1-\alpha)\frac{\log 2}{\log A}} \right).$$

As $A > 2$ is arbitrary, let us choose A such that $(1-\alpha)\dfrac{\log 2}{\log A} \geq 1 - 2\alpha$. This gives us the final condition on

$$\lambda \leq \frac{c_\beta}{2C_0 \log C} |\log\varepsilon|^{1-2\alpha}.$$

Note that we take this scaling so as to have the biggest λ possible in the hypothesis, pushing the associated error at the same level as the truncation error above, which is the limiting one. It yields

$$C^{C_0\lambda} e^{-2^{K-K^\alpha}} \leq \exp\left(-\frac{c_\beta}{2} |\log\varepsilon|^{1-2\alpha} \right).$$

The final verification is the condition $p_\mu \leq 2^{-K}$ of Proposition 4.7.1, which is satisfied with room to spare considering the choices above. Piling all of this, the pruning error is bigger than all the other ones, and we end up with the very last inequality for ε small enough

$$\|F_n^\varepsilon(t) - G_n(t)\|_{\mathbb{L}^\infty(\mathcal{E}_n^t(\varepsilon_d))} \leq n^{cn} \exp\left(-\frac{c_\beta}{2} |\log\varepsilon|^{1-2\alpha} \right).$$

Eventually, the indicator $\mathbb{1}_{\mathcal{E}_n^t(\varepsilon_d)}$ of the set of past-excluding configurations (4.43) pointwise converges, as ε goes to 0, to the indicator of the following set of full measure

$$\Big\{ \underline{z}_n \in \mathcal{D}^n \ , \ \forall 1 \leq i < j \leq n, \ x_i \neq x_j \text{ and } v_i - v_j \notin \mathrm{Vect}(x_i - x_j) \Big\},$$

which concludes the proof of Theorem 1. □

Chapter 5

Combinatorics of the cumulants

The cumulants are obtained in Chapter 6 as the coefficients in the expansion in power series of the *cumulant generating function*, defined as the functional

$$\log \mathbb{E}\left[\exp\left(\mu \pi_t^\varepsilon[H]\right)\right].$$

They are an alternative description of the law of a random variable, equivalent to the knowledge of its moments: the said expansion of the cumulant generating function thus contains all the information about the moments of the empirical measure, which can be retrieved through the cumulants. These objects are called that way because of their additive property for independant random variables.

More precisely, thanks to the link (2.19) between moments and correlation functions, there exists a way to define the cumulants from the correlation functions (F_n^ε) of the system. The combinatorics of the logarithm and exponential that define their generating function (Section 6.1) makes appear a decomposition of the dynamics according to partitions into independent clusters, which leads to the Definition 5.1 of the cumulants.

Looking closely to this formula, it is clear that the cumulants measure the defect of factorization of the correlation functions, i.e. the correlations between the system's particles. And indeed, the precise study of the cumulants of the dynamics, led in the following Chapter 6, will emphasize the fact that the cumulants are asymptotically supported on rare correlating events of the dynamics, associated to interactions between particles. More exactly, the n-th cumulant (f_n^ε) is asymptotically supported on the trajectories implying exactly $(n-1)$ of these rare encounters, through explicit formulas that decompose the pseudo-trajectories previously defined (Section 4.2) into aggregates and clusters of interaction, which are divided into *recollisions* and *overlaps* between particles.

In the present chapter, we hence give the combinatorial definition of the cumulants based on the correlation functions, and discuss it until showing the injectivity of the cumulants through their *inversion formula*, allowing to retrieve the correlation functions from the cumulants (Section 5.1). Section 5.2 is dedicated to highlighting the combinatorial stakes of the inversion formula, which was proven before through analytical methods [12].

The second part of this chapter begins with Section 5.3, introducing a specific formula for the cumulants of functionals written as a product of interactions between some objects, which is typically the case of the exclusion condition (2.1). These *cumulants of an exclusion* can be decomposed into connected graphs of interaction, and this formula leads to a strong control of these objects thanks to the *tree inequality* (Proposition 5.3.1), which bounds this decomposition by a sum over the trees, instead of all the connected graphs. This tree inequality will prove itself very useful to get bounds on the cumulants of the dynamics, in Section 6.5.

Eventually, we use this analysis to prove in the last sections of this chapter the estimates on the partition functions, that we used in Chapter 4.

5.1 Cumulants

The definition of the cumulants is based on a decomposition into partitions, so that for $\sigma \in \mathcal{P}_n$ a partition of $[\![1,n]\!]$, we denote $|\sigma|$ the number of subsets $(\sigma_i)_{1\leqslant i\leqslant|\sigma|}$ that compose this partition, which is not to be confused with the cardinal $|\sigma_i|$ of one of these subsets. Eventually, we denote $\mathcal{P}_n^k \subset \mathcal{P}_n$ the set of partitions $\sigma \in \mathcal{P}_n$ that contain exactly $k = |\sigma|$ subsets.

Definition 5.1.1 (Cumulants)**.** The cumulants associated to a family $(G_n)_{n\geqslant 1}$ are defined as

$$g_n(\underline{z}_n, \underline{\ell}_n) \doteq \sum_{\sigma\in\mathcal{P}_n} (-1)^{|\sigma|-1}(|\sigma|-1)! G_{[\sigma]}(\underline{z}_n, \underline{\ell}_n), \tag{5.1}$$

where for any partition $\sigma \in \mathcal{P}_n$, we denote

$$G_{[\sigma]}(\underline{z}_n, \underline{\ell}_n) = \prod_{i=1}^{|\sigma|} G_{|\sigma_i|}(\underline{z}_{\sigma_i}, \underline{\ell}_{\sigma_i}).$$

Note that the n-th cumulant g_n is constructed from the correlation functions (G_i) for $i \leq n$. Indeed, it decomposes the interactions between n particles into products of interactions within the subsets of every possible partition, to measure the defects of independence. One may easily check that for a tensorized family $(G_n = G_1^{\otimes n})$, all the cumulants (g_n) vanish for $n \geq 2$.

We denote (f_n^ε) the cumulants associated to the hierarchy (F_n^ε). Note for example that the second cumulant is $f_2^\varepsilon = F_2^\varepsilon - F_1^{\varepsilon\otimes 2}$, encoding the defect of independence between pairs of particles. One will see in Section 6.3.2 that when expanding the pseudo-trajectory formula, this corresponds to the rare dynamics in which a distinguished couple of particles interact together. Section 5.3 below is dedicated to the study of the cumulants of the exclusion indicators $(\mathbb{1}_{\mathcal{X}_n^\varepsilon})$, denoted ϕ_n.

Proposition 5.1.1 (Inversion formula)**.** *With the definition above, the injectivity of cumulants is a consequence of the following inversion formula*

$$G_n = \sum_{\sigma\in\mathcal{P}_n} g_{[\sigma]}. \tag{5.2}$$

Proof. We start this proof with the following combinatorial identity, satisfied for any $r \geq 2$,

$$\sum_{k=1}^{r} \sum_{\sigma\in\mathcal{P}_r^k} (-1)^k \prod_{i=1}^{k} (|\sigma_i|-1)! = 0, \tag{5.3}$$

which is shown in [12, Lemma 2.5.1] using the Taylor series of $x \mapsto \exp(\log(1+x))$. Note that it can also be proved using combinatorics arguments (see the following Section 5.3, Lemma 5.2.1). We can hence introduce artificially the sum of all the possible $G_{[\rho]}$ appearing in the cumulants' formula, making each of them vanish thanks to the latter identity (5.3). We do this summing over partitions σ *of the subsets* (ρ_i) that compose the partition ρ (in the notation below, $r = |\rho|$):

$$\begin{aligned} G_n &= G_n + \sum_{r=2}^{n} \sum_{\rho\in\mathcal{P}_n^r} (-1)^r G_{[\rho]} \sum_{k=1}^{r} \sum_{\sigma\in\mathcal{P}_r^k} (-1)^k \prod_{i=1}^{k} (|\sigma_i|-1)! \\ &= \sum_{r=1}^{n} \sum_{\rho\in\mathcal{P}_n^r} \sum_{k=1}^{r} \sum_{\sigma\in\mathcal{P}_r^k} \prod_{i=1}^{k} \left[(-1)^{|\sigma_i|-1}(|\sigma_i|-1)! \prod_{j\in\sigma_i} G_{\rho_j} \right] \end{aligned}$$

using the definition of $G_{[\rho]}$ and the fact that $r = \sum |\sigma_i|$. The trick now is to invert the partitions: seeing $\sigma \in \mathcal{P}_{|\rho|}$ as a coarser partition than ρ, it is similar as taking a partition $\tilde{\sigma}$ of $[\![1,n]\!]$, and then a

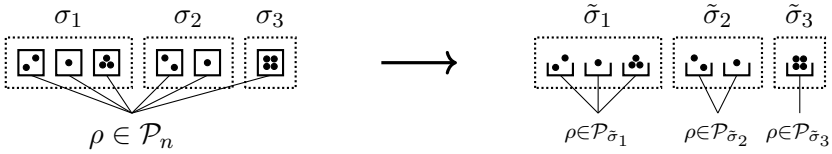

Figure 5.1: Partition indexing

partition $\rho \in \mathcal{P}_{\tilde{\sigma}_i}$ of *each subset* $\tilde{\sigma}_i$ (cf. Fig. 5.1). Doing so, the cardinal of a subset $|\sigma_i|$ becomes the number of subsets in the partition ρ of σ_i, so that inverting the partitions we get

$$G_n = \sum_{k=1}^{n} \sum_{\sigma \in \mathcal{P}_n^k} \prod_{i=1}^{k} \sum_{\rho \in \mathcal{P}_{\sigma_i}} (-1)^{|\rho|-1}(|\rho|-1)! G_{[\rho]},$$

which concludes the proof. □

5.2 Combinatorics of the inversion formula

We prove here the identity (5.3) at the origin of the inversion formula (5.2) for the cumulants, through combinatorial methods. We recall this formula in the following lemma.

Lemma 5.2.1. *For any $r \geqslant 1$, one has*

$$\sum_{k=1}^{r+1} (-1)^k \sum_{\sigma \in \mathcal{P}_{r+1}^k} \prod_{i=1}^{k} (|\sigma_i| - 1)! = 0. \tag{5.4}$$

Proof. We start introducing the following mapping

$$\begin{array}{ccc} \mathcal{P}_{r+1}^k & \longrightarrow & \mathcal{P}_r^{k-1} \amalg \mathcal{P}_r^k \\ \{\sigma_1, \ldots, \sigma_k\} & \mapsto & \{\check{\sigma}_1, \ldots, \check{\sigma}_k\} \end{array}$$

where $\check{\sigma}_i = \sigma_i \setminus \{r+1\}$ denotes the subsets of σ from which we have removed $(r+1)$. Inverting this mapping, for a $\sigma \in \mathcal{P}_r^{k-1}$, we have k choices for the subset $(r+1)$ belongs to; and otherwise for a $\sigma \in \mathcal{P}_r^k$, the element $(r+1)$ must form a partition subset on its own. This way, one can write

$$\begin{aligned} \sum_{\sigma \in \mathcal{P}_{r+1}^k} \prod_{i=1}^{k} (|\sigma_i| - 1)! &= \sum_{j=1}^{k} \sum_{\sigma \in \mathcal{P}_r^k} |\sigma_j| \prod_{i=1}^{k} (|\sigma_i| - 1)! + \sum_{\sigma \in \mathcal{P}_r^{k-1}} \prod_{i=1}^{k-1} (|\sigma_i| - 1)! \\ &= r \sum_{\sigma \in \mathcal{P}_r^k} \prod_{i=1}^{k} (|\sigma_i| - 1)! + \sum_{\sigma \in \mathcal{P}_r^{k-1}} \prod_{i=1}^{k-1} (|\sigma_i| - 1)! \,, \end{aligned}$$

since by construction $\sum_j |\sigma_j| = r$. Thus, decomposing as above the sum (5.4), we can perform an index shift on k to gather it back (the extreme terms, summing over $\mathcal{P}_r^{r+1}$ and $\mathcal{P}_r^0$, vanish). We get

$$\begin{aligned} \sum_{k=1}^{r+1} (-1)^k \sum_{\sigma \in \mathcal{P}_{r+1}^k} \prod_{i=1}^{k} (|\sigma_i| - 1)! &= (r-1) \sum_{k=1}^{r} (-1)^k \sum_{\sigma \in \mathcal{P}_r^k} \prod_{i=1}^{k} (|\sigma_i| - 1)! \\ &= (r-1)(r-2) \times \cdots \times 0 \times \sum_{k=1}^{1} (-1)^1 \times 0! \end{aligned}$$

iterating the computation, which concludes the proof. The importance of the cancellations to get rid of a big combinatorial factor is clear here. □

5.3 Cumulants of the exclusion

This section is devoted to the study of the cumulants of the exclusion indicator associated with the hard sphere domain (2.1) (see Section 5.1 for the definition of the cumulants). The exclusion between particles may be generalized to the exclusion between aggregates and clusters (see Section 6.3.2), yet the following results and computations remain identical. The most crucial statement is the *tree inequality* (Proposition 5.3.1), which provides a strong bound on the integral of these objects, used in the following to estimate cumulants in Section 6.5, and the grand canonical function in Section 5.4.

Denoting $\mathcal{G}_S$ the set of graphs on a set S and $\mathcal{G}_n \doteq \mathcal{G}_{[\![1,n]\!]}$ the set of graphs on $\{1,\dots,n\}$, one may write

$$\begin{aligned}\mathbb{1}_{\mathcal{X}_n^\varepsilon}(x_1,\dots,x_n) &= \prod_{1\le i<j\le n}(1-\mathbb{1}_{x_i\sim x_j})\\ &= \sum_{G\in\mathcal{G}_n}\prod_{\{i,j\}\in E_G}(-\mathbb{1}_{x_i\sim x_j}).\end{aligned}$$

One can even further decompose the graphs into their connected components. We denote $\mathcal{C}_S \subset \mathcal{G}_S$ the set of *connected* graphs on S and $\mathcal{P}_n$ the set of partitions of $\{1,\dots,n\}$, so that we can write

$$\mathbb{1}_{\mathcal{X}_n^\varepsilon}(x_1,\dots,x_n) = \sum_{\sigma\in\mathcal{P}_n}\prod_{k=1}^{|\sigma|}\left(\sum_{G_k\in\mathcal{C}_{\sigma_k}}\prod_{\{i,j\}\in E_{G_k}}(-\mathbb{1}_{x_i\sim x_j})\right).$$

Hence, thanks to the uniqueness due to the inversion formula (Proposition 5.1.1), the cumulants of the exclusion are given by

$$\phi_k(x_1,\dots,x_k) \doteq \sum_{G\in\mathcal{C}_k}\prod_{\{i,j\}\in E_G}(-\mathbb{1}_{x_i\sim x_j}). \tag{5.5}$$

The very specific structure of these cumulants yields a strong bound on them, called the tree inequality, exposed in the following Proposition. This bound on the integral of the cumulants allows a strong control of the particle correlations, used in Section 5.4 to gain estimates on the partition function, and in Section 6.5.2 to bound the initial cumulants.

Proposition 5.3.1 (Tree inequality)**.**

(i) The modulus of the cumulants may be controlled restricting the sum defining them to the trees $\mathcal{T}_k \subset \mathcal{C}_k$ (i.e. to the minimally connected graphs) as such:

$$|\phi_k(x_1,\dots,x_k)| \le \sum_{T\in\mathcal{T}_k}\prod_{\{i,j\}\in E_T}\mathbb{1}_{x_i\sim x_j}.$$

(ii) As a consequence, we have the following control over their integral

$$\int|\phi_k(\underline{x}_k)|\mathrm{d}\underline{x}_k \le k^{k-2}(|\mathcal{B}_d|\varepsilon^d)^{k-1}.$$

Proof. The proof of this proposition relies on a partition scheme due to Penrose [52], and may also be found in [12].

1. The key argument is to find a map $\pi : \mathcal{C}_k \to \mathcal{T}_k$ such that for any tree $T \in \mathcal{T}_k$, there is a connected graph $R(T) \in \mathcal{C}_k$ satisfying

$$\pi^{-1}(T) = \{G \in \mathcal{C}_k \ , \ E_T \subset E_G \subset E_{R(T)}\}.$$

This means that we can partition $\mathcal{C}_k$ into subsets corresponding each to a single tree, and containing all the graphs that are both compatible with this tree and smaller than an upper graph $R(T)$. We will prove later the existence of such a partition.

Now, we decompose the sum defining the k-th cumulant according to this mapping, and using its structure we get

$$\begin{aligned}\sum_{G\in\mathcal{C}_k}\prod_{\{i,j\}\in E_G}(-\mathbb{1}_{i\sim j}) &= \sum_{T\in\mathcal{T}_k}\sum_{G\in\pi^{-1}(T)}\prod_{\{i,j\}\in E_G}(-\mathbb{1}_{i\sim j}) \\ &= \sum_{T\in\mathcal{T}_k}\left(\prod_{\{i,j\}\in E_T}(-\mathbb{1}_{i\sim j})\right)\left(\sum_{E'\subset E_{R(T)}\setminus E_T}\prod_{\{i,j\}\in E'}(-\mathbb{1}_{i\sim j})\right) \\ &= \sum_{T\in\mathcal{T}_k}\left(\prod_{\{i,j\}\in E_T}(-\mathbb{1}_{i\sim j})\right)\left(\prod_{\{i,j\}\in E_{R(T)}\setminus E_T}(1-\mathbb{1}_{i\sim j})\right)\end{aligned}$$

reversing the usual computation so as to harness the cancellations, which yields the result since $1 - \mathbb{1}_{i\sim j} \in \{0, 1\}$.

Let us now expose the Penrose partition scheme. To construct the representative $T \in \mathcal{T}_k$ of a connected graph G, we will choose the vertex 1 as its root, and explore the graph from there, always favouring the lowest vertices when choosing a new edge. Formally, we proceed by generations of same distance to the root $d(1, \cdot)$, on the tree in construction. At each generation, starting from the currently connected vertices, we add the edges of E_G connecting these vertices to non-connected ones, and whenever a conflict happens—which would create a cycle—the lowest currently connected vertex has priority to connect with the new one. This iterated procedure leads to a tree T such that $E_T \subset E_G$.

Then, to construct $R(T)$, we search an algorithm to retrieve some information on E_G from the knowledge of T. For each edge $\{i, j\} \in E_G \setminus E_T$, in the procedure to construct T, at the generation when the first among i and j was connected to the root 1 (let us say i), then either j gets connected at the same generation, and then $d(1, i) = d(1, j)$, either it gets connected at the next generation, since they are connected in G. Since we supposed $\{i, j\} \notin E_T$, it precisely means that some other vertex—within the generation of i—had priority to claim j. Hence, in that case, $d(1, j) = d(1, i) + 1$ and the parent $p(j)$ of j is lower than i.

A good candidate for $R(T)$ is thus T at which we add the vertices $\{i, j\}$ such that $d(1, i) = d(1, j)$, or such that $d(1, i) = d(1, j) + 1$ when $p(j) < i$. One may check that with this choice, every graph G satisfying $E_T \subset E_G \subset E_{R(T)}$ has T as its tree representative, which concludes the construction we needed.

2. By the first part of the proposition, the problem is reduced to the integration over the vertices of a tree, for which we know a very simple algorithm. We start integrating over a leaf i_ℓ of T, which appears in only one condition $\mathbb{1}_{i_\ell\sim j}$, and we then iterate for a new leaf until the tree is

reduced to a single root, so that

$$\begin{aligned}\int |\phi_k| &\leq \int \sum_{T\in\mathcal{T}_k} \prod_{\{i,j\}\in E_T} \mathbb{1}_{i\sim j}\mathrm{d}\underline{x}_k \\ &\leq \sum_{T\in\mathcal{T}_k} |\mathcal{B}_d|\varepsilon^d \int \prod_{\{i,j\}\in E_{T\setminus\{i_\ell\}}} \mathbb{1}_{i\sim j}\mathrm{d}x_1\dots\mathrm{d}\check{x}_{i_\ell}\dots\mathrm{d}x_k \\ &\leq \sum_{T\in\mathcal{T}_k} (|\mathcal{B}_d|\varepsilon^d)^{k-1} \\ &= k^{k-2}(|\mathcal{B}_d|\varepsilon^d)^{k-1},\end{aligned}$$

concluding with Cayley's formula, that gives the number of trees on $[\![1,k]\!]$. □

5.4 Partition function estimates

In this section, we prove Proposition 4.4.1, which yields the following estimate on the partition function, for μ large enough in our mixed low density scaling ($S_{\varepsilon,\mu,\lambda}$):

$$\frac{1}{\mathcal{Z}_\mu}\sum_{q,r\geqslant 0}\frac{(\lambda C_0)^q\mu^r}{q!r!}\int \mathbb{1}_{\mathcal{X}^\varepsilon_{q+r}} \leq C_d^{C_0\lambda}.$$

First of all, let us use the symmetry of the particles (among each labelled group) to observe that the partition function can be rewritten as

$$\begin{aligned}\mathcal{Z}_\mu &= \sum_{p\geqslant 0}\sum_{\underline{\ell}_p\in\Lambda_p}\frac{\lambda^{|\underline{\ell}_p|}\mu^{p-|\underline{\ell}_p|}}{p!}\int (M_\beta\varphi_0)^{\otimes\underline{\ell}_p}(\underline{z}_{\underline{\ell}_p})\mathbb{1}_{\mathcal{X}^\varepsilon_p}(\underline{x}_p)\mathrm{d}\underline{x}_p\mathrm{d}\underline{v}_{\underline{\ell}_p} \\ &= \sum_{p\geqslant 0}\sum_{k=0}^{p}\frac{\lambda^k\mu^{p-k}}{k!(p-k)!}\int (M_\beta\varphi_0)^{\otimes k}(\underline{z}_k)\mathbb{1}_{\mathcal{X}^\varepsilon_p}(\underline{x}_p)\mathrm{d}\underline{x}_p\mathrm{d}\underline{v}_k \qquad (5.6)\\ &= \sum_{p,q\geqslant 0}\frac{\lambda^q\mu^p}{q!p!}\int (M_\beta\varphi_0)^{\otimes q}(\underline{x}_q)\mathbb{1}_{\mathcal{X}^\varepsilon_{p+q}}(\underline{x}_{p+q})\mathrm{d}\underline{x}_{p+q}\mathrm{d}\underline{v}_q. \qquad (5.7)\end{aligned}$$

We now start by proving the computational lemma below, giving an explicit and exact formulation of the partition function using the cumulants of the exclusion, defined in Section 5.3 above.

Lemma 5.4.1. *For all $\lambda,\mu>0$, with (ϕ_k) the cumulants associated to the exclusion $(\mathbb{1}_{\mathcal{X}^\varepsilon_k})$, one has*

$$\mathcal{Z}_\mu = \exp\left(\sum_{(k,l)\neq(0,0)}\frac{\mu^k\lambda^l}{k!\ l!}\int (M_\beta\varphi_0)^{\otimes l}\phi_{k+l}\right). \qquad (5.8)$$

Proof. We start from the formulation (5.7) of the partition function, and we will write the following cumulant expansion, denoting $\mathcal{P}^s_{p+q}$ the partitions of $[\![1,p+q]\!]$ into s subsets,

$$\begin{aligned}\mathcal{Z}_\mu &= 1+\sum_{p,q\neq 0,0}\frac{\mu^p\lambda^q}{p!q!}\sum_{s=1}^{p+q}\sum_{\sigma\in\mathcal{P}^s_{p+q}}\int\prod_{k=1}^{s}\phi_{|\sigma_k|}(\underline{x}_{\sigma_k})(M_\beta\varphi_0)^{\otimes q}(\underline{x}_q)\mathrm{d}\underline{x}_{p+q} \\ &= 1+\sum_{p,q\neq 0,0}\frac{\mu^p\lambda^q}{p!q!}\sum_{s=1}^{p+q}\sum_{\substack{(k_i,l_i)\neq(0,0)\\ \sum k_j=p,\sum l_j=q}}\frac{1}{s!}\frac{p!}{k_1!\cdots k_s!}\frac{q!}{l_1!\cdots l_s!}\int\prod_{i=1}^{s}\phi_{k_i+l_i}(\underline{x}_{k_i+l_i})(M_\beta\varphi_0)^{\otimes l_i}(\underline{x}_{l_i})\mathrm{d}\underline{x}_{k_i+l_i}.\end{aligned}$$

To perform this last equality, denoting $P = [\![1, p]\!]$ and $Q = [\![p+1, p+q]\!]$, we consider the following surjection that counts the number of elements from each partition subset in both P and Q, defined up to an arbitrary choice of a partition order:

$$\begin{array}{rccc} \Phi : & \mathcal{P}^s_{p+q} & \longrightarrow & \left\{(\underline{k}_s, \underline{\ell}_s) \;\middle|\; (k_i, l_i) \neq (0,0), \sum k_j = p, \sum l_j = q\right\} \\ & \sigma & \mapsto & (|\sigma_1 \cap P|, \dots, |\sigma_s \cap P|, |\sigma_1 \cap Q|, \dots, |\sigma_s \cap Q|). \end{array}$$

Its defect of injectivity is indeed given by

$$\sharp\left\{\sigma \in \mathcal{P}^s_{p+q}\ ,\ \Phi(\sigma) = (\underline{k}_s, \underline{\ell}_s)\right\} = \frac{1}{s!} \cdot \frac{p!}{k_1! \cdots k_s!} \cdot \frac{q!}{l_1! \cdots l_s!},$$

providing the combinatorial factors. Now, permuting the sums so as to get rid of the condition on the value of the index sums, we get

$$\begin{aligned} \mathcal{Z}_\mu &= 1 + \sum_{s \geqslant 1} \frac{1}{s!} \prod_{i=1}^{s} \left(\sum_{(k_i,l_i) \neq (0,0)} \frac{\mu^{k_i}}{k_i!} \frac{\lambda^{l_i}}{l_i!} \int \phi_{k_i+l_i}(\underline{x}_{k_i+l_i}) (M_\beta \varphi_0)^{\otimes l_i}(\underline{x}_{l_i}) \mathrm{d}\underline{x}_{k_i+l_i} \right) \\ &= \exp\left(\sum_{(k_i,l_i) \neq (0,0)} \frac{\mu^{k_i} \lambda^{l_i}}{k_i! l_i!} \int \phi_{k_i+l_i} \cdot (M_\beta \varphi_0)^{\otimes l_i} \right), \end{aligned} \tag{5.9}$$

concluding the proof. □

Proof of the proposition. Now, Lemma 5.4.1 applied to both the numerator and the denominator—that have the same structure—gives

$$\frac{1}{\mathcal{Z}_\mu} \sum_{p,q \geqslant 0} \frac{\mu^p (\lambda C_0)^q}{p! q!} \int \mathbb{1}_{\mathcal{X}^\varepsilon_{p+q}} = \exp\left(\sum_{(k,l) \neq 0,0} \frac{\mu^k \lambda^l}{k!\ l!} \int \phi_{k+l} \cdot \left[C_0^l - (M_\beta \varphi_0)^{\otimes l} \right] \right).$$

The terms in the sum are vanishing for $l = 0$, so that

$$\begin{aligned} \left| \sum_{(k,l) \neq 0,0} \frac{\mu^k \lambda^l}{k!\ l!} \int \phi_{k+l} \cdot \left[C_0^l - (M_\beta \varphi_0)^{\otimes l} \right] \right| &\leq \sum_{\substack{k \geqslant 0 \\ l \geqslant 1}} \frac{\mu^k \lambda^l}{k!\ l!} \int |\phi_{k+l}| \cdot 2 C_0^l \\ &\leq 2 \sum_{r \geqslant 1} \sum_{l=1}^{r} \frac{\mu^{r-l} (\lambda C_0)^l}{(r-l)!\ l!} \int |\phi_r| \\ &\leq 2 \sum_{r \geqslant 1} \sum_{l=1}^{r} \frac{\mu^{r-l} (\lambda C_0)^l}{(r-l)!\ l!} r^{r-2} (|\mathcal{B}_d| \varepsilon^d)^{r-1}, \end{aligned}$$

by the point *(ii)* of Proposition 5.3.1, stemming from the tree inequality. Using Stirling's approximation, we have for any $l \leq r$

$$\frac{r^{r-2}}{(r-l)!\ l!} \leq \frac{e^r}{r^2} \cdot \frac{r!}{(r-l)!\ l!} \leq \frac{(2e)^r}{r^2},$$

so that

$$\left| \sum_{(k,l) \neq 0,0} \frac{\mu^k \lambda^l}{k!\ l!} \int \phi_{k+l} \cdot \left[C_0^l - (M_\beta \varphi_0)^{\otimes l} \right] \right| \leq 4 e C_0 \lambda \sum_{r \geqslant 1} \sum_{l=1}^{r} \frac{\mu^{r-l} (\lambda C_0)^{l-1}}{r^2} (2e |\mathcal{B}_d| \varepsilon^d)^{r-1}.$$

Eventually, thanks to the scaling $\mu\varepsilon^{d-1} = 1$ and $1 \ll \lambda \ll \mu$, we have

$$\begin{aligned}\sum_{r\geqslant 1}\sum_{l=1}^{r}\frac{\mu^{r-l}(\lambda C_0)^{l-1}}{r^2}(2e|\mathcal{B}_d|\varepsilon^d)^{r-1} &\leq \sum_{r\geqslant 1}\sum_{l=1}^{r}\frac{\mu^{r-1}}{r^2}(2e|\mathcal{B}_d|\varepsilon^d)^{r-1}\\ &\leq \sum_{r\geqslant 1}(2e|\mathcal{B}_d|\varepsilon)^{r-1}\\ &\leq 2,\end{aligned}$$

concluding the proof. □

5.5 Asymptotic study of the canonical partition functions

We take here the opportunity of the previous study of the grand canonical partition function to expose briefly the asymptotical behaviour of the *canonical* partition functions (2.12), which also appear in the grand canonical partition function, defined for every $N \geq 0$ as

$$\mathcal{Z}_N^{\varepsilon,c} \doteq \int_{\mathbb{T}^{dp}} \mathbb{1}_{\mathcal{X}_N^\varepsilon}(\underline{x}_N)\mathrm{d}\underline{x}_N.$$

In particular, we justify the fact that the random grand canonical number of particles $\mathcal{N}$, whose law is given in Section 2.4, gets close to a Poisson variable when μ goes to infinity in the Boltzmann-Grad scaling. Indeed, at fixed $N \in \mathbb{N}^*$, the Lebesgue's dominated convergence theorem asserts that

$$\mathcal{Z}_N^{\varepsilon,c} \xrightarrow[\varepsilon\to 0]{} 1, \tag{5.10}$$

so that the cumulative distribution function of $\mathcal{N}$ will behave asymptotically as the one of a Poisson law pointwise. Indeed, as μ goes to infinity, the probability $\mathbb{P}[\mathcal{N} = N]$ at fixed N thus behaves like

$$e^{-\mu-\lambda}\frac{(\mu+\lambda)^N}{N!}, \tag{5.11}$$

thanks to the estimate on the grand canonical partition function in the previous Section 5.4.

Nevertheless, one may want to know what happens to the canonical partition functions in the Boltzmann–Grad limit (i.e. such that $N\varepsilon^{d-1} = 1$). Thanks to the exclusion condition of $\mathcal{D}_N^\varepsilon$, one can be sure that the conditions $|x_i - x_j| > \varepsilon/2$ are all disjoint. Since $\varepsilon/2$ is the radius of the spheres, a way to see these conditions is to say that the *center* of a particle cannot enter another particle. Hence, taking this small margin we may integrate over these disjoint conditions to get, integrating over x_N and then iterating,

$$\begin{aligned}\mathcal{Z}_N^{\varepsilon,c} &= \int_{\mathbb{T}^{dp}}\prod_{i\neq j}\mathbb{1}_{|x_i-x_j|>\varepsilon}\mathrm{d}\underline{x}_N\\ &\leq \left(1-(N-1)|\mathcal{B}_d|\frac{\varepsilon^d}{2^d}\right)\int_{\mathbb{T}^{d(N-1)}}\prod_{i\neq j}\mathbb{1}_{|x_i-x_j|>\varepsilon}\mathrm{d}\underline{x}_{N-1}\\ &\leq \prod_{i=1}^{N-1}\left(1-i|\mathcal{B}_d|\frac{\varepsilon^d}{2^d}\right),\end{aligned}$$

so that

$$\log\mathcal{Z}_N^{\varepsilon,c} \leq \sum_{i=1}^{N-1}\log\left(1-i|\mathcal{B}_d|\frac{\varepsilon^d}{2^d}\right), \tag{5.12}$$

and by the concavity inequality $\log(1-x) \leq -x$, we have for $d \geq 3$ that

$$\log \mathcal{Z}_N^{\varepsilon,c} \leq \sum_{i=1}^{N-1} \left(-i|\mathcal{B}_d| \frac{\varepsilon^d}{2^d} \right) = -|\mathcal{B}_d| \frac{\varepsilon^d}{2^d} \frac{N(N-1)}{2} = -\frac{|\mathcal{B}_d|}{2^{d+1}} \varepsilon (N-1) \xrightarrow[N\to\infty]{} -\infty, \tag{5.13}$$

in the Boltzmann–Grad scaling, so that eventually for $d \geq 3$, we get

$$\mathcal{Z}_N^{\varepsilon,c} \xrightarrow[N\to\infty]{N^{-1}=\varepsilon^{d-1}} 0.$$

This is an interesting phenomenon: because the canonical partition function vanishes asymptotically, the estimate (5.11) above on the distribution of $\mathcal{N}$ does not hold for N around the expectation $\lambda+\mu$ of the Poisson law – where the mass is concentrated.

Note that we also use this estimate in Section 10.2.1 to discuss the optimality of our estimates of initial proximity between the BBGKY correlation functions and their limit.

Chapter 6

Cumulants of the nonideal Rayleigh gas

To study further than the first order convergence of the empirical measure (Corollary 4.1.1), we introduced in Section 2.5 the fluctuation field of this measure around its expected value. Chapter 7 is dedicated to presenting the limit of this fluctuation field in Theorem 2, and to stating a large deviation principle for the empirical measure in Theorem 3. This analysis stems from our work presented in [33].

These results are proved thanks to the cumulants, introduced in the previous Chapter 5, which are statistical objects finer than the correlation functions, capturing the finer scales of the dynamics and allowing to rescale its rare events, to characterize their limit behaviour.

In the present chapter, we show the convergence in short times of these cumulants to limit objects, with a full convergence rate in ε thanks to a new precise computation on the dynamics' cycles, introduced in Section 1.5 and detailed in Chapter 8.

First of all, we exhibit the link between the system's statistics and the cumulants, introducing the *cumulant generating function* in Section 6.1. Then, defining aggregates and clusters of interaction in Section 6.3, we reparametrize the pseudo-trajectories already introduced in Section 4.2 in a way that makes appear the rare correlating events that drive the evolution of the cumulants, eventually encoding them in dynamics trees in Section 6.4.

Section 6.2 motivates that expansion by presenting the cumulant hierarchy in a naive way, highlighting the difficulty to deal directly with this hierarchy.

6.1 Cumulant generating function

The cumulant generating function is the functional $\log \mathbb{E}\left[\exp\left(\mu\pi_t^\varepsilon[H]\right)\right]$, containing all the information on the moments of the empirical measure. Using the identity (2.19) between correlation functions and observables, the formal expansion of this functional leads [12] to the definition of the *cumulants* (Section 5.1). We prove here rigourously the said expansion of the cumulant generating function (6.3).

By linearity, and using the fact that before having been assigned a tag, the particles are exchangeable, one has

$$\begin{aligned}\mathbb{E}\left[\exp\left(\sum_{i=1}^{\mathcal{N}} H(Z_{\varepsilon,i}^{[t]}, L_i)\right)\right] &= 1 + \sum_{k\geqslant 1}\frac{1}{k!}\mathbb{E}\left[\left(\sum_{i=1}^{\mathcal{N}} H(Z_{\varepsilon,i}^{[t]}, L_i)\right)^k\right] \\ &= 1 + \sum_{k\geqslant 1}\frac{1}{k!}\mathbb{E}\left[\sum_{n=1}^{k}\frac{1}{n!}\sum_{\substack{k_1+\cdots+k_n=k\\(k_j\geqslant 1)_{j\leq n}}}\frac{k!}{k_1!\dots k_n!}\sum_{\substack{(i_j\leqslant \mathcal{N})_{j\leq n}\\ i_j\neq i_{j'}}} H_{i_1}^{k_1}\dots H_{i_n}^{k_n}\right],\end{aligned}$$

denoting $H_i \doteq H(Z^{[t]}_{\varepsilon,i}, L_i)$, and expanding the power k by partitioning the resulting sum according to the number of different particles implied in each product. Hence, using the relation (2.19) between observables and correlation functions, and permuting the sums to get rid of the sum over k, we get (once again extending the correlation functions by 0 outside of their domain)

$$\begin{aligned}\mathbb{E}\left[\exp\left(\sum_{i=1}^{\mathcal{N}} H(Z_i^t, L_i)\right)\right] &= 1 + \sum_{n\geqslant 1}\frac{1}{n!}\sum_{\underline{\ell}_n\in\Lambda_n}\lambda^{|\underline{\ell}_n|}\mu^{n-|\underline{\ell}_n|}\int F_n^\varepsilon(t,\underline{\ell}_n)\prod_{i=1}^{n}\left(\sum_{k_i\geqslant 1}\frac{1}{k_i!}H(z_i,\ell_i)^{k_i}\right)\\ &= 1 + \sum_{n\geqslant 1}\frac{1}{n!}\sum_{\underline{\ell}_n\in\Lambda_n}\lambda^{|\underline{\ell}_n|}\mu^{n-|\underline{\ell}_n|}\int F_n^\varepsilon(t,\underline{\ell}_n)(e^H-1)^{\otimes n}(\underline{\ell}_n). \qquad (6.1)\end{aligned}$$

Now that we dispose of an expansion for this expectancy in terms of correlation functions, let us see how the cumulants appear along with a logarithm. We start from the formula (6.1) above and use the inversion formula (5.2). Hence, using the exchangeability of particles to reduce the partitions to the number of elements in each of their subsets, we get

$$\begin{aligned}&\mathbb{E}\left[\exp\left(\sum_{i=1}^{\mathcal{N}} H(Z_i^{[t]}, L_i)\right)\right]\\ &\quad= 1 + \sum_{n\geqslant 1}\frac{1}{n!}\sum_{\underline{\ell}_n\in\Lambda_n}\lambda^{|\underline{\ell}_n|}\mu^{n-|\underline{\ell}_n|}\sum_{\sigma\in\mathcal{P}_n}\prod_{i=1}^{|\sigma|}\int_{\mathcal{D}^{|\sigma_i|}} f^\varepsilon_{\sigma_i}(t,\underline{\ell}_{\sigma_i})(e^H-1)^{\otimes\sigma_i}(\underline{\ell}_{\sigma_i})\\ &\quad= 1 + \sum_{n\geqslant 1}\frac{1}{n!}\sum_{s=1}^{n}\frac{1}{s!}\sum_{\substack{p_1+\ldots+p_s=n\\(p_i\geqslant 1)_{i\leqslant s}}}\frac{n!}{p_1!\ldots p_s!}\prod_{i=1}^{s}\sum_{\underline{\ell}^{(i)}\in\Lambda_{p_i}}\lambda^{|\underline{\ell}^{(i)}|}\mu^{p_i-|\underline{\ell}^{(i)}|}\int_{\mathcal{D}^{p_i}} f^\varepsilon_{p_i}(t,\underline{\ell}^{(i)})(e^H-1)^{\otimes p_i}(\underline{\ell}^{(i)}),\end{aligned}$$

where the denominator $s!$ stems from the arbitrary order that we impose on the partitions' subsets. We have also split the labels $\underline{\ell}_n \in \Lambda_n$ into the labels $\underline{\ell}^{(i)} \in \Lambda_{p_i}$ on each subset. Eventually, we sum over n to relax the condition on the subset cardinals p_i, and factorize everything as

$$\mathbb{E}\left[\exp\left(\sum_{i=1}^{\mathcal{N}} H(Z_i^{[t]}, L_i)\right)\right] = 1 + \sum_{s\geqslant 1}\frac{1}{s!}\left(\sum_{p\geqslant 1}\frac{1}{p!}\sum_{\underline{\ell}_p\in\Lambda_p}\lambda^{|\underline{\ell}_p|}\mu^{p-|\underline{\ell}_p|}\int_{\mathcal{D}^p} f^\varepsilon_p(t,\underline{\ell}_p)(e^H-1)^{\otimes p}(\underline{\ell}_p)\right)^s,$$

which makes appear the exponential of the quantity defined below.

Definition 6.1.1 (Cumulant generating function)**.** Thanks to the computation above, the two following definitions are equivalent to define the *cumulant generating function*, from the empirical measure and from the cumulants:

$$\mathfrak{G}^{[t]}_\varepsilon[H] \doteq \log\mathbb{E}\left[\exp\left(\sum_{i=1}^{\mathcal{N}} H(Z_i^{[t]}, L_i)\right)\right] \qquad (6.2)$$

$$\doteq \sum_{p\geqslant 1}\frac{1}{p!}\sum_{\underline{\ell}_p\in\Lambda_p}\lambda^{|\underline{\ell}_p|}\mu^{p-|\underline{\ell}_p|}\int_{\mathcal{D}^p} f^\varepsilon_p(t,\underline{\ell}_p)(e^H-1)^{\otimes p}(\underline{\ell}_p). \qquad (6.3)$$

Note that it is not directly a generating function as one can be used to, since it is not an expansion in powers of the observable H, but in powers of its exponential, which makes appear *combinations of cumulants* when deriving along H, not directly cumulants.

Let us finally observe that if the observable is of the form $\hat{H}(z,\ell) = h(z)\mathbb{1}_{\ell=1}$, (i.e. counting only the tagged particles) then the cumulant generating function writes

$$\mathfrak{G}^{[t]}_\varepsilon[\hat{H}] = \sum_{p\geqslant 1}\frac{\lambda^p}{p!}\int_{\mathcal{D}^p} f^\varepsilon_p(t,\underline{1}_p)(e^{\hat{H}}-1)^{\otimes p}. \qquad (6.4)$$

We do not renormalize yet the cumulant generating function, since according to whether the observable H weights all the particles or only the tagged ones, the suitable scale will be μ or λ.

6.2 Naive computation of the cumulant equations

6.2.1 Cumulant hierarchy

Before entering the details of the cumulant expansion based on aggregates and clusters of interaction, which will be later decomposed along dynamics trees, let us motivate this analysis. Indeed, one could start instead from the BBGKY hierarchy on the correlation functions, stated in Proposition 2.6.1, and use the combinatorics of the cumulants to find the hierarchy they satisfy. Nevertheless, as we show in this section, this non-linear hierarchy is quite difficult to handle, and does not yield as much a priori information on the cumulants, as did the hierarchy on the canonical marginals.

Let us compute, for instance, the equations satisfied by the transport of the two first cumulants. The first cumulant corresponds to the first correlation function, so that using the equation on F_1^ε given by the hierarchy (2.25) and the inversion formula (Proposition 5.1.1), one can find an equation on the first cumulant depending on the second one. Avoiding to write down the dependence on the tags of the particles for simplicity, we get

$$\begin{aligned}(\partial_t + v\cdot\nabla_x) f_1^\varepsilon &= \mathcal{C}_1 F_2^\varepsilon \\ &= \mathcal{C}_1 f_2^\varepsilon + \mathcal{C}_1 \left(f_1^\varepsilon\right)^{\otimes 2}.\end{aligned}$$

Because of the structure of the inversion formula, this equation makes appear all the lower orders than the order 2, and a first non-linearity in the first cumulant. We will not detail the general formula for the equation on f_n^ε, for it is more interesting to see technically how the cancellations occur in the following example: for the second cumulant f_2^ε, the same results as previously lead to

$$\begin{aligned}(\partial_t + \underline{v}\cdot\nabla_{\underline{x}}) f_2^\varepsilon &= (\partial_t + v\cdot\nabla_x)\left[F_2^\varepsilon - (F_1^\varepsilon)^{\otimes 2}\right] \\ &= \mathcal{C}_2 F_3^\varepsilon - F_1^\varepsilon \otimes \mathcal{C}_1 F_2^\varepsilon - \mathcal{C}_1 F_2^\varepsilon \otimes F_1^\varepsilon.\end{aligned}$$

Expanding now the correlation functions in cumulants, exact cancellations happen that greatly simplifies the equation; for instance, from the formula

$$F_3^\varepsilon = f_3^\varepsilon - f_1^\varepsilon \otimes f_2^\varepsilon - f_2^\varepsilon \otimes f_1^\varepsilon - f_1^\varepsilon(z_2) f_2^\varepsilon(z_1, z_3) + (f_1^\varepsilon)^{\otimes 3},$$

the term $\mathcal{C}_2 F_3^\varepsilon$ makes appear a term

$$\mathcal{C}_2 (f_1^\varepsilon)^{\otimes 3} = f_1^\varepsilon \otimes \mathcal{C}_1 (f_1^\varepsilon)^{\otimes 2} + \mathcal{C}_1 (f_1^\varepsilon)^{\otimes 2} \otimes f_1^\varepsilon$$

which simplifies with the cumulant terms stemming from the expansion of F_2^ε. The same cancellation happens for the other terms stemming from F_2^ε, and in the end it remains

$$\begin{aligned}(\partial_t + \underline{v}\cdot\nabla_{\underline{x}}) f_2^\varepsilon &= \mathcal{C}_2 f_3^\varepsilon + \mathcal{C}_2(f_2^\varepsilon \otimes f_1^\varepsilon) \\ &+ \int \Big[\langle \omega, v_{\mathrm{c}} - v_1\rangle f_1^\varepsilon(z_1) f_2^\varepsilon(z_2, x_1 + \varepsilon\omega, v_{\mathrm{c}}) + \langle \omega, v_{\mathrm{c}} - v_2\rangle f_1^\varepsilon(z_2) f_2^\varepsilon(z_1, x_2 + \varepsilon\omega, v_{\mathrm{c}})\Big] \mathrm{d}\omega \mathrm{d}v_{\mathrm{c}},\end{aligned} \tag{6.5}$$

where the last terms come from operators $\mathcal{C}_2$ partially compensated. Once again, this equation implies all the orders lower than the order 3, in a nonlinear way. These equations are given to emphasize the difficulty of dealing directly with them; starting from Section 6.3, we harness an alternative method to find a more relevant equation on the cumulants.

6.2.2 Coarser cumulants

Another idea that is sometimes used in the litterature, is to use a coarser decomposition in cumulants around a tensorized ansatz [54]; this is typically the choice made by Deng, Hani and Ma in their paper deriving the Boltzmann equation on large time scales [24]. We present here this alternative definition for curiosity.

Moreover, in the Rayleigh gas setting, it is quite natural to see that decomposition appear from the classical cumulant definition: let us start with the Definition 5.1 of the cumulants. In the case of a single tagged particle, only correlation functions depending on the first particle are expected to be perturbed: let us hence formally replace the other correlation functions by the Maxwellian equilibrium ansatz. For example, the second cumulant becomes

$$\tilde{f}_2^\varepsilon = F_2^\varepsilon - F_1^\varepsilon \otimes M_\beta,$$

and in general we write thanks to the factorized property of the ansatz

$$\begin{aligned}\tilde{f}_n^\varepsilon &= \sum_{\substack{\sigma_0 \subset [\![1,n]\!] \\ \sigma_0 \ni 1}} F_{\sigma_0}^\varepsilon \sum_{\sigma \in \mathcal{P}_{n-|\sigma_0|}} (-1)^{|\sigma|}|\sigma|! M_\beta^{\otimes \sigma_0^c} \\ &= \sum_{\substack{A \subset [\![1,n]\!] \\ A \ni 1}} F_A M_\beta^{\otimes n-|A|}(-1)^{n-|A|},\end{aligned}$$

by the combinatorics of the Stirling numbers of the second kind, appearing in the Touchard polynomials. Eventually, we retrieve the following formula appearing in the litterature

$$\tilde{f}_n^\varepsilon \doteq \sum_{A \subset [\![2,n]\!]} (-1)^{|A|} F_{A^c}^\varepsilon M_\beta^{\otimes A},$$

with the following inverse formula, far simpler to prove combinatorically than Proposition 5.1.1,

$$F_n^\varepsilon = \sum_{\substack{B \subset [\![1,n]\!] \\ B \ni 1}} \tilde{f}_B^\varepsilon M_\beta^{\otimes B^c} = \sum_{B \subset [\![2,n]\!]} \tilde{f}_{B^c}^\varepsilon M_\beta^{\otimes B}.$$

The main asset of these coarser cumulants is that, in our case, the direct naive hierarchy is linear. Indeed, we can write from the formulas above that

$$\begin{aligned}(\partial_t - \underline{v}\cdot\nabla_{\underline{x}})\tilde{f}_n^\varepsilon &= \sum_{1 \in A \subset [\![1,n]\!]} (-1)^{n-|A|} M_\beta^{\otimes A^c} (\partial_t - \underline{v}\cdot\nabla_{\underline{x}}) F^\varepsilon \\ &= \sum_{1 \in A \subset [\![1,n]\!]} (-1)^{n-|A|} M_\beta^{\otimes A^c} \mathcal{C}_{|A|} \left[\sum_{1 \in B \subset A \cup \{n+1\}} \tilde{f}_B^\varepsilon M_\beta^{\otimes B^c} \right] \\ &= \sum_{1 \in A \subset [\![1,n]\!]} (-1)^{n-|A|} M_\beta^{\otimes A^c} \sum_{a \in A} \sum_{1 \in B \subset A \cup \{n+1\}} \{\tilde{f}_B^\varepsilon M_\beta^{\otimes B^c}\}^{a,n+1}\end{aligned}$$

where the operator

$$\{\tilde{f}_B^\varepsilon M_\beta^{\otimes B^c}\}^{a,n+1} \doteq \int \langle \omega, v_{n+1} - v_a \rangle [\tilde{f}_B^\varepsilon M_\beta^{\otimes B^c}](\underline{z}_A, x_a + \varepsilon\omega, v_{n+1}) \mathrm{d}\omega \mathrm{d}v_{n+1}$$

corresponds to the part of the collision operator (2.24) where particles a and $(n+1)$ collide. Inverting the perspective $B \subset A$, the sums might be arranged as

$$(\partial_t - \underline{v}\cdot\nabla_{\underline{x}})\tilde{f}_n^\varepsilon = \sum_{1 \in B \subset [\![1,n+1]\!]} \sum_{a \in [\![1,n]\!]} \{\tilde{f}_B^\varepsilon M_\beta^{\otimes B^c}\}^{a,n+1} \sum_{a \in A \supset B \setminus \{n+1\}} (-1)^{n-|A|}.$$

Now, observing that we have the combinatorial equality

$$\sum_{a\in A\supset B\setminus\{n+1\}}(-1)^{n-|A|}=\mathbb{1}_{B\setminus\{1,n+1\}\cup\{a\}=[\![1,n+1]\!]},$$

the remaining values of B are $[\![1,n]\!]$, $[\![1,n+1]\!]$, $[\![1,n]\!]\setminus\{a\}$ and $[\![1,n+1]\!]\setminus\{a\}$ for $a\neq 1$. Finally, since the terms where two particles distributed at equilibrium collide vanish by the boundary condition (like in the proof of the BBGKY hierarchy, Proposition 2.6.1), we get

$$(\partial_t-\underline{v}\cdot\nabla_{\underline{x}})\tilde{f}_n^\varepsilon=\sum_{1\leqslant a\leqslant n}\{\tilde{f}_n^\varepsilon M_\beta(v_{n+1})\}^{a,n+1}+\{\tilde{f}_{n+1}^\varepsilon\}^{a,n+1}+\sum_{2\leqslant a\leqslant n}\{\tilde{f}_n^\varepsilon(\underline{z}_{[\![1,n+1]\!]\setminus\{a\}})M_\beta(v_a)\}^{a,n+1}.$$

This equation does not imply anymore the lower orders than the order n, and is completely linear. Those coarser cumulants seem relevant to study the behaviour of the tagged particle in the Rayleigh gas. In practice, we prefer the tagged model which is more adapted to our statistical study since it allows to define an empirical measure of a large amount of tagged particles.

6.3 Reparametrization of the trajetories along rare interactions

Instead of the descriptions presented in the previous section, we will favour a decomposition of the cumulants according to the clusters formed by the interactions between particles, happening in the dynamics. This computation leads us to an explicit formula that makes clearly appear the rare dynamics events on which the cumulants are supported (see the discussion in the introducing Section 1.4).

Once again, the first step to understand the cumulants is to find an equation implying only other cumulants, which we do by computing an expansion of the dynamics, based on the interactions between the particles (Lemma 6.3.1).

This first expansion is adapted from [12, Chapter 3, *Tree expansions of the hard-sphere dynamics*], for the general indistinguishable case. Our purpose to find the expansion is to start with the pseudo-trajectory equation on the correlation functions, and to identify the cumulants in an expansion similar to the one characterizing them (see the inversion formula in Proposition 5.1.1).

6.3.1 Pseudo-trajectory measure

We start from the pseudo-trajectory formulation (4.9); recall that a pseudo-trajectory is fully determined by its final configuration $\underline{z}_n=\underline{z}_n^{[t]}$, and the following parameters: number of collisions, a collision history, collision times, collision angles and collision velocities, summed up in the parametrizing vector

$$\Psi_n\doteq(k,\chi_k,\underline{t}_k,\underline{\omega}_k,\underline{v}_k^*)\in\coprod_{k\geqslant 0}\{k\}\times\mathcal{H}_{n,k}\times T_k(t)\times\left(\mathbb{S}^{d-1}\times\mathbb{R}^d\right)^k,$$

referring to the definitions of the collision times (4.6) and collision history (4.7)

$$\chi_k\doteq(\underline{m}_k,\underline{\ell}_k^*,\underline{s}_k)\in\mathcal{H}_{n,k}\doteq\mathcal{M}_{n,k}\times\Lambda_k\times\{\pm1\}^k.$$

Hence, denoting $v_{n+i}=v_i^*$ the velocities of added particles, and introducing the measure

$$\mathrm{d}\nu_{[t]}(\Psi_n)\doteq p_\mu^{|\underline{\ell}_k^*|}\mathrm{d}\underline{t}_k\mathrm{d}\underline{\omega}_k\mathrm{d}\underline{v}_k^*\prod_{i=1}^k s_i\langle\omega_i,v_{n+i}-v_{m_i}^{[t_i^+]}\rangle_+,\tag{6.6}$$

the pseudo-trajectory formulation rewrites as

$$F_n^\varepsilon(t)=\int F^\varepsilon\left(0,\underline{z}_{\Psi_n}^{[0]}\right)\,\mathrm{d}\nu_{[t]}(\Psi_n),\tag{6.7}$$

where $\underline{z}^{[0]}_{\Psi_n}$ denotes the initial configuration deduced from the pseudo-trajectory, according to the construction given in Section 4.2 (the initial configuration $\underline{z}^{[0]}_{\Psi_n}$ also includes the *tags* of the corresponding particles). Note finally that the sums over k and χ_k in the pseudo-trajectory formulation result from the domain of integration of the measure $\nu_{[t]}$, and so remain implicit.

The formula giving an expression for the expectation of the empirical measure according to the correlation functions (2.19), may be generalized [12, Proposition 3.3.1] to observables $H_n(\underline{z}_n^{[0,t]})$ depending on the whole trajectory on $[0,t]$, as

$$\mathbb{E}\left[\sum_{1\leq i_k\neq i_j\leq \mathcal{N}} H_n(Z_{i_1}^{[0,t]}, L_{i_1}, \dots, Z_{i_n}^{[0,t]}, L_{i_n})\right] = \mu^n \sum_{\underline{\ell}_n\in\Lambda_n} p_\mu^{|\underline{\ell}_n|} \int_{\mathcal{D}_n^\varepsilon} \mathrm{d}\underline{z}_n \int F^\varepsilon(0, \underline{z}^{[0]}_{\Psi_n}) H_n(\underline{z}^{[0,t]}_{\Psi_n}) \mathrm{d}\nu_{[t]}(\Psi_n),$$

where $H_n(\underline{z}^{[0,t]}_{\Psi_n})$ is projecting the whole trajectory on the trajectories of the n first particles. The object that we will study, for tensorized observables, is hence the *H-weighted correlation function*

$$F_n^\varepsilon[H](t, \underline{z}_n, \underline{\ell}_n) \doteq \int F^\varepsilon(0, \underline{z}^{[0]}_{\Psi_n}) H^{\otimes n}(\underline{z}^{[0,t]}_{\Psi_n})\ \mathrm{d}\nu_{[t]}(\Psi_n). \tag{6.8}$$

Note that for $H \equiv 1$, we retrieve the correlation functions. Moreover, the cumulant generating function (6.2) also generalizes to obervables depending on the whole trajectory $H_n(\underline{z}_n^{[0,t]})$, as follows

$$\begin{aligned}\mathfrak{G}_\varepsilon^{[0,t]}[H] &\doteq \log \mathbb{E}\left[\exp\left(\sum_{i=1}^{\mathcal{N}} H(Z_i^{[0,t]}, L_i)\right)\right] \\ &= \sum_{p\geqslant 1} \frac{1}{p!} \sum_{\underline{\ell}_p\in\Lambda_p} \lambda^{|\underline{\ell}_p|} \mu^{p-|\underline{\ell}_p|} \int_{\mathcal{D}^p} f_p^\varepsilon \left[e^H - 1\right](t, \underline{\ell}_p).\end{aligned} \tag{6.9}$$

Indeed, the computation of Section 6.1 are identical for the expansion of this generalized version of the cumulant generating function. The following section gives a formula for the H-weighted cumulants $f_p^\varepsilon[H]$.

6.3.2 Expansion and equation on the cumulants

Starting from the integral formulation (6.7) for the pseudo-trajectory formula, we will perform an expansion based on the interactions between the particles, to make appear an expansion in cumulants (5.1), eventually identifying the cumulants by injectivity, due to the inversion formula (Proposition 5.1.1). This expansion is a first illustration of the link between cumulants and dynamical interactions.

We start by splitting the pseudo-trajectories into *non-interacting aggregates*, to factorize the pseudo-trajectory measure. At a fixed pseudo-trajectory $\Psi_n = (k, \chi_k, \underline{t}_k, \underline{\omega}_k, \underline{v}_k)$, for a set of particles $A \subset [\![1,n]\!]$, we will denote

$$P(A) \subset A \cup [\![n+1, n+k]\!] \tag{6.10}$$

the set of all particles contained in the pseudo-trajectory stemming from A (depending on the history χ_k). Then, if $\mathbb{1}_{p\not\sim q}^{[0,t]}$ is the indicator that particles p and q never collided on $[0,t]$ during the pseudo-trajectory $(\underline{z}_n, \Psi_n)$, we denote for A, A' two subsets of $[\![1,n]\!]$,

$$\mathbb{1}_{A\not\sim A'} \doteq \prod_{p\in P(A)} \prod_{q\in P(A')} \mathbb{1}_{p\not\sim q}^{[0,t]}$$

the indicator that no particle stemming from A encountered any particle stemming from A', during the whole pseudo-dynamics on $[0,t]$. Under the condition $A \not\sim A'$, the pseudo-trajectories are independent and the measure and observable factorize as

$$\mathrm{d}\nu_{[t]}(\Psi_{A\cup A'})H^{\otimes A\cup A'}(\underline{z}^{[0,t]}_{\Psi_{A\cup A'}}) = \mathrm{d}\nu_{[t]}(\Psi_A)H^{\otimes A}(\underline{z}^{[0,t]}_{\Psi_A}) \times \mathrm{d}\nu_{[t]}(\Psi_{A'})H^{\otimes A'}(\underline{z}^{[0,t]}_{\Psi_{A'}}).$$

We keep this factorized writing for the moment, to remember that the pseudo-trajectories are defined and constructed independently on each aggregate. In practice, they behave as if the particles from two different aggregates could not interact: they overlap one another when they meet.

On the other hand, we denote the *aggregating condition* $\mathrm{agg}(A)$ the indicator that all the particles in the aggregate A are connected through collisions in their pseudo-trajectories, i.e. that there exists a path $(i_1,\dots,i_{|A|}) \in [\![1,|A|]\!]^{|A|}$ such that

$$\{i_1,\dots,i_{|A|}\} = [\![1,|A|]\!] \quad \text{and} \quad \forall j \in [\![1,\ |A|-1]\!],\ \mathbb{1}^{[0,t]}_{A_{i_j}\sim A_{i_{j+1}}} = 1. \tag{6.11}$$

This eventually leads to the following conditioning according to the partition $\kappa \in \mathcal{P}_n$ into aggregates:

$$F^\varepsilon_n[H](t) = \sum_{\kappa\in\mathcal{P}_n} \int \left[\prod_{i=1}^{|\kappa|} \mathrm{agg}(\kappa_i)\ \mathrm{d}\nu_{[t]}(\Psi_{\kappa_i})H^{\otimes\kappa_i}(\underline{z}^{[0,t]}_{\Psi_{\kappa_i}})\right]\left(\prod_{1\leqslant i<j\leqslant|\kappa|} \mathbb{1}_{\kappa_i\not\sim\kappa_j}\right) F^\varepsilon(0,\underline{z}^{[0]}_{\Psi_n}).$$

Henceforth, we denote the measure weighted by the observable

$$\mathrm{d}\nu^{[H]}_{[0,t]}(\Psi_n) \doteq H^{\otimes n}(\underline{z}^{[0,t]}_{\Psi_n})\mathrm{d}\nu_{[t]}(\Psi_n). \tag{6.12}$$

Now, still in the idea of factorizing, we want to decorrelate the condition of exclusion between the aggregates $\mathbb{1}_{\kappa_i\not\sim\kappa_j}$, using the cumulants of the exclusion (Definition 5.1, studied specifically in Section 5.3) thanks to which we write

$$\prod_{1\leqslant i<j\leqslant|\kappa|} \mathbb{1}_{\kappa_i\not\sim\kappa_j} = \sum_{\rho\in\mathcal{P}_{|\kappa|}} \phi_{[\rho]}(\kappa_1,\dots,\kappa_{|\kappa|})$$

recalling the notation

$$\phi_{[\rho]}(\kappa_1,\dots,\kappa_{|\kappa|}) = \prod_{i=1}^{|\rho|} \phi_{|\rho_i|}(\underline{\kappa}_{\rho_i}).$$

Finally, we still need to expand the initial distribution $F^\varepsilon(0,\underline{z}^{[0]}_{\Psi_n})$ to completely factorize the formula, to make appear a cumulant expansion. We need to expand it in a coarser way than the partition ρ, to be compatible with the product $\phi_{[\rho]}$ above, so that we consider the *cluster cumulants*, defined by the expansion

$$F^\varepsilon(0,\underline{z}^{[0]}_{\Psi_{\rho_1}},\dots,\underline{z}^{[0]}_{\Psi_{\rho_{|\rho|}}}) = \sum_{\sigma\in\mathcal{P}_{|\rho|}} f^{\varepsilon,\rho}_{[\sigma]}(0,\underline{z}^{[0]}_{\Psi_{\rho_1}},\dots,\underline{z}^{[0]}_{\Psi_{\rho_{|\rho|}}}) \tag{6.13}$$

due once again to the inversion formula (Proposition 5.1.1). This expansion is made in clusters, and so *depends on the partition of the aggregates* $\rho \in \mathcal{P}_{|\kappa|}$. The following notation $\sigma \lhd \rho \lhd \kappa$ means that the partition σ is coarser than ρ, which is coarser then κ, and in the end we write

$$F^\varepsilon_n[H](t) = \sum_{\kappa\in\mathcal{P}_n} \int \left[\prod_{i=1}^{|\kappa|} \mathrm{agg}(\kappa_i)\ \mathrm{d}\nu^{[H]}_{[0,t]}(\Psi_{\kappa_i})\right] \sum_{\sigma\lhd\rho\lhd\kappa} \phi_{[\rho]} f^{\varepsilon,\rho}_{[\sigma]}(0).$$

To identify with a cumulant expansion, the last step is to use the same trick as in the proof of the inversion formula to invert the partitions, starting by considering a partition σ of $[\![1,n]\!]$, then considering a partition ρ *on each subset* σ_j. This is made possible by to the compatibility condition

$$f^{\varepsilon,\rho}_{\sigma_j} = f^{\varepsilon,\rho_{|\sigma_j}}_{\sigma_j},$$

and thanks to the factorizing identity

$$\phi_{[\rho]} f^{\varepsilon,\rho}_{[\sigma]} = \prod_{i=1}^{|\rho|} \phi_{\rho_i} \prod_{j=1}^{|\sigma|} f^{\varepsilon,\rho}_{\sigma_j} = \prod_{j=1}^{|\sigma|} \left[f^{\varepsilon,\rho}_{\sigma_j} \prod_{i\in\sigma_j} \phi_{\rho_i} \right].$$

Since the initial cluster cumulants $f^{\varepsilon,\rho}_n$ do not depend on the subdivision κ, we can also invert κ and ρ to finally get the cumulant expansion

$$F^{\varepsilon}_n[H](t) = \sum_{\sigma\in\mathcal{P}_n} \prod_{j=1}^{|\sigma|} \int \sum_{\rho\in\mathcal{P}_{\sigma_j}} f^{\varepsilon,\rho}_{\sigma_j}(0) \prod_{j=1}^{|\rho|} \left[\sum_{\kappa\in\mathcal{P}_{\rho_j}} \phi_{\rho_j} \prod_{i=1}^{|\kappa|} \mathrm{agg}(\kappa_i)\ \mathrm{d}\nu^{[H]}_{[0,t]}(\Psi_{\kappa_i}) \right],$$

whence the following lemma by injectivity of the cumulants.

Lemma 6.3.1. *The cumulants satisfy the following integral equation, in terms of aggregates and clusters of interaction*

$$f^{\varepsilon}_n[H](t,\underline{z}_n,\underline{\ell}_n) = \sum_{\rho\in\mathcal{P}_n} \int f^{\varepsilon,\rho}_n(0,\underline{z}^{[0]}_{\Psi_{\rho_1}},\dots,\underline{z}^{[0]}_{\Psi_{\rho_{|\rho|}}}) \prod_{j=1}^{|\rho|} \left[\sum_{\kappa\in\mathcal{P}_{\rho_j}} \phi_{\rho_j} \prod_{i=1}^{|\kappa|} \mathrm{agg}(\kappa_i)\ \mathrm{d}\nu^{[H]}_{[0,t]}(\Psi_{\kappa_i}) \right]. \tag{6.14}$$

Note that the indicators $\mathrm{agg}(\kappa_i)$ and the cumulants $\phi_{[\rho]}$ depend on the whole pseudo-trajectory, and hence depend on the time t.

6.3.3 Initial cluster cumulants

This section is dedicated to proving Lemma 6.3.2 below, yielding an explicit formulation of the initial cluster cumulants implicitly defined in (6.13), and useful to find bounds in Section 6.5.2. We denote

$$\aleph_{|\rho|} \doteq \{\underline{z}^{[0]}_{\Psi_{\rho_i}}\ ,\ 1\le i\le|\rho|\} \quad\text{and}\quad \Gamma_p \doteq \{z^*_i\ ,\ 1\le i\le p\}$$

the set of clusters and the set of integrated particles, $N \doteq |\Psi_{\rho_1}| + \dots + |\Psi_{\rho_{|\rho|}}|$ the total number of particles contained in the clusters, and

$$\left[\mathbb{1}_{\mathcal{X}_{(\cdot)}}\right]^{\otimes\aleph_{|\rho|}} \doteq \prod_{\underline{z}\in\aleph_{|\rho|}} \mathbb{1}_{\mathcal{X}_{|\underline{z}|}}(\underline{z})$$

the indicator that *within* each cluster, the particles exclude themselves. Finally, we denote as before $\mathbb{1}_{x\sim y} = 1 - \mathbb{1}_{x\not\sim y}$ the exclusion condition between two subsets of particles x and y (potentially clusters), and for $S\subset\aleph_{|\rho|}$, $k\le p$ and $l\le q$, we introduce the *cumulants of the cluster exclusion*

$$\phi_{S,k+l} \doteq \sum_{G\in\mathcal{C}_{S\cup[\![k+l]\!]}} \prod_{\{x,y\}\in E_G} (-\mathbb{1}_{x\sim y}),$$

where $\mathcal{C}_A$ stands for the connected graphs on a set A.

Lemma 6.3.2 (Explicit formula for the initial cluster cumulants)**.** *For any $\lambda,\mu>0$, with the notation above, the initial cluster cumulants can be written as*

$$f^{\varepsilon,\rho}_n(0,\underline{z}_{\Psi_{\rho_1}},\dots,\underline{z}_{\Psi_{\rho_{|\rho|}}}) = \left[\mathbb{1}_{\mathcal{X}_{(\cdot)}}\right]^{\otimes\aleph_{|\rho|}} M_\beta^{\otimes N} \varphi_0^{\otimes\underline{\ell}_N} \sum_{p,q\geqslant 0} \frac{\lambda^p\mu^q}{p!q!} \int \varphi_0^{\otimes p} M_\beta^{\otimes p+q} \phi_{\aleph_{|\rho|},p+q}.$$

Proof. To obtain an explicit formulation for the initial cluster cumulants, we will identify them using the following characterization

$$F^\varepsilon(0, \underline{z}^{[0]}_{\Psi_{\rho_1}}, \dots, \underline{z}^{[0]}_{\Psi_{\rho_{|\rho|}}}) = \sum_{\sigma \in \mathcal{P}_{|\rho|}} f^{\varepsilon,\rho}_{[\sigma]}(\underline{z}^{[0]}_{\Psi_{\rho_1}}, \dots, \underline{z}^{[0]}_{\Psi_{\rho_{|\rho|}}}). \tag{6.15}$$

Using the exchangeability of particles, we have

$$\begin{aligned} F^\varepsilon(0, \underline{z}^{[0]}_{\Psi_{\rho_1}}, \dots, \underline{z}^{[0]}_{\Psi_{\rho_{|\rho|}}}) &= \frac{1}{\mathcal{Z}_\mu} \sum_{p \geqslant 0} \sum_{\underline{\ell}^*_p \in \Lambda_p} \frac{\lambda^{|\underline{\ell}^*_p|} \mu^{p - |\underline{\ell}^*_p|}}{p!} \int \varphi_0^{\otimes \tilde{\underline{\ell}}_{N+p}} M_\beta^{\otimes N+p} \mathbb{1}_{\mathcal{X}^\varepsilon_{N+p}} \mathrm{d}\underline{z}^*_p \\ &= \frac{1}{\mathcal{Z}_\mu} \sum_{p \geqslant 0} \sum_{q=1}^{p} \frac{\lambda^q \mu^{p-q}}{q!(p-q)!} \int \varphi_0^{\otimes \underline{\ell}_N} \varphi_0^{\otimes q} M_\beta^{\otimes N+p} \mathbb{1}_{\mathcal{X}^\varepsilon_{N+p}} \mathrm{d}\underline{z}^*_p \end{aligned}$$

To retrieve a cumulant formulation like (6.15) above, we will expand into cumulants the exclusion condition—which is the only obstruction to independence. To get rid of the partition function $\mathcal{Z}_\mu$ in the process, we will not expand the condition according to the integrating variables $\underline{z}^*_p$, to make appear the partition function at the numerator. More precisely, decomposing the exclusion condition within each cluster, we write

$$\mathbb{1}_{\mathcal{X}_{N+p}}(\underline{z}^{[0]}_{\Psi_{\rho_1}}, \dots, \underline{z}^{[0]}_{\Psi_{\rho_{|\rho|}}}, \underline{z}^*_p) = \left[\mathbb{1}_{\mathcal{X}_{(\cdot)}}\right]^{\otimes \aleph_{|\rho|}} \times \mathbb{1}_{\hat{\mathcal{X}}_{|\rho|+p}}(\underline{z}^{[0]}_{\Psi_{\rho_1}}, \dots, \underline{z}^{[0]}_{\Psi_{\rho_{|\rho|}}}, \underline{z}^*_p),$$

with

$$\begin{aligned} \mathbb{1}_{\hat{\mathcal{X}}_{|\rho|+p}}(\underline{z}^{[0]}_{\Psi_{\rho_1}}, \dots, \underline{z}^{[0]}_{\Psi_{\rho_{|\rho|}}}, \underline{z}^*_p) &= \prod_{x,y \in \aleph_{|\rho|}} \mathbb{1}_{x \not\sim y} \prod_{x \in \aleph_{|\rho|}, y \in \Gamma_p} \mathbb{1}_{x \not\sim y} \prod_{x,y \in \Gamma_p} \mathbb{1}_{x \not\sim y} \\ &= \sum_{G \in \mathcal{G}_{(\aleph_{|\rho|} \cup \Gamma_p)}} \prod_{\{x,y\} \in E_G} (-\mathbb{1}_{x \sim y}). \end{aligned}$$

We want now to split the sum above according to the partition induced by the connected components of the graph G, as for the standard cumulants of the exclusion (5.5). Nevertheless, since we want to make appear the partition function, we will compute a coarser splitting. Indeed, we will merely isolate the part of the graph which is not connected to any cluster of $\aleph_{|\rho|}$, i.e. the subset $B \subset \Gamma_p$ of integrated particles that are only connected between themselves. We still decompose the rest of the graph into its connected components, yielding a partition of $\aleph_{|\rho|} \cup B^c$ in which each subset has to contain a cluster (otherwise it would have been kept in B), which we denote $\sigma \in \tilde{\mathcal{P}}[\aleph_{|\rho|}, B^c]$. Hence, one can write

$$\begin{aligned} \mathbb{1}_{\hat{\mathcal{X}}_{|\rho|+p}}(\underline{z}^{[0]}_{\Psi_{\rho_1}}, \dots, \underline{z}^{[0]}_{\Psi_{\rho_{|\rho|}}}, \underline{z}^*_p) &= \sum_{B \subset \Gamma_p} \sum_{G \in \mathcal{G}_B} \prod_{\{x,y\} \in E_G} (-\mathbb{1}_{x \sim y}) \sum_{\sigma \in \tilde{\mathcal{P}}[\aleph_{|\rho|}, B^c]} \prod_{i=1}^{|\sigma|} \sum_{G \in \mathcal{C}_{\sigma_i}} \prod_{\{x,y\} \in E_G} (-\mathbb{1}_{x \sim y}) \\ &= \sum_{B \subset \Gamma_p} \mathbb{1}_{\mathcal{X}_{|B|}}(\underline{z}^*_B) \sum_{\sigma \in \tilde{\mathcal{P}}[\aleph_{|\rho|}, B^c]} \prod_{i=1}^{|\sigma|} \phi_{\sigma_i}, \end{aligned}$$

gathering the first sum over $\mathcal{G}_B$ by inverting the usual expansion, and recognizing cumulants of the exclusion in their form (5.5) (see Section 5.3). In the end, a partition $\sigma \in \tilde{\mathcal{P}}[\aleph_{|\rho|}, B^c]$ is a partition of $\aleph_{|\rho|}$ on which some particles from B^c are added, either tagged by $\underline{\ell}^*_p$ or not. We will use the symmetry of particles (like in the study of the partition function, Section 5.4) to reduce these added particles to their numbers of 1-tags $k_1, \dots, k_{|\sigma|} \geq 0$ and of 0-tags $l_1, \dots, l_{|\sigma|} \geq 0$, and similarly for

the particles in B, in numbers $k_0, l_0 \geq 0$. Omitting the indicator $\left[\mathbb{1}_{\mathcal{X}_{(\cdot)}}\right]^{\otimes \aleph_{|\rho|}}$ to gain lisibility (it factorizes and distributes very easily), we thus write

$$
\begin{aligned}
&F^{\varepsilon}\left[0, \underline{z}^{[0]}_{\Psi_{\rho_1}}, \dots, \underline{z}^{[0]}_{\Psi_{\rho_{|\rho|}}}\right] \\
&= \frac{\varphi_0^{\otimes \underline{\ell}_N}}{\mathcal{Z}_\mu} \sum_{p\geqslant 0} \sum_{q=1}^{p} \frac{\lambda^q \mu^{p-q}}{q!(p-q)!} \sum_{\sigma \in \mathcal{P}_{\aleph_{|\rho|}}} \sum_{\substack{k_0+\dots+k_{|\sigma|}=q \\ l_0+\dots+l_{|\sigma|}=p-q}} \frac{q!}{k_0!\dots k_{|\sigma|}!} \frac{(p-q)!}{l_0!\dots l_{|\sigma|}!} \int \varphi_0^{\otimes q} M_\beta^{\otimes N+p} \mathbb{1}_{\mathcal{X}^{\varepsilon}_{k_0+l_0}} \prod_{i=1}^{|\sigma|} \phi_{\sigma_i, k_i+l_i} \\
&= \frac{\varphi_0^{\otimes \underline{\ell}_N} M_\beta^{\otimes N}}{\mathcal{Z}_\mu} \sum_{k_0, l_0 \geqslant 0} \frac{\lambda^{k_0}\mu^{l_0}}{k_0! l_0!} \int \varphi_0^{\otimes k_0} M_\beta^{\otimes l_0 + k_0} \mathbb{1}_{\mathcal{X}^{\varepsilon}_{k_0+l_0}} \times \sum_{\sigma \in \mathcal{P}_{\aleph_{|\rho|}}} \prod_{i=1}^{|\sigma|} \sum_{k_i, l_i \geqslant 0} \frac{\lambda^{k_i}\mu^{l_i}}{k_i! l_i!} \int \varphi_0^{\otimes k_i} M_\beta^{\otimes l_i + k_i} \phi_{\sigma_i, k_i+l_i} \\
&= \sum_{\sigma \in \mathcal{P}_{\aleph_{|\rho|}}} \prod_{i=1}^{|\sigma|} M_\beta^{\otimes \sigma_i} \varphi_0^{\otimes \underline{\ell}_{\sigma_i}} \sum_{k_i, l_i \geqslant 0} \frac{\lambda^{k_i}\mu^{l_i}}{k_i! l_i!} \int \mathrm{d}\underline{z}^*_{l_i+k_i} \varphi_0^{\otimes k_i} M_\beta^{\otimes l_i + k_i} \phi_{\sigma_i, k_i+l_i},
\end{aligned}
$$

recognizing the partition function $\mathcal{Z}_\mu$ at the numerator. The lemma is thus proved by identification once added back the indicator $\mathbb{1}_{\mathcal{X}_{(\cdot)}}^{\otimes \aleph_{|\rho|}}$. □

6.4 Dynamics trees

Starting from the formulation (6.14) of the cumulants in terms of pseudo-trajectories, we will rewrite this integral to make appear the *correlations*' history between the particles. Indeed, the cumulants encode the small defects of particles' independence, which correspond to fortuitous encounters happening between the pseudo-trajectories of the n considered particles. In fact, we prove that asymptotically, the n-th cumulant f_n^{ε} is supported over trajectories implying exactly $(n-1)$ of these fortuitous encounters, thus connecting all the pseudo-trajectories. This way, each of these interactions has to be clustering, to eventually form a minimally connected graph.

We will control these fortuitous interactions between pseudo-trajectories in the integrated form

$$
\sum_{\rho \in \mathcal{P}_n} \int \mathrm{d}\underline{z}_n \int f_n^{\varepsilon,\rho}(0, \underline{z}^{[0]}_{\Psi_{\rho_1}}, \dots, \underline{z}^{[0]}_{\Psi_{\rho_{|\rho|}}}) \prod_{j=1}^{|\rho|} \left[\sum_{\kappa \in \mathcal{P}_{\rho_j}} \phi_{\rho_j} \prod_{i=1}^{|\kappa|} \mathrm{agg}(\kappa_i)\ \mathrm{d}\nu^{[H]}_{[0,t]}(\Psi_{\kappa_i}) \right], \tag{6.16}
$$

which is the integral over $\underline{z}_n$ of $f_n^{\varepsilon}[H](t, \underline{z}_n, \underline{\ell}_n)$ in its form (6.14). The integral over the endstate $\underline{z}_n$ allow to act on the arrival positions $\underline{x}_n$ of the trajectories to make the fortuitous interactions appear or disappear. In the end, we will perform a change of these variables $\underline{x}_n$ that harnesses these interactions.

To that end, these fortuitous encounters will be recorded in *dynamics trees*, allowing us to express the conditions of their existence. They stem from two different sources: first, *recollisions* appear within the aggregates (κ_i) to make them connected; and on the other hand, on each cluster ρ_j of aggregates, the extended cumulants of their mutual exclusion ϕ_{ρ_j} make appear *overlapping* conditions between the aggregates, recalling that when two different aggregates meet, they overlap one another without interacting. This formulation in dynamics trees will be the first step to prove bounds on the cumulants, and to compute their limit (Sections 6.5.2 and 6.6.3).

6.4.1 Clustering recollisions

As explained above, within a typical aggregate $\kappa_i \subset [\![1, n]\!]$, denoting $A \doteq \kappa_i$ and $a \doteq |A|$, each pseudo-trajectory Ψ_A contains recollisions (6.11) that connect the aggregate altogether, according to the condition $\mathrm{agg}(A)$.

Definition 6.4.1 (Clustering recollisions)**.** In a given pseudo-trajectory, looked at backwards in time starting from time t, we call *clustering recollision* the first recollision connecting the pseudo-trajectories stemming from two different particles. In an aggregate A, we order these clustering recollisions backwards in time from 1 to $(a-1)$, which defines a *recollision tree* $T^{\mathrm{c}}(\underline{z}_{\Psi_A}^{[0,t]}) \in \mathcal{T}_A^{\prec}$ whose ordered edges record these recollisions: two particles $m, m' \in A \subset [\![1,n]\!]$ are connected in this tree if and only if a clustering recollision happens between the pseudo-trajectories stemming from m and m'. Eventually, we define

$$(\tau_i^{\mathrm{c}}, \omega_i^{\mathrm{c}})_{1 \leqslant i \leqslant a-1} \in ([0,t] \times \mathbb{S}^{d-1})^{a-1}$$

the ordered collision times and angles at which the recollision occurs.

For simplicity, we denote $T_A^{\mathrm{c}} \doteq T^{\mathrm{c}}(\underline{z}_{\Psi_A}^{[0,t]})$. We now partition according to the associated tree

$$\mathrm{agg}(A) = \sum_{\Upsilon \in \mathcal{T}_A^{\prec}} \mathbb{1}_{T_A^{\mathrm{c}} = \Upsilon}.$$

Under the condition $T_A^{\mathrm{c}} = \Upsilon$, we will perform a change of variables that harnesses each of the clustering recollision conditions. To do so, we need to know *which particles*, from the pseudo-trajectories stemming from $m, m' \in A$, collided to connect them. Recall that $P(m)$ denotes the set of all particles added in the pseudo-trajectory stemming from m. Then, for every edge $e = (m, m') \in E_\Upsilon$, we define $\mathrm{col}_e(A)$ the pair of particles $(p_e, q_e) \in P(m) \times P(m')$ that collided on $(0,t)$ to connect the pseudo-trajectories of m and m', when creating the edge e. Eventually, we also partition according to which particle collided with which, for each clustering recollision:

$$\mathrm{agg}(A) = \sum_{\Upsilon \in \mathcal{T}_A^{\prec}} \mathbb{1}_{T_A^{\mathrm{c}} = \Upsilon} \sum_{\substack{p_e \in P(m), q_e \in P(m') \\ e=(m,m') \in \mathbb{E}_\Upsilon}} \prod_{e \in E_\Upsilon} \mathbb{1}_{(p_e,q_e) = \mathrm{col}_e(A)}.$$

We introduce the following notation for the indicator that the clustering particles are those we want (the Fraktur $\mathfrak{S}$ is chosen after the historical German word for collisions *Stoß*, at the origin of the concept of molecular chaos *Stoßzahlansatz* [29])

$$\mathfrak{S}_{(p_e,q_e)_\Upsilon}[A] \doteq \prod_{e \in E_\Upsilon} \mathbb{1}_{(p_e,q_e) = \mathrm{col}_e(A)}.$$

We can now harness the successive clustering conditions, which correspond to the ordered edges of the tree T_A^{c}, enumerated $(e_1, \dots, e_{a-1}) = ((m_1, m_1'), \dots, (m_{a-1}, m_{a-1}'))$ backwards in time. The relevant variables that we want to make appear are the times and angles of the collisions, when the current integration variables are the arrival positions $\underline{x}_A$ at time t.

As we are interested in the relative positions of the particles implied in the clustering recollisions, we start with the following change of variable of Jacobian 1, denoting $\overline{x}_A$ the *barycenter of the positions* $\underline{x}_A$,

$$\underline{x}_A \mapsto \left(\overline{x}_A, (\vec{x}_e \doteq x_{p_e} - x_{q_e})_{e \in E_\Upsilon}\right),$$

where we take the convention $p_e > q_e$, to be consistent in the following with the measure ν. Thus, once recursively determined the clustering conditions associated to all the edges preceding an edge e such that $\mathrm{col}_e(A) = (p_e, q_e)$, the condition associated with this edge states that at time τ_e^{c}, the relative position $x_{p_e}(\tau_e^{\mathrm{c}}) - x_{q_e}(\tau_e^{\mathrm{c}})$ must belong to the sphere of radius ε, defining the recollision angle $\omega_e^{\mathrm{c}} \in \mathbb{S}^{d-1}$. Hence, denoting τ_{d} the time of the closest deflection that underwent p_e or q_e between t and τ_e^{c}, and Δx_{d} the relative distance travelled between t and τ_{d}, the relative positions at time t might be retrieved from

$$x_{p_e} - x_{q_e} = \varepsilon \omega_e^{\mathrm{c}} - (\tau_e^{\mathrm{c}} - \tau_{\mathrm{d}})(v_{p_e}(\tau_e^{\mathrm{c}+}) - v_{q_e}(\tau_e^{\mathrm{c}+})) - \Delta x_{\mathrm{d}}. \tag{6.17}$$

The parameters $(\tau_e^{\mathrm{c}}, \omega_e^{\mathrm{c}})$ are unique because we consider the very first time (backwards) at which p_e and q_e meet, so that the mapping (6.17) above is invertible: we consider the local change of variable

$$x_{p_e} - x_{q_e} = \vec{x}_e \mapsto (\tau_e^{\mathrm{c}}, \omega_e^{\mathrm{c}}) \in [0, \tau_{e'}^{\mathrm{c}}] \times \mathbb{S}^{d-1},$$

where e' is the edge ordered right before e. Since Δx_{d} is a piecewise affine function recording the part of the dynamics that does not depend on τ_e^{c} (but depends on the previous recursively determined clustering conditions, the dependency in τ_e^{c} being explicit in (6.17)), the Jacobian of this change of variables is

$$\varepsilon^{d-1} \langle v_{p_e}(\tau_e^{\mathrm{c}+}) - v_{q_e}(\tau_e^{\mathrm{c}+}), \omega_e^{\mathrm{c}} \rangle_+ = \mu^{-1} \langle v_{p_e}(\tau_e^{\mathrm{c}+}) - v_{q_e}(\tau_e^{\mathrm{c}+}), \omega_e^{\mathrm{c}} \rangle_+. \tag{6.18}$$

Iterating this computation, we change the variables $(\vec{x}_e)_{e \in E_\Upsilon}$ to the ordered times $\underline{\tau}_{a-1}^{\mathrm{c}}$ and angles $\underline{\omega}_{a-1}^{\mathrm{c}}$ of clustering recollisions (also indexed by the ordered edges of E_Υ), finally leading to

$$\begin{aligned} &\int \mathrm{d}\underline{x}_A \Big[\mathbb{1}_{T_A^{\mathrm{c}} = \Upsilon} \mathfrak{S}_{(p_e, q_e)_\Upsilon}[A] \Big] \mathrm{d}\nu_{[0,t]}^{[H]}(\Psi_A) \\ &\quad = \int \frac{\mathrm{d}\overline{x}_A}{\mu^{a-1}} \mathrm{d}\underline{\omega}_{a-1}^{\mathrm{c}} \mathrm{d}\underline{\tau}_{a-1}^{\mathrm{c}} \Big[\mathbb{1}_{T_A^{\mathrm{c}} = \Upsilon} \mathfrak{S}_{(p_e, q_e)_\Upsilon}[A] \Big] \mathrm{d}\nu_{[0,t]}^{[H]}(\Psi_A) \prod_{e \in E_\Upsilon} \langle v_{p_e}(\tau_e^{\mathrm{c}+}) - v_{q_e}(\tau_e^{\mathrm{c}+}), \omega_e^{\mathrm{c}} \rangle_+. \end{aligned}$$

6.4.2 Clustering overlaps

Now for a general cluster $R = \rho_j$, of size $r = |R|$, we expand the cumulant

$$\phi_R = \sum_{G \in \mathcal{C}_{|\kappa|}} \prod_{\{i,j\} \in E_G} (-\mathbb{1}_{\kappa_i \sim \kappa_j})$$

making appear *overlap conditions* $\mathbb{1}_{\kappa_i \sim \kappa_j}$. At fixed pseudo-trajectory parameters Ψ_R, changing the barycenter $\overline{x}_{\kappa_i}$ of an aggregate moves rigidly the whole aggregate pseudo-trajectory, since by construction the trajectories are defined independently on each aggregate. That way, we can act on the barycenters to make them match the overlaps given by a given graph $G \in \mathcal{C}_{|\kappa|}$. In the same fashion as for the recollision trees, we define the following objects.

Definition 6.4.2 (Clustering overlaps)**.** In a given pseudo-trajectory, we call *clustering overlap* the first overlap (backwards in time) appearing between independently defined aggregates, connecting them according to the overlap condition discussed above. As for recollisions, clustering overlaps define an *overlap tree* $T^{\mathrm{ov}}(\underline{z}_{\Psi_R^{[0,t]}}) \in \mathcal{T}_{|\kappa|}^{\prec}$, and for each edge $e = \{m, m'\}$ associated to an overlap, we define

$$\tau_e^{\mathrm{ov}} = \sup \Big\{ 0 \le s \le t \ , \ \mathbb{1}_{\kappa_m \sim \kappa_{m'}}^{[s,t]} = 1 \Big\}$$

its overlap time (arbitrarily taking the latest possible, to make them consistent with recollisions when constructing pseudo-trajectories backwards in time), along with the associated overlap angle ω_e^{ov}.

As for the recollision trees, we denote $T_R^{\mathrm{ov}} \doteq T^{\mathrm{ov}}(\underline{z}_{\Psi_R^{[0,t]}})$ the overlap tree. Now, we partition the expansion of the cumulants according to the associated tree, treating separately when the graph appearing in the sum is the overlap tree, and when it presents some additional cycles. Denoting $\mathcal{C}_{|\kappa|}(\Upsilon)$ the connected graphs containing Υ, we have

$$\begin{aligned} \phi_R = &\sum_{\Upsilon \in \mathcal{T}_{|\kappa|}^{\prec}} \mathbb{1}_{T_R^{\mathrm{ov}} = \Upsilon} \prod_{\{i,j\} \in E_\Upsilon} (-\mathbb{1}_{\kappa_i \sim \kappa_j}) \quad + \quad \sum_{\Upsilon \in \mathcal{T}_{|\kappa|}^{\prec}} \mathbb{1}_{T_R^{\mathrm{ov}} = \Upsilon} \sum_{G \in \mathcal{C}_{|\kappa|}(\Upsilon) \setminus \{\Upsilon\}} \prod_{\{i,j\} \in E_G} (-\mathbb{1}_{\kappa_i \sim \kappa_j}) \\ \doteq &\qquad \phi_R^{[\mathrm{tree}]} \qquad + \qquad \phi_R^{[\mathrm{cycle}]}. \end{aligned} \tag{6.19}$$

Focusing first on the tree part, one can write

$$\sum_{\kappa\in\mathcal{P}_R}\phi_R^{[\mathrm{tree}]}\prod_{i=1}^{|\kappa|}\mathrm{agg}(\kappa_i)\mathrm{d}\nu_{[0,t]}^{[H]}(\Psi_{\kappa_i})=(-1)^{|\kappa|-1}\sum_{\Upsilon\in\mathcal{T}_{|\kappa|}^{\prec}}\mathbb{1}_{T_R^{\mathrm{ov}}=\Upsilon}\prod_{i=1}^{|\kappa|}\mathrm{agg}(\kappa_i)\mathrm{d}\nu_{[0,t]}^{[H]}(\Psi_{\kappa_i}),$$

the overlap conditions being included in the overlap tree matching condition. At fixed overlap tree $\Upsilon=T_R^{\mathrm{ov}}$, we act now on the aggregate barycenters that appeared during the change of variable harnessing the recollisions. Recall that moving these barycenters moves rigidly the aggregate pseudo-trajectories. Like for the clustering recollisions, we hence focus on the relative positions of these barycenters through the change of variable, of Jacobian 1,

$$(\overline{x}_{\kappa_i})_{i\leqslant|\kappa|}\mapsto\left(\overline{x}_R,(\vec{x}_e\doteq x_{p_e}-x_{q_e})_{e\in E_\Upsilon}\right),$$

conditionning on the overlapping particles (p_e,q_e) associated to the edge e, as it was done for recollisions.

6.4.3 Clustering trees

At this point, we observe that the knowledge of a recollision tree on each aggregate, and of an overlap tree between these aggregates, is equivalent to the knowledge of a global decorated *clustering tree* $T_R^\star\in\mathcal{T}_r^{\prec,\star}$, recording all the clustering interactions between the r particles of a cluster R, and recording whether it is a recollision or an overlap through a decoration on each edge. This leads to the mapping

$$\begin{aligned}\mathcal{T}_{|\kappa|}^{\prec}\times\prod_{i=1}^{|\kappa|}\mathcal{T}_{|\kappa_i|}^{\prec}\quad&\longrightarrow\quad\mathcal{T}_r^{\prec,\star}\\ T_R^{\mathrm{ov}},(T_{\kappa_i}^{\mathrm{c}})_{i\leqslant|\kappa|}\quad&\longmapsto\quad T_R^\star.\end{aligned}$$

The decorations are denoted $\underline{s}_{E_\Upsilon}$ by analogy with the scattering labels of the pseudo-trajectory histories (4.7): indeed, this time again, we choose that a sign $+1$ corresponds to a scattering (i.e. a recollision), and a sign (-1) to no scattering (i.e. an overlap). In the decorated clustering tree, the aggregates correspond to the decorated connected components retrieved when removing the overlap edges (we denote $\mathfrak{CC}^\star(\Upsilon)$ the set of these decorated connected components), so that the tree part of our cluster measure writes

$$\sum_{\kappa\in\mathcal{P}_R}\phi_R^{[\mathrm{tree}]}\prod_{i=1}^{|\kappa|}\mathrm{agg}(\kappa_i)\mathrm{d}\nu_{[0,t]}^{[H]}(\Psi_{\kappa_i})=\sum_{\Upsilon\in\mathcal{T}_R^{\prec,\star}}(-1)^{|\mathfrak{CC}^\star(\Upsilon)|-1}\int\mathbb{1}_{T_R^\star=\Upsilon}\prod_{A\in\mathfrak{CC}^\star(\Upsilon)}\mathrm{d}\nu_{[0,t]}^{[H]}(\Psi_A).$$

For each global tree $\Upsilon\in\mathcal{T}_R^{\prec,\star}$, we thus have $(r-1)$ encounter times and angles $(\tau_e^\star,\omega_e^\star)_{e\in E_\Upsilon}$, either associated to a recollision or to an overlap, according to the decorations $(s_e)_{e\in E_\Upsilon}$. Once computed the recollision changes of variable in each aggregate (i.e. decorated connected component of Υ), we compute the same on their barycenters to harness the overlaps, eventually leading to the variables $(\overline{x}_R,\underline{\tau}_{r-1}^\star,\underline{\omega}_{r-1}^\star)$. Since the overlap change of variable has the same Jacobian as the recollision one (6.18), we end up with

$$\begin{aligned}\int\mathrm{d}\underline{x}_R\sum_{\kappa\in\mathcal{P}_R}\phi_R^{[\mathrm{tree}]}\prod_{i=1}^{|\kappa|}\mathrm{agg}(\kappa_i)\mathrm{d}\nu_{[0,t]}^{[H]}(\Psi_{\kappa_i})=&\sum_{\Upsilon\in\mathcal{T}_R^{\prec,\star}}\sum_{\substack{p_e\in P(m),q_e\in P(m')\\e=(m,m')\in E_\Upsilon}}\int\frac{\mathrm{d}\overline{x}_R}{\mu^{r-1}}\mathrm{d}\underline{\omega}_{E_\Upsilon}^\star\mathrm{d}\underline{\tau}_{E_\Upsilon}^\star\\&\times\mathbb{1}_{T_R^\star=\Upsilon}\mathfrak{S}_{(p_e,q_e)_\Upsilon}[R]\prod_{e\in E_\Upsilon}s_e\langle v_{p_e}(\tau_e^{\star+})-v_{q_e}(\tau_e^{\star+}),\omega_e^\star\rangle_+\prod_{A\in\mathfrak{CC}^\star(\Upsilon)}\mathrm{d}\nu_{[0,t]}^{[H]}(\Psi_A).\end{aligned}$$

Now, keeping in mind that the pseudo-trajectories do not interact between decorated connected components of the clustering tree, one may gather back the measures $\nu^{[H]}_{[0,t]}$ on the whole set R. This means that we consider a unique history

$$(k, \underline{m}_k, \underline{\ell}^*_k, \underline{s}_k, \underline{t}_k, \underline{\omega}_k, \underline{v}^*_k)$$

for all the dynamics, although the pseudo-trajectories are still independently defined on each aggregate. Moreover, we want to keep track of the time ordering between the particle adjunctions and the clustering encounters. To that end, we will add to each edge $e \in E_\Upsilon$ of the clustering tree the information of the time interval $[t_{j+1}, t_j]$ (between two particle adjunctions) in which the clustering encounter occur. This way, adding this information to the knowledge of which particles are involved in the clustering encounter, each edge $e = \{m, m'\}$ is associated with the triplet

$$(p_e, q_e, i_e) \in P(m) \times P(m') \times [\![0, k]\!],$$

such that $\tau_e \in [t_{i_e+1}, t_{i_e}]$. Keeping the notation $\mathfrak{S}_{(p_e,q_e,i_e)}$ for this triplet's compatibility, we write

$$\int \mathrm{d}\underline{x}_R \sum_{\kappa\in\mathcal{P}_R} \phi_R^{[\mathrm{tree}]} \prod_{i=1}^{|\kappa|} \mathrm{agg}(\kappa_i)\mathrm{d}\nu^{[H]}_{[0,t]}(\Psi_{\kappa_i}) = \sum_{\Upsilon\in\mathcal{T}_R^{\prec,\star}} \sum_{\substack{p_e,q_e,i_e \\ e\in E_\Upsilon}} \int \frac{\mathrm{d}\overline{x}_R}{\mu^{r-1}} \mathrm{d}\underline{\omega}^\star_{E_\Upsilon} \mathrm{d}\underline{\tau}^\star_{E_\Upsilon} \mathbb{1}_{T^\star_R=\Upsilon} \mathfrak{S}_{(p_e,q_e,i_e)_\Upsilon}[R] \times \prod_{e\in E_\Upsilon} s_e \langle v_{p_e}(\tau_e^{\star+}) - v_{q_e}(\tau_e^{\star+}), \omega^\star_e\rangle_+ \, \mathrm{d}\nu^{[H]}_{[0,t]}(\Psi_R).$$

With all this in mind, we are now able to gather all the particle adjunctions and clustering encounters into a single tree encoding the whole dynamics. Indeed, at fixed number of added particles k, the choice of the history $(\underline{s}_k, \underline{m}_k)$ contained in the measure ν, along with the clustering information, may be encoded in a dynamics tree $T^{\mathrm{d}}_R \in \mathcal{T}^{\prec,\star}_{r+k}$, in which two vertices are connected either if a clustering encounter happens between them, or if one of them was added to the other one, i.e. if they form a couple $(n + j, m_j)$, with the associated signed decoration. The edges are time ordered from the ordered clustering conditions in $\Upsilon = T^\star_R$, and the intervals $(i_e)_{e\in E_\Upsilon}$ defined above. This provides the following mapping

$$\begin{array}{ccccccccccc} \mathcal{T}_R^{\prec,\star} & \times & [\![1, r+k]\!]^{E_\Upsilon} & \times & [\![0,k]\!]^{E_\Upsilon} & \times & \{\pm 1\}^k & \times & \mathcal{M}_{R,k} & \to & \mathcal{T}^{\mathrm{d}}_{R,k} \subset \mathcal{T}^{\prec,\star}_{r+k} \\ T^\star_R & , & (p_e, q_e)_e & , & (i_e)_e & , & \underline{s}_k & , & \underline{m}_k & \mapsto & T^{\mathrm{d}}_R \end{array}$$

with the condition $p_e, q_e \in P(m) \times P(m')$ for every $e = \{m, m'\} \in E_\Upsilon$. This mapping is injective, and made bijective by restriction to its image $\mathcal{T}^{\mathrm{d}}_{R,k} \subset \mathcal{T}^{\prec,\star}_{r+k}$, containing all the admissible dynamics trees. More precisely, an admissible dynamics tree is such that the added particles from $[\![r+1, r+k]\!]$ appear in increasing order, and in particular do not have encounters before appearing. For such a dynamics tree, the global dynamics might be recovered, starting from the highest ordered edge (the closest to time 0) and reconstructing the trajectories up to time t, as in the example given in Figure 6.1 (note that in this example the edge 0 is not admissible as it would connect the vertices 4 and 6 before they appear). From the dynamics, the parameters $(T^\star_R, (p_e, q_e, i_e)_e, \underline{s}_k, \underline{m}_k)$ can be retrieved, making the mapping bijective. Recalling the expression (6.6) of the measure, this lets us with encounter times $\underline{\tau}_{E_\Upsilon}$, angles $\underline{\omega}_{E_\Upsilon}$, stemming either from the adjunction of a particle in the pseudo-trajectory expansion, or from a clustering encounter (recollision or overlap). Generalizing the notation $\langle v_m(\tau_e{}^+) - v_{m'}(\tau_e{}^+), \omega_e\rangle_+$ to the adjunction of particles (even if in this case one of the

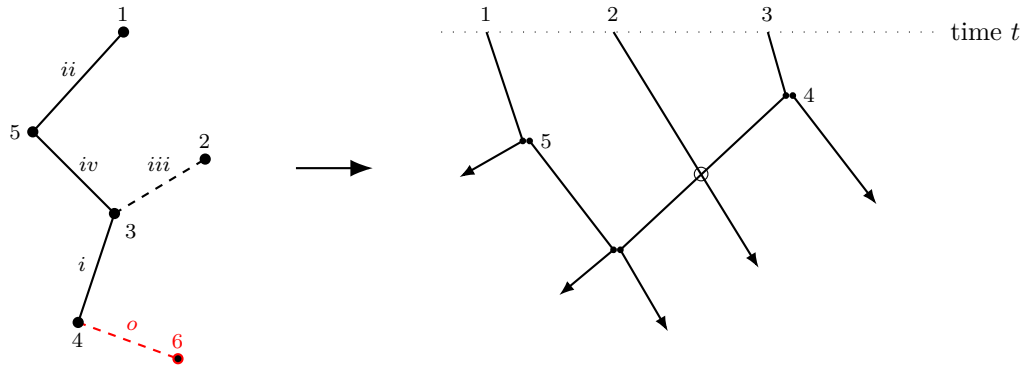

Figure 6.1: Example of retrieving the pseudo-trajectory dynamics (right) from the dynamics tree (left)

particles does not really exist at time τ_e^+), one can write the condensed measure

$$\int \mathrm{d}\underline{x}_R \sum_{\kappa\in\mathcal{P}_R} \phi_R^{[\mathrm{tree}]} \prod_{i=1}^{|\kappa|} \mathrm{agg}(\kappa_i)\mathrm{d}\nu_{[0,t]}^{[H]}(\Psi_{\kappa_i})$$
$$= \sum_{k\geqslant 0} \sum_{\underline{\ell}_k\in\Lambda_k} \sum_{\Upsilon\in\mathcal{T}_{R,k}^{\mathrm{d}}} \int \frac{p_\mu^{|\underline{\ell}_k|}}{\mu^{r-1}} \mathrm{d}\overline{x}_R \mathrm{d}\underline{v}_k^* H^{\otimes R} \mathbb{1}_{T_R^{\mathrm{d}}=\Upsilon} \prod_{e=\{m,m'\}\in E_\Upsilon} s_e\langle v_m(\tau_e{}^+) - v_{m'}(\tau_e{}^+), \omega_e\rangle_+ \mathrm{d}\omega_e \mathrm{d}\tau_e.$$

Although the order in the velocities' difference above do not change the calculus (as we integrate ω_e over the whole symmetric sphere), recall anyway that this order has been chosen such that $m > m'$. Summing everything up, we get the following proposition.

Proposition 6.4.1 (Dynamics tree formula for the integrated cumulants)**.** *For any time $t > 0$, the cumulants decompose into two terms*

$$f_n^\varepsilon[H](t) = f_n^\varepsilon[H]^{[\mathrm{tree}]}(t) + f_n^\varepsilon[H]^{[\mathrm{cycle}]}(t),$$

the first one containing only trees in its expansion, and the other including cycles. Indeed, the integral of the first tree term rewrites as the expansion

$$\int f_n^\varepsilon[H]^{[\mathrm{tree}]}(\underline{z}_n)\mathrm{d}\underline{z}_n = \sum_{\rho\in\mathcal{P}_n} I_n^{[\rho]}[H](t,\underline{\ell}_n),$$

where

$$I_n^{[\rho]}[H](t,\underline{\ell}_n) \doteq \int f_n^{\varepsilon,\rho}(0, \underline{z}_{\Psi_{\rho_1}}^{[0]}, \dots, \underline{z}_{\Psi_{\rho_{|\rho|}}}^{[0]}) \mathrm{d}\underline{v}_n \prod_{j=1}^{|\rho|} \frac{\mathrm{d}\overline{x}_{\rho_j}}{\mu^{|\rho_j|-1}} \sum_{k_j\geqslant 0} \sum_{\underline{\ell}_{k_j}} \sum_{\Upsilon\in\mathcal{T}_{\rho_j,k_j}^{\mathrm{d}}} p_\mu^{|\underline{\ell}_{k_j}|} H^{\otimes\rho_j} \mathbb{1}_{T_{\rho_j}^{\mathrm{d}}=\Upsilon}$$
$$\times \mathrm{d}\underline{v}_{k_j}^* \prod_{e\in E_\Upsilon} s_e\langle v_m(\tau_e{}^+) - v_{m'}(\tau_e{}^+), \omega_e\rangle_+ \mathrm{d}\omega_e \mathrm{d}\tau_e. \tag{6.20}$$

The term $f_n^\varepsilon[H]^{[\mathrm{cycle}]}$ corresponds to a similar expansion, stemming from the part $\phi_{\rho_j}^{[\mathrm{cycle}]}$ of the exclusion cumulants (6.19). Recall that the cluster cumulants $f_n^{\varepsilon,\rho}$ were defined in (6.13).

The term $f_n^\varepsilon[H]^{[\mathrm{cycle}]}$ will be controlled in the following Section 6.5.1.

6.5 Integrability bounds

We present here integrability bounds for the cumulants, based on the formula above (Proposition 6.4.1). First, we show how to reduce the study of the cycle part to the study of the tree part, making appear additional constraints on the way, to show that the cycle part will be negligible in the limit. Secondly, we bound this tree part on short times in Proposition 6.5.1.

6.5.1 Discarding overlap cycles: a tree inequality

As announced, we start by controlling the part of the cumulant expansion containing cycles. A cycle in the overlap conditions imposes a strong geometric constraint, which will provide smallness (Chapter 8). But first, we will compute a *tree inequality* to simplify the sum over all the connected graphs. To do this, we will harness the cancellations due to the signs, using the same trick as in the proof of Proposition 5.3.1. Indeed, recall that the cycle part of the exlusion cumulants writes, for a general cluster R,

$$\phi_R^{[\mathrm{cycle}]} = \sum_{\Upsilon \in \mathcal{T}_{|\kappa|}^{\prec}} \mathbb{1}_{T^{\mathrm{ov}}(R)=\Upsilon} \sum_{G \in \mathcal{C}_{|\kappa|}(\Upsilon)\setminus\{\Upsilon\}} \prod_{\{i,j\}\in E_G} (-\mathbb{1}_{\kappa_i \sim \kappa_j}).$$

Denoting $\mathbb{1}_R^{\emptyset}$ the indicator that the global dynamics contains a cycle, the sum over the cycling graphs rewrites as

$$\begin{aligned}\sum_{G \in \mathcal{C}_{|\kappa|}(\Upsilon)\setminus\{\Upsilon\}} \prod_{\{i,j\}\in E_G} (-\mathbb{1}_{\kappa_i \sim \kappa_j}) &= \mathbb{1}_R^{\emptyset} \prod_{\{i,j\}\in E_\Upsilon} (-\mathbb{1}_{\kappa_i \sim \kappa_j}) \sum_{E' \subset E_\Upsilon^c} \prod_{\{i,j\}\in E'} (-\mathbb{1}_{\kappa_i \sim \kappa_j}) \\ &= \mathbb{1}_R^{\emptyset} \prod_{\{i,j\}\in E_\Upsilon} (-\mathbb{1}_{\kappa_i \sim \kappa_j}) \prod_{\{i,j\}\in E_\Upsilon^c} (1 - \mathbb{1}_{\kappa_i \not\sim \kappa_j})\end{aligned}$$

computing the inverse expansion of the exclusion cumulants, the latter product being smaller than 1. We are hence brought back to the tree case, and dominate the cycle part by the tree part, with the additional strong cycle condition

$$\begin{aligned}\int f_n^{\varepsilon}[H]^{[\mathrm{cycle}]} \leq \sum_{\rho \in \mathcal{P}_n} \int f_n^{\varepsilon,\rho}(0) \mathrm{d}\underline{v}_n \prod_{j=1}^{|\rho|} \frac{\mathrm{d}\overline{x}_{\rho_j}}{\mu^{|\rho_j|-1}} \sum_{k_j \geqslant 0} \sum_{\underline{\ell}_{k_j}} \sum_{\Upsilon \in \mathcal{T}^{\mathrm{d}}_{\rho_j,k_j}} p_\mu^{|\underline{\ell}_{k_j}|} H^{\otimes \rho_j} \mathbb{1}_{T^{\mathrm{d}}_{\rho_j}=\Upsilon} \\ \times \mathrm{d}\underline{v}^*_{k_j} \prod_{e \in E_\Upsilon} s_e \langle v_m(\tau_e{}^+) - v_{m'}(\tau_e{}^+), \omega_e \rangle_+ \mathrm{d}\omega_e \mathrm{d}\tau_e \times \mathbb{1}^{\emptyset}_{\rho_j}.\end{aligned}$$

This term is negligible in front of the tree one, because of the strong geometric cycle condition, as stated in Section 6.6.2.

6.5.2 Bounding the cumulants on short times

We hence need to study the tree part of the integrated cumulants, written (Proposition 6.4.1)

$$\begin{aligned}\int f_n^{\varepsilon}[H]^{[\mathrm{tree}]}(t) = \sum_{\rho \in \mathcal{P}_n} \int f_n^{\varepsilon,\rho}(0) \mathrm{d}\underline{v}_n \prod_{j=1}^{|\rho|} \frac{\mathrm{d}\overline{x}_{\rho_j}}{\mu^{|\rho_j|-1}} \sum_{k_j \geqslant 0} \sum_{\underline{\ell}_{k_j}} \sum_{\Upsilon \in \mathcal{T}^{\mathrm{d}}_{\rho_j,k_j}} \int \mathrm{d}\underline{v}^*_{k_j} \mathbb{1}_{T^{\mathrm{d}}_{\rho_j}=\Upsilon} \\ \times \prod_{e \in E_\Upsilon} s_e \langle v_m(\tau_e{}^+) - v_{m'}(\tau_e{}^+), \omega_e \rangle_+ \mathrm{d}\omega_e \mathrm{d}\tau_e.\end{aligned} \tag{6.21}$$

As in [12], this bound is only valid on short times, considering that we do not have a priori bounds for the cumulants, unlike for the correlation functions (Section 4.4).

Proposition 6.5.1 (Cumulant bound)**.** *For μ large enough in the mixed scaling ($S_{\varepsilon,\mu,\lambda}$), there exists a time T_β depending on β and d such that for any $t < T_\beta$, one has for an absolute constant $C > 0$ that*

$$\left| \int f_n^\varepsilon[H]^{[\mathrm{tree}]}(t) \right| \leq \frac{C^n n!}{\mu^{n-1}} \|H\|_\infty^n.$$

More precisely, we have

$$\left| \int f_n^\varepsilon[H]^{[\mathrm{tree}]}(t) - I_n^{[\![1,n]\!]}[H](t) \right| \leq \frac{C^n n!}{\mu^{n-1}} \|H\|_\infty^n \cdot \varepsilon. \tag{6.22}$$

The latter inequality specifies that the leading term in the integral formula for the cumulants is the one corresponding to the trivial partition $\rho = \{[\![1,n]\!]\}$.

Proof. **First step: initial cluster cumulants.** To get bounds on this cumulant, we will start integrating the *initial* cluster cumulants, of which we recall the following expression (Lemma 6.3.2), where $N \doteq |\Psi_{\rho_1}| + \cdots + |\Psi_{\rho_{|\rho|}}|$ denotes the total number of particles contained in the clusters,

$$f_n^{\varepsilon,\rho}(0, \underline{z}^{[0]}_{\Psi_{\rho_1}}, \dots, \underline{z}^{[0]}_{\Psi_{\rho_{|\rho|}}}) = \left[\mathbb{1}_{\mathcal{X}_{(\cdot)}}\right]^{\otimes \aleph_{|\rho|}} M_\beta^{\otimes N} \varphi_0^{\otimes \underline{\ell}_N} \sum_{p,q \geqslant 0} \frac{\lambda^p \mu^q}{p!q!} \int \mathrm{d}\underline{z}^*_{p+q} \varphi_0^{\otimes p} M_\beta^{\otimes p+q} \phi_{\aleph_{|\rho|},p+q}.$$

Using the definition (4.15) of C_0 to control M_β and φ_0, we have

$$\int \left| f_n^{\varepsilon,\rho}(0, \underline{z}^{[0]}_{\Psi_{\rho_1}}, \dots, \underline{z}^{[0]}_{\Psi_{\rho_{|\rho|}}}) \right| \prod_{k=1}^{|\rho|} \mathrm{d}\overline{x}_{\rho_k} \leq C_0^N e^{-\beta \|\underline{v}_N\|^2} \sum_{p,q \geqslant 0} \frac{(C_0\lambda)^p \mu^q}{p!q!} \int M_\beta^{\otimes p+q} \left| \phi_{\aleph_{|\rho|},p+q} \right| \prod_{k=1}^{|\rho|} \mathrm{d}\overline{x}_{\rho_k} \mathrm{d}\underline{z}^*_{p+q},$$

and we apply the tree inequality (Proposition 5.3.1, *i.*) to the cumulant of the exclusion

$$\left| \phi_{\aleph_{|\rho|},p+q} \right| \leq \sum_{T \in \mathcal{T}_{\aleph_{|\rho|} \cup [\![p+q]\!]}} \prod_{\{x,y\} \in E_G} \mathbb{1}_{x \sim y}.$$

Like in the proof of the bound on these cumulants (Proposition 5.3.1, *ii.*), we use the integration variables $\underline{z}^*_{p+q}$ and $(\overline{x}_{\rho_k})_k$, the latter moving rigidly the clusters $(\underline{x}_{\Psi_k})_k$. Integrating over successive leaves of the tree, removing the edge $\{i,j\}$ leads to a factor $|\Psi_{\rho_i}| \cdot |\Psi_{\rho_j}| C_d \varepsilon^d$, depending on the number of particles in each cluster. For this reason, this time we need to discriminate according to the degrees $d_1, \dots, d_{|\rho|+p+q}$ of the vertices $\Psi_{\rho_1}, \dots, \Psi_{\rho_{|\rho|}}, x_1^*, \dots, x_{p+q}^*$. Since the number of trees on $[\![1,m]\!]$ with prescribed degrees $d_1, \dots, d_m$ is equal to

$$\frac{(m-2)!}{\prod_{i=1}^m (d_i - 1)!},$$

we get (also integrating the density M_β over $\underline{v}^*_{p+q}$)

$$\begin{aligned} &\int \left| f_n^{\varepsilon,\rho}(0, \underline{z}^{[0]}_{\Psi_{\rho_1}}, \dots, \underline{z}^{[0]}_{\Psi_{\rho_{|\rho|}}}) \right| \prod_{k=1}^{|\rho|} \mathrm{d}\overline{x}_{\rho_k} \\ &\qquad \leq C_0^N e^{-\beta \|\underline{v}_N\|^2} \sum_{p,q \geqslant 0} \frac{(C_0\lambda)^p \mu^q}{p!q!} \varepsilon^{d(|\rho|+p+q-1)} \sum_{d_1, \dots, d_{|\rho|+p+q}} \frac{(|\rho|+p+q-2)!}{\prod_{i=1}^{|\rho|+p+q} (d_i - 1)!} \prod_{i=1}^{|\rho|} |\Psi_{\rho_i}|^{d_i}. \end{aligned}$$

Now, we observe that

$$\frac{(|\rho|+p+q-2)!}{p!q!} = \binom{p+q}{p} \binom{p+q+|\rho|-2}{p+q} (|\rho|-2)! \leq \binom{p+q}{p} 2^{p+q+|\rho|-2} (|\rho|-2)!\,.$$

We write on the other hand

$$\prod_{i=1}^{|\rho|}\sum_{d_i\geqslant 1}\frac{|\Psi_{\rho_i}|^{d_i}}{(d_i-1)!}\leq\prod_{i=1}^{|\rho|}|\Psi_{\rho_i}|\exp(|\Psi_{\rho_i}|)\leq e^{2N},$$

and similarly

$$\prod_{i=1}^{p+q}\sum_{d_{|\rho|+i}\geqslant 1}\frac{1}{(d_{|\rho|+i}-1)!}\leq e^{p+q}.$$

We eventually get, since $|\rho|\leq N$ and $C_0\lambda\leq\mu$,

$$\begin{aligned}\int\left|f_n^{\varepsilon,\rho}(0,\underline{z}^{[0]}_{\Psi_{\rho_1}},\dots,\underline{z}^{[0]}_{\Psi_{\rho_{|\rho|}}})\right|\prod_{k=1}^{|\rho|}\mathrm{d}\overline{x}_{\rho_k}&\leq(2e^2C_0)^Ne^{-\beta\|\underline{v}_N\|^2}(|\rho|-2)!\varepsilon^{d(|\rho|-1)}\sum_{p,q\geqslant 0}\binom{p+q}{p}(2\mu\varepsilon^d)^{p+q}\\&\leq(2e^2C_0)^Ne^{-\beta\|\underline{v}_N\|^2}(|\rho|-2)!\varepsilon^{d(|\rho|-1)}\sum_{r\geqslant 0}(4\varepsilon)^r,\end{aligned}$$

eventually leading, for an absolute constant C, to

$$\int\left|f_n^{\varepsilon,\rho}(0,\underline{z}^{[0]}_{\Psi_{\rho_1}},\dots,\underline{z}^{[0]}_{\Psi_{\rho_{|\rho|}}})\right|\prod_{k=1}^{|\rho|}\mathrm{d}\overline{x}_{\rho_k}\leq(CC_0)^Ne^{-\beta\|\underline{v}_N\|^2}(|\rho|-2)!\varepsilon^{d(|\rho|-1)}.\tag{6.23}$$

Second step: bounding the collision kernels. The observable H being bounded, we can dominate it roughly. Moreover, let us observe that the factors bounding the initial cumulants (6.23) decompose on the clusters as

$$(CC_0)^Ne^{-\beta\|\underline{v}_N\|^2}=\prod_{j=1}^{r}(CC_0)^{|\Psi_{\rho_j}|}e^{-\beta\|\underline{v}_{\Psi_{\rho_j}}\|^2},\tag{6.24}$$

so that for a generic cluster $R=\rho_j$, we harness the associated velocity decay, to study the cluster collisions in

$$S_R\doteq\sum_{k\geqslant 0}\sum_{\underline{\ell}_k\in\Lambda_k}p_\mu^{|\underline{\ell}_k|}\sum_{\Upsilon\in\mathcal{T}^{\mathrm{d}}_{R,k}}\int\mathrm{d}\underline{v}_{r+k}\mathbb{1}_{T^{\mathrm{d}}_{\rho_j}=\Upsilon}\prod_{e\in E_\Upsilon}s_e\langle v_m(\tau_e{}^+)-v_{m'}(\tau_e{}^+),\omega_e\rangle_+\mathrm{d}\omega_e\mathrm{d}\tau_e e^{-\beta\|\underline{v}_{r+k}\|^2}.$$

With our notation, $r+k=|\Psi_R|$. Since we just bounded the dependency on the initial value, the trajectories do not depend anymore on the particles' tags, allowing us to bound roughly the sum over $\underline{\ell}_k$, using that $p_\mu\leq 1$. We will use the velocity decay to bound the velocities appearing in the collision kernels. We bound each edge separately, starting from the furthest from time t, so that the other collision kernels will only contain velocities that do not depend on the considered edge.

For each edge corresponding to a clustering condition, using the Cauchy-Schwarz inequality, we bound all the possibilities for this edge by

$$2\sum_{m,m'=1}^{r+k}(|v_m(\tau_e^{\star+})|+|v_{m'}(\tau_e^{\star+})|)\leq 4(r+k)\sqrt{(r+k)\|\underline{v}_{r+k}\|^2},\tag{6.25}$$

where the factor 2 stems from the choice of the edge's decoration. For each edge associated to a particle's adjunction, since one of the vertices corresponds to the particle that is added, we only have to sum over the choice of the second particle as

$$2\sum_{m=1}^{r+k}(|v_m(\tau_e^{\star+})|+|v_{m'}(\tau_e^{\star+})|)\leq 2\sqrt{(r+k)\|\underline{v}_{r+k}\|^2}.\tag{6.26}$$

Determining whether the edge is a clustering condition or a particle's adjunction corresponds to an additional factor 2^{r+k}. In the end, harnessing the velocity decay (6.24) and integrating the ordered times, we get

$$\begin{aligned} S_R &\leq \sum_{k\geqslant 0} 8^k \int \mathrm{d}\underline{v}_{r+k}\mathrm{d}\underline{\omega}_{E_\Upsilon}\mathrm{d}\underline{\tau}_{E_\Upsilon}(r+k)^{r-1}\left(\sqrt{(r+k)\|\underline{v}_{r+k}\|^2}\right)^{r+k-1} e^{-\beta\|\underline{v}_{r+k}\|^2} \\ &\leq \sum_{k\geqslant 0} 8^k \frac{t^{r+k-1}}{(r+k-1)!}(r+k)^{r-1}\sqrt{r+k}^{r+k-1}\left(C_\beta\sqrt{r+k}\right)^{r+k-1} \\ &\leq \sum_{k\geqslant 0}(\hat{C}_\beta t)^{r+k-1}(r+k)^{r-1}e^{r+k}, \end{aligned} \tag{6.27}$$

using in the end that $(r+k)^{r+k-1} \leq (r+k-1)!e^{r+k}$.

Last step: combinatorial manipulations. We now gather it all to bound the cumulants using their expression (6.21) from Proposition 6.4.1. Using the exchangeability of particles to reduce the partition $\rho \in \mathcal{P}_n$ to the cardinal of its subsets, and denoting $C_H \doteq \|H\|_\infty$, we write for a constant C_β depending on the temperature and dimension that

$$\begin{aligned} \left|\int f_n^\varepsilon[H]^{[\mathrm{tree}]}(t)\right| &\leq \sum_{i=1}^n \sum_{r_1+\cdots+r_i=n} \frac{(i-2)!\varepsilon^{d(i-1)}n!}{i!r_1!\dots r_i!}\frac{C_H^n}{\mu^{n-i}}\prod_{j=1}^i\sum_{k_j\geqslant 0}(C_\beta C_0 t)^{r_j+k_j-1}(r_j+k_j)^{r_j-1} \\ &\leq \frac{C_H^n n!}{\mu^{n-1}}\sum_{i=1}^n \varepsilon^{i-1}\prod_{j=1}^i\sum_{r_j\geqslant 0}\sum_{k_j\geqslant 0}(C_\beta C_0 t)^{r_j+k_j-1}e^{k_j+r_j} \end{aligned}$$

in the scaling $\mu\varepsilon^d = \varepsilon$, and harnessing the denominators $r_j!$ to control the terms $(r_j+k_j)^{r_j-1}$. Now, for t small enough the series are convergent (and the term $r_j = k_j = 0$ actually does not appear, as it corresponds to the empty tree), so that we get

$$\begin{aligned} \left|\int f_n^\varepsilon[H]^{[\mathrm{tree}]}(t)\right| &\leq \frac{C_H^n n!}{\mu^{n-1}}\sum_{i=1}^n \varepsilon^{i-1}\cdot 4^i \\ &\leq 4\frac{C_H^n n!}{\mu^{n-1}}(1+8\varepsilon), \end{aligned}$$

which concludes the proof. The second point (6.22) of the proposition is proved observing that the term 8ε corresponds to the sum for $i \geq 2$, i.e. to the sum over the non-trivial partitions. □

6.6 Limit cumulants

Since the cumulants f_n^ε decrease very quickly as n increases (Proposition 6.5.1), we only need the convergence of the first cumulant to compute the large deviation principle, and the convergence of the fluctuation field. Indeed, in the rescaling $(\lambda^{n-1}f_n^\varepsilon)$ that appears in the statistical study of the tagged particles, the cumulants vanish for $n \geqslant 2$, as soon as $\frac{\lambda}{\mu}$ goes to zero. Nevertheless, for completeness, we also compute their limit in the rescaling $(\mu^{n-1}f_n^\varepsilon)$. The corresponding formula could be used to capture the fine scales of the dynamics in a further study.

6.6.1 Rare encounters of tagged particles

First of all, like in Section 4.7 for the correlation functions, we will show that the encounters between tagged particles are very rare. Indeed, when we have bounded roughly the sum over the possible

tags $\underline{\ell}_k \in \Lambda_k$ by 2^k, one could have looked at the influence of the encounters with at least one tagged particle, which corresponds to the sum

$$\sum_{\substack{\underline{\ell}_k \in \Lambda_k \\ \underline{\ell}_k \neq \underline{0}_k}} p_\mu^{|\underline{\ell}_k|} = \sum_{i=1}^{k} \binom{k}{i} p_\mu^i \leq p_\mu 2^k.$$

This leads to the exact same bound as the previous one, with an additional factor $p_\mu \ll 1$. In the end, we get the estimate presented in the proposition below.

Proposition 6.6.1 (Rare tagged encounters)**.** *Denoting*

$$\int f_n^\varepsilon [H]^{[\mathrm{tree}],\underline{0}}(t)$$

the integrated cumulants where the domain of integration of $\mathrm{d}\nu$ *is restricted to* $\{\underline{\ell}_k^* = \underline{0}_k\}$*, one has in the usual mixed scaling* ($S_{\varepsilon,\mu,\lambda}$)*, for any* t *small enough and an absolute constant* $C > 0$*, that*

$$\left| \int f_n^\varepsilon [H]^{[\mathrm{tree}]}(t) - \int f_n^\varepsilon [H]^{[\mathrm{tree}],\underline{0}}(t) \right| \leq \frac{C^n n!}{\mu^{n-1}} \|H\|_\infty^n \cdot p_\mu.$$

6.6.2 Discarding cycles

In the expansion of the integrated cumulants in terms of dynamics trees (Section 6.4), we emphasized that non-clustering encounters may happen, either stemming from a non-clustering overlap, or from a non-clustering collision. We state here that the dynamics presenting such cycles are negligible in the said expansion, in particular proving the smallness of the cycle part of the expansion (Section 6.5.1). Using a more precise computation than the previous method [11], we achieve an optimal bounding factor in ε instead of $\varepsilon|\log\varepsilon|$.

Proposition 6.6.2 (Cycles are rare in the dynamics)**.** *We have the following estimate on the expansion proved in Proposition 6.4.1 for the integrated cumulants, under the constraint that a cycle happens in the dynamics:*

$$\left| \sum_{\rho \in \mathcal{P}_n} \int f_n^{\varepsilon,\rho}(0) \mathrm{d}\underline{v}_n \prod_{j=1}^{|\rho|} \frac{\mathrm{d}\overline{x}_{\rho_j}}{\mu^{|\rho_j|-1}} \sum_{k_j \geqslant 0} \sum_{\Upsilon \in \mathcal{T}^{\mathrm{d}}_{\rho_j,k_j}} H^{\otimes \rho_j} \mathbb{1}_{T^{\mathrm{d}}_{\rho_j} = \Upsilon} \right.$$
$$\left. \times \mathrm{d}\underline{v}^*_{k_j} \mathrm{d}\underline{\omega}_{E_\Upsilon} \mathrm{d}\underline{\tau}_{E_\Upsilon} \prod_{e \in E_\Upsilon} s_e \langle v_m(\tau_e{}^+) - v_{m'}(\tau_e{}^+), \omega_e \rangle_+ \times \mathbb{1}^{\emptyset}_{\rho_j} \right| \leq \frac{C^n n!}{\mu^{n-1}} \|H\|_\infty^n \cdot \varepsilon.$$

The cycle condition imposes strong geometric constraints that result in a additional factor ε *in the usual bounds for the integrated cumulants. The dynamics implying cycles are thus negligible in the expansion above.*

The proof of this proposition is given in Chapter 8, based on geometric estimates.

6.6.3 Convergence of the integrated cumulants

Now that we stated that the cycles and the other tagged particles asymptotically have a negligible impact on the dynamics of n fixed particles, we go back to the expression (6.20) given in Proposition 6.4.1 for the integral of cumulants, to determine their limit (Proposition 6.6.3 below). Indeed,

by Propositions 6.6.1 and 6.6.2 above, up to an error of order $(\varepsilon + p_\mu)$, the pseudo-trajectories $\underline{z}_{n+k}^{[0,t]}$ only include clustering encounters, and none of the added particles is tagged. Hence, the velocities of these pseudo-trajectories only depend on the dynamics tree $T^{\mathrm{d}}_{[\![n]\!],k}$ and on the dynamics parameters in the integral, so that they are equal to the velocities of the limit pseudo-trajectories $\underline{\zeta}_{n+k}^{[0,t]}$. This way, similarly as in the discussions around Lemma 4.8.3 and the identification (4.47) of the initial pseudo-trajectories, the positions of both pseudo-trajectories are $(k\varepsilon)$-close, and in particular they are identical for the n final particles. Since the only tagged particles are among these n final particles, and since the equilibrium M_β only depends on the velocities, we get

$$[\varphi_0^{\otimes \underline{\ell}_n} M_\beta^{\otimes n+k}](\underline{\zeta}_{n+k}^{[0]}) = [\varphi_0^{\otimes \underline{\ell}_n} M_\beta^{\otimes n+k}](\underline{z}_{n+k}^{[0]}).$$

The observable $H^{\otimes n}$ also only depends on the n studied particles, so that one can bound

$$\begin{aligned}
&\left| H^{\otimes n}(\underline{\zeta}_n^{[0,t]})[\varphi_0^{\otimes \underline{\ell}_n} M_\beta^{\otimes n+k}](\underline{\zeta}_{n+k}^{[0]}) - H^{\otimes n}(\underline{z}_n^{[0,t]}) F^\varepsilon_{n+k}(0, \underline{z}_{n+k}^{[0]}) \right| \\
&\quad = \left| H^{\otimes n}(\underline{z}_n^{[0,t]}) \right| \cdot \left| [\varphi_0^{\otimes \underline{\ell}_n} M_\beta^{\otimes n+k}](\underline{z}_{n+k}^{[0]}) - F^\varepsilon_{n+k}(0, \underline{z}_{n+k}^{[0]}) \right| \\
&\quad \leq \left| H^{\otimes n}(\underline{z}_n^{[0,t]}) \right| \cdot C_0^{n+k} e^{-\frac{\beta}{4}\|\underline{v}_{n+k}\|^2} \varepsilon,
\end{aligned}$$

by the initial error studied in Proposition 4.3.1. Eventually, recalling the result (6.22) of Proposition 6.5.1, the leading term in the cumulant expansion corresponds to the case of a single cluster $\rho_1 = [\![1, n]\!]$, once again with an error of order ε. We end up with the following limit formula for the integrated cumulants.

Proposition 6.6.3 (Convergence of the cumulants)**.** *For $t > 0$ small enough, the integrated cumulants $\int f_n^\varepsilon[H](t, \underline{\ell}_n)$ introduced in (6.16), converge as ε goes to 0 in the scaling $(S_{\varepsilon,\mu,\lambda})$ towards the following limit formula*

$$\begin{aligned}
&\int f_n[H](t, \underline{\ell}_n) \qquad (6.28)\\
&\quad \doteq \sum_{k \geqslant 0} \sum_{\Upsilon \in \mathcal{T}^{\mathrm{d}}_{[\![n]\!],k}} \int \frac{\mathrm{d}\underline{x}\mathrm{d}\underline{v}_{n+k}}{\mu^{n-1}} \mathrm{d}\underline{\omega}_{E_\Upsilon} \mathrm{d}\underline{\tau}_{E_\Upsilon} \prod_{e \in E_\Upsilon} s_e \langle v_m^{[\tau_e^+]} - v_{m'}^{[\tau_e^+]}, \omega_e \rangle_+ H^{\otimes n}[\varphi_0^{\otimes \underline{\ell}_n} M_\beta^{\otimes n+k}](\underline{\zeta}_{n+k}^{[0]}),
\end{aligned}$$

where none of the added particles in the pseudo-trajectories are tagged, and with the quantitative bound

$$\left| \int f_n[H](t, \underline{\ell}_n) - \int f_n^\varepsilon[H](t, \underline{\ell}_n) \right| \leq \frac{C^n n!}{\mu^{n-1}} \|H\|_\infty^n \cdot (\varepsilon + p_\mu)\,.$$

Let us observe finally that some of the trees in the formula above do not contribute to the sum. Indeed, imagine that in a tree two added particles (hence non-tagged ones), both meet as their first (forwards) encounter at a time τ_e. Then, changing the sign of the encounter leads to a weight

$$-s_e \langle v_m^{[\tau_e^+]} - v_{m'}^{[\tau_e^+]}, \omega_e \rangle_+ M_\beta\left(v_m^{[0]\prime}\right) M_\beta\left(v_{m'}^{[0]\prime}\right) = -s_e \langle v_m^{[\tau_e^+]} - v_{m'}^{[\tau_e^+]}, \omega_e \rangle_+ M_\beta\left(v_m^{[0]}\right) M_\beta\left(v_{m'}^{[0]}\right),$$

using the equilibrium structure. Note that since they are added, they do not contribute to the weight $\varphi_0^{\otimes \underline{\ell}_n} H^{\otimes n}$, so that the contributions of this tree and of its counterpart with a changed sign cancel out. In particular, for the first limit cumulant $f_1 = F_1$, as pictured in Figure 6.2, the only

shape of tree that contributes is the linear one. Hence, it is enough to know the signs associated to each encounter, and one may write

$$\int F_1[H](t,\ell) \tag{6.29}$$
$$= \sum_{k\geqslant 0}\sum_{\underline{s}_k}\int \mathrm{d}z_1 \mathrm{d}\underline{v}_k^* \mathrm{d}\underline{\omega}_k \mathrm{d}\underline{\tau}_k \prod_{i=1}^{k} s_i \langle v_1^{[\tau_i^+]} - v_{1+i}^{[\tau_i^+]}, \omega_i\rangle_+ H(\zeta_1^{[0,t]})[\varphi_0^{\otimes \ell} M_\beta^{\otimes 1+k}](\underline{\zeta}_{1+k}^{[0]}).$$

Fortunately, this expansion coincides with the pseudo-trajectory formulation (4.13) of the solution to the linear Rayleigh–Boltzmann equation (2.13).

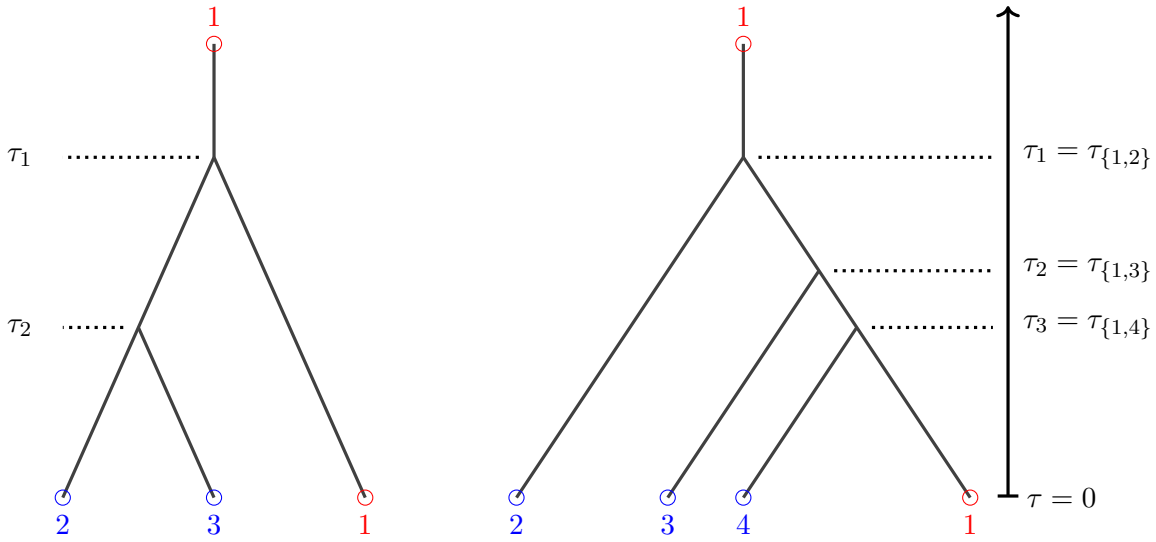

Figure 6.2: Left: example of non-contributing dynamics tree in the expansion (6.28) of the first correlation function. Right: only contributing tree for 3 added particles.

6.6.4 Convergence of the cumulant generating function

We study here the convergence of the cumulant generating function in the case (6.4) of an observable $H = \widehat{H}\mathbb{1}_{\ell=1}$ weighting only the tagged particles, generalized to observables depending on the pseudo-trajectory $\underline{z}^{[0,t]}$ in the whole time interval $[0,t]$ as in (6.9). It writes

$$\mathfrak{G}_\varepsilon^{[0,t]}[H] = \sum_{p\geqslant 1}\frac{\lambda^p}{p!}\int f_p^\varepsilon \left[e^H - 1\right](t,\underline{1}_p).$$

For $p \geq 2$, using the bounds on the cumulants (Proposition 6.5.1), one has

$$\sum_{p\geqslant 2}\frac{\lambda^p}{p!}\left|\int f_p^\varepsilon \left[e^H-1\right](t,\underline{1}_p)\right| \leq \lambda \sum_{p\geqslant 2}\left(\frac{\lambda}{\mu}\right)^{p-1}\left(C\|e^H-1\|_\infty\right)^p$$
$$\leq \lambda \times 2\frac{\lambda}{\mu}\left(C\|e^H-1\|_\infty\right)^2$$

as soon as $2\lambda C\|e^H - 1\|_\infty \leq \mu$ in the scaling ($S_{\varepsilon,\mu,\lambda}$). Hence, rescaling properly the generating function, we get the following proposition thanks to the convergence of the first cumulant (Proposition 6.6.3).

Proposition 6.6.4 (Convergence of the cumulant generating function)**.** *For any time t smaller than the short time T_β considered in Proposition 6.5.1, still in the mixed scaling $(S_{\varepsilon,\mu,\lambda})$, the rescaled cumulant generating function converges as*

$$\frac{1}{\lambda}\mathfrak{G}_\varepsilon^{[0,t]}[H] \xrightarrow[\varepsilon\to 0]{} \int F_1[e^H-1](t,1) = \int F_1[e^H](t,1) - 1. \tag{6.30}$$

All the cumulants of order greater than 2 vanish in this scaling, at the opposite of the non-linear version [12] in which they contribute to add non-linearity in the limiting generating function. Next section is dedicated to the equations driving this limit.

6.6.5 Hamilton–Jacobi equations for the limit cumulant generating function

For observables that behave according to the structure of the trajectories, i.e. of the form

$$H(z^{[0,t]}) = g(t, z^{[t]}) - \int_0^t [\partial_s - v\cdot\nabla_x] g(s, z(s))\mathrm{d}s$$

as introduced in Section 7.1, we will study the limit cumulant generating function (see the previous Section 6.6.4), denoted

$$\mathcal{I}(t,g) \doteq \int \tilde{F}_1 \left[\exp\left(g_t - \int_0^t (\partial_s - v\cdot\nabla_x) g_s \right) \right](t). \tag{6.31}$$

It is relevant to consider observables in the functional space

$$g \in \mathbb{B}_{T,\beta} \doteq \left\{ h \;\middle|\; \exists C>0 :\ \forall t\leqslant T,\ \left\| (h(t,v) - \frac{\beta}{4}|v|^2)_+ \right\|_{\mathbb{L}^\infty(\mathcal{D})} + \|(\partial_t - v\cdot\nabla_x)h(t)\|_{\mathbb{L}^\infty(\mathcal{D})} < C \right\}. \tag{6.32}$$

Indeed, the relevant variable that will appear as boundary condition of a Boltzmann equation will be $e^g(t)$ (see the proof of Proposition 6.6.6). Note that the time of validity of Theorem 3 depends on this norm C chosen for $g \in \mathbb{B}_{T,\beta}$. One may choose to extend this class of functions to observables growing as small inverse Gaussians, using part of the exponential decay of the cumulants to compensate this growth (see [12, Chapter 7]), yet that would mean losing control on the solutions to the Hamilton-Jacobi system below (Proposition 6.6.5).

We will use the formula (6.29) above to find the Hamilton–Jacobi equation it satisfies. Observe that the term $k=0$ in this expansion corresponds to the initial value $\mathcal{I}(0,g)$. For any $k\geqslant 1$, we split the dynamics tree in two, to isolate the influence of particle 2 at time τ_1. To this extent, let us define $\underline{\widetilde{s}}_{k-1} \doteq (s_2,\dots,s_k)$, and similarly $\underline{\widetilde{v}}_{k-1}, \underline{\widetilde{\omega}}_{k-1}, \underline{\widetilde{\tau}}_{k-1}$, and $\underline{\widetilde{\zeta}}_k \doteq (\zeta_1,\zeta_3,\dots,\zeta_{1+k})$. We split according to the sign s_1, which labels the first collision (between v_1 and $v_2 = v_1^*$), writing

$$\begin{aligned}
&\mathcal{I}(t,g) - \mathcal{I}(0,g) \qquad (6.33)\\
&= \int \mathrm{d}z_1\mathrm{d}v_2\mathrm{d}\omega_1\mathrm{d}\tau_1 \langle v_1 - v_2, \omega_1\rangle_+ M_\beta(v_2') \sum_{k\geqslant 1}\sum_{\underline{\widetilde{s}}} \int \mathrm{d}\underline{\widetilde{v}}\mathrm{d}\underline{\widetilde{\omega}}\mathrm{d}\underline{\widetilde{\tau}} \prod_{i=2}^k s_i \langle v_1^{[\tau_i^+]} - v_{1+i}^{[\tau_i^+]}, \omega_i\rangle_+ \\
&\qquad \times \exp\left(g(t,\zeta_1^{[t]}) - \int_0^t (\partial_s - v\cdot\nabla_x) g(s,\zeta_1^{[s]}) \right) [\varphi_0 M_\beta^{\otimes k}](\underline{\widetilde{\zeta}}_k^{[0]}) \\
&- \int \mathrm{d}z_1\mathrm{d}v_2\mathrm{d}\omega_1\mathrm{d}\tau_1 \langle v_1 - v_2, \omega_1\rangle_+ M_\beta(v_2) \sum_{k\geqslant 1}\sum_{\underline{\widetilde{s}}} \int \mathrm{d}\underline{\widetilde{v}}\mathrm{d}\underline{\widetilde{\omega}}\mathrm{d}\underline{\widetilde{\tau}} \prod_{i=2}^k s_i \langle v_1^{[\tau_i^+]} - v_{1+i}^{[\tau_i^+]}, \omega_i\rangle_+ \\
&\qquad \times \exp\left(g(t,\zeta_1^{[t]}) - \int_0^t (\partial_s - v\cdot\nabla_x) g(s,\zeta_1^{[s]}) \right) [\varphi_0 M_\beta^{\otimes k}](\underline{\widetilde{\zeta}}_k^{[0]}),
\end{aligned}$$

where the pseudo-trajectory $\underset{\sim}{\zeta}_k^{[0,t]}$ corresponds to the scattering case $s_1 = 1$ in the first term, and to the overlapping case $s_1 = -1$ in the second one. Now, by the fundamental theorem of calculus for the transport equation, since there is no collision in the pseudo-trajectory on $[\tau_1, t]$, one has

$$g(t,\zeta_1(t)) - \int_0^t (\partial_s - v\cdot\nabla_x) g(s,\zeta_1(s)) = g(\tau_1,\zeta_1(\tau_1^+)) - \int_0^{\tau_1} (\partial_s - v\cdot\nabla_x) g(s,\zeta_1(s)).$$

In the overlapping case, we have $g(\tau_1,\zeta_1(\tau_1^+)) = g(\tau_1, x_1^{[\tau_1]}, v_1) = g(\tau_1,\zeta_1(\tau_1^-))$, yet there is a discontinuity in the scattering case. Indeed, in the scattering case, writing

$$g(\tau_1,\zeta_1(\tau_1^+)) = g(\tau_1, x_1^{[\tau_1]}, v_1) - g(\tau_1, x_1^{[\tau_1]}, v_1') + g(\tau_1, x_1^{[\tau_1]}, v_1'),$$

and recalling that the mapping $(v_1', v_2') \mapsto (v_1, v_2)$ is of Jacobian 1, the first term in the expansion (6.33) above writes exactly as the second one, with an additional factor

$$\exp\left(g(\tau_1, x_1^{[\tau_1]}, v_1') - g(\tau_1, x_1^{[\tau_1]}, v_1)\right).$$

This way, the expansion (6.33) of the cumulant generating function corresponds to an integral over time of the same expansion at time τ_1, with an additional weight depending on $z_1(\tau_1)$: this is precisely the partial derivative of the functional $\mathcal{I}(t,g)$ with respect to $g(t)$ as an independent variable, in the direction of the said weight (the functional $\mathcal{I}(t,g)$ is clearly analytical in this variable $g(t)$ by the expansion that we used above). Hence, one can write

$$\mathcal{I}(t,g) - \mathcal{I}(0,g) = \int_0^t \mathrm{d}\tau \frac{\partial \mathcal{I}}{\partial g(t)}(\tau, g)\left[\int \mathrm{d}z_1 \mathrm{d}v_2 \mathrm{d}\omega \langle v_1 - v_2, \omega\rangle_+ M_\beta(v_2)(e^{g(\tau,z_1')-g(\tau,z_1)} - 1)\right].$$

One may identify the partial derivative with the function $z \mapsto \partial_{g(t)}\mathcal{I}(t,g,z)$ such that

$$\frac{\partial \mathcal{I}}{\partial g(t)}(t,g)\,[h] = \int_{\mathcal{D}} \partial_{g(t)}\mathcal{I}(t,g,z) h(z)\mathrm{d}z.$$

The function $z \mapsto \partial_{g(t)}\mathcal{I}(t,g,z)$ is shown [12] to be continuous in x, with values in the space of measures weighted by the inverse of the Maxwellian M_β^{-1}. Hence, we are left with

$$\mathcal{I}(t,g) = \mathcal{I}(0,g) + \int_0^t \mathrm{d}\tau \int \mathrm{d}z_1 \mathrm{d}v_2 \mathrm{d}\omega \langle v_1 - v_2, \omega\rangle_+ M_\beta(v_2) \partial_{g(t)}\mathcal{I}(\tau,g,z_1)(e^{g(\tau,z_1')-g(\tau,z_1)} - 1), \quad (6.34)$$

yielding the following proposition.

Proposition 6.6.5 (Hamilton–Jacobi system for the limit cumulant generating function)**.** *Introducing the Hamiltonian*

$$\mathcal{H}(q,p) \doteq \int \mathrm{d}z_1 \mathrm{d}v_2 \mathrm{d}\omega \langle v_1 - v_2, \omega\rangle_+ M_\beta(v_2) q(z_1)(e^{p(x_1,v_1)-p(x_1,v_1')} - 1),$$

for any time $t < T_\beta$ (see Propositions 6.5.1 and 6.6.4), the limit cumulant generating function is a mild solution of the equation

$$\partial_t \mathcal{I}(t,g) = \mathcal{H}\left(\partial_{g(t)}\mathcal{I}(t,g), g(t)\right),$$

in the sense of (6.34)*.*

At fixed $t > 0$ and $g \in \mathbb{B}_{t,\beta}$ (defined above in (6.32)), this Hamiltonian equation incites to introduce the following Hamilton–Jacobi system

$$\begin{cases} (\partial_s - v\cdot\nabla_x)q^{[t]} = \dfrac{\partial\mathcal{H}}{\partial p}(q^{[t]},p^{[t]}) & , \quad q^{[t]}(0) = M\varphi_0\exp(p^{[t]}(0)), \\ (\partial_s - v\cdot\nabla_x)(p^{[t]}-g) = -\dfrac{\partial\mathcal{H}}{\partial q}(q^{[t]},p^{[t]}) & , \quad p^{[t]}(t) = g(t), \end{cases} \tag{6.35}$$

where the unknowns $(q^{[t]},p^{[t]})$ are meant to find the minimizing values of $\Big(\partial_{g(t)}\mathcal{I}(t,g),g(t)\Big)$ for this Hamiltonian. Next proposition is dedicated to proving that the mild Hamiltonian solution

$$\hat{\mathcal{I}}(t,g) \doteq \mathcal{I}(0,g) + \int_0^t \mathrm{d}s \int_{\mathcal{D}} q^{[t]}(s)(\partial_s - v\cdot\nabla_x)(p^{[t]}(s)-g(s)) + \int_0^t \mathcal{H}(q^{[t]}(s),p^{[t]}(s))\mathrm{d}s \tag{6.36}$$

is well-defined, and to identify it with the functional $\mathcal{I}(t,g)$.

Proposition 6.6.6 (Identification of the Hamiltonian solutions)**.** *For any time $t > 0$ and any observable $g \in \mathbb{B}_{t,\beta}$, the Hamilton–Jacobi system (6.35) admits a unique global solution $(q^{[t]},p^{[t]})$ such that $(q^{[t]}e^{-p^{[t]}},e^{p^{[t]}}) \in \mathbb{L}^\infty\Big([0,t],\mathcal{F}_{1,\beta/4}\Big)^2$, and the functional $\hat{\mathcal{I}}(t,g)$ defined as (6.36) from this solution coincides on $[0,t]$ with our functional*

$$\mathcal{I}(t,g) = \hat{\mathcal{I}}(t,g).$$

Proof. To prove the wellposedness of the equation, we compute the change of unknowns

$$\begin{cases} \gamma(s) = e^{g(s)} \\ \theta(s) = (\partial_s - v\cdot\nabla_x)g(s), \end{cases}$$

and we consider the functional $\mathcal{J}(t,\theta,\gamma) \doteq \mathcal{I}(t,g)$. For this functional, the formula for the partial derivative with respect with γ is even simpler: where the derivation of the term $\gamma = e^g$ with respect to e^g let it invariant, the derivation with respect with γ makes it disappear. Thus, in the previous formulas, we have to add it back in the weight corresponding to the direction of the derivation. The associated Hamiltonian is hence

$$\hat{\mathcal{H}}(\chi,\eta) \doteq \int \mathrm{d}z_1\mathrm{d}v_2\mathrm{d}\omega\langle v_1 - v_2,\omega\rangle_+ M_\beta(v_2)\chi(z_1)(\eta(z_1') - \eta(z_1)), \tag{6.37}$$

for the variables $\chi \doteq qe^{-p}$ and $\eta \doteq e^p$, and the Hamilton–Jacobi system writes as

$$\begin{cases} (\partial_s - v\cdot\nabla_x)\chi + \theta\chi = \dfrac{\partial\hat{\mathcal{H}}}{\partial\eta}(\chi,\eta) & , \quad \chi(0) = M_\beta\varphi_0, \\ (\partial_s - v\cdot\nabla_x)\eta - \theta\eta = -\dfrac{\partial\hat{\mathcal{H}}}{\partial\chi}(\chi,\eta) & , \quad \eta(t) = \gamma(t). \end{cases}$$

This system is equivalent to the following linear Boltzmann–Hamilton–Jacobi system

$$\begin{cases} (\partial_s - v\cdot\nabla_x)\chi = -\theta\chi + \displaystyle\int \mathrm{d}v_2\mathrm{d}\omega\langle v - v_2,\omega\rangle_+\Big(M_\beta(v_2')\chi(z') - M_\beta(v_2)\chi(z)\Big) \\ (\partial_s - v\cdot\nabla_x)\eta = +\theta\eta - \displaystyle\int \mathrm{d}v_2\mathrm{d}\omega\langle v - v_2,\omega\rangle_+ M_\beta(v_2)\Big(\eta(z') - \eta(z)\Big). \end{cases} \tag{6.38}$$

Contrary to [12], these equations are decoupled, since the coupling was stemming from the non-linearity. Moreover, they are not symmetrical: these linear equations are very close to the Rayleigh–Boltzmann equation (2.13), yet the first one has the same collision kernel as the equation on $M_\beta\varphi$,

and the second one the same as the equation on φ. As we saw in Section 3.4 in which we introduced this system, in our functional setting this system admits a unique global positive solution

$$(\chi,\eta)\in\mathbb{L}^\infty\left([0,t],\ \mathcal{F}_{1,\beta/4}\times\mathcal{F}_{1,-\beta/4}\right),$$

proving the first part of the proposition.

To perform the identification, we start to show it on small times. We prove that

$$\mathcal{J}(t,\theta,\gamma)=\hat{\mathcal{J}}(t,\theta,\gamma)\ \left(\doteq\hat{\mathcal{I}}(t,g)\right),$$

where the second term is defined through the same change of unknowns. Both functionals are mild solutions to the same Hamilton–Jacobi equation (see for example [12] for the algebraic details). It is hence enough to show that there exists a unique solution to this mild equation in a regularity space common to both functionals.

Denoting $\mathcal{B}_{R,\beta}$ the $(\mathcal{F}_{1,-\beta/4})$-ball of radius $R>0$, let us define the norm

$$|||\mathcal{J}(t)|||_{R,\beta}\doteq\sup_{\substack{\|\theta\|_\infty\leqslant R\\ \gamma\in\mathcal{B}_{R,\beta}}}|\mathcal{J}(t,\theta,\gamma)|,$$

and let us assume the regularity condition, for every $0<\beta<\beta'$,

$$\forall G\in\mathcal{C}^0(\mathcal{D}),\left[\forall z\in\mathcal{D},|G(z)|\leq RC_\beta|v|e^{\frac{\beta}{4}|v|^2}\right]\Rightarrow\left|\int\partial_\gamma\mathcal{J}(t,\theta,\gamma)\ G\right|\leq\frac{R\tilde{C}_\beta}{\sqrt{\beta'-\beta}}|||\mathcal{J}(t)|||_{R,\beta'},\quad(6.39)$$

for some explicit constants $C_\beta,\tilde{C}_\beta$ depending continuously on β. Then, considering the Hamilton–Jacobi equation (6.34) and the modified Hamiltonian $\hat{\mathcal{H}}$ defined in (6.37), we have for any functionals $\mathcal{J},\mathcal{J}'$ satisfying the regularity asumption (6.39) above, and γ in the ball $\mathcal{B}_{R,\beta}$, that

$$\left|\hat{\mathcal{H}}(\partial_\gamma\mathcal{J},\gamma)-\hat{\mathcal{H}}(\partial_\gamma\mathcal{J}',\gamma)\right|\leq\left|\int\mathrm{d}z\mathrm{d}v_2\mathrm{d}\omega\langle v-v_2,\omega\rangle_+M_\beta(v_2)\left[\partial_\gamma\mathcal{J}-\partial_\gamma\mathcal{J}'\right](z)\left|\gamma(z')-\gamma(z)\right|\right|.\quad(6.40)$$

Using the fact that $\gamma\in\mathcal{B}_{R,\beta}$, we have on the one hand for any $z\in\mathcal{D}$,

$$\begin{aligned}\left|\int\mathrm{d}v_2\mathrm{d}\omega\langle v-v_2,\omega\rangle_+M_\beta(v_2)|\gamma(z)|\right|&\leq Re^{\frac{\beta}{4}|v|^2}\nu_\beta(v)\\&\leq Re^{\frac{\beta}{4}|v|^2}C_\beta|v|,\end{aligned}$$

with the notation (3.5) for the loss factor $\nu_\beta(v)$. On the other hand, using Lemma 3.3.1 to rewrite the collision operator in terms of its integral kernel, we observe that

$$\begin{aligned}\left|\int\mathrm{d}v_2\mathrm{d}\omega\langle v-v_2,\omega\rangle_+M_\beta(v_2)|\gamma(z')|\right|&\leq R\int\mathrm{d}v_2\mathrm{d}\omega\langle v-v_2,\omega\rangle_+M_\beta(v_2)e^{\frac{\beta}{4}|v'|^2}\\&\leq RC_\beta\int\frac{\mathrm{d}\eta\ e^{\frac{\beta}{4}|\eta|^2}}{|\eta-v|^{d-2}}e^{-\beta\left[\frac{|\eta-v|^2}{8}+\frac{|\eta|^2-|v|^2}{4}+\frac{\left(|\eta|^2-|v|^2\right)^2}{8|\eta-v|^2}\right]}\\&\leq RC_\beta e^{\frac{\beta}{4}|v|^2}\int\frac{\mathrm{d}\eta}{|\eta-v|^{d-2}}e^{-\beta\left[\frac{|\eta-v|^2}{8}+\frac{\left(|\eta|^2-|v|^2\right)^2}{8|\eta-v|^2}\right]},\end{aligned}$$

so that we recognize precisely the collision kernel of the modified collision operator (3.8). Thanks to its bound shown in Section 3.3.2, Lemma 3.3.3, we get

$$\left|\int\mathrm{d}v_2\mathrm{d}\omega\langle v-v_2,\omega\rangle_+M_\beta(v_2)|\gamma(z')|\right|\leq\overline{C}_\beta R\frac{e^{\frac{\beta}{4}|v|^2}}{1+|v|}.$$

In the end, the functional in z integrated against $\left[\partial_\gamma \mathcal{J} - \partial_\gamma \mathcal{J}'\right]$ in (6.40) satisfies the assumptions of the regularity condition (6.39), so that

$$\left|\hat{\mathcal{H}}(\partial_\gamma \mathcal{J}, \gamma) - \hat{\mathcal{H}}(\partial_\gamma \mathcal{J}', \gamma)\right| \leq \frac{\tilde{C}_\beta}{\sqrt{\beta' - \beta}} |||\mathcal{J}(t)|||_{R,\beta'}.$$

This inequality is precisely the hypothesis of the abstract Cauchy–Kovalevskaya theorem stated in [12, Appendix A], for equations of the form (6.34) that we consider. According to this theorem, there exists a short time on which there exists a unique solution to the mild equation on $\mathcal{J}$, with the regularity (6.39) that we imposed. To show that both functionals $\mathcal{J}$ and $\hat{\mathcal{J}}$ are identical on short times, it is now enough to show that they share this regularity assumption. It is trivial in the case of $\hat{\mathcal{J}}$ since by construction we have

$$\partial_\gamma \hat{\mathcal{J}}(t, \theta, \gamma) = \chi(t).$$

For the other one, we use its analyticity in γ to write for any $\lambda \in \mathbb{R}$ that

$$\int \partial_\gamma \mathcal{J}(t, \theta, \gamma)(z) G(z) \mathrm{d}z = \frac{1}{2\pi\lambda} \int_0^{2\pi} \mathcal{J}(t, \theta, \gamma + e^{i\theta}\lambda G) e^{-i\theta} \mathrm{d}\theta.$$

Since we assumed that for any $z \in \mathcal{D}$,

$$\begin{aligned} G(z) &\leq R C_\beta |v| e^{\frac{\beta}{4}|v|^2} \\ &\leq R \frac{\tilde{C}_\beta}{\sqrt{\beta' - \beta}} e^{\beta'|v|^2}, \end{aligned}$$

if we choose

$$\lambda = \frac{\sqrt{\beta' - \beta}}{R\tilde{C}_\beta},$$

we obtain

$$\gamma + e^{i\theta}\lambda G \in \mathcal{B}_{R,\beta'}.$$

Eventually, thanks to the analytical formula, we retrieve exactly the wanted regularity domination (6.39).

Now that the identification is established on short times, on any time interval $[0, t]$, one has uniform bounds on $\hat{\mathcal{J}}$ thanks to the long-time existence result on the linear Boltzmann–Hamilton–Jacobi system. Hence, after the first small time of identification, since $\mathcal{J} = \hat{\mathcal{J}}$, both functionals still belong to the same functional framework, allowing to extend the proof of the uniqueness until any fixed large time t, concluding the proof. □

Chapter 7

Statistical fluctuations and large deviations

To analyse further than the first-order convergence of the empirical measure (Corollary 4.1.1), we study in this section the fluctuation field of this measure around its expected value, and present its limit. Eventually, we state a large deviation principle for the empirical measure, that we prove in the following sections.

This study is performed thanks to finer objects than the correlation functions, called *cumulants*, that capture the finer scales of the dynamics and allow to rescale its rare events to characterize them. The previous Chapter 6 is dedicated to the analysis of these cumulants: we show the convergence in short times of these cumulants to limit objects, with a full convergence rate in ε thanks to a new precise computation presented in Chapter 8.

7.1 Statistical refinements: fluctuations and large deviations

As discussed in Section 2.5, the empirical measure of the tagged particles, defined in (2.21) for an observable H, can be seen as the observation of a measure $\tilde{\pi}_t^\varepsilon \in \mathcal{M}(\mathcal{D})$ on the domain $\mathcal{D}$, writing

$$\tilde{\pi}_t^\varepsilon[H] = \int H(z)\mathrm{d}\tilde{\pi}_t^\varepsilon(z).$$

The family $(\tilde{\pi}_s^\varepsilon)_{0\leqslant s\leqslant t}$ defines a measure on the trajectories of $\mathcal{D}^{[0,t]}$. The set $\mathrm{Traj}([0,t],\mathcal{M}(\mathcal{D}))$ of such measures is endowed with the Skorokhod topology. On the other hand, we have defined the *fluctuation field*

$$\zeta_t^\varepsilon = \sqrt{\lambda}(\tilde{\pi}_t^\varepsilon - \mathbb{E}\,[\tilde{\pi}_t^\varepsilon]),$$

to capture the next small order after the law of large numbers (4.3).

Theorem 2 (Convergence of the fluctuation field)**.** *There exists a time $T > 0$ such that, in the mixed scaling ($S_{\varepsilon,\mu,\lambda}$), the fluctuation field defined above converges in law on $[0,T]$ to a Gaussian process (ζ_t), whose equal-time covariance is given for any $t < T$ by*

$$\mathbb{E}\Big[\zeta_t[g]\zeta_t[h]\Big] = \int_{\mathcal{D}} M(v)\varphi(t,z)g(z)h(z)\mathrm{d}z, \tag{7.1}$$

where φ denotes the solution to the linear Rayleigh–Boltzmann equation (2.13).

Indeed, unlike in [12] where the limit fluctuation field satisfies a linear stochastic equation of the form

$$\mathrm{d}\tilde{\zeta}_t = \mathcal{L}\tilde{\zeta}_t\ \mathrm{d}t + \mathrm{d}\tilde{\eta}_t$$

driven by the linearized Boltzmann operator (3.3), here the limit fluctuation field is trivial and does not depend on the second limit cumulant; there is no interference between the tagged particles, on the mere condition that $\lambda \ll \varepsilon^{1-d}$, without any phase transition between this scaling and the nonlinear scaling $\lambda \sim \alpha\varepsilon^{1-d}$. The proof of this theorem is given in Section 7.3, using the properties of cumulants that have been established in Chapter 6.

To study the *large deviations* of the dynamics, we will harness a weaker topology than the Skorokhod one. To that end, for a measure $\mathfrak{m} = (\mathfrak{m}_s)_{s\in[0,t]} \in \mathrm{Traj}([0,t], \mathcal{M}(\mathcal{D}))$, and an observable $h \in \mathcal{C}_c^\infty([0,t]\times\mathcal{D})$, we define the *filtered mean*

$$\{h, \mathfrak{m}\}_t = \int_{\mathcal{D}} h(t,z)\mathrm{d}\mathfrak{m}_t(z) - \int_0^t \int_{\mathcal{D}} (\partial_s + v\cdot\nabla_x)h(s,z)\mathrm{d}\mathfrak{m}_s(z), \tag{7.2}$$

that filters the transported part of the considered observables (see Section 6.6.5 and below to justify the use of this filtered mean). The first quantity that will be relevant for the large deviation principle will be the limit object $\mathcal{I}(t,h)$, that is defined in (6.31) as the limit of an expectancy, and which can also be defined as the mild solution (Proposition 6.6.6) to the Hamilton–Jacobi system

$$\begin{cases} (\partial_s - v\cdot\nabla_x)q^{[t]} = \dfrac{\partial\mathcal{H}}{\partial p}(q^{[t]}, p^{[t]}) & , \quad q^{[t]}(0) = M\varphi_0, \\ (\partial_s - v\cdot\nabla_x)(p^{[t]} - h) = -\dfrac{\partial\mathcal{H}}{\partial q}(q^{[t]}, p^{[t]}) & , \quad p^{[t]}(t) = h(t), \end{cases} \tag{7.3}$$

with the Hamiltonian

$$\mathcal{H}\,(q,p) \doteq \int \mathrm{d}v_2\mathrm{d}\omega\langle v_1 - v_2, \omega\rangle_+ M_\beta(v_2)q(z_1)(e^{p(z_1)-p(z_1')} - 1),$$

in the sense of

$$\mathcal{I}(t,h) = \mathcal{I}(0,h) + \int_0^t \mathrm{d}s \int_{\mathcal{D}} q^{[t]}(s)(\partial_s - v\cdot\nabla_x)(p^{[t]}(s) - h(s)) + \int_0^t \mathcal{H}(q^{[t]}(s), p^{[t]}(s))\mathrm{d}s. \tag{7.4}$$

More precisely, we are interested in its Legendre transform, defined for $\mathfrak{v} \in \mathrm{Traj}([0,t], \mathcal{M}(\mathcal{D}))$ as

$$\mathbf{\Lambda}(t,\mathfrak{v}) \doteq \sup_{h\in\mathbb{B}_{t,\beta}} \Big[\{h,\mathfrak{v}\} - \mathcal{I}(t,h) - 1\Big], \tag{7.5}$$

where the supremum is taken over observables in $\mathbb{B}_{t,\beta}$, defined in (6.32) as the set of observables with bounded transport, and such that e^h is uniformly dominated by the inverse $\frac{\beta}{4}$–Gaussian.

Eventually, for the lower bound of the large deviation principle, we need to consider the set $\mathbf{S}_t$ of strong solutions, on $[0,t]$, of a biased linear Boltzmann equation of the form

$$(\partial_s - v\cdot\nabla_x)\mathfrak{v} = \int \mathrm{d}v_c\mathrm{d}\omega\langle v - v_c, \omega\rangle_+ M_\beta(v_c)\left(\mathfrak{v}(v')e^{p(z)-p(z')} - \mathfrak{v}(v)e^{p(z')-p(z)}\right), \tag{7.6}$$

for some $p \in \mathbb{B}_{t,\beta}$. The large deviation principle might then be formulated as follows.

Theorem 3 (Large deviations of the empirical measure)**.** *In our mixed scaling ($S_{\varepsilon,\mu,\lambda}$), considering the tagged empirical measure (2.22), there exists a time $T > 0$ such that, for any $t \in (0,T]$, we have the following large deviation upper bound*

$$\limsup_{\varepsilon\to 0} \frac{1}{\lambda}\log\mathbb{P}(\tilde{\pi}_t^\varepsilon \in \mathbf{F}) \le -\inf_{\mathfrak{v}\in\mathbf{F}} \mathbf{\Lambda}(t,\mathfrak{v}), \tag{7.7}$$

when $\mathbf{F}$ is a closed set in the Skorokhod topology. Additionally, when $\mathbf{O}$ is an open set in this topology, one has the large deviation lower bound

$$\liminf_{\varepsilon\to 0} \frac{1}{\lambda}\log\mathbb{P}(\tilde{\pi}_t^\varepsilon \in \mathbf{O}) \ge -\inf_{\mathfrak{v}\in\mathbf{O}\cap\mathbf{S}_t} \mathbf{\Lambda}(t,\mathfrak{v}). \tag{7.8}$$

Note that the most useful result is the upper bound on the probability of deviation, as one can see for example in Section 9.4.3, where we use it for the binomial distribution. In our Theorem 3, the upper bound has no restriction on its infimum. Nevertheless, the lower bound, which precises that the upper bound is optimal, is here restricted (like in [12]) to solutions not that far from the Boltzmann linear equation, since they must be solutions to the biased equation (7.6). The proof of this theorem is the subject of Section 7.4, once again based on the convergence of the cumulants. For this reason, since without a priori bounds on these objects our method does not allow to show their convergence on large times, the theorems above are restricted as in [12] to short times.

7.2 Tightness

We expose here tightness results for the empirical measure and the fluctuation field, useful to extend weak results, in the sense of observables, to results in the strong Skorokhod topology on the set of trajectories $\mathrm{Traj}([0,t],\mathcal{M}(\mathcal{D}))$.

The results of this section are given without complete proofs, which can be found in the paper dealing with the fluctuations and large deviations of the general symmetric hard-sphere dynamics [12]. Indeed, these proofs rely on the bounds on the cumulants, that we proved in Section 6.5.2 in our mixed model, and are otherwise identical.

Proposition 7.2.1. *There exists a distance d, based on normalized bounded observables, and associated to the strong Skorokhod topology on* $\mathrm{Traj}([0,t],\mathcal{M}(\mathcal{D}))$*, such that*

$$\lim_{A\to+\infty}\lim_{\lambda\to+\infty}\frac{1}{\lambda}\log\mathbb{P}\left[\sup_{s\in[0,t]}d(0,\tilde{\pi}^{\varepsilon}_{s})\geq A\right]=-\infty, \tag{7.9}$$

and for any $\eta>0$,

$$\lim_{\delta\to+\infty}\lim_{\lambda\to+\infty}\frac{1}{\lambda}\log\mathbb{P}\left[\sup_{|s-s'|<\delta}d(\tilde{\pi}^{\varepsilon}_{s},\tilde{\pi}^{\varepsilon}_{s'})>\eta\right]=-\infty. \tag{7.10}$$

Proof. As an example, we show the first result (7.9), which is the easiest one and for this reason not completely detailed in [12]. Let us define the random set containing the labels of the tagged particles

$$\mathcal{S}_{\lambda}\doteq\Big\{1\leq i\leq\mathcal{N}\ ,\ L_{i}=1\Big\}.$$

Noticing that the number $|\mathcal{S}_{\lambda}|$ of tagged particles does not change with time, and since whichever normalized observable $(h_i)_{i\in\mathbb{N}}$ appearing in the distance d is bounded, we have

$$\begin{aligned}d(0,\tilde{\pi}^{\varepsilon}_{s})&=\sum_{i\in\mathbb{N}}\frac{1}{\lambda}\sum_{j\in\mathcal{S}_{\lambda}}h_{i}(Z^{[0,s]}_{\varepsilon,j})\\&\leq\frac{|\mathcal{S}_{\lambda}|}{\lambda}\sum_{i\in\mathbb{N}}\|h_{i}\|_{\infty}.\end{aligned}$$

The latter sum being normalized, the condition $d(0,\tilde{\pi}^{\varepsilon}_{t})\geq A$ is reduced to asking, for a constant $C>0$ depending on these observables, that

$$\frac{|\mathcal{S}_{\lambda}|}{\lambda}\geqslant CA.$$

Thus, we have

$$\mathbb{P}\left[\sup_{s\in[0,t]}d(0,\tilde{\pi}^{\varepsilon}_{t})\geq A\right]\leq\mathbb{P}\big[|\mathcal{S}_{\lambda}|\geq CA\lambda\big]\leq\frac{\mathbb{E}\left[2^{|\mathcal{S}_{\lambda}|}\right]}{2^{CA\lambda}}$$

by the Markov inequality. We know very well the initial distribution discussed in Section 2.4, and in particular we have a formula (5.7) for the partition function, that harnesses symmetry to write $q = |\underline{\ell}_p|$ the number of tagged particles in the following computation

$$\begin{aligned}\mathbb{E}\left[2^{|\mathcal{S}_\lambda|}\right] &= \frac{1}{\mathcal{Z}_\mu}\sum_{p,q\geqslant 0} 2^q \cdot \frac{\lambda^q\mu^p}{p!q!}\int M_\beta^{\otimes p+q}\varphi_0^{\otimes p}\mathbb{1}_{\mathcal{X}^\varepsilon_{p+q}} \\ &= \frac{1}{\mathcal{Z}_\mu}\sum_{p,q\geqslant 0}\left[\sum_{l=0}^{q}\frac{q!}{l!(q-l)!}\right]\frac{\lambda^q\mu^p}{p!q!}\int M_\beta^{\otimes p+q}\varphi_0^{\otimes q}\mathbb{1}_{\mathcal{X}^\varepsilon_{p+q}}.\end{aligned}$$

Hence, we use that $\mathbb{1}_{\mathcal{X}^\varepsilon_{p+q}} \leq \mathbb{1}_{\mathcal{X}^\varepsilon_{p+q-l}}$ and invert the sums, eventually computing an index shift to get

$$\begin{aligned}\mathbb{E}\left[2^{|\mathcal{S}_\lambda|}\right] &\leq \frac{1}{\mathcal{Z}_\mu}\sum_{l\geqslant 0}\frac{(\lambda\|\varphi_0\|)^l}{l!}\sum_{\substack{p\geqslant 0\\ q\geqslant l}}\frac{\lambda^{q-l}\mu^p}{p!(q-l)!}\int M_\beta^{\otimes p+q-l}\varphi_0^{\otimes q-l}\mathbb{1}_{\mathcal{X}^\varepsilon_{p+q-l}} \\ &\leq \sum_{l=0}^{q}\frac{(\lambda\|\varphi_0\|)^l}{l!}\cdot\frac{1}{\mathcal{Z}_\mu}\sum_{p,q\geqslant 0}\frac{\lambda^q\mu^p}{p!q!}\int M_\beta^{\otimes p+q}\varphi_0^{\otimes q}\mathbb{1}_{\mathcal{X}^\varepsilon_{p+q}} \\ &= e^{\lambda\|\varphi_0\|},\end{aligned}$$

recognizing the partition function $\mathcal{Z}_\mu$. In the end, we obtain

$$\mathbb{P}\left[\sup_{s\in[0,t]} d(0,\tilde{\pi}^\varepsilon_t)\geq A\right] \leq \exp\Big(\lambda\|\varphi_0\| - C\log 2A\lambda\Big),$$

which concludes the proof of the first statement in the mixed scaling ($S_{\varepsilon,\mu,\lambda}$).

The second statement (7.10) follows from the previous bound and the estimate on the cumulants given in Proposition 6.5.1, with the same proof as in [12, Proposition 7.3.2]. □

Proposition 7.2.2 (Tightness of the fluctuation field)**.** *There exists a distance $\tilde{d}$, based on some normalized bounded observables, and associated to the strong Skorokhod topology on* $\mathrm{Traj}([0,t],\mathcal{M}(\mathcal{D}))$*, such that*

$$\lim_{A\to+\infty}\lim_{\mu\to+\infty}\mathbb{P}\left[\sup_{s\in[0,t]}\tilde{d}(0,\zeta^\varepsilon_s)\geq A\right] = 0$$

and for any $\eta > 0$,

$$\lim_{\delta\to 0}\lim_{\mu\to+\infty}\mathbb{P}\left[\sup_{|s-s'|<\delta}\tilde{d}(\zeta^\varepsilon_s,\zeta^\varepsilon_{s'})>\eta\right] = 0. \tag{7.11}$$

The proof of this proposition is once again identical to the one in [12, Proposition 6.2.3], using the bounds proved in Proposition 6.5.1. Note that in the integrated form, dominating roughly the bounded observables, it is easy to remark that the bounding estimates that are true in the non-linear symmetric case remain true in our linear tagged model, since by symmetry one can rewrite the sum over the tags $\underline{\ell}_p$ as

$$\sum_{\underline{\ell}_p\in\Lambda_p}\lambda^{|\underline{\ell}_p|}\mu^{p-|\underline{\ell}_p|}\int M_\beta^{\otimes p}\varphi_0^{\otimes\underline{\ell}_p}\mathbb{1}_{\mathcal{X}^\varepsilon_p}\mathrm{d}\underline{z}_p = \mu^p\int M_\beta^{\otimes p}\left(\frac{\lambda}{\mu}\varphi_0+1\right)^{\otimes p}\mathbb{1}_{\mathcal{X}^\varepsilon_p}\mathrm{d}\underline{z}_p,$$

which formally corresponds to a bounded symmetric initial data $[M_\beta(p_\mu\varphi_0+1)]$.

7.3 Convergence of the fluctuation field

Since the fluctuation field (ζ_t^ε) defined in (2.23) is tight by Proposition 7.2.2, identifying its limit moments is enough to characterize its limit, as they decrease fast enough (see the method of moments in [8, Theorem 30.1]). Hence, to identify the limit fluctuation field with a Gaussian process, and to find its covariance, we consider the following sampled observable

$$H(z^{[0,t]}, \ell) = \mathbb{1}_{\ell=1} \sum_{j=1}^{J} \psi_j(z^{[\theta_j]}).$$

For simplicity, we denote $\tilde{f}_n(t) \doteq f_n(t, \underline{\ell}_n = \underline{1}_n)$ and $\tilde{F}_1(t) \doteq F_1(t, \ell_1 = 1)$ the cumulants associated to the tagged particles only. Recall that the random set $\mathcal{S}_\lambda$ contains the labels of tagged particles. With the same notation as in Corollary 4.1.1, we have

$$\zeta_t^\varepsilon[H] = \frac{1}{\sqrt{\lambda}} \sum_{j=1}^{J} \left[\sum_{i \in \mathcal{S}_\lambda} \psi_j\left(Z_{\varepsilon,i}^{[\theta_j]}\right) - \lambda \int \tilde{F}_1^\varepsilon(\theta_j)\psi_j \right].$$

To characterize the law of this fluctuation field, we look at its Fourier transform, using the generalized cumulant generating function (6.9) to write

$$\mathbb{E}\left[e^{i\zeta_t^\varepsilon[H]}\right] = \exp\left(\mathfrak{G}_\varepsilon^{[0,t]}\left[\frac{iH}{\sqrt{\lambda}}\right]\right) \exp\left(-i\sqrt{\lambda}\sum_{j=1}^{J}\int \tilde{F}_1^\varepsilon(\theta_j)\psi_j\right). \tag{7.12}$$

Expanding the cumulant generating function (6.9) yields

$$\begin{aligned}\mathfrak{G}_\varepsilon^{[0,t]}\left[\frac{iH}{\sqrt{\lambda}}\right] &= \sum_{p\geqslant 1}\frac{\lambda^p}{p!}\int \tilde{f}_p^\varepsilon\left[e^{\frac{i}{\sqrt{\lambda}}H} - 1\right] \\ &= \sum_{p\geqslant 1}\frac{\lambda^p}{p!}\int \tilde{f}_p^\varepsilon\left[\frac{i}{\sqrt{\lambda}}H - \frac{1}{2\lambda}H^2 + O\left(\frac{\|H\|}{\sqrt{\lambda}}\right)^3\right].\end{aligned}$$

Using the estimates on the cumulants stated in Proposition 6.5.1, and the convexity of $x \mapsto (1+x)^p$, we bound for any $p \geqslant 2$

$$\frac{\lambda^p}{p!}\left|\int \tilde{f}_p^\varepsilon\left[\frac{i}{\sqrt{\lambda}}H + O\left(\frac{\|H\|}{\sqrt{\lambda}}\right)^2\right]\right| \leq \frac{\lambda^p C^p}{\mu^{p-1}} \cdot \left[\frac{\|H\|^p}{\lambda^{\frac{p}{2}}} + 2^p O\left(\frac{\|H\|}{\sqrt{\lambda}}\right)^{p+1}\right],$$

so that

$$\sum_{p\geqslant 2}\frac{\lambda^p}{p!}\left|\int \tilde{f}_p^\varepsilon\left[e^{\frac{i}{\sqrt{\lambda}}H} - 1\right]\right| \leq 2(C\|H\|)^2\frac{\lambda}{\mu}.$$

Then the cumulant generating function writes

$$\mathfrak{G}_\varepsilon^{[0,t]}\left[\frac{iH}{\sqrt{\lambda}}\right] = \int \tilde{F}_1^\varepsilon\left[i\sqrt{\lambda}H - \frac{H^2}{2} + O\left(\frac{\|H\|}{\sqrt{\lambda}}\right)^3\right] + 2(C\|H\|)^2\frac{\lambda}{\mu}$$

where the first term simplifies in the Fourier transform (7.12). Eventually, in the mixed scaling $(S_{\varepsilon,\mu,\lambda})$ this provides the following convergence

$$\mathbb{E}\left[e^{i\zeta_t^\varepsilon[H]}\right] \xrightarrow[\varepsilon\to 0]{} \exp\left(-\frac{1}{2}\sum_{i,j=1}^{J}\int \tilde{F}_1\left[\psi_i(z^{[\theta_i]})\psi_j(z^{[\theta_j]})\right]\right)$$

thanks to the convergence of the integrated cumulants shown in Proposition 6.6.3. By the method of moments mentioned above, and thanks to the tightness (7.11) of the fluctuation field, ζ_t^ε converges to a Gaussian process ζ_t, with time-observable covariance

$$\mathbb{E}\Big[\zeta_s[g]\zeta_t[h]\Big] = \int \tilde{F}_1 \left[g(z^{[s]})h(z^{[t]})\right].$$

At each time, it is hence characterized by its covariance (7.1) with respect to observables. This concludes the proof of Theorem 2, recalling that the expansion of the integral above has been identified with the expansion (6.29) of the solution $M_\beta\varphi$ to the Rayleigh–Boltzmann equation. □

7.4 Large deviations of the empirical measure

We explain here how the convergence of the cumulant generating function (Sections 6.6.4 and 6.6.5) leads to the large deviation principle for the empirical measure (Theorem 3), following the method of [12].

Upper bound Let $\mathbf{F}$ be a closed set for the Skorokhod topology. In particular, $\mathbf{F}$ is also closed for the weaker topology given by the opens of the form

$$\mathbf{O}_{h,\delta}(\mathfrak{v}) \doteq \Big\{\mathfrak{m} \in \mathrm{Traj}([0,t],\mathcal{M}(\mathcal{D}))\ ,\ |\{h,\mathfrak{m}-\mathfrak{v}\}| < \delta\Big\},$$

for observables $h \in \mathcal{C}_c^\infty$ and measures $\mathfrak{v} \in \mathrm{Traj}([0,t],\mathcal{M}(\mathcal{D}))$, where $\delta > 0$ is fixed (we recall the definition (7.2) of the transport filtered mean). For any open set of this form, one can write

$$\mathbb{P}(\tilde{\pi}_t^\varepsilon \in \mathbf{O}_{h,\delta}(\mathfrak{v})) \leq \mathbb{E}\left[\exp\Big(\lambda\{h,\tilde{\pi}_t^\varepsilon\} - \lambda\{h,\mathfrak{v}\} + \lambda\delta\Big)\right].$$

Now, since by definition

$$\{h,\tilde{\pi}_t^\varepsilon\} = \frac{1}{\lambda}\sum_{i\in\mathcal{S}_\lambda}\left[h\left(t,Z_i^{[t]}\right) + \int_0^t (\partial_s + v\cdot\nabla_x)h\left(s,Z_i^{[s]}\right)\right],$$

and harnessing the definition (6.9) of the cumulant generating function, we get

$$\mathbb{P}(\tilde{\pi}_t^\varepsilon \in \mathbf{O}_{h,\delta}(\mathfrak{v})) \leq \exp\left(\mathfrak{G}_\varepsilon^{[0,t]}\left[h_t + \int(\partial_s + v\cdot\nabla_x)h_s\right] - \lambda\{h,\mathfrak{v}\} + \lambda\delta\right).$$

Taking the limit superior, thanks to the convergence (6.30) of the generating function, and using the notation $\mathcal{I}(t,g)$ for the limit cumulant generating function (6.31), one has

$$\limsup_{\varepsilon\to 0}\frac{1}{\lambda}\log\mathbb{P}(\tilde{\pi}_t^\varepsilon \in \mathbf{O}_{h,\delta}(\mathfrak{v})) \leq \mathcal{I}(t,h) - 1 - \{h,\mathfrak{v}\} + \delta.$$

By definition of the Legendre transform (7.5), for our fixed $\delta > 0$ there exists an observable $g \in \mathbb{B}_{t,\beta}$ such that

$$\{g,\mathfrak{v}\} - \mathcal{I}(t,g) + 1 > \mathbf{\Lambda}(t,\mathfrak{v}) - \delta,$$

so that

$$\limsup_{\varepsilon\to 0}\frac{1}{\lambda}\log\mathbb{P}(\tilde{\pi}_t^\varepsilon \in \mathbf{O}_{g,\delta}(\mathfrak{v})) \leq -\mathbf{\Lambda}(t,\mathfrak{v}) + 2\delta.$$

By the tightness result stated in Proposition 7.2.1, $\mathbf{F}$ is in fact compact, and one can extract a finite covering of open sets $\mathbf{F} \subset \cup_{i=1}^k \mathbf{O}_{g_i,\delta}(\mathfrak{v}_i)$, so that

$$\limsup_{\varepsilon\to 0}\frac{1}{\lambda}\log\mathbb{P}(\tilde{\pi}_t^\varepsilon \in \mathbf{F}) \leq -\inf_{i\leqslant k}\mathbf{\Lambda}(t,\mathfrak{v}_i) + 2\delta \leq -\inf_{\mathfrak{v}\in\mathbf{F}}\mathbf{\Lambda}(t,\mathfrak{v}) + 2\delta.$$

The result (7.7) follows, considering that $\delta > 0$ may be chosen arbitrarily small.

Lower bound The lower bound follows from more elaborate methods, that works only for measures $\mathfrak{v}$ such that the Legendre transform $\mathbf{\Lambda}(t, \mathfrak{v})$ is reached for an observable $h \in \mathbb{B}_{t,\beta}$, which is the case when $\mathfrak{v}$ is a strong solution of the biased Boltzmann–Hamilton–Jacobi equation (6.35)

$$(\partial_s - v \cdot \nabla_x)\mathfrak{v} = \int \mathrm{d}v_{\mathrm{c}}\mathrm{d}\omega\langle v - v_{\mathrm{c}}, \omega\rangle_+ M_\beta(v_{\mathrm{c}}) \left(\mathfrak{v}(v')e^{p(z)-p(z')} - \mathfrak{v}(v)e^{p(z')-p(z)}\right),$$

for some $p \in \mathbb{B}_{t,\beta}$, whence the restriction on the infimum defining the lower bound. The algebraic details are exaclty the same as in [12, Chapter 7] and proceed of industrious topological considerations, so that we do not replicate them here. □

Chapter 8

Geometric control of dynamics cycles

We prove here Proposition 6.6.2, adding the analysis of geometric cycle constraints to the bounds proved in Section 6.5.2. Thanks to a fine computation to handle the appearing singularities (Section 8.4), we achieve an optimal convergence rate in a full power of ε, better than the previous existing one [11]. Section 1.5 in the introduction gives some context and insights on this proof, and the methods we use in it.

8.1 Parametrizing the cycle

First of all, it will be useful in the following to parametrize the encounters in terms of the angle σ instead of ω (see Section 2.2 for the associated change of variables). For a general cluster $R = \rho_j$, at fixed number of added particles k_j and fixed labels, we want to show that the cycle condition in the following integral

$$\sum_{\Upsilon \in \mathcal{T}^{\mathrm{d}}_{R,k}} \int \mathbb{1}_{T^{\mathrm{d}}_R = \Upsilon} \mathrm{d}\underline{v}_{r+k} \mathrm{d}\underline{\sigma}_{E_\Upsilon} \mathrm{d}\underline{\tau}_{E_\Upsilon} \prod_{e \in E_\Upsilon} s_e |v_m(\tau_e{}^+) - v_{m'}(\tau_e{}^+)| e^{-\beta \|\underline{v}_{r+k}\|^2} \times \mathbb{1}^{\emptyset}_R \tag{8.1}$$

leads to similar bounds as without the cycle constraint (see (6.27) and the final Section 8.5 of this chapter), with an additional small factor ε. This way, we will then be able to use the same computation as in Section 6.5.2, when bounding the integrated cumulants, gaining smallness from the cycle.

We have denoted $\underline{v}_{r+k} = (\underline{v}_R, \underline{v}^*_k)$, and we define $\mathbf{V} = \max(1, \|\underline{v}_{r+k}\|_2)$ to control the total energy. For simplicity, we will not precise in all the following, every time we use an adverb of time, that *time is looked at backwards*.

Let us hence suppose that two particles, say i and j, create the first cycle at a time $t_{\mathrm{c}} \in [\tau_{c+1}, \tau_c]$, through a non-clustering collision or overlap. The cycling condition imposes strong geometric constraints, providing smallness when integrating over well-chosen parameters in the dynamics, restrained to small geometric volumes. Nevertheless, to integrate over a collision angle in (8.1), we need to make sure that the velocities appearing in the product over the edges do not depend on this angle: we will hence start identifying the corresponding edges, and sum over them to make the associated velocities disappear like in (6.25) and (6.26).

The parametrization of the cycle will depend on whether one of both particles i or j has undergone a deflection between t and τ_c or not. We hereafter define the relevant interactions to parametrize the cycle. Should it be the case, let us denote k the particle that deflected i at the closest time $\tau_{\mathrm{d}} \geq \tau_c$, and if such a deflection never happened let us denote k the particle that overlapped i at a closest time $\tau_{\mathrm{ov}} \geq \tau_c$. One can arbitrarily choose i, among i and j, to be the closest to have been deflected, or to have been overlapped if none of both has ever been deflected. Eventually, something that might happen is that the first connection between i and j (before their cycle) stems from i overlapping a fourth particle (call it l), after having encountered k (see i, j, k, l in Fig. 8.1).

The choice of this configuration $(i,j,k,l) \in [\![1, r+k]\!]^4$ and of $(\tau_c, \tau_{\rm d}, \tau_{\rm ov}) \subset \{\tau_p\}_{p\leq r+k-1}$ corresponds to a combinatorial factor of order $(r+k)^7$.

Since the first cycle happens between τ_c and τ_{c+1}, before the time τ_c every encounter is clustering, registered in the tree Υ, and every velocity in the dynamics thus only depends on the signs and angles associated to the edges of Υ. This way, we may sum over these edges like in Section 6.5.2, as soon as we do it in an order respecting the interdependence among the encounters.

The set $K \subset E_\Upsilon$ of edges possibly impacted by the collision between i and k at time $\tau_{\rm d}$ is defined as follows: we start with all the edges between τ_{c+1} and 0, since the cycle happens before (as we look at time backwards, time 0 is *after* the cycle occurs). Then, we can define the connected component of k when removing the edge $\tau_{\rm d}$ between i and k, component of which we add to K all the edges after the deflection time $\tau_{\rm d}$ (see the definition of the dynamics tree in Fig. 6.1). Eventually, we add to K all the potential overlaps undergone by i after $\tau_{\rm d}$, apart from the one with l if appropriate, since we need it to close the cycle. We hence *condition on this set* K, which corresponds to a factor 2^c once c is fixed, and we can sum beforehand over all these edges as in (6.25) and (6.26). To be finally able to integrate over the deflection angle $\sigma_{\rm d}$ associated with the time $\tau_{\rm d}$ without impacting velocities in the product over the edges, it only remains to dominate roughly the one associated with the overlap time $\tau_{\rm ov}$ in the deflection case, as follows:

$$|v_i({\tau_{\rm ov}}^+) - v_l({\tau_{\rm ov}}^+)| \leq 2\mathbf{V}.$$

This factor will be found back in the final estimation (8.10). We will now treat both cases separately: as said before, if one of both particles has been deflected before τ_c, we will use the angle $\sigma_{\rm d}$ of the corresponding collision to parametrize the cycle condition. Else, we will use the distance between the aggregates involved in the closest overlap. Both ways will raise some singularities in velocities, that we will control afterwards, in Section 8.4.

8.2 Deflected case

If one of the particles has been deflected before τ_c, we have fixed the closest deflection, involving i and k at time $\tau_{\rm d}$. Taking the encounter time just before $\tau_{\rm d}$ as a reference (call it τ_0), we shall denote u_i, u_j, u_k the velocities of particles i,j,k between τ_0 and $\tau_{\rm d}$, and u_i', u_j', u_k' these velocities between $\tau_{\rm d}$ and $t_{\rm c}$ (cf. Fig. 8.1). We first suppose that $k \neq j$. Then, there are three possibilites for the origin of particle j, considering that at time $t_{\rm c}$ it creates a cycle with i: it can stem from the connected component C_i of i at time τ_0, from the connected component C_k of k at time τ_0, or from the connected component C_l of a particle l overlapping i at a time $\tau_{\rm ov}$, between $\tau_{\rm d}$ and τ_c (Fig. 8.1). The dependency of $x_i - x_j$ along the setting at τ_0 is different in each case.

▷ If j is in the connected component of i (Fig. 8.1, top left), this is the simplest case and

$$[x_i - x_j](t_{\rm c}) = [x_i - x_j](\tau_0) + (\tau_{\rm d} - \tau_0)[u_i - u_j] + (t_{\rm c} - \tau_{\rm d})[u_i' - u_j].$$

▷ If j is in the connected component of k (Fig. 8.1, top right), then

$$\begin{aligned}[x_i - x_j](t_{\rm c}) &= [x_i - x_k + x_k - x_j](\tau_{\rm d}) + (t_{\rm c} - \tau_{\rm d})[u_i' - u_j] \\ &= \varepsilon\omega_{\rm d} + [x_k - x_j](\tau_0) + (\tau_{\rm d} - \tau_0)[u_k - u_j] + (t_{\rm c} - \tau_{\rm d})[u_i' - u_j].\end{aligned}$$

▷ Eventually, if j is in the connected component of l (Fig. 8.1, bottom left), then

$$\begin{aligned}[x_i - x_j](t_{\rm c}) &= [x_i - x_l + x_l - x_j](\tau_{\rm ov}) + (t_{\rm c} - \tau_{\rm ov})[u_i' - u_j] \\ &= \varepsilon\omega_{\rm ov} + [x_l - x_j](\tau_0) + (\tau_{\rm ov} - \tau_0)[u_l - u_j] + (t_{\rm c} - \tau_{\rm ov})[u_i' - u_j].\end{aligned}$$

Actually, it may happen that u_l is deflected between τ_0 and $\tau_{\rm ov}$, yet it only requires to change the term $(\tau_{\rm ov} - \tau_0)[u_l - u_j]$, splitting it according to each segment between two deflections.

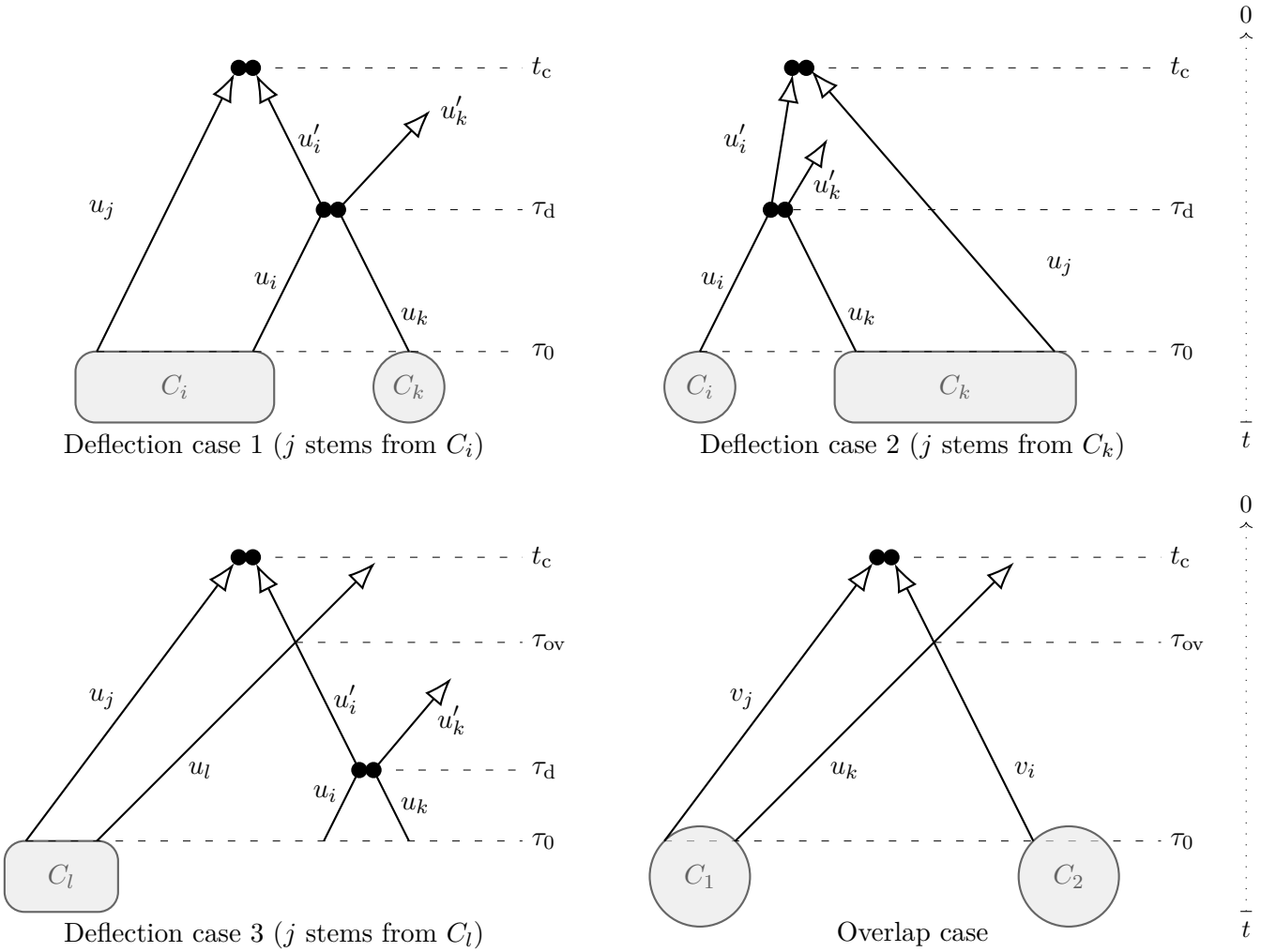

Figure 8.1: The three deflection cases, and the overlap case

In each case, using the cycle condition $[x_i - x_j](t_c) = \varepsilon\omega_c + \zeta$, for a $\zeta \in \mathbb{Z}^d$ due to the periodicity of the domain and satisfying $|\zeta| \leq t\mathbf{V}$, one can write

$$(t_c - \tau_*)[u'_i - u_j] = \Delta x(\tau_*) + \varepsilon\omega_*, \tag{8.2}$$

where $\tau_* \in \{\tau_d, \tau_{ov}\}$, with $\Delta x(\tau_*)$ is independent of ω_d (see the explicit formula (8.5)), and where $\omega_* \in \omega_c - \{0, \omega_d, \omega_{ov}\}$ satisfies $|\omega_*| \leq 2$. This relationship (8.2) defines a cone to which $u'_i - u_j$ must belong to achieve the cycle, whose height depends on the relative position of i and j at time τ_*: if $\Delta x(\tau_*)$ is large enough compared to ε, we will be able to control the height of this cone, and hence its angle, which constrains σ_d. Otherwise, it will provide a strong condition on the encounter times. First, if

$$|\Delta x(\tau_*)| \geq 4\varepsilon, \tag{8.3}$$

then

$$\Big|(t_c - \tau_*)[u'_i - u_j]\Big| \geq \frac{|\Delta x(\tau_*)|}{2},$$

so that

$$\frac{1}{|t_c - \tau_*|} \leq \frac{4\mathbf{V}}{|\Delta x(\tau_*)|}. \tag{8.4}$$

Now, the value of $\Delta x(\tau_*)$ is respectively given by

$$\Delta x(\tau_*) = \begin{cases} [x_j - x_i](\tau_0) + (\tau_{\rm d} - \tau_0)[u_j - u_i] & \text{if } j \in C_i, \\ [x_k - x_j](\tau_0) + (\tau_{\rm d} - \tau_0)[u_k - u_j] & \text{if } j \in C_k, \\ [x_l - x_j](\tau_0) + (\tau_{\rm ov} - \tau_0)[u_l - u_j] & \text{if } j \in C_l, \end{cases} \tag{8.5}$$

which is affine in $\tau_* \in \{\tau_{\rm d}, \tau_{\rm ov}\}$. Hence, denoting $(\tau_* - \tau_0^*)\Delta u$ the projection of $\Delta x(\tau_*)$ on the relative velocity $\Delta u \in \{u_j - u_i, u_k - u_j, u_l - u_j\}$ according to the considered case, one has

$$|\Delta x(\tau_*)| \geq |(\tau_* - \tau_0^*)\Delta u|.$$

Thus, using (8.2) and (8.4), we know that

$$u_i' - u_j = \frac{\Delta x(\tau_*) + \varepsilon\omega_*}{|t_{\rm c} - \tau_*|}$$

belongs to a cylinder of width at most

$$\frac{4\varepsilon \mathbf{V}}{|\Delta x(\tau_*)|} \leq \frac{4\varepsilon \mathbf{V}}{|(\tau_* - \tau_0^*)\Delta u|},$$

(which contains the previous cone of controlled height, cf Fig. 8.2, **a.**). Hence, u_i' also belongs to such a cylinder, since u_j remains unchanged. Now, the deflection condition states that

$$|u_i' - (u_i + u_k)/2| = |u_i - u_k|/2,$$

so that $u_i' - (u_i + u_k)/2$, whose direction is given by $\sigma_{\rm d}$ (see Fig. 2.2), also has to belong to a sphere of radius $|u_i - u_k|/2$. The intersection of this sphere with the previous cylinder is included in the union of two cones, of which solid angle is maximum when the cylinder is tangent to the sphere (cf. Fig. 8.2, **b.**), namely

$$C_d \min\left[1, \left(\frac{\varepsilon \mathbf{V}}{|(\tau_* - \tau_0^*)\Delta u| \cdot |u_i - u_k|}\right)^{d-1}\right].$$

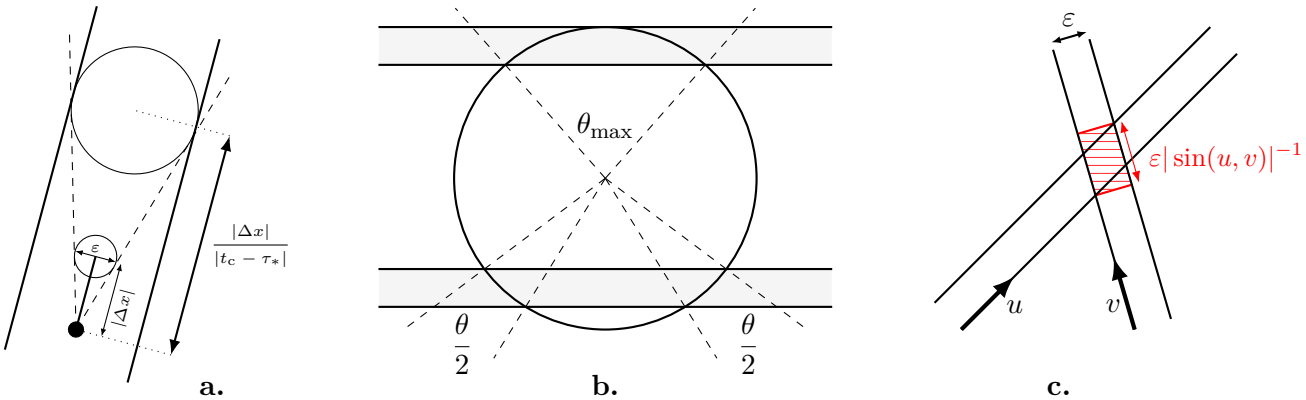

Figure 8.2: Geometrical estimates

Eventually, denoting $\mathbb{1}_{i \between j}$ the condition that i and j create the first cycle within the tree Υ, we can bound the following integral using that $d \geq 3$,

$$\int \mathbb{1}_{i\between j} \mathrm{d}\sigma_{\mathrm{d}} \mathrm{d}\tau_* \leq C_d \sum_{|\zeta| \leqslant t\mathbf{V}} \int \min \left[1, \left(\frac{\varepsilon \mathbf{V}}{|(\tau_* - \tau_0^*)\Delta u| \cdot |u_i - u_k|}\right)^{d-1}\right] \mathrm{d}\tau_* \tag{8.6}$$

$$\leq C_d (t\mathbf{V})^d \left(\frac{\varepsilon \mathbf{V}}{|\Delta u| \cdot |u_i - u_k|} + (d-2)\left[\frac{\varepsilon \mathbf{V}}{|\Delta u| \cdot |u_i - u_k|}\right]^{(d-1)-(d-2)}\right)$$

$$\leq \tilde{C}_d \frac{t^d \mathbf{V}^{d+1} \cdot \varepsilon}{|\Delta u| \cdot |u_i - u_k|}. \tag{8.7}$$

Finally, if the condition (8.3) is not satisfied, then the condition $|\tau_* - \tau_0^*| \leq 2\varepsilon/|\Delta u|$ provides an even better bound integrating over τ_*, with the same singularity $|\Delta u|^{-1}$.

The case $k = j$ is treated in a similar manner, without singularity since the disjunction on the height of the cone is not necessary: the cycle must occur because of a periodic shift $\zeta \neq 0_{\mathbb{Z}^d}$, necessarily providing a height larger than 1, which yields a negligible term (of order ε^{d-1}, see for instance [11, proof of Proposition B.2]).

8.3 Non-deflected case

If none of both particles i and j has ever been deflected, we have considered the closest overlap, involving i and k at time τ_{ov}. Taking the encounter time just before τ_{ov} as a reference, call it τ_0, we will use the same notation as previously, knowing that none of the velocities changes between τ_0 and τ_{ov} and that the velocities of i and j are given by their initial velocities v_i and v_j (see Fig. 8.1, bottom right). Then, the overlap at time τ_{ov} and the cycle creation at time t_{c} give respectively the following conditions

$$\begin{cases} x_k(\tau_0) - x_i(\tau_0) + (\tau_{\mathrm{ov}} - \tau_0)(u_k - v_i) = \zeta_{\mathrm{ov}} + \varepsilon\omega_{\mathrm{ov}} \\ x_j(\tau_0) - x_i(\tau_0) + (t_{\mathrm{c}} - \tau_0)(v_j - v_i) = \zeta_{\mathrm{c}} + \varepsilon\omega_{\mathrm{c}}, \end{cases} \tag{8.8}$$

for some $(\zeta_{\mathrm{ov}}, \zeta_{\mathrm{c}}, \omega_{\mathrm{ov}}, \omega_{\mathrm{c}}) \in (\mathbb{Z}^d)^2 \times (\mathbb{S}^{d-1})^2$. Since before τ_c all encounters are clustering, removing the two encounters t_{c} and τ_{ov} divides the past encounters that involve i and j into two connected components: C_1 containing j and k and C_2 containing i. By construction, when $\vec{x}_{\mathrm{ov}}$ varies alone, both dynamics components C_1 and C_2 move rigidly one with respect to the other, and the distance $x_k(\tau_0) - x_j(\tau_0)$ remains fixed, so that

$$\vec{x}_{\mathrm{ov}} = x_k(\tau_0) - x_i(\tau_0) = [x_k(\tau_0) - x_j(\tau_0)] + [x_j(\tau_0) - x_i(\tau_0)]$$

has to belong (8.8) to two cylinders of axes $(u_k - v_i)$ and $(v_j - v_i)$ and of common width ε.

If $j \neq k$, the volume of the intersection of these cylinders is of order $\varepsilon^d |\sin(u_k - v_i, v_j - v_i)|^{-1}$ (cf. Fig. 8.2, **c.**), so that with the same notation as in the previous deflected case (8.6), recalling the changes of variables (6.18) and (2.5), we have

$$\int \mathbb{1}_{i\between j} \mathrm{d}\sigma_{\mathrm{ov}} \mathrm{d}\tau_{\mathrm{ov}} = \frac{\mu}{|v_i - u_k|} \int \mathbb{1}_{i\between j} \mathrm{d}\vec{x}_{\mathrm{ov}} \leq C_d \frac{(t\mathbf{V})^{2d} \cdot \varepsilon}{|\sin(u_k - v_i, v_j - v_i)| \cdot |v_i - u_k|}. \tag{8.9}$$

If $j = k$, since none of the particles has been deflected, this means that the cycle is due to the periodic conditions with $\zeta_{\mathrm{ov}} \neq \zeta_{\mathrm{c}}$. Hence, the difference of both lines of the system (8.8) provides

$$(\tau_{\mathrm{ov}} - t_{\mathrm{c}})(u_j - u_i) = (\zeta_{\mathrm{ov}} - \zeta_{\mathrm{c}}) + \varepsilon(\omega_{\mathrm{ov}} - \omega_{\mathrm{c}}),$$

so that for ε small enough $(u_j - u_i)$ must belong to a cone of opening at most 3ε, and integrating as before over v_i and v_j provides a negligible term (of order ε^{d-1}, see once again [11, proof of Proposition B.2] for instance).

8.4 Handling the singularities

Now, we are left with some singularities to handle in our bounds (8.7) and (8.9). To do so, we will either: use some of the relative velocities appearing in the product over the edges to cancel them, use a previous deflection to integrate them, or integrate them using the initial velocities $\underline{v}_{r+k}$ in the case where there is no such deflection. First, the singularity $|u_i - u_k|^{-1}$ in (8.7) and (8.9) appears in the product over the edges in the integral (8.1) that we want to bound, so that it cancels out. The remaining singularities above hence consist in

$$\frac{1}{|u_j - u_i|} + \frac{1}{|u_j - u_k|} + \frac{1}{|u_j - u_l|} + \frac{1}{|\sin(u_k - v_i, v_j - v_i)|}.$$

For one of the three first singularities, of the form, $|u_j - u_n|^{-1}$, we will discriminate on the history of j and n.

If j or n has been deflected by a particle m at a closest time $\tau_{\tilde{\mathrm{d}}}$, we will integrate over this collision's parameters. If this deflection is between j and n, by the scattering identity $|u_j - u_n| = |u_j^\star - u_n^\star|$ between post and pre-collisional velocities, the singularity cancels out in the product over the edges. Otherwise, let us say by symmetry that j is colliding $m \neq n$, so that in particular u_n does not depend on $\sigma_{\tilde{\mathrm{d}}}$. Using the deflection equation (2.4), we write

$$\begin{aligned}\int \frac{\mathrm{d}\sigma_{\tilde{\mathrm{d}}}\mathrm{d}\tau_{\tilde{\mathrm{d}}}}{|u_j - u_n|} &= \int \mathrm{d}\sigma_{\tilde{\mathrm{d}}}\mathrm{d}t_{\tilde{\mathrm{d}}} \left| \frac{u_j^\star + u_m^\star}{2} - u_n + \frac{|u_j^\star - u_m^\star|}{2}\sigma_{\tilde{\mathrm{d}}} \right|^{-1} \\ &= \frac{2}{|u_j^\star - u_m^\star|} \int \mathrm{d}\sigma_{\tilde{\mathrm{d}}}\mathrm{d}\tau_{\tilde{\mathrm{d}}} \left| \frac{u_j^\star + u_m^\star - 2u_n}{|u_j^\star - u_m^\star|} + \sigma_{\tilde{\mathrm{d}}} \right|^{-1}.\end{aligned}$$

We are brought back to studying an integral of the following form, computed in hyperspherical coordinates (cf. Section 2.2) for $w = (1, 0, \dots, 0)$, its maximum value being reached for any $|w| = 1$,

$$\int \frac{\mathrm{d}\sigma}{|w + \sigma|} = C_d \int_0^\pi \frac{\sin^{d-2}\theta}{\sqrt{1 - \cos\theta}} \mathrm{d}\theta = \tilde{C}_d.$$

The remaining singularity $|u_j^\star - u_m^\star|^{-1}$, due to the collision, now appears in the product over the edges in (8.1) and hence get cancelled like $|u_i - u_k|^{-1}$.

Nevertheless, to be able to integrate over these parameters $(\sigma_{\tilde{d}}, \tau_{\tilde{d}})$, we first need to dispose of the velocities that are impacted by them: as we did for K in the beginning of this section, we fix the corresponding set J of edges, and sum over them beforehand (along with the choice of K, this choice of two disjoint sets corresponds to a factor 3^{c}).

If neither j nor n has ever been deflected before τ_{d}, we integrate directly the singularity over the velocity v_j at time 0, using part of the exponential decay $e^{-\frac{\beta}{2}|v_j|^2}$, as the singularity is locally integrable in dimension $d > 1$.

The sine singularity only appears in the non-deflected case, and so is integrated in the same way over v_i and v_j, using for example once again hyperspherical coordinates

$$\int \frac{e^{-{v_j}^2-{v_i}^2}}{|\sin(u_k-v_i,v_j-v_i)|}\mathrm{d}v_j\mathrm{d}v_i = \int\left(\int \frac{e^{-(v+v_i)^2-{v_i}^2}}{|\sin(u_k-v_i,v)|}\mathrm{d}v\right)\mathrm{d}v_i$$
$$\leq \int\left(C_d\int r^{d-1}e^{-r^2+2|v_i|r}\frac{\sin^{d-2}\theta}{|\sin\theta|}\mathrm{d}\theta\mathrm{d}r\right)e^{-{v_i}^2}\mathrm{d}v_i \leq \tilde{C}_d.$$

8.5 Final estimate

In the end, we have obtained enough smallness and there is no more singularity, so that we can eventually sum over all the remaining edges, and conclude the domination as in Section 6.5.2, yielding the same bound as (6.27). The choice of the disjoint sets $K, J \subset E_\Upsilon$ gives a factor 3^c, which becomes $3^{r+k}/2$ with the sum over c, so that we get the following final bound (the constant C stemming from the different cases)

$$\sum_{\Upsilon\in\mathcal{T}^{\mathrm{d}}_{R,k}}\int \mathbb{1}_{T^{\mathrm{d}}_R=\Upsilon}\mathrm{d}\underline{v}_{r+k}\mathrm{d}\underline{\sigma}_{E_\Upsilon}\mathrm{d}\underline{\tau}_{E_\Upsilon}\prod_{e\in E_\Upsilon}s_e|v_m(\tau_e{}^+)-v_{m'}(\tau_e{}^+)|e^{-\beta\|\underline{v}_{r+k}\|^2}\times\mathbb{1}^{\emptyset}_R \tag{8.10}$$
$$\leq C(r+k)^7 3^{r+k}\frac{t^{r+k-1}}{(r+k-1)!}\int \mathrm{d}\underline{v}_{r+k}e^{-\beta\mathbf{V}^2}(r+k)^{r-1}\left(\sqrt{(r+k)\mathbf{V}^2}\right)^{r+k-1}\cdot\mathbf{V}^{2d+1}\varepsilon$$
$$\leq \varepsilon\cdot(\tilde{C}t)^{r+k-1}(r+k)^{r-1}.$$

Compare this bound with (6.27), in Section 6.5 dedicated to the bound on the cumulants (Proposition 6.5.1):

$$\sum_{\Upsilon\in\mathcal{T}^{\mathrm{d}}_{R,k}}\int \mathbb{1}_{T^{\mathrm{d}}_R=\Upsilon}\mathrm{d}\underline{v}_{r+k}\prod_{e\in E_\Upsilon}s_e\langle v_m(\tau_e{}^+)-v_{m'}(\tau_e{}^+),\omega_e\rangle_+\mathrm{d}\omega_e\mathrm{d}\tau_e e^{-\beta\|\underline{v}_{r+k}\|^2}$$
$$\leq (C_d t)^{r+k-1}(r+k)^{r-1},$$

which led, in the following paragraph *Last step: combinatorial manipulations* in the latter proposition's proof, to the bound

$$\left|\int f^{\varepsilon}_n[H]^{[\mathrm{tree}]}(t)\right| \leq \frac{C^n_H n!}{\mu^{n-1}}\sum_{i=1}^{n}\varepsilon^{i-1}\prod_{j=1}^{i}\sum_{r_j\geqslant 0}\sum_{k_j\geqslant 0}(C_d t)^{r_j+k_j-1}e^{k_j+r_j}.$$

Here, the constants are possibly different, but we gain an additional factor ε on each cluster R of size r_j. Note that more precisely, τ_{d} or τ_{ov} has been integrated before, and v_i and v_j also might have been integrated before with the singularities, yet it only changes constants in this bound. Eventually, since the number i of clusters is greater than 1, there is always at least one power of ε added to the bound above, whence the proposition.

Also note that the leading term in the bound above is the one corresponding to a single cluster (i.e. to $i = 1$), in which we exactly gain a factor ε.

Finally, let us sum up the whole strategy of proof: we fixed a configuration of cycle

$$[i, j, k, l, (\tau_c, \tau_{\mathrm{d}}, \tau_{\mathrm{ov}}), J, K],$$

then summed over all the edges in K whose associated velocities would have been impacted by the collision angle σ_{d}, so that we could integrate over the collision parameters σ_{d}, and τ_{d} or τ_{ov}, or $\vec{x}_{\mathrm{ov}}$. This made appear some singularities that we have handled by summing first over the edges of J, to free some collision parameters or velocities, eventually integrating over them. □

Chapter 9

Long time hindrances and solutions

This chapter proposes to reflect on our long time derivation techniques, all of them based on Lanford's method, in a kind of meta-analysis of the obstacles and solutions to derivations on more than short times.

First of all, we discard a big amount of methods by a small heuristic argument based on the time irreversibility of the limit solution, showing that a long-time derivation has to rely on the global history of the system's dynamics, keeping memory of all the interactions since the initial time.

We then explain how the pruning method presented in Chapter 4 performs such a procedure, which hindrances it resolves exactly, and to what it corresponds technically, hence exhibiting the need for a priori bounds. The following Section 9.3 recalls or details different ways of obtaining these a priori bounds, and why in the case of cumulants we still face obstructions.

Eventually, the last section of this chapter is an opening towards an alternative method to bound the successive-collision operators, which consists in computing bounds in an $\mathbb{L}^1$-space in velocities so as to be able to harness large deviation results, to try to get rid of the bad factor n^{cn} appearing in the quantitative bounds for the n-th marginal, in Theorem 1. This method allows to explore the possibilities of displacing the long-time obstruction from a loss of control on the number of particles to a loss of control on the temperature.

As discussed in the introduction, we do not detail the new method calculated by Deng, Hani and Ma [24] (to that end, see for example the paper by Bodineau, Gallagher, Saint-Raymond and Simonella [14]), yet the following meta-analysis provides an insight of the difficulties to which they had to respond.

9.1 The dead-end of a method without history

We first harness the limit irreversibility of the system to justify heuristically the fact that any method to compute a long time derivation must keep track of the full history of the dynamics. Indeed, since Lanford's method shows the derivation on a short time t_1, one may want to use the rate of the convergence of the correlation functions F_n^ε to the tensor product of identical solutions of the Boltzmann equation f, to restart Lanford's method from t_1, eventually covering large times iterating this method. Actually, that was historically the first argument to try to derive the linear Rayleigh–Boltzmann equation in the long time, using the a priori bounds to push the derivation further in time, step by step.

More precisely, let us imagine that one can show that in some functional space X, the error at a time $t_1 > 0$ can be bounded from the error at time 0 as

$$\|F_n^\varepsilon(t_1) - f^{\otimes n}(t_1)\|_X \leq C(1,n)\|F_n^\varepsilon(0) - f^{\otimes n}(0)\|_X, \tag{9.1}$$

for a constant $C(1,n)$—(or more generally a bound depending on the initial error for every higher correlation function $(F^\varepsilon_{n+k})_{k\geqslant 0}$ appearing in the hierarchy). Imagining that the constant is not too bad, and assuming strong estimates on the solution f of the Boltzmann equation, one may try to iterate this method K times, on successive times $t_2 < ... < t_K$ diverging to infinity, hence covering arbitrary large times.

Nevertheless, should such a method work, one could choose a time t_i halfway to t_K, and restart Lanford's method from the error

$$\|F^\varepsilon_n(t_i) - f^{\otimes n}(t_i)\|_X, \tag{9.2}$$

but for the reversed dynamics, looked at backwards in time, which merely corresponds to the Newton microscopic equations

$$\frac{\mathrm{d}x_i}{\mathrm{d}t} = -v_i, \qquad \frac{\mathrm{d}v_i}{\mathrm{d}t} = 0,$$

and to inverting formulas between pre- and post-collisional velocities. The corresponding transport operators are

$$\tilde{\Theta}_i(t) = \Theta_i(-t),$$

and the pre- and post-velocities are inverted in the collision operators. The same study as Lanford's show that this dynamics leads to the Boltzmann equation backwards in time [10]. Since the bounds at time t_i ignore the previous history, the large time derivation now leads to the convergence of the first correlation function to the solution to the forward, then backward Boltzmann equation, with inversion of the velocities at time t_i:

$$\tilde{f}(t) = \begin{cases} f(t,x,v) & \text{for } t \in [0,t_i] \\ f(t_i - t, x, -v) & \text{for } t \in [t_i, t_K]. \end{cases}$$

That solution should coincide with the solution to the Boltzmann equation by uniqueness of the limit, which contradicts the irreversibility of this solution, which relaxes in large times to the Maxwellian state. Hence, there is no hope for such a method, without memory, to work.

9.2 Pruning methods

From the previous section, one can see that an iterating method to derive a Boltzmann equation needs to have memory, and to keep track of the dynamics history. In a very elaborate, and industrious way, Deng, Hani and Ma [24] define a clever algorithm to show that the pathological pseudo-trajectories have a negligible influence on the evolution of correlation functions. This method allows them to derive the Boltzmann equation on large times, assuming bounds on the regular solutions to the Boltzmann equation, uniformly in time.

In this section, we detail the technical obstacles that our pruning method allows to overcome, and explain its ideas from a computational point of view. Indeed, in the case of the Rayleigh gas, in a simpler way, one can use the a priori bounds on the correlation functions to discard the pseudo-trajectories containing too many collisions. Looking at the whole dynamics history, we choose to consider trajectories that grow less than exponentially in time, this way determining a favoured direction of time: it keeps track indeed of the whole evolution of particles, in a far coarser way than [24].

This method can be seen as a pruning of the trees constructed from the pseudo-trajectories (Section 4.6), and the key point is to discard the pruned-out trajectories (the ones containing too may particles). In the method that we presented in Chapter 4, it is made thanks to the *a priori bounds* on the correlation functions, since each pruning appears at a certain time t_i^{p}, and makes appear the correlation functions $(F^\varepsilon_n(t_i^{\mathrm{p}}))_{n\geqslant 0}$ in the pruned-out term.

From a technical point of view, when we iterate the Dyson expansion (4.4), like we do in the pruning computation (4.28), each successive-collision operator $Q_{N_{i-1},\underline{\ell}^*_{j_i}}$ makes appear a factor C^{N_i} due to the Cauchy–Schwarz estimate on the collision kernels. If one would ignore these factors and perform an expansion without taking them into account, since the Lanford time depends on the initial bound, which would get bigger by a factor C^{N_i} at each step, each further expansion would be computed on a downgraded time interval

$$h_i = C^n C^{n+j_1} \dots C^{n+J_K} h_1,$$

resulting in a (very quickly) converging series

$$\sum_{i \geqslant 1} h_i < \infty,$$

leading to a convergence on short times. The link between time and number of collisions is further discussed in Section 9.4.

The key point in the pruning computation, to perform a long time derivation, is to set apart these factors C^n, factorizing all of them in a big constant, to let the iterated time intervals remain of the same order, eventually obtaining a (slowly but surely) diverging time series. Nevertheless, in return we need to control the size of these stacking factors

$$C^n C^{n+j_1} \dots C^{n+J_K},$$

which depends on the number of collisions $(j_1, \dots, j_K)$. This is precisely the reason why we need to control the number of these collisions, by pruning the trajectory trees. Eventually, since the stacking terms above, that have been set aside, have a controlled growth, we are able to compensate them by a small fraction of the converging rate ε (Section 4.8). In the end, as we said before, it remains to control the size of the pruned-out term, thanks to a priori estimates.

Next section discusses the methods used to get a priori bounds.

9.3 A priori bounds

As we presented in Section 4.4, we can get a priori bounds on the canonical marginals from the fact that their initial data is controlled by a Maxwellian distribution, which is stable by the transport flow, and the fact that the transport flow preserves such bounds. To get bounds on the grand canonical correlation functions from the ones on the canonical distributions, we had to perform a combinatorial analysis of the grand canonical distribution function (Section 5.4), eventually leading to useful a priori estimates, stated in Proposition 4.4.2.

Another way to get such estimates, that we present here for curiosity and later studies, is to use the link between correlation functions and the moments of the empirical measure (2.19), thus harnessing more deeply the reversible structure of the microscopic flow.

Note that for the cumulants, the first method has no chance to work, because of the non-linearity of the equations they satisfy (6.5). A method like the one we present below has more chance to yield a priori bounds on them, since the cumulants are also directly linked to the moments of the empirical measure through their generating function (Section 6.1, Definition 6.1.1).

Indeed, let us observe that the cumulant generating function is defined (6.2) as

$$\mathbb{E}\left[e^{\mu \pi^\varepsilon_t[H]}\right] = \frac{1}{\mathcal{Z}_\mu} \sum_{n \geqslant 0} \sum_{\underline{\ell}_n} \frac{\lambda^{|\underline{\ell}_n|} \mu^{n-|\underline{\ell}_n|}}{n!} \int \mathrm{d}\underline{z}_n \mathbb{1}_{\mathcal{X}^\varepsilon_n}(\underline{x}_n) \varphi_0^{\otimes \underline{\ell}_n}(\underline{z}_{\underline{\ell}_n}) M_\beta^{\otimes n}(\underline{v}_n) e^{\sum H(z_i^{[t]}, \ell_i)}.$$

On the other hand, when we have performed its expansion into cumulants, we showed halfway the following expansion (6.1) in correlation functions

$$\mathbb{E}\left[e^{\mu\pi_t^\varepsilon[H]}\right] = 1 + \sum_{n\geqslant 1}\frac{1}{n!}\sum_{\underline{\ell}_n\in\Lambda_n}\lambda^{|\underline{\ell}_n|}\mu^{n-|\underline{\ell}_n|}\int F_n^\varepsilon(t,\underline{\ell}_n)(e^H-1)^{\otimes n}(\underline{\ell}_n).$$

Both formulas clearly exhibit analyticity with respect to the observable H, so that we introduce the observable uH, for $u\in\mathbb{R}$ close to 0, and differentiate according to this parameter both writings.

In $u=0$, we get heuristical bounds for all times $t>0$ on the derivatives from the first formula by writing

$$\begin{aligned}\partial_u^s\mathbb{E}\left[e^{\mu\pi_t^\varepsilon[uH]}\right]_{u=0} &= \frac{1}{\mathcal{Z}_\mu}\sum_{n\geqslant 0}\sum_{\underline{\ell}_n}\frac{\lambda^{|\underline{\ell}_n|}\mu^{n-|\underline{\ell}_n|}}{n!}\int \mathrm{d}\underline{z}_n\mathbb{1}_{\mathcal{X}_n^\varepsilon}(\underline{x}_n)\varphi_0^{\otimes\underline{\ell}_n}(\underline{z}_{\underline{\ell}_n})M_\beta^{\otimes n}(\underline{v}_n)\left(\sum_{i=1}^n H(z_i^{[t]},\ell_i)\right)^s\\ &\leq \frac{\|H\|^s}{\mathcal{Z}_\mu}\sum_{n\geqslant 0}\sum_{\underline{\ell}_n}n^s\frac{\lambda^{|\underline{\ell}_n|}\mu^{n-|\underline{\ell}_n|}}{n!}\int \mathrm{d}\underline{z}_n\mathbb{1}_{\mathcal{X}_n^\varepsilon}(\underline{x}_n)\varphi_0^{\otimes\underline{\ell}_n}(\underline{z}_{\underline{\ell}_n})M_\beta^{\otimes n}(\underline{v}_n)\\ &= \|H\|^s\times\mathbb{E}\left[\mathcal{N}^s\right].\end{aligned}$$

On the other hand, we retrieve the correlation functions from the second formula, writing for example

$$\partial_u\mathbb{E}\left[e^{\mu\pi_t^\varepsilon[uH]}\right]_{u=0} = \sum_\ell\lambda^\ell\mu^{1-\ell}\int F_1^\varepsilon(t,\ell)H(\ell),$$

then

$$\partial_u^2\mathbb{E}\left[e^{\mu\pi_t^\varepsilon[uH]}\right]_{u=0} = \sum_\ell\lambda^\ell\mu^{1-\ell}\int F_1^\varepsilon(t,\ell)H^2(\ell) + 2\sum_{\underline{\ell}_2}\lambda^{|\underline{\ell}_2|}\mu^{2-|\underline{\ell}_2|}\int F_2^\varepsilon(t,\ell)H(\ell_1)H(\ell_2),$$

etc. As we commented when we defined the cumulant generating function, the observables $(e^H-1)^{\otimes n}$ make appear combinatorial factors, but we still get good bounds for small correlation functions: for example, we just proved that for any $t>0$

$$\left|\lambda\int F_1^\varepsilon(t,0)H(0)+\mu\int F_1^\varepsilon(t,1)\right| \leq \|H\|\cdot\mathbb{E}[\mathcal{N}]\sim_{\varepsilon\to 0}\|H\|\cdot\mu,$$

which could also be refined by looking at observables that only consider tagged particles (see for example (6.4) in the case of the cumulant generating function).

Nevertheless, this method does not work directly for high correlation functions, or for cumulants, because of the combinatorial factors. Changing the combinatorics of the generating functions might allow to get rid of this technical obstruction.

Let us also observe that similarly at the limit, characterizing limit cumulants as derivatives of the limit cumulant generating function could lead to bounds on these limit cumulants, provided some bounds on the limit cumulant generating function.

Finally, let us observe that the naive a priori bound on the cumulants, using their Definition 5.1 and the a priori bound (4.19) on the correlation functions, yields by the same usual decomposition of the partitions (as in Lemma 5.4.1 or the final step of the proof of Proposition 6.5.1),

$$\begin{aligned}|f_n^\varepsilon(t)| &\leq \sum_{\sigma\in\mathcal{P}_n}(|\sigma|-1)!F_{[\sigma]}^\varepsilon(t)\\ &\leq \sum_{j=1}^n\frac{(j-1)!}{j!}\sum_{\substack{k_1+\cdots+k_j=n\\ k_1,\ldots,k_j\geqslant 1}}\frac{n!}{k_1!\ldots k_j!}C_0^n C^{C_0\lambda j}.\end{aligned}$$

Ignoring the condition on the sum of indices $k_1 + \cdots + k_j$, we sum over each one of these indices to find the final bound

$$|f_n^\varepsilon(t)| \leq C_0^n n! \sum_{j=1}^{n} C^{C_0 \lambda j} (e-1)^j$$
$$\leq C_0^n n! \cdot \tilde{C}^{\lambda n}.$$

In itself, this would not be that terrible of a bound, but the thing is that we lost all the fine compensations between correlation functions, that yielded the factors $\varepsilon^{d(n-1)}$ in their initial bound (6.23), which are highly needed to get bounds on the cumulants at time $t > 0$ (see the proof of Proposition 6.5.1). The cumulants are small objects, constructed on fine cancellations in the dynamics, which makes very hard to prove a priori bounds on them.

9.4 Bounding the collision operators in an $\mathbb{L}^1$ setting

In this section, we present a heuristics that modifies the way we bound the successive-collision operators, leading to a different way of controlling the pruned Dyson expansion (4.28). Although we do not exhaustively detail the proof of the whole derivation, we give improved estimates on the main term of the Dyson expansion, in Propositions 9.4.4 and 9.4.5.

This method relies on large deviation methods, used to justify the fact that the velocities cannot concentrate around zero: this way, the kinetic energy

$$\|\underline{v}_n\|^2 = \sum_{i=1}^{n} |v_i|^2$$

has to be big enough, so that the Maxwellian weight

$$\exp\left(-(\beta - \beta')\|\underline{v}_n\|^2\right) \tag{9.3}$$

stemming from the initial control, has to provide better smallness than the Cauchy–Schwarz computation. Nevertheless, these large deviation methods only work in an $\mathbb{L}^1_v$ setting, when we look at the average behaviour of the collision operators, and is immediatly hindered in the previous $\mathbb{L}^\infty$ setting, in which rare events such as concentration of velocities around 0 have a great weight.

Using this method, we displace the obstruction to large times from a limitation on the number of collisions to a loss of temperature. The fact that these two parameters usually cause a restriction to short times can be seen in the proof of the wellposedness of the BBGKY hierarchy for general initial data. In [34, Proposition 5.4.1], the collision operator applied to the whole hierarchy $\mathbf{F}$ satisfies a bound of the form

$$\|\mathcal{C}\mathbf{F}\|_{\beta',\mu'} \leq C_\beta \left(\frac{1}{\beta - \beta'} + \frac{1}{\mu - \mu'}\right) \|\mathbf{F}\|_{\beta,\mu},$$

where $\beta' < \beta$ tune the temperature, and $\mu' < \mu$ weight the number of particles implied, directly linked to the number of collisions implied in the trajectories. This estimate suffers both from a loss of control on the temperature and on the number of particles, because of the Cauchy–Scwharz argument that absorbs the velocities

$$\sum_{i=1}^{n} |v_i|$$

appearing in the collision operators, using part of the exponential decay (9.3), eventually making appear the number of particles and the temperature. By a classical Banach argument, the loss on this operator leads to a loss of control on the solution over time, eventually stopping the process in

short time once all the controls are exhausted. Along with the discussion of Section 9.2, that gives a nice philosophical insight into the fact that time and number of collisions are deeply connected, and that the short time of existence of the solution to the general Boltzmann equation is precisely due to the overabundance of correlated collisions in the dynamics. The same kind of bound might be found in various situations concerning the Boltzmann equation, for example in the short time variant of our Proposition 6.6.6, in [12, Proposition 7.2.1]. In the following, we try to gain on the loss over the number of particles, downgrading the loss over the temperature, in an $\mathbb{L}^1_v$-framework.

We hence consider the weighted spaces

$$\mathcal{F}^1_\beta \doteq \mathbb{L}^1_v(M_\beta^{-1})\mathbb{L}^\infty_x$$

and

$$\mathcal{F}^\infty_\beta \doteq \mathbb{L}^\infty_v(M_\beta^{-1})\mathbb{L}^\infty_x,$$

eventually denoting $\mathbb{L}^1_\beta \doteq \mathbb{L}^1_v(M_\beta^{-1})$.

We do not consider the tags in this heuristical section, imagine for example the case of a single tagged particle in a gas initially at equilibrium, like in [9, 31]. Like we did in Chapter 4, we want to bound an expansion of the form

$$\|F^\varepsilon_n(t)\|_\beta \leq \sum_{m\geqslant 0} \|Q_{n,m}(t)F^\varepsilon_{n+m}(0)\|_\beta. \tag{9.4}$$

In the preceding Section 9.2, we explained how the pruning method allows to control the stacking factors C^n stemming from the bound on $Q_{n,m}$. We propose here to get rid of these factors in an $\mathbb{L}^1_\beta$ framework, to upgrade the dependency in n of the convergence rate for the n-th marginal, in Theorem 1. Indeed, if one gets rid of these stacking factors, one could expect a way better convergence rate and time scaling for the validity of the theorem, as we saw in Section 9.2, and in the computations of Chapter 4, that these factors are the main obstruction to upgrade these estimates. Nevertheless, the $\mathbb{L}^1_\beta$ method comes at the cost of a different dependency on the temperature increments performed to bound each operator. Indeed, where the Cauchy–Schwarz arguments (see Proposition 4.5.1) led to a bound in

$$e^n\left(\frac{C_d\ t}{\sqrt{(\beta-\beta')}}\right)^k,$$

we go here to a bound in

$$\left(\frac{C_d\ t}{\beta-\beta'}\right)^k,$$

getting rid of the dependency in n, yet losing on the decay in $(\beta-\beta')$. This decay is crucial because in a decomposition in K time intervals, each successive-collision operator is estimated with an increment of order

$$\beta-\beta' \sim \frac{\beta_0}{K},$$

so that it is deeply linked to the size of the total time interval, which is not directly improved by this heuristic method.

For any $n \geqslant 0$, we assume that initially the $\mathcal{F}^1_\beta$-norms are small, with the idea that through the large deviation heuristics one can propagate this smallness. We consider the natural initial hypothesis, similar to the one proved in Proposition 4.3.1,

$$\|F^\varepsilon_n(0)\|_{\mathcal{F}^1_\beta} \leq {C_0}^n\varepsilon. \tag{9.5}$$

On the other hand, we know that the large deviation heuristics cannot propagate smallness in $\mathcal{F}_\beta^\infty$-norm, so that we merely assume for all times $t \geqslant 0$ the usual a priori bounds that can be found in [9, 31] in their non-mixture version, comparable to the bounds (4.19) that can be found in Chapter 4. Namely, we assume

$$\|F_n^\varepsilon(t)\|_{\mathcal{F}_\beta^\infty} \leq {C_0}^n. \tag{9.6}$$

We present in the following section the main decomposition of the operators on which the heuristics relies, then prove the essential results, before explaining how this method leads to an alternative long time derivation in $\mathcal{F}_\beta^1$, in the last section of this chapter.

9.4.1 Heuristics of the large deviation method

Recall the definition of the successive-collision operator (without tags in this section)

$$Q_{n,m}(t) \doteq \int_0^t \int_0^{t_1} \cdots \int_0^{t_{m-1}} \Theta_n(t-t_1)\mathcal{C}_n\Theta_{n+1}(t_1-t_2)\ldots\mathcal{C}_{n+m-1}\Theta_{n+m}(t_m)\mathrm{d}t_m\ldots\mathrm{d}t_1.$$

Following the classical method to estimate this operator, we will use a fraction of the exponential decay to resorb the sum of the velocities, writing $e^{\beta\|\underline{v}_n\|^2} = e^{\beta'\|\underline{v}_{n+1}\|^2}e^{-(\beta'-\beta)\|\underline{v}_n\|^2}e^{-\beta'|v_{n+1}|^2}$. The new computational idea consists in observing that if the velocities do not concentrate on too small norms, the exponential gain yields far better estimates; it will hence remain to control the configurations where the velocities concentrates around 0, in the $\mathbb{L}^1_\beta$ norm in velocities, thanks to a large deviation principle.

First, for non-pathological configurations (when the velocities do not concentrate around 0), we have the following lemma on the exponential gain.

Lemma 9.4.1 (Control under non-concentration assumptions)**.** *Let us fix $\eta > 0$ a threshold for the modulus of the velocities. We assume that there is a large enough proportion of velocities that are greater than η, i.e. that for a proportion $p \in (0,1)$*

$$\sharp\Big\{v_i \;\Big|\; |v_i| \geq \eta\ ,\ 1 \leq i \leq N\Big\} \geq pN. \tag{9.7}$$

The set of velocities $\underline{v}_N \in \mathbb{R}^{dN}$ satisying this condition (9.7) is denoted $A_\eta^{(N)}$. Then, for any inverse tempertaure $\lambda > 0$ one has

$$e^{-\lambda\|\underline{v}_N\|^2}\mathbb{1}_{\underline{v}_N \in A_\eta^{(N)}} \leq \frac{1}{e\lambda pN\eta^2}.$$

Proof. The proof is elementary; we use the fact that for $\underline{v}_N \in A_\eta^{(N)}$

$$\|\underline{v}_N\|^2 = \sum_{\substack{i=1\\|v_i|<\eta}}^N |v_i|^2 + \sum_{\substack{i=1\\|v_i|\geqslant\eta}}^N |v_i|^2 \geq 0 + pN\eta^2,$$

and then observe that $x \geq 0 \Rightarrow xe^{-x} \leq e^{-1}$ to deduce

$$e^{-\lambda\|\underline{v}_N\|^2} \leq e^{-\lambda pN\eta^2} \leq \frac{1}{e\lambda pN\eta^2}.$$

□

Starting from the definition (9.4.1) of the successive-collision operator, we want to bound each collision operator $\mathcal{C}_k$ on its time interval $[\tau_c, \tau] \doteq [t_{k-n+1}, t_{k-n}]$. The $\mathbb{L}^1_\beta$-norm is preserved by the

transport operators since the exponential weight only depends on the kinetic energy, so that for a general function $G_{k+1} \in \mathcal{F}^1_{\beta'}$, we can compute

$$\|\Theta(\tau-\tau_c)\mathcal{C}_k G_{k+1}(\tau_c,\underline{x}_k)\|_{\mathbb{L}^1_\beta} \leq \int \mathrm{d}\omega \mathrm{d}\underline{v}_{k+1} \sum_{i=1}^{k} (|v_i^{[\tau_c]}| + |v_{k+1}|)\cdot |G_{k+1}(\underline{z}_k, x_i+\varepsilon\omega, v_{k+1})| e^{\beta\|\underline{v}_k\|^2} + \int \mathrm{d}\omega \mathrm{d}\underline{v}_{k+1} \sum_{i=1}^{k} (|v_i^{[\tau_c]}| + |v_{k+1}|)\cdot |G_{k+1}(\underline{z}_k^\star, x_i+\varepsilon\omega, v_{k+1}^\star)| e^{\beta\|\underline{v}_k\|^2}$$

where $v_i^{[\tau_c]}$ is determined by the velocities $\underline{v}_k = \underline{v}_k^{[\tau]}$ and the backwards transport flow. Using the usual change of variable that harnesses the reversibility of the flow, the study of both terms above can be brought back to the study of the first one.

For this term, the idea is to split the integral defining the collision operators, according to the non-concentration assumption (9.7) that defines the set of velocities $A_\eta^{(N)}$. More precisely, at fixed η, let us define

$$\begin{aligned} \mathcal{C}_k = \quad & \mathcal{C}_k \mathbb{1}_{A_\eta^{(k)}} \quad + \quad \mathcal{C}_k \mathbb{1}_{\overline{A_\eta^{(k)}}} \\ \doteq \quad & \mathcal{C}_k^\sharp \quad + \quad \mathcal{C}_k^\flat, \end{aligned}$$

where $\mathcal{C}_k^\sharp$ contains the good non-concentration cardinal assumption and $\mathcal{C}_k^\flat$ the pathological one. Then, we write

$$\begin{aligned} \Theta_n \mathcal{C}_n \Theta_{n+1} \dots \mathcal{C}_{n+m-1} = \Theta_n \mathcal{C}_n^\sharp \Theta_{n+1} \dots \mathcal{C}_{n+m-1}^\sharp \\ + \sum_{k=0}^{m-1} \Theta_n \mathcal{C}_n \dots \mathcal{C}_{n+k-1}\ \Theta_{n+k}\mathcal{C}_{n+k}^\flat\ \Theta_{n+k+1}\mathcal{C}_{n+k+1}^\sharp \dots \mathcal{C}_{n+m-1}^\sharp, \end{aligned} \tag{9.8}$$

and according to this decomposition we define naturally

$$Q_{n,m}(t) \doteq Q_{n,m}^\sharp(t) + Q_{n,m}^\flat(t). \tag{9.9}$$

We are left with two different terms to estimate, each one of them being the subject of one of both following sections. We start by bounding the successions of collision operators in both terms, to emphasize the origin of the different factors in the estimate, and we postpone the time integration leading to the final estimate on the successive-collision operators to Section 9.4.4 for both terms.

9.4.2 Bounding the non-pathological term

We use here Lemma 9.4.1 to control the first non-concentrated term, to obtain the following result.

Proposition 9.4.1 (Bound on the non-concentrated part)**.** *Considering an initial temperature $\beta_0 > 0$, and an increment $\delta\beta < \beta_0/2$, for any $F_{n+m} \in \mathcal{F}^1_{\beta_0}$, we have*

$$\|\Theta_n \mathcal{C}_n^\sharp \Theta_{n+1} \dots \mathcal{C}_{n+m-1}^\sharp F_{n+m}\|_{\mathcal{F}^1_{\beta_0-\delta\beta}} \leq \left(\frac{2mC_d[1+\beta_0^{-\frac{1}{2}}]}{\delta\beta\cdot p\eta^2}\right)^m \|F_{n+m}\|_{\mathcal{F}^1_{\beta_0}},$$

where the constant C_d only depends on the dimension.

Proof. We choose to denote $N \doteq n+m$, and for any $\underline{x}_{N-1} \in \mathbb{T}^{d(N-1)}$ we bound the $\mathbb{L}^1_\beta$-norm, with respect to the velocities, of the collision operator, by the triangle inequality

$$\begin{aligned} \|C_{N-1}^\sharp \Theta_N F_N\|_{\mathbb{L}^1_\beta} \leq \sum_{i=1}^{N-1} \int \mathrm{d}\omega \mathrm{d}\underline{v}_N |v_i - v_N| \left[\Theta_N F_N\right](\underline{z}_{N-1}, x_i+\varepsilon\omega, v_N) e^{\beta\|\underline{v}_{N-1}\|^2} \mathbb{1}_{\underline{v}_{N-1}\in A_\eta^{(N-1)}} \\ + \sum_{i=1}^{N-1} \int \mathrm{d}\omega \mathrm{d}\underline{v}_N |v_i - v_N| \left[\Theta_N F_N\right](\underline{z}_{N-1}^\star, x_i+\varepsilon\omega, v_N^\star) e^{\beta\|\underline{v}_{N-1}\|^2} \mathbb{1}_{\underline{v}_{N-1}\in A_\eta^{(N-1)}}. \end{aligned}$$

Let us deal with the first gain term of the collision operator—the other one is computed similarly. Writing that $|v_i - v_N| \leq 1 + |v_N| + |v_i|^2$, we have (ignoring the loss term, treated similarly)

$$\begin{aligned}
&\|C^\sharp_{N-1}\Theta_N F_N\|_{\mathbb{L}^1_\beta} \\
&= \sum_{i=1}^{N-1} \int \mathrm{d}\omega \mathrm{d}\underline{v}_N |v_i - v_N| \left[\Theta_N F_N\right](\underline{z}_{N-1}, x_i + \varepsilon\omega, v_N) e^{\beta'\|\underline{v}_N\|^2 - \beta'\|\underline{v}_N\|^2} e^{\beta\|\underline{v}_{N-1}\|^2} \mathbb{1}_{\underline{v}_{N-1}\in A_\eta^{(N-1)}} \\
&\leq \sum_{i=1}^{N-1} \int \mathrm{d}\omega \mathrm{d}\underline{v}_N \left(\sup_{\mathbb{T}^{dN}} \left[\Theta_N F_N\right](\cdot, \underline{v}_N) e^{\beta'\|\underline{v}_N\|^2}\right) (1 + |v_N|) e^{-\beta'|v_N|^2} \left\{ e^{-(\beta'-\beta)\|\underline{v}_{N-1}\|^2} \mathbb{1}_{\underline{v}_{N-1}\in A_\eta^{(N-1)}} \right\} \\
&\quad + \sum_{i=1}^{N-1} \int \mathrm{d}\omega \mathrm{d}\underline{v}_N \left(\sup_{\mathbb{T}^{dN}} \left[\Theta_N F_N\right](\cdot, \underline{v}_N) e^{\beta'\|\underline{v}_N\|^2}\right) |v_i|^2 e^{-(\beta'-\beta)\|\underline{v}_N\|^2}
\end{aligned}$$

For the first of the two terms above, we apply Lemma 9.4.1 on the factor between curly brackets to harness the non-concentration assumption, and we bound the velocity $|v_N| e^{-\beta'|v_N|^2} \leq (2e\beta')^{-\frac{1}{2}}$, so that we get

$$\begin{aligned}
&\|C^\sharp_{N-1}\Theta_N F_N\|_{\mathbb{L}^1_\beta} \\
&\leq \sum_{i=1}^{N-1} \int \mathrm{d}\omega \mathrm{d}\underline{v}_N \left(\sup_{\mathbb{T}^{dN}} \left[\Theta_N F_N\right](\cdot, \underline{v}_N) e^{\beta'\|\underline{v}_N\|^2}\right) \left(1 + \frac{1}{\sqrt{2e\beta'}}\right) \cdot \frac{e^{-1}}{(\beta'-\beta)(N-1)p\eta^2} \\
&\qquad + \sum_{i=1}^{N-1} \int \mathrm{d}\omega \mathrm{d}\underline{v}_N \left(\sup_{\mathbb{T}^{dN}} \left[\Theta_N F_N\right](\cdot, \underline{v}_N) e^{\beta'\|\underline{v}_N\|^2}\right) |v_i|^2 e^{-(\beta'-\beta)\|\underline{v}_N\|^2} \\
&\leq \frac{c + C(\beta')^{-\frac{1}{2}}}{(\beta'-\beta)(N-1)p\eta^2} \sum_{i=1}^{N-1} \int \mathrm{d}\omega \mathrm{d}\underline{v}_N \left(\sup_{\mathbb{T}^{dN}} \left[\Theta_N F_N\right](\cdot, \underline{v}_N) e^{\beta'\|\underline{v}_N\|^2}\right) \\
&\qquad + \int \mathrm{d}\omega \mathrm{d}\underline{v}_N \left(\sup_{\mathbb{T}^{dN}} \left[\Theta_N F_N\right](\cdot, \underline{v}_N) e^{\beta'\|\underline{v}_N\|^2}\right) \|\underline{v}_N\|^2 e^{-(\beta'-\beta)\|\underline{v}_N\|^2} \\
&\leq \frac{c + C(\beta')^{-\frac{1}{2}}}{(\beta'-\beta)(N-1)p\eta^2} (N-1)|\mathbb{S}_d| \cdot \|F_N\|_{\mathcal{F}^1_{\beta'}} + |\mathbb{S}_d| \cdot \|F_N\|_{\mathcal{F}^1_{\beta'}} \frac{e^{-1}}{\beta'-\beta},
\end{aligned}$$

using the fact the transport operator preserves the $\mathcal{F}^1_{\beta'}$-norm. Note that at the penultimate lign above, we dominated the kinetic energy of the $(N-1)$ first particles by the kinetic energy of all the N particles. As this bound is uniform in $\underline{x}_{N-1} \in \mathbb{T}^{d(N-1)}$, we eventually have

$$\|C^\sharp_{n+m-1}\Theta_{n+m}(t_m) F_{n+m}\|_{\mathcal{F}^1_\beta} \leq \frac{C\left(1 + \beta'^{-\frac{1}{2}}\right)}{(\beta'-\beta)p\eta^2} \|F_{n+m}\|_{\mathcal{F}^1_{\beta'}}.$$

Now, we will iterate this computation m times to control the succession of non-concentrated collision operators, choosing a constant increment

$$\beta' - \beta = \frac{\delta\beta}{2m},$$

so that the successive inverse temperature β' remain between β_0 and $\beta_0/2$ by the condition $\delta\beta < \beta_0/2$. Eventually, this leads to

$$\|\Theta_n \mathcal{C}^\sharp_n \Theta_{n+1} \dots \mathcal{C}^\sharp_{n+m-1} F_{n+m}\|_{\mathcal{F}^1_{\beta_0-\delta\beta}} \leq \left(\frac{2mC[1 + \beta_0^{-\frac{1}{2}}]}{\delta\beta \cdot p\eta^2}\right)^m \|F_{n+m}\|_{\mathcal{F}^1_{\beta_0}}.$$

This concludes the proof of the proposition. The factor m^m will be resorbed by the time integration in Section 9.4.4, thanks to the denominator $m!$. □

9.4.3 Bounding the concentrated term: large deviation method

The pathologically concentrated second term implying $\mathcal{C}^\flat$ is dealt with using a large deviation argument, and the a priori bounds in $\mathcal{F}^\infty_\beta$. For a general term of the form

$$\mathfrak{C}^{(k)}_{n,m}(\underline{t}_m) \doteq \Theta_n(t-t_1)\mathcal{C}_n \dots \mathcal{C}_{n+k-1}\ \Theta_{n+k}(t_k - t_{k+1})\mathcal{C}^\flat_{n+k}\ \Theta_{n+k+1}(t_{k+1}-t_{k+2})\mathcal{C}^\sharp_{n+k+1}\dots\mathcal{C}^\sharp_{n+m-1},$$

one can have the idea to discriminate the way we bound it on the value of n. Indeed, the large deviation method only provides smallness for large values of n, and requires a priori bounds in $\mathcal{F}^\infty_\beta$. Nevertheless, let us imagine that one has a strong control in $\mathcal{F}^1_\beta$ of the initial proximity (or on the proximity at a certain time from which we start our Dyson expansion); then for n small enough, one can treat the pathological term as it is now classical to do in the litterature [9, 31], making appear a factor c^n, which may not be that big if n is not too big, with the hope of compensating it thanks to the initial proximity in $\mathcal{F}^1_\beta$.

Indeed, when looking closely at the usual way how we bound the quantity

$$\frac{(n+m)^m}{m!} \leq e^{n+m}$$

appearing in the estimates of the successive-collision operators, one realizes that a finer Stirling control can lead to a bound in

$$\frac{(n+m)^m}{m!} \leq c^n C^m,$$

with c arbitrarily close to 1, up to taking C bigger (see Lemma 9.4.2 in the following section).

We thus provide the following proposition, with two different bounds on the pathological term, one classical with initial smallness in $\mathcal{F}^1_\beta$, and one using the large deviation argument, yet requiring bounds in $\mathcal{F}^\infty_\beta$.

Proposition 9.4.2 (Two bounds on the concentrated term)**.** *For any initial inverse temperature β_0, and inverse temperature increment $\delta\beta < \beta_0/2$, one has the following usual bound on the concentrated term*

$$\|\mathfrak{C}^{(k)}_{n,m}(\underline{t}_m)F_{n+m}\|_{\mathcal{F}^1_{\beta_0-\delta\beta}} \leq \left(\frac{C(n+m)}{\sqrt{\delta\beta}}\right)^m \|F_{n+m}\|_{\mathcal{F}^1_{\beta_0}},$$

and the following one, harnessing a large deviation principle

$$\|\mathfrak{C}^{(k)}_{n,m}(\underline{t}_m)F_{n+m}\|_{\mathcal{F}^1_{\beta_0-\delta\beta}} \leq \frac{\delta^{n+k}_{\eta,p}}{\sqrt{\delta\beta}}\left(C_{\beta_0}\frac{n+m}{\sqrt{\delta\beta}}\right)^m \|F_{n+m}\|_{\mathcal{F}^\infty_{\beta_0}},$$

where the large deviation rate depends on the parameters η, p defining the concentrating contition as

$$\begin{cases} \delta_{\eta,p} \doteq \exp\left[-p\log\left(\dfrac{p}{\overline{p}_{\eta,\delta\beta}}\right) - (1-p)\log\left(\dfrac{1-p}{1-\overline{p}_{\eta,\delta\beta}}\right)\right], \\ \overline{p}_{\eta,\delta\beta} \doteq \mathbb{P}\left[|\hat{V}_1| \geq \eta\right], \end{cases} \tag{9.10}$$

with $\hat{V}_1$ a centered Gaussian distribution of variance $(\delta\beta)^{-1}$.

Proof. **First classical part.** We adapt here the classical method, adapted to the $\mathcal{F}^1_\beta$ framework, in the idea of using this bound for small values of n. Like we just computed in the previous section, we write once again

$$\begin{aligned}\|C_{N-1}\Theta_N F_N\|_{\mathbb{L}^1_\beta} \leq &\sum_{i=1}^{N-1}\int \mathrm{d}\omega\mathrm{d}\underline{v}_N |v_i - v_N|\left[\Theta_N F_N\right](\underline{z}_{N-1}, x_i+\varepsilon\omega, v_N)e^{\beta\|\underline{v}_{N-1}\|^2} \\ &+ \sum_{i=1}^{N-1}\int \mathrm{d}\omega\mathrm{d}\underline{v}_N |v_i - v_N|\left[\Theta_N F_N\right](\underline{z}^\star_{N-1}, x_i+\varepsilon\omega, v^\star_N)e^{\beta\|\underline{v}_{N-1}\|^2}.\end{aligned}$$

Once again ignoring the second term, which is still being computed in a similar way thanks to the classical change of variable pre- to post-collisional, we write by the same usual Cauchy–Schwarz argument as in (4.25) that

$$\begin{aligned}\|C_{N-1}\Theta_N F_N\|_{\mathbb{L}^1_\beta} &\leq \sum_{i=1}^{N-1}\int \mathrm{d}\omega \mathrm{d}\underline{v}_N \left(\sup_{\mathbb{T}^{dN}} \left[\Theta_N F_N\right](\cdot,\underline{v}_N) e^{\beta'\|\underline{v}_N\|^2}\right) |v_i| e^{-(\beta'-\beta)\|\underline{v}_N\|^2} \\ &\quad + \sum_{i=1}^{N-1}\int \mathrm{d}\omega \mathrm{d}\underline{v}_N \left(\sup_{\mathbb{T}^{dN}} \left[\Theta_N F_N\right](\cdot,\underline{v}_N) e^{\beta'\|\underline{v}_N\|^2}\right) |v_N| e^{-\beta'|v_N|^2} \\ &\leq \int \mathrm{d}\omega \mathrm{d}\underline{v}_N \left(\sup_{\mathbb{T}^{dN}} \left[\Theta_N F_N\right](\cdot,\underline{v}_N) e^{\beta'\|\underline{v}_N\|^2}\right) \sqrt{N-1}\sqrt{\|\underline{v}_{N-1}\|^2}\; e^{-(\beta'-\beta)\|\underline{v}_N\|^2} \\ &\quad + \frac{N-1}{\sqrt{2e\beta'}} |\mathbb{S}_d| \cdot \|F_N\|_{\mathcal{F}^1_{\beta'}}.\end{aligned}$$

We get as in the proof of Proposition 9.4.1

$$\|C_{n+m-1}\Theta_{n+m}F_{n+m}\|_{\mathcal{F}^1_\beta} \leq \frac{\sqrt{n+m-1}}{e\sqrt{\beta'-\beta}}|\mathbb{S}_d|\cdot\|F_{n+m}\|_{\mathcal{F}^1_{\beta'}} + \frac{n+m-1}{\sqrt{2e\beta'}}|\mathbb{S}_d|\cdot\|F_{n+m}\|_{\mathcal{F}^1_{\beta'}},$$

and iterate with the same increment $\beta'-\beta = \delta\beta/(2m)$ to get

$$\|\mathfrak{C}^{(k)}_{n,m}(\underline{t}_m)F_{n+m}\|_{\mathcal{F}^1_{\beta_0-\delta\beta}} \leq \left(\frac{C(n+m)}{\sqrt{\delta\beta}}\right)^m \|F_{n+m}\|_{\mathcal{F}^1_{\beta_0}}, \tag{9.11}$$

concluding the first part of the proposition.

Large deviation argument. We enter now the key argument of this heuristic. Integrating over the condition $\underline{v}_n \notin A^{(n)}_\eta$ due to the operator $\mathcal{C}^\flat_{n+k}$, we will get smallness thanks to a large deviation argument, in the idea of using the associated bound for large values of n.

Recall the expression

$$\mathfrak{C}^{(k)}_{n,m}(\underline{t}_m) = \Theta_n(t-t_1)\mathcal{C}_n\ldots\mathcal{C}_{n+k-1}\;\Theta_{n+k}(t_k-t_{k+1})\mathcal{C}^\flat_{n+k}\;\Theta_{n+k+1}(t_{k+1}-t_{k+2})\mathcal{C}^\sharp_{n+k+1}\ldots\mathcal{C}^\sharp_{n+m-1},$$

of the pathological term. The **first step** is to bound the non-concentrated collision operators

$$\mathcal{C}^\sharp_{n+k+1}\ldots\mathcal{C}^\sharp_{n+m-1}.$$

Here, we do not expect smallness from an initial value, but from the concentrated condition in $\mathcal{C}^\flat_{n+k}$, so that for these collision operators we can as well harness the a priori $\mathcal{F}^\infty_\beta$ bounds, instead of an $\mathcal{F}^1_\beta$ one. In fact, we will need an $\mathcal{F}^\infty_\beta$ bound to compute the large deviation principle, as it is the $\mathbb{L}^\infty$-proximity of densities that yields proximity of the associated probabilities. Bounding crudely the indicator of non-concentration, we get as in the proof of Proposition 4.5.1 that

$$\|\Theta_{n+k+1}\mathcal{C}^\sharp_{n+k+1}\ldots\mathcal{C}^\sharp_{n+m-1}F_{n+m}\|_{\mathcal{F}^\infty_{\beta_0-\frac{\delta\beta}{3}}} \leq \left(C_{\beta_0}\frac{n+m}{\sqrt{\delta\beta}}\right)^{m-k-1}\|F_{n+m}\|_{\mathcal{F}^\infty_{\beta_0}}. \tag{9.12}$$

Note that we could have chosen to bound these operators as we did in Proposition 9.4.1, since they are non-concentrated.

The **second step** is precisely the large deviation argument. This latter requires $\mathcal{F}^\infty_\beta$-bounds, but only provides a control in $\mathcal{F}^1_\beta$.

We write for any positive functional $F_{n+k+1} \in \mathcal{F}^{\infty}_{\lambda'}$, for $\lambda < \lambda'$

$$\begin{aligned}
&\|C^{\flat}_{n+k} F_{n+k+1}\|_{\mathbb{L}^1_\lambda} \\
&\quad \leq \sum_{i=1}^{n+k} \int \mathrm{d}\omega \mathrm{d}\underline{v}_{n+k+1} |v_i - v_{n+k+1}| F_{n+k+1}(\underline{z}_{n+k}, x_i + \varepsilon\omega, v_{n+k+1}) e^{\lambda \|\underline{v}_{n+k}\|^2} \mathbb{1}_{\underline{v}_{n+k} \notin A^{(n+k)}_\eta} \\
&\qquad + \sum_{i=1}^{n+k} \int \mathrm{d}\omega \mathrm{d}\underline{v}_{n+k+1} |v_i - v_{n+k+1}| F_{n+k+1}(\underline{z}^\star_{n+k}, x_i + \varepsilon\omega, v^\star_{n+k+1}) e^{\lambda \|\underline{v}_{n+k}\|^2} \mathbb{1}_{\underline{v}_{n+k} \notin A^{(n+k)}_\eta}.
\end{aligned}$$

Ignoring once again (for the last time) the second collisional term, treated similarly with the same bounds, we compute the usual Cauchy–Schwarz inequality as in (4.25) with half of the exponential weight, and keep half of it for the later large deviation argument, writing

$$\begin{aligned}
&\|C^{\flat}_{n+k} F_{n+k+1}\|_{\mathbb{L}^1_\lambda} \\
&\leq \sum_{i=1}^{n+k} \int \mathrm{d}\omega \mathrm{d}\underline{v}_{n+k+1} |v_i - v_{n+k+1}| \cdot \|F_{n+k+1}\|_{\mathcal{F}^{\infty}_{\lambda'}} e^{-(\lambda'-\lambda)\|\underline{v}_{n+k}\|^2} e^{-\lambda'|v_{n+k+1}|^2} \mathbb{1}_{\underline{v}_{n+k} \notin A^{(n+k)}_\eta} \\
&\leq \|F_{n+k+1}\|_{\mathcal{F}^{\infty}_{\lambda'}} \int \mathrm{d}v_{n+k+1} e^{-\lambda'|v_{n+k+1}|^2} \int_{\overline{A}^{(n+k)}_\eta} \mathrm{d}\underline{v}_{n+k} \left[C\sqrt{\frac{n+k}{\lambda'-\lambda}} + (n+k)|v_{n+k+1}| \right] e^{-\frac{\lambda'-\lambda}{2}\|\underline{v}_{n+k}\|^2} \\
&\leq \|F_{n+k+1}\|_{\mathcal{F}^{\infty}_{\lambda'}} \tilde{C}_{\lambda'} \left(\sqrt{\frac{n+k}{\lambda'-\lambda}} + (n+k) \right) \int_{\overline{A}^{(n+k)}_\eta} \mathrm{d}\underline{v}_{n+k} e^{-\frac{\lambda'-\lambda}{2}\|\underline{v}_{n+k}\|^2},
\end{aligned}$$

integrating over v_{n+k+1}, which makes appear a constant $\tilde{C}_{\lambda'}$ depending continuously on the dimension and on λ'. Now that we have dominated the integral above using an $\mathbb{L}^\infty$-bound on F_{n+k+1}, to use our large deviation argument we will express it as a probability: the integrand is proportional to the joint density of independant and identical centered Gaussian distributions $(\hat{V}_i)_{1 \leqslant i \leqslant n+k}$ with variance $(\lambda' - \lambda)^{-1}$. Then, considering the non-concentration condition (9.7), let us observe that belonging or not to the set A^{n+k}_η of non-pathological velocities, depends on how many of the velocities' norms excess η. Hence, denoting E_{n+k} a binomial random variable of parameters $\left(n+k, \mathbb{P}\left[|\hat{V}_1| \geq \eta\right]\right)$, we have

$$\begin{aligned}
\sqrt{\frac{\lambda'-\lambda}{2\pi}} \int_{\overline{A}^{(n+k)}_\eta} \mathrm{d}\underline{v}_{n+k} e^{-\frac{\lambda'-\lambda}{2}\|\underline{v}_{n+k}\|^2} &= \mathbb{P}\left[\sharp\{1 \leq i \leq n+k \ , \ |\hat{V}_i| \geq \eta\} \leq p(n+k)\right] &(9.13)\\
&= \mathbb{P}\left[E_{n+k} \leq p(n+k)\right]. &(9.14)
\end{aligned}$$

This crucial step requires on its own an increment that does not depend on m, as it tunes the variance of our random variables: we opt for

$$\lambda' - \lambda = \frac{\delta\beta}{3}. \tag{9.15}$$

Henceforth, by the explicit large deviation principle for the binomial distribution (see for example the book by Tomas Dominguez and Jean-Christophe Mourrat [28, Exercise 2.22]), the probability that the velocities concentrate close to zero vanishes exponentially with $n+k$. More precisely, denoting

$$\begin{cases}
\overline{p}_{\eta,\delta\beta} \doteq \mathbb{P}\left[|\hat{V}_1| \geq \eta\right], \\
\delta_{\eta,p} \doteq \exp\left[-p\log\left(\dfrac{p}{\overline{p}_{\eta,\delta\beta}}\right) - (1-p)\log\left(\dfrac{1-p}{1-\overline{p}_{\eta,\delta\beta}}\right)\right],
\end{cases}$$

we have for any $N \in \mathbb{N}$ large enough that

$$\mathbb{P}\left[E_N \leq pN\right] \leq \delta_{\eta,p}^N. \tag{9.16}$$

With the initial given inverse temperature β_0, taking any velocity threshold η allows to choose a proportion $p < \overline{p}_{\eta,\delta\beta}$ such that $\delta_{\eta,p} < 1$, and vice versa. Eventually, it all boils down to the following bound

$$\|C_{n+k}^\flat F_{n+k+1}\|_{\mathcal{F}_\beta^1} \leq C_{\beta_0} \frac{n+k}{\delta\beta} \|F_{n+k+1}\|_{\mathcal{F}_{\beta'}^\infty} \, \delta_{\eta,p}^{n+k}. \tag{9.17}$$

The **last step** is to bound in $\mathcal{F}_\beta^1$-norms the remaining collision operators

$$\Theta_n(t-t_1)\mathcal{C}_n \dots \mathcal{C}_{n+k-1},$$

like in the first part of the proposition proved above (9.11), yielding eventually with the large deviation bound (9.12) the second and last estimate of this proposition. □

9.4.4 Time integration

Before computing the time integration, we prove the refined Stirling bound in the following lemma.

Lemma 9.4.2 (Stirling refinement)**.** *For any $c > 1$, there exists a absolute constant $C > 1$ such that for any $n, m \geq 1$,*

$$\frac{(n+m)^m}{m!} \leq C^m c^n. \tag{9.18}$$

Proof. Using Robbins–Stirling bounds, one has

$$\begin{aligned}
\frac{(n+m)^m}{m!} &\leq e^m \left(\frac{n+m}{m}\right)^m \\
&\leq e^m \exp\left[m \log\left(1+\frac{n}{m}\right)\right] &(9.19)\\
&\leq e^m \exp\left[m\left(C + c\frac{n}{m}\right)\right] &(9.20)\\
&\leq e^{m(1+C)} e^{cn},
\end{aligned}$$

using comparative growths of the affine function $[x \mapsto cx]$ and of the logarithm between ligns (9.19) and (9.20), which concludes the proof. □

From an analysis of the rate function (9.10) defining $\delta_{\eta,p}$, one can tune this rating parameter to be arbitrarily small, up to degrading the parameters η, p appearing in the other constants of this method. In this section, let us hence fix these parameters such that $\delta_{\eta,p} < 1$.

Proposition 9.4.3 (Estimates on the successive-collision operators)**.** *Let us consider any initial inverse temperature β_0, and inverse temperature increment $\delta\beta < \beta_0/2$. Then, the bound on the non-concentrated part of the successive-collision operator is completely freed from its dependency in n, namely*

$$\|Q_{n,m}^\sharp(t) F_{n+m}\|_{\mathcal{F}_{\beta_0-\delta\beta}^1} \leq \left(\frac{tC_{\beta_0}}{\delta\beta \cdot p\eta^2}\right)^m \|F_{n+m}\|_{\mathcal{F}_{\beta_0}^1}.$$

On the other hand, we still have at hand two different ways of bounding its concentrated part, which depends on n but at any prescribed exponential rate, up to increasing the exponential rate in m. More

precisely, for any $c > 1$, there exists a constant $C_\beta > 1$ depending on c and β_0, such that one can dominate by the $\mathcal{F}^1_{\beta_0}$-norm as

$$\|Q^\flat_{n,m}(t)F_{n+m}\|_{\mathcal{F}^1_{\beta_0-\delta\beta}} \leq c^n \left(\frac{C_{\beta_0}t}{\sqrt{\delta\beta}}\right)^m \|F_{n+m}\|_{\mathcal{F}^1_{\beta_0}},$$

or by the $\mathcal{F}^\infty_{\beta_0}$-norm, through a large deviation argument, as

$$\|Q^\flat_{n,m}(t)F_{n+m}\|_{\mathcal{F}^1_{\beta_0-\delta\beta}} \leq \frac{(c\delta_{\eta,p})^n}{\sqrt{\delta\beta}} \left(\frac{\tilde{C}_{\beta_0}t}{\sqrt{\delta\beta}}\right)^m \|F_{n+m}\|_{\mathcal{F}^\infty_{\beta_0}}.$$

Proof. Recalling the definition of the time ensemble (4.6) on which we integrate, and harnessing Proposition 9.4.1, we have

$$\begin{aligned}\|Q^\sharp_{n,m}(t)F_{n+m}\|_{\mathcal{F}^1_{\beta_0-\delta\beta}} &\leq \int_{T_m(t)} \mathrm{d}\underline{t}_m \left(\frac{C_{d,\beta_0}m}{\delta\beta\cdot p\eta^2}\right)^m \|F_{n+m}\|_{\mathcal{F}^1_{\beta_0}} \\ &\leq \frac{t^m}{m!}\left(\frac{C_{d,\beta_0}m}{\delta\beta\cdot p\eta^2}\right)^m \|F_{n+m}\|_{\mathcal{F}^1_{\beta_0}} \\ &\leq \left(\frac{t\tilde{C}_{d,\beta_0}}{\delta\beta\cdot p\eta^2}\right)^m \|F_{n+m}\|_{\mathcal{F}^1_{\beta_0}},\end{aligned}$$

using at the last line the fact that $m^m \leq e^m m!$, proving the first estimate of the proposition.

Now, it is time to apply the optimized Stirling estimate stated in Lemma 9.4.2, with the idea of having a controlled bad constant c^n. We compute as before, applying Proposition 9.4.2 to the succession of collision operators appearing in the concentrated part of the decomposition (9.8),

$$\begin{aligned}\|Q^\flat_{n,m}(t)F_{n+m}\|_{\mathcal{F}^1_{\beta_0-\delta\beta}} &\leq m\frac{t^m}{m!}\left(\frac{C(n+m)}{\sqrt{\delta\beta}}\right)^m \|F_{n+m}\|_{\mathcal{F}^1_{\beta_0}} \\ &\leq c^n \left(\frac{\tilde{C}t}{\sqrt{\delta\beta}}\right)^m \|F_{n+m}\|_{\mathcal{F}^1_{\beta_0}},\end{aligned}$$

applying the said lemma at the last line. Similarly, we observe that given that $\delta_{\eta,p} < 1$, the worst term among the values of k for the large deviation decay is the one of order n, so that as before, using the second part of Proposition 9.4.2, we get

$$\begin{aligned}\|Q^\flat_{n,m}(t)F_{n+m}\|_{\mathcal{F}^1_{\beta_0-\delta\beta}} &\leq m\frac{t^m}{m!}\cdot\frac{\delta^n_{\eta,p}}{\sqrt{\delta\beta}}\left(C_{\beta_0}\frac{n+m}{\sqrt{\delta\beta}}\right)^m \|F_{n+m}\|_{\mathcal{F}^\infty_{\beta_0}} \\ &\leq \frac{(c\delta_{\eta,p})^n}{\sqrt{\delta\beta}}\left(\frac{\tilde{C}_{\beta_0}t}{\sqrt{\delta\beta}}\right)^m \|F_{n+m}\|_{\mathcal{F}^\infty_{\beta_0}}.\end{aligned}$$

This concludes the proof of Proposition 9.4.3. □

At fixed $\varepsilon > 0$, one can choose to use either one of the two last bounds of Proposition 9.4.3 on the concentrated term, according to the value of n: if it is large enough one can use the large deviation principle to justify that the pathological concentration of velocities is rare, and otherwise the fact that n is not that large allows a good control of the term in c^n.

In practice, let us set two different thresholds for this disjunction, then verify that they are compatible. On the one hand, if for $\gamma \in (0,1)$ we assume

$$n \leq -\frac{\gamma\log\varepsilon}{\log c},$$

then we have $c^n \leq \varepsilon^{-\gamma}$, and consequently

$$\|Q^\flat_{n,m}(t)F_{n+m}\|_{\mathcal{F}^1_{\beta_0-\delta\beta}} \leq \varepsilon^{-\gamma}\left(\frac{\tilde{C}t}{\sqrt{\delta\beta}}\right)^m \|F_{n+m}\|_{\mathcal{F}^1_{\beta_0}},$$

expecting the initial closeness in $\mathcal{F}^1_{\beta_0}$ to compensate the term in $\varepsilon^{-\gamma}$. On the other hand, if

$$n \geq \frac{\log\varepsilon}{\log(c\delta_{\eta,p})},$$

then we get $(c\delta_{\eta,p})^n \leq \varepsilon$, so that

$$\|Q^\flat_{n,m}(t)F_{n+m}\|_{\mathcal{F}^1_{\beta_0-\delta\beta}} \leq \frac{\varepsilon}{\sqrt{\delta\beta}}\left(\frac{\tilde{C}_{\beta_0}t}{\sqrt{\delta\beta}}\right)^m \|F_{n+m}\|_{\mathcal{F}^\infty_{\beta_0}}.$$

Now, for both conditions to cover all possible values of n, we need that

$$\frac{\log\varepsilon}{\log(c\delta_{\eta,p})} \leq -\frac{\alpha\log\varepsilon}{\log c}, \quad \text{i.e.} \quad c^{1+\frac{1}{\alpha}}\delta_{\eta,p} \leq 1, \tag{9.21}$$

which is true up to choosing c small enough, hence increasing the constant rating the exponential growth in m, yet this constant only rescales linearly the long time interval on which we compute our study.

9.4.5 Deriving long time results, a different pruning

We finally explain in this section how a pruning method constructed on the decomposition of the successive-collision operators into concentrated and non-concentrated parts can lead to long time results on the convergence of the marginals F^ε_n, freed from the pathological constant n^{cn} appearing in Theorem 1. In fact, our study initially works for high marginals, yet we show in the end how to retrieve information on the low ones.

Indeed, we have now the whole toolbox to perform our long time derivation in $\mathcal{F}^1_{\beta_0}$. We perform a tree pruning like we did in (4.28), yielding at the first step

$$F^\varepsilon_n(t) = \sum_{j_1\leqslant 2} Q^\sharp_{n,j_1}(h_1)F^\varepsilon_{N_1}(t-h_1) + \sum_{j_1\leqslant 2} Q^\flat_{n,j_1}(h_1)F^\varepsilon_{N_1}(t-h_1) + \sum_{j_1>2} Q_{n,j_1}(h_1)F^\varepsilon_{N_1}(t-h_1)$$

yet here we are going to stop the pathological concentrated term as well, putting it aside in another remainder, eventually writing

$$F^\varepsilon_n(t) = \sum_{(j_i\leqslant 2^i)_{1\leqslant i\leqslant K}} Q^\sharp_{n,j_1}(h_1)\dots Q^\sharp_{N_{K-1},j_K}(h_K)F^\varepsilon_{N_K}(0) + R^{\flat,[K]}_n(t) + \tilde{R}^{[K]}_n(t),$$

with the following new remainders, using the same notation for the time steps (4.26),

$$R^{\flat,[K]}_n(t) \doteq \sum_{k=1}^K \sum_{(j_i\leqslant 2^i)_{i\leqslant k}} Q^\sharp_{n,j_1}(h_1)\dots Q^\sharp_{N_{k-2},j_{k-1}}(h_{k-1})Q^\flat_{N_{k-1},j_k}(h_k)F^\varepsilon_{N_k}(t^{\mathrm{p}}_k), \tag{9.22}$$

and

$$\tilde{R}^{[K]}_n(t) \doteq \sum_{k=1}^K \sum_{(j_i\leqslant 2^i)_{i\leqslant k}} Q^\sharp_{n,j_1}(h_1)\dots Q^\sharp_{N_{k-2},j_{k-1}}(h_{k-1}) \sum_{j_k>2^k} Q_{N_{k-1},j_k}(h_k)F^\varepsilon_{N_k}(t^{\mathrm{p}}_k).$$

The optimized study of the latter pruned-out term would require further adjustments to get an optimal bound, that we do not compute here. Nevertheless, we detail here the very good estimates that we obtain on the main term (Proposition 9.4.4) and on the pathological concentrated remainder (Proposition 9.4.5). The latter is more powerful for marginals of high order, so that in the end we justify how to retrieve information on the lower ones, keeping reasonable bounds.

Proposition 9.4.4 (Estimate on the main part)**.** *With our initial proximity assumption (9.5), and the a priori bounds (9.6), the main term of the expansion above is bounded for ε small enough by*

$$\left\| \sum_{(j_i \leqslant 2^i)_{1\leqslant i\leqslant K}} Q^\sharp_{n,j_1}(h_1)\dots Q^\sharp_{N_{K-1},j_K}(h_K) F^\varepsilon_{N_K}(0) \right\|_{\mathcal{F}^1_{\beta_0/2}} \leq C_0^n C^{A^K} \varepsilon^{\frac{d-1}{4(d+1)}},$$

for any $A > 2$, as soon as K is large enough. The factor C^{nK}, which led to the bad factor n^{cn} in Theorem 1, thus disappeared.

Proof. Harnessing the initial proximity hypothesis (9.5) for $F^\varepsilon_{N_K}(0)$, we write

$$\|Q^\sharp_{n,j_1}(h_1)\dots Q^\sharp_{N_{K-1},j_K}(h_K) F^\varepsilon_{N_K}(0)\|_{\mathcal{F}^1_{\beta_0/2}} \leq C_0^n K^{j_1+\dots+j_K} (CC_0h_1)^{j_1}\dots(CC_0h_K)^{j_K}\varepsilon,$$

using the bounds of the first part of Proposition 9.4.3, with uniform increments

$$\delta\beta = \frac{\beta_0}{2K}.$$

We observe that $j_1 + \dots + j_K \leq 2^{K+1}$. Note that like in the proof of Proposition 4.7.1, we can asymptotically bound the appearing factor

$$K^{2^{K+1}} \leq e^{A^K},$$

for any $A > 2$. This bound is thus similar to the one in the said proof, but without the factor C^{nK}, which was previously leading to the bad factor n^{cn} in the convergence rate of Theorem 1. Apart from this, the new bound behaves as well as previously, yielding similar estimates as in the conclusion of Section 4.8, the power of ε stemming from the bound (4.49), performing the same truncations to guarantee the proximity of pseudo-trajectories. □

Proposition 9.4.5 (Estimates of the pathological concentrated terms)**.** *For any inverse temperature β_0, the remainder due to the exclusion of the concentrated terms might be estimated by*

$$\|R_n^{\flat,[K]}(t)\|_{\mathcal{F}^1_{\beta_0/2}} \leq C_0^n e^{A^K} (c\delta_{\eta,p})^n,$$

for any $A > 2$, as soon as K is large enough.

Proof. Each term of the sum defining the remainder (9.22) is of the form

$$Q^\sharp_{n,j_1}(h_1)\dots Q^\sharp_{N_{k-2},j_{k-1}}(h_{k-1}) Q^\flat_{N_{k-1},j_k}(h_k) F^\varepsilon_{N_k}(t_k^{\mathrm{p}}),$$

stopped at an intermediate time at which we will apply the a priori bounds (9.6) in $\mathcal{F}^\infty_{\beta_0}$. The key computation is to distribute correctly the temperature increment $\delta\beta$. Making it uniform on all the successive-collision operators above would alter the parameter $\delta_{\eta,p}$, that intrisically depends on $\delta\beta$ through its definition (9.10), disrupting the estimate. The solution is to split it in two, taking a fixed increment

$$\delta\beta = \frac{\beta_0}{4}$$

for the concentrated step, then splitting the remaining increment uniformly into steps of size

$$\delta\beta = \frac{\beta_0}{4k},$$

for the non-concentrated collision operators, eventually leading to the following bound, harnessing the results of Proposition 9.4.3,

$$\begin{aligned}\|Q^\sharp_{n,j_1}(h_1)\dots Q^\sharp_{N_{k-2},j_{k-1}}(h_{k-1})Q^\flat_{N_{k-1},j_k}(h_k)F^\varepsilon_{N_k}(t^{\mathrm{p}}_k)\|_{\mathcal{F}^1_{\beta_0/2}}&\\ \leq K^{2^{K+1}}(Ch_1)^{j_1}\dots(Ch_{k-1})^{j_{k-1}}(Ch_k)^{j_k}(c\delta_{\eta,p})^{N_{k-1}}C_0^{N_k}&\\ \leq K^{2^{K+1}}(CC_0h_1)^{j_1}\dots(CC_0h_k)^{j_k}(c\delta_{\eta,p})^{n}C_0^{n}.&\end{aligned}$$

We bound as in the beginning of this section the first factor, and conclude similarly as for the estimates of Chapter 4, completing the proof. □

To conclude, observe now that this method works for large values of n, since it relies on the smallness of $(c\delta_{\eta,p})^n$. Nevertheless, the lower marginals can be retrieved from the high orders, since the latter contain more information, though it means that the quantitative bound is still weighted by a factor C_0^n, with n large.

We will place ourself in the simpler framework of a convergence rate in ε, that absorbs the term e^{A^K} in the good scaling. In reality, should anyone write this heuristics exhaustively, one would need to replace it with something more close to the convergence rate given in Proposition 4.6.1 for the pruned-out remainder, yet the idea rem ains the same.

Indeed, let us consider the canonical framework, so that the following formula is true for any integers $0 \leqslant k \leqslant n$

$$F_k(\underline{z}_k) = \int \mathrm{d}\underline{z}^*_{n-k} F_n(\underline{z}_k, \underline{z}^*_{n-k}),$$

so that the optimal convergence rate would be

$$\begin{aligned}\|F_k - F_k^{\lim}\|_{\mathbb{L}^1} &\leq \|F_n - F_n^{\lim}\|_{\mathbb{L}^1}\\ &\leq C_0^n\varepsilon^\alpha,\end{aligned}$$

with the following condition imposed by our large deviation heuristics

$$(c\delta_{\eta,p})^n \leq \varepsilon^\alpha.$$

Thus, we need to exploit a value of n that satisfies simultaneously the condition above and such that

$$C_0{}^n \leq \varepsilon^{-\gamma},$$

for some $0 < \gamma < \alpha < 1$, eventually leading to a convergence rate in $\varepsilon^{\alpha-\gamma}$. For some n to exist in this range, it requires

$$\alpha \log C_0 \leqslant \gamma |\log(c\delta_{\eta,p})|$$

which is satisfied up to considering $(c\delta_{\eta,p})$ small enough, which can be done playing with the parameters η, p in the definition (9.10), and also in part by making the constant c closer to 1, thus making the constant C from the Stirling Lemma 9.4.2 bigger, and downgrading the dependency in η and p of the bounds on the non-concentrated term, yet that only rescale linearly the large time horizon.

That concludes this heuristical section, dedicated to harness a large deviation argument to get rid of the bad dependency in n of the bounds of Theorem 1, at least for the main term of the expansion, by displacing the loss of control on the number of collisions to a loss of control on the temperature.

Chapter 10

Perspectives

We present in this small last chapter some perspectives to generalize the results studied in the present thesis, or their adaptation to different models, exposing some prospective ideas that may pave the way to the continuation of this work.

10.1 Long-time bounds on the cumulants

The main perspective, after this thesis, is to derive the asymptotic fluctuation and large deviation results in large times using the closeness to equilibrium of the system, and the linearity of the limit equations. We present here some prospective ideas implying pruning methods, fine combinatorial analysis of the trajectories, or coarser cumulants.

10.1.1 Pruning methods

A first idea stems from the observation that in the bound of the cumulants shown in Proposition 6.5.1, the leading term corresponds to the decomposition of the initial cluster cumulants along the trivial partition $\rho = [\![1, n]\!]$. This initial trivial cumulant is none other than the correlation function F_n^ε, for which we have a priori bounds, proved in Section 4.4.

This leading term is hence fit for a pruning process as the one computed in Chapter 4 to derive in long time the limit of the correlation functions.

This method would hence require to deal, on large times, with the negligible terms corresponding with the decompositions in other non-trivial partitions, putting them aside and proving that their influence remains negligible. The three main difficulties are the following one.

First, it demands a precise control of the stacking factors appearing in large times, as discussed in Section 9.2 on the pruning methods, yet it should be made easier thanks to the explicit and detailed calculus of Sections 6.4 and 6.5 on the cumulants and their bounds.

Secondly, we study in this thesis the evolution of the cumulants f_n^ε, which correspond to the cluster cumulants $f_n^{\varepsilon,\rho}$ associated to the partition $\rho = \{\{1\}, \dots, \{n\}\}$. We should extend this study to the equations describing the evolution of all the generalized cluster cumulants, but they should formally behave similarly.

Finally, the main obstacle is the fact that the initial cumulants are shown in (6.23) to be decreasing with the size of the cumulants as $\varepsilon^{d(|\rho|-1)}$. Nevertheless, in the case of the fully decomposed cumulants that we study (with $|\rho| = n$ as discussed in the paragraph above), their size at time t is proved in Proposition 6.5.1 to be bounded by $\varepsilon^{(d-1)(n-1)}$. Even their difference to the limit cumulants (Proposition 6.6.3) is always tuned by an additional factor ε, and not by a factor decreasing with n as ε^n. The optimality of this bound is in particular discussed in Section 10.2.1. In any case, this

downgrading bound makes harder to use this pruning method and to justify that the non-trivial decompositions remain negligible in large times.

10.1.2 Deng–Hani–Ma method

The work of Deng, Hani and Ma [24] introduced very fine new methods to deal with the geometric dynamics of the dilute gases, and specifically with pathological trajectories, leading to a long-time derivation of the Boltzmann equation, assuming uniform bounds on its regular solutions.

More precisely, combining the usual geometric study of the billiards dynamics with combinatorial results like the Burago lemma [18], and computing in a very subtle way a combinatorial algorithm of integration of the variables driving the dynamics, they succeed in discarding pathological trajectories, which are correlated between several time layers. That eventually allows them to compare the solution of the Boltzmann equation with a well-chosen ansatz close to the original dynamics [14].

Although their study remains based on uniform bounds for the limit Boltzmann equation, which are still an open problem, using their method in a linear framework would be perfectly adapted, since these uniform bounds are true in the linear case. Indeed, adapting their fine analysis of the dynamics to the study of the cumulants and correlation functions of the Rayleigh gas, it should lead to extending on large times the statistical description presented in this thesis. This would allow to catch more precisely the nature of the correlations of the system. Their method still remains particularly technical and computational.

10.1.3 Coarser cumulants

Finally, the coarser cumulants described in Section 6.2.2 have all the good properties for their limit to be described in large times, with a priori bounds directly stemming from the ones on F_n^ε. It could be interesting to try to link them to some statistical quantities, possibly of a simplified ideal Rayleigh gas model. Indeed, as they allow to describe a single tagged particle in a gas, one could imagine a model of non-interacting copies of this particle in a gas, getting rid of the correlations that are difficult to deal with. This way, one could expect the large deviations of the empirical measure of such independent copies to be driven by those linearized coarser cumulants, whose study could be performed on long times.

Possibly, because of the rigid structure of these coarser cumulants as tensorized against the equilibrium, one could also imagine to relax it by considering coarser cumulants against a more general ansatz, for example

$$\check{F}_n^\varepsilon(t, \underline{z}_n) \doteq F_n^\varepsilon(t, \underline{z}_n, \underline{0}_n)$$

the correlation functions of the non-tagged particles, which are close to equilibrium. This would lead to the cumulants

$$\overline{f}_n^\varepsilon = \sum_{\substack{\sigma \in \mathcal{P}_n \\ 1 \in \sigma_1}} (-1)^{|\sigma|+1} (|\sigma|-1)! F_{\sigma_1}^\varepsilon \prod_{i=2}^{|\sigma|} \check{F}_{\sigma_i}^\varepsilon, \tag{10.1}$$

with the inverting formula

$$F_n^\varepsilon = \sum_{\substack{\sigma \in \mathcal{P}_n \\ 1 \in \sigma_1}} \overline{f}_{\sigma_1}^\varepsilon \prod_{i=2} \check{f}_{\sigma_i}^\varepsilon, \tag{10.2}$$

the functions $\check{f}_{\sigma_i}^\varepsilon$ being the cumulants of the $(\check{F}_n^\varepsilon)$.

This model could be the key to refine statistically the ideal Rayleigh gas, or other simplified versions of our study, possibly then deducing some information on the nonideal Rayleigh gas.

10.2 Complementary prospective results

10.2.1 Small data

In the details of the proof of Proposition 6.5.1 on the bound on the cumulants, the dependency in the initial data C_0 is explicit. In similar studies, it is well-known that the small Lanford time of derivation depends on this initial bound. For initial data arbitrarily small, close to vaccum, this time can be arbitrarily large. This phenomenon has first been exhibited by Reinhard Illner and Mario Pulvirenti in [53, 42], after they found an alternative method in dimension 2 to prove arbitrarily large time derivation for a *fixed* initial data small enough, harnessing the dispersion of particles in the case of particles evolving in the full space $\mathbb{R}^2$ [41].

Knowing that the limit function, solution to a linear equation, is well-posed for large times, one could want to apply this result to the difference between the correlation function and its limit, which is indeed small enough initially (at least of order ε, thanks to Proposition 4.3.1), to derive long time results in the general case. Nevertheless, the method used by Illner and Pulvirenti requires a degrowth of the initial data in $F_n^\varepsilon(0)$ in z_0^n, with z_0 small enough.

Actually, the optimality of our bound in ε is a consequence of the study of the canonical partition function that we performed in Section 5.5. It is easier to see in the canonical setting, where the initial bound comes from the estimate [9, Appendix A]

$$1 \leq \frac{\mathcal{Z}_n^{\varepsilon,c}}{\mathcal{Z}_{n+p}^{\varepsilon,c}} \leq (1 - C_d\varepsilon)^{-p}.$$

The computation of Section 5.5 yields the lower bound

$$\begin{aligned}\frac{\mathcal{Z}_n^{\varepsilon,c}}{\mathcal{Z}_{n+p}^{\varepsilon,c}} &\geq \prod_{i=n}^{n+p-1} (1 - \tilde{C}_d i\varepsilon^d) \\ &\geq \left(1 - \frac{\tilde{C}_d}{2}\varepsilon\right)^p\end{aligned}$$

for example for n big enough compared to ε, using the low density limit $(n+p)\varepsilon^{d-1} = 1$. Hence, this asymptotic bound on which depends the initial proximity is optimal.

Nevertheless, the initial cumulants have such initial bounds, which one could want to harness to derive long time results. This will not work directly because of the more complex structure of the equation on the cumulants (6.5), yet using alternative forms of the cumulants, such as the coarser ones presented in Section 10.1.3, could lead to interesting results.

Eventually, adding dispersion methods like the one by Illner and Pulivirenti could also help the long-time derivations of the cumulants in the whole space $\mathbb{R}^d$.

10.2.2 Rescaled limit cumulants

In our study, the cumulants of the tagged particles are rescaled in the cumulant generating function such that they make appear the moments of the empirical measure of the tagged particles. Doing so, since their size depends on the particles' diameter and dynamics, which are tuned by the Boltzmann-Grad scaling, all the cumulants above the first one vanish in their generating function (see Section 6.6.4).

Nevertheless, to better understand the dynamics of the tagged particles, one could get interested in a differently rescaled generating function, that would not correspond to the statistical description of the empirical measure, but would capture all the fine limit information about the cumulants. We already computed the limits of the cumulants rescaled as such, and their generating function should be driven by a linearized version of the Hamilton–Jacobi system similar to the one presented in [55].

Understanding precisely the limit behaviour of this functional and its derivatives (which make appear the cumulants), one could expect to comprehend better the loss of information in the correlation functions that lead to a limit irreversible system, through the vanishing of the cumulants. This would be part of the more general problem of reversibility and of understanding the generation of chaos, which still has a lot of opportunities to explore.

10.2.3 Conclusion

In this thesis, we introduced a new mixture model for the nonideal Rayleigh gas, based on tags on the particles. Through an analysis of its combinatorial properties, we explored its asymptotic behaviour, described in a mixed Rayleigh–Boltzmann mesoscopic scaling: this has been the occasion to question the long time behaviour of such systems, for which we improved and precised the convergence rates of correlation functions.

To refine this description, thanks to the mixture structure, we introduced the empirical measure of tagged particles, and derived the limit of its fluctuations and large deviations, yet only on short times because of the complexity appearing in the study of the cumulants. Despite this limitation, our study allowed to explore the over-diluted regime and to emphasize there the absence of phase transition in the small statistical scales.

The main perspective for later studies continuating this work would be to derive the results on the cumulants on large times, to extend the latter statistical refinements. To that end we proposed some potential solutions, trying to better apprehend the hindrances on the way.

Finally, this study was also the opportunity to explore the behaviour of various linear versions of the Boltzmann equation, along with their functional frameworks. Eventually, we have been able to precise the geometrical study of the particles' dynamics to improve the quantitative control of the pathological cycling trajectories, finally obtaining a full convergence rate for the cumulants in short times.

Thank you for reading! Merci pour votre lecture !

Notation index

t	Time horizon	2.1
ε	Particles' diameter	2.1
$\underline{z}_N = (\underline{x}_N, \underline{v}_N) \in \mathcal{D}^N$	Particles' state vector	2.1
$\mathcal{X}_N^\varepsilon, \mathcal{D}_N^\varepsilon$	Hard sphere domains (in position space, in phase space)	(2.1)
${v_i}', {v_j}', {v_i}^\star, {v_j}^\star$	Post-collisional, pre-collisional velocities	(2.2)
ω, σ	Scattering angles	(2.3)
$M_\beta(x,v)$	Maxwellian equilibrium	(2.11)
$W_N^\varepsilon(t, \underline{z}_n, \underline{\ell}_n)$	Canonical particles' density in phase space	2.3
φ, φ_0	Solution to Rayleigh–Boltzmann equation, initial perturbation	(2.13)
λ, μ	Chemical potentials (tagged particles, equilibrium particles)	$(S_{\varepsilon,\mu,\lambda})$
$p_\mu = \lambda\mu^{-1}$	Tagged particle ratio	4.2
$\underline{\ell}_n \in \Lambda_n,\ \lvert\underline{\ell}_n\rvert$	Tags' vector, its cardinality	2.4, 4.2
$\varphi_0^{\otimes \underline{\ell}_n}(\underline{z}_{\underline{\ell}_n})$	Initial perturbation of tagged particles	2.4
$F_n^\varepsilon(t, \underline{z}_n, \underline{\ell}_n)$	Correlation functions	2.4
$\mathcal{Z}_\mu$	Grand canonical partition function	(2.17)
$H_n, H^{\otimes n}$	Smooth observables	2.4
$\mathcal{C}_n^\ell$	Collision operators	(2.26)
$\pi_t^\varepsilon[H], \tilde{\pi}_t^\varepsilon[H]$	Empirical measure (non-tagged one, tagged one)	(2.20)(2.21)
$Q_{n,\underline{\ell}_k^*}(t), Q^{\lim}_{n,\underline{0}_k}(t)$	Successive-collision operators, limit versions	(4.5)(4.12)
$T_k(t)$	Set of ordered times	(4.6)
$\mathcal{M}_{n,k}$	Set of admissible ordered added particles	4.2
$\chi_k \doteq (\underline{m}_k, \underline{\ell}_k^*, \underline{s}_k) \in \mathcal{H}_{n,k}$	History vector of a pseudo-trajectory	(4.7)
$\underline{z}_n^{[t]}, \underline{\zeta}_n^{[t]}$	Pseudo-trajectory at time t, limit version	(4.8)(4.13)
$G_n = M_\beta^{\otimes n}\varphi^{\otimes \underline{\ell}_n}$	Limit correlation function	4.2
$\lVert f_k\rVert_{k,\beta}$, $\mathcal{F}_{k,\beta}$	Sub-Gaussian norm and space	(4.14)
C_0	Initial density bound	(4.15)
K	Tree pruning parameter	4.6
$\underline{h}_K, t_k^{\mathrm{p}}$	Time cutting intervals and steps	(4.26)
$R_n^{[K]}(t)$	Pruned-out term	(4.29)
$\widehat{G}_n = G_n - R_n^{[K],\lim}$	Pruned limit correlation function	4.6
$\mathbf{V}, \delta$	Truncation parameters, in velocities and time separation	4.8
$\mathrm{Traj}([0,t], \mathcal{M}(\mathcal{D}))$	Set of trajectories on $\mathcal{M}(\mathcal{D})$	7.1
ζ_t^ε	Fluctuation field of the tagged empirical measure	(2.23)
$\{h, \mathfrak{m}\}_t$	Filtered mean of the observable h against measure $\mathfrak{m}$	(7.2)
$\mathcal{H}(q,p)$	Hamiltonian governing the limit cumulants	(7.3)
$\mathcal{I}(t,h), \mathbf{\Lambda}(t,\mathfrak{v})$	Limit cumulant generating function, its Legendre transform	(6.31)
$\mathfrak{G}_\varepsilon^{[t]}[H]$	Cumulant generating function	(6.2)
$G_{[\sigma]} = \prod_{i=1}^{\lvert\sigma\rvert} G_{\lvert\sigma_i\rvert}$	Decomposition of G_n along the partition $\sigma \in \mathcal{P}_n$	(5.1)
f_n^ε, f_n	Cumulants of the correlation functions, limit version	(5.1)

ϕ_n	Cumulants of the exclusion condition $\mathbb{1}_{\mathcal{X}_n^\varepsilon}$	(5.1)
$\Psi_n = (k, \chi_k, \underline{t}_k, \underline{\omega}_k, \underline{v}_k^*)$	Pseudo-trajectory parametrizing vector	6.3.1
$\mathrm{d}\nu_{[t]}(\Psi_n)$	Pseudo-trajectory measure	(6.6)
$\mathrm{d}\nu_{[0,t]}^{[H]}(\Psi_n)$	Pseudo-trajectory H-weighted measure	(6.12)
$F_n^\varepsilon[H](t, \underline{z}_n, \underline{\ell}_n)$	H-weighted correlation function	(6.8)
$f_n^\varepsilon[H](t, \underline{z}_n, \underline{\ell}_n)$	Cumulants of the H-weighted correlation functions	(6.14)
$P(A)$	Particles stemming from A	6.3.2
$\mathbb{1}_{A \not\sim A'}$	Indicator of non-interaction	6.3.2
$\mathrm{agg}(A)$	Indicator of aggregation	6.3.2
$\aleph_{\lvert\rho\rvert}$, Γ_p	Set of clusters, set of particles	6.3.3
$\phi_{S,k+l}$	Cumulants of the cluster exclusion	6.3.3
$\mathcal{C}_A$	Connected graphs on A	6.3.3
$T_A^{\mathrm{c}} = T^{\mathrm{c}}(\underline{z}_{\Psi_A}^{[0,t]}), \tau_i^{\mathrm{c}}, \omega_i^{\mathrm{c}}$	Recollision tree, recollision times and angles	6.4
$\mathfrak{S}_{(p_e,q_e)_\Upsilon}[A]$	Indicator of clustering compatibility	6.4
$\overline{x}_A$	Barycenter of the positions $\underline{x}_A$	6.4
$T_R^{\mathrm{ov}} = T^{\mathrm{ov}}(\underline{z}_{\Psi_R}^{[0,t]}), \tau_i^{\mathrm{ov}}, \omega_i^{\mathrm{ov}}$	Overlap tree, overlap times and angles	6.4
$\mathcal{C}_{\lvert\kappa\rvert}(\Upsilon)$	Connected graphs containing the tree Υ	6.4
$\phi_R = \phi_R^{[\mathrm{tree}]} + \phi_R^{[\mathrm{cycle}]}$	Decomposition of the cumulants in tree and cycle part	6.4
$T_R^\star, \tau_i^\star, \omega_i^\star$	Clustering tree, clustering times and angles	6.4
$\mathfrak{CC}^\star(\Upsilon)$	Set of decorated connected components	6.4
T_R^{d}	Dynamics tree	6.4
$f_n^\varepsilon[H]^{[\mathrm{tree}]}(t), f_n^\varepsilon[H]^{[\mathrm{cycle}]}(t)$	Decomposition of the cumulant in tree and cycle part	(6.20)
$I_n^{[\rho]}[H](t, \underline{\ell}_n)$	ρ-contribution to the tree cumulant integral	(6.20)
$\mathbb{B}_{T,\beta}$	Functional space of the large deviation observables	6.32
$\mathcal{B}_{R,\beta}$	$\mathcal{F}_{1,\beta/4}$-ball of radius R	6.6.5
$\mathcal{J}(t, \theta, \gamma)$	Limit cumulant generating function in different variables	6.6.5
$\hat{\mathcal{J}}(t, \theta, \gamma)$	Hamiltonian solution	6.6.5
$\lVert\!\lVert\mathcal{J}(t)\rVert\!\rVert_{R,\beta}$	Norm on the functionals above, used to identify them	6.6.5
$\mathcal{S}_\lambda$	Random set of tagged particles	7.2
$\mathcal{F}_\beta^1, \mathcal{F}_\beta^\infty$	Weighted functional spaces	9.4.1

Bibliography

[1] R. K. Alexander. *The infinite hard-sphere system*. ProQuest LLC, Ann Arbor, MI, 1975. Thesis (Ph.D.)–University of California, Berkeley.

[2] G. Allaire, X. Blanc, B. Després, and F. Golse. *Transport et diffusion*. Éditions de l'École polytechnique, 2018.

[3] I. Ampatzoglou, J. K. Miller, and N. Pavlović. A rigorous derivation of a Boltzmann system for a mixture of hard-sphere gases. *SIAM J. Math. Anal.*, 54(2):2320–2372, 2022.

[4] N. Ayi. From Newton's law to the linear Boltzmann equation without cut-off. *Comm. Math. Phys.*, 350(3):1219–1274, 2017.

[5] B. Aylaj, N. Bellomo, L. Gibelli, and D. Knopoff. *Crowd dynamics by kinetic theory modeling—complexity, modeling, simulations, and safety*, volume 36 of *Synthesis Lectures on Mathematics and Statistics*. Springer, Cham, 2022. Reprint of the 2021 original.

[6] C. Bardos, F. Golse, and D. Levermore. Fluid dynamic limits of kinetic equations. I. Formal derivations. *J. Statist. Phys.*, 63(1-2):323–344, 1991.

[7] C. Bardos, F. Golse, and D. Levermore. Fluid dynamic limits of kinetic equations. II. Convergence proofs for the Boltzmann equation. *Comm. Pure Appl. Math.*, 46(5):667–753, 1993.

[8] P. Billingsley. *Probability and measure*. Wiley Series in Probability and Mathematical Statistics. John Wiley & Sons, New York-Chichester-Brisbane, 1979.

[9] T. Bodineau, I. Gallagher, and L. Saint-Raymond. The Brownian motion as the limit of a deterministic system of hard-spheres. *Invent. Math.*, 203(2):493–553, 2016.

[10] T. Bodineau, I. Gallagher, L. Saint-Raymond, and S. Simonella. One-sided convergence in the Boltzmann-Grad limit. *Ann. Fac. Sci. Toulouse Math. (6)*, 27(5):985–1022, 2018.

[11] T. Bodineau, I. Gallagher, L. Saint-Raymond, and S. Simonella. Long-time correlations for a hard-sphere gas at equilibrium. *Comm. Pure Appl. Math.*, 76(12):3852–3911, 2023.

[12] T. Bodineau, I. Gallagher, L. Saint-Raymond, and S. Simonella. Statistical dynamics of a hard sphere gas: fluctuating Boltzmann equation and large deviations. *Ann. of Math. (2)*, 198(3):1047–1201, 2023.

[13] T. Bodineau, I. Gallagher, L. Saint-Raymond, and S. Simonella. Long-time derivation at equilibrium of the fluctuating Boltzmann equation. *Ann. Probab.*, 52(1):217–295, 2024.

[14] T. Bodineau, I. Gallagher, L. Saint-Raymond, and S. Simonella. Derivation of the Boltzmann equation from hard-sphere dynamics (after Y. Deng, Z. Hani, and X. Ma), 2026.

[15] L. Boltzmann. *Lectures on gas theory*. University of California Press, Berkeley-Los Angeles, Calif., 1964. Translated by Stephen G. Brush.

[16] L. Boudin and F. Salvarani. Opinion dynamics: kinetic modelling with mass media, application to the Scottish independence referendum. *Physica A: Statistical Mechanics and its Applications*, 444:448–457, 2016.

[17] L. Boudin and L. Trussardi. Concentration effects in a kinetic model with wealth and knowledge exchanges. *La Matematica*, 3(1):166–195, Jan. 2024.

[18] D. Burago, S. Ferleger, and A. Kononenko. Uniform estimates on the number of collisions in semi-dispersing billiards. *Ann. of Math. (2)*, 147(3):695–708, 1998.

[19] C. Cercignani, R. Illner, and M. Pulvirenti. *The mathematical theory of dilute gases*, volume 106 of *Applied Mathematical Sciences*. Springer-Verlag, New York, 1994.

[20] P. M. Chaikin and T. C. Lubensky. *Mean-field theory*, page 144–212. Cambridge University Press, 1995.

[21] S. Chapman and T. G. Cowling. *The mathematical theory of non-uniform gases: An account of the kinetic theory of viscosity, thermal conduction, and diffusion in gases*. Cambridge University Press, New York, 1939.

[22] J. Dalton. *A New System of Chemical Philosophy*. R. Bickerstaff, Strand, London, 1808.

[23] P. Degond, A. Frouvelle, and S. Merino-Aceituno. A new flocking model through body attitude coordination. *Math. Models Methods Appl. Sci.*, 27(6):1005–1049, 2017.

[24] Y. Deng, Z. Hani, and X. Ma. Hilbert's sixth problem: derivation of fluid equations via Boltzmann's kinetic theory, 2025. Preprint.

[25] L. Desvillettes and M. Pulvirenti. The linear Boltzmann equation for long-range forces: a derivation from particle systems. *Math. Models Methods Appl. Sci.*, 9(8):1123–1145, 1999.

[26] T. Dolmaire and A. Nota. Boltzmann-Grad limit for the inelastic Lorentz gas: Part I. Existence, uniqueness, and rigorous derivation via weak convergence, 2025.

[27] T. Dolmaire and J. J. L. Velázquez. Collapse of inelastic hard spheres in dimension $d \geq 2$. *Journal of Nonlinear Science*, 34(6):111, Oct 2024.

[28] T. Dominguez and J.-C. Mourrat. *Statistical mechanics of mean-field disordered systems—a Hamilton-Jacobi approach*. Zurich Lectures in Advanced Mathematics. EMS Press, Berlin, 2024.

[29] P. Ehrenfest and T. Ehrenfest. *The conceptual foundations of the statistical approach in mechanics*. Cornell University Press, Ithaca, NY, 1959. Translated by M. J. Moravcsik.

[30] L. Erdős and D. Q. Tuyen. Central limit theorems for the one-dimensional Rayleigh gas with semipermeable barriers. *Comm. Math. Phys.*, 143(3):451–466, 1992.

[31] F. Fougères. On the derivation of the linear Boltzmann equation from the nonideal Rayleigh gas. *Journal of Statistical Physics*, 191, 10 2024.

[32] F. Fougères. About a nonideal Rayleigh gas mixture model, 2026. Preprint.

[33] F. Fougères. Cumulants of the Rayleigh gas mixture model: statistical results, 2026. Preprint.

[34] I. Gallagher, L. Saint-Raymond, and B. Texier. *From Newton to Boltzmann: hard spheres and short-range potentials*. Zurich Lectures in Advanced Mathematics. European Mathematical Society (EMS), Zürich, 2013.

[35] I. Gallagher and I. Tristani. On the convergence of smooth solutions from Boltzmann to Navier-Stokes. *Ann. H. Lebesgue*, 3:561–614, 2020.

[36] T. Gianoli, J.-F. Boussuge, P. Sagaut, and J. de Laborderie. Development and validation of Navier-Stokes characteristic boundary conditions applied to turbomachinery simulations using the lattice Boltzmann method. *Internat. J. Numer. Methods Fluids*, 95(4):528–556, 2023.

[37] R. T. Glassey. *The Cauchy problem in kinetic theory*. Society for Industrial and Applied Mathematics (SIAM), Philadelphia, PA, 1996.

[38] F. Golse. On the periodic Lorentz gas and the Lorentz kinetic equation. *Ann. Fac. Sci. Toulouse Math. (6)*, 17(4):735–749, 2008.

[39] F. Golse and L. Saint-Raymond. The Navier-Stokes limit for the Boltzmann equation. *C. R. Acad. Sci. Paris Sér. I Math.*, 333(9):897–902, 2001.

[40] H. Grad. Asymptotic equivalence of the Navier-Stokes and nonlinear Boltzmann equations. In *Proc. Sympos. Appl. Math., Vol. XVII*, pages 154–183. Amer. Math. Soc., Providence, RI, 1965.

[41] R. Illner and M. Pulvirenti. Global validity of the Boltzmann equation for a two-dimensional rare gas in vacuum. *Comm. Math. Phys.*, 105(2):189–203, 1986.

[42] R. Illner and M. Pulvirenti. Global validity of the Boltzmann equation for two- and three-dimensional rare gas in vacuum. Erratum and improved result. *Comm. Math. Phys.*, 121(1):143–146, 1989.

[43] A. Jebrane and A. E. Mousaoui. A hybrid mesoscopic/agent-based model for crowd dynamics with emotional contagion. December 2025. Preprint.

[44] F. G. King. *BBGKY hierarchy for positive potentials*. ProQuest LLC, Ann Arbor, MI, 1975. Thesis (Ph.D.)–University of California, Berkeley.

[45] O. E. Lanford, III. Time evolution of large classical systems. In *Dynamical systems, theory and applications (Rencontres, Battelle Res. Inst., Seattle, Wash., 1974)*, volume Vol. 38 of *Lecture Notes in Phys.*, pages 1–111. Springer, Berlin-New York, 1975.

[46] O. E. Lanford, III. On a derivation of the Boltzmann equation. In *International Conference on Dynamical Systems in Mathematical Physics (Rennes, 1975)*, volume No. 40 of *Astérisque*, pages 117–137. Soc. Math. France, Paris, 1976.

[47] J. L. Lebowitz and H. Spohn. Steady state self-diffusion at low density. *J. Statist. Phys.*, 29(1):39–55, 1982.

[48] X. Lu. A modified Boltzmann equation for Bose-Einstein particles: isotropic solutions and long-time behavior. *J. Statist. Phys.*, 98(5-6):1335–1394, 2000.

[49] K. Matthies, G. Stone, and F. Theil. The derivation of the linear Boltzmann equation from a Rayleigh gas particle model. *Kinet. Relat. Models*, 11(1):137–177, 2018.

[50] K. Matthies and T. Syntaka. Derivation of kinetic and diffusion equations from a hard-sphere rayleigh gas using collision trees and semigroups, 2024. arXiv:2405.04449v1, to appear in LMS lecture notes.

[51] A. Nota, R. Winter, and B. Lods. Kinetic description of a Rayleigh gas with annihilation. *J. Stat. Phys.*, 176(6):1434–1462, 2019.

[52] O. Penrose. Convergence of fugacity expansions for classical systems. *Statistical mechanics: foundations and applications*, page 101, 1967.

[53] M. Pulvirenti. Global validity of the Boltzmann equation for a three-dimensional rare gas in vacuum. *Comm. Math. Phys.*, 113(1):79–85, 1987.

[54] M. Pulvirenti and S. Simonella. The Boltzmann-Grad limit of a hard sphere system: analysis of the correlation error. *Invent. Math.*, 207(3):1135–1237, 2017.

[55] C. Qi. Global solution of a functional Hamilton-Jacobi equation associated with a hard sphere gas, 2024.

[56] L. Saint-Raymond. From Boltzmann's kinetic theory to Euler's equations. *Phys. D*, 237(14-17):2028–2036, 2008.

[57] H. Spohn. *Kinetic Equations from Hamiltonian Dynamics: The Markovian Approximations*, pages 183–211. Springer Vienna, Vienna, 1988.

[58] H. Spohn. *Large Scale Dynamics of Interacting Particles*, volume vol. 174 of *Theoretical and Mathematical Physics*. Springer, 1991.

[59] S. Ukai. On the existence of global solutions of mixed problem for non-linear Boltzmann equation. *Proc. Japan Acad.*, 50:179–184, 1974.

[60] H. van Beijeren, O. E. Lanford, III, J. L. Lebowitz, and H. Spohn. Equilibrium time correlation functions in the low-density limit. *J. Statist. Phys.*, 22(2):237–257, 1980.

[61] C. Villani. A review of mathematical topics in collisional kinetic theory. In *Handbook of mathematical fluid dynamics, Vol. I*, pages 71–305. North-Holland, Amsterdam, 2002.

[62] Y. Wang and Y. Ma. lbmnth: A unified lattice boltzmann framework for coupled neutronics-thermal-hydraulics analysis. *Annals of Nuclear Energy*, 166:108750, 2022.

[63] G. Wissocq and P. Sagaut. Hydrodynamic limits and numerical errors of isothermal lattice Boltzmann schemes. *J. Comput. Phys.*, 450:Paper No. 110858, 61, 2022.

RÉSUMÉ

Cette thèse s'inscrit dans la mécanique statistique des gaz, qui s'intéresse à décrire des fluides très peu denses dans leur comportement moyen, à partir de leur modélisation microscopique. Dans le cas précis que nous étudions, nous supposons qu'un gaz observé de très près se comporte comme un ensemble de boules de billard idéales s'entrechoquant dans le vide : c'est le modèle des sphères dures.
Lorsque l'on regarde ces molécules de plus loin, en observant leur densité, il est possible de décrire son évolution grâce à une équation due à Ludwig Boltzmann en 1872.
Depuis les années 1970 et les travaux d'Oscar Lanford, les mathématiciens étudient en détails le lien entre ces échelles microscopique et mésoscopique, appelé limite cinétique. La présente thèse décrit un cas particulier de modèle de gaz, proche de son état d'équilibre, appelé gaz de Rayleigh non-idéal, et s'intéresse aux équations de type Boltzmann qui apparaissent dans cette limite pour décrire son comportement statistique.

MOTS CLÉS

Théorie cinétique, Mécanique statistique des gaz, Limites d'échelle, Équations aux dérivées partielles, Théorème de Lanford

ABSTRACT

This thesis is part of statistical mechanics of gases, which describes low-density fluids in their average behaviour, from their microscopic modelization. In the precise case that we study, we suppose that a gas, when observed very closely, behaves like ideal billiard balls colliding in the void: this is what defines the hard sphere model.
When looking at these molecules from further away, and observing their density, one can describe its evolution thanks to an equation due to Ludwig Boltzmann in 1872.
Since the 1970s and Oscar Lanford's work, mathematicians have studied in detail the link between these microscopic and mesoscopic scales, called the kinetic limit. The present thesis describes a specific case of gas model, close to its equilibrium state, called nonideal Rayleigh gas; we are interested in the Boltzmann-like equations that appear in this limit to describe its statistical behaviour.

KEYWORDS

Kinetic theory, Statistical mechanics of gases, Scaling limits, Partial differential equations, Lanford theorem